INTERNATIONAL CONFERENCE

MEĐUNARODNA KONFERENCIJA

MEETING POINT OF THE SCIENCE AND PRACTICE IN THE FIELDS OF CORROSION, MATERIALS AND ENVIRONMENTAL PROTECTION

STECIŠTE NAUKE I PRAKSE U OBLASTIMA KOROZIJE, ZAŠTITE MATERIJALA I ŽIVOTNE SREDINE

PROCEEDINGS

KNJIGA RADOVA

Under the auspicies of the
MINISTRY OF SCIENCE, TECHNOLOGICAL DEVELOPMENT AND INNOVATION OF THE REPUBLIC OF SERBIA

Pod pokroviteljstvom
MINISTARSTVO NAUKE, TEHNOLOŠKOG RAZVOJA I INOVACIJA REPUBLIKE SRBIJE

May 28-31, 2024 : : Divčibare, Serbia

CIP - Каталогизација у публикацији
Народна библиотека Србије, Београд

620.193/.197(082)(0.034.2)
621.793/.795(082)(0.034.2)
667.6(082)(0.034.2)
502/504(082)(0.034.2)
66.017/.018(082)(0.034.2)

МЕЂУНАРОДНА конференија YuCorr (25 ; 2024 ; Дивчибаре)
Meeting point of the science and practice in the fields of corrosion, materials and environmental protection [Elektronski izvor] : proceedings = Stecište nauke i prakse u oblastima korozije, zaštite materijala i životne sredine : knjiga radova / XXV YuCorr International Conference, May 28-31, 2024, Divčibare, Serbia = XXV YuCorr Međunarodna konferencija ; [organized by] Serbian Society of Corrosion and Materials Protection ... [et al.]] = [organizatori Udruženje inženjera Srbije za koroziju i zaštitu materijala ... [et al.] ; [editors, urednici Miroslav Pavlović, Marijana Pantović Pavlović, Miomir Pavlović]. - Beograd : Serbian Society of Corrosion and Materials Protection UISKOZAM = Udruženje inženjera Srbije za koroziju i zaštitu materijala UISKOZAM, 2024 (Beograd : UISKOZAM). - 1 elektronski optički disk (CD-ROM) ; 12 cm
Sistemski zahtevi: Nisu navedeni. - Nasl. sa naslovne strane dokumenta. - Radovi na engl. i srp. jeziku. - Tiraž 200. - Bibliografija uz većinu radova. - Abstracts.

ISBN 978-86-82343-31-8

а) Премази, антикорозиони -- Зборници б) Превлаке, антикорозионе -- Зборници в) Антикорозиона заштита -- Зборници г) Животна средина -- Заштита -- Зборници д) Наука о материјалима -- Зборници

COBISS.SR-ID 146962185

XXV YUCORR – International Conference | *Međunarodna konferencija*

PUBLISHED BY | *IZDAVAČ*
SERBIAN SOCIETY OF CORROSION AND MATERIALS PROTECTION (UISKOZAM)
UDRUŽENJE INŽENJERA SRBIJE ZA KORZIJU I ZAŠTITU MATERIJALA (UISKOZAM),
Kneza Miloša 7a/II, 11000 Beograd, Srbija, tel/fax: +381 11 3230 028, *office@uiskozam.rs; www.uiskozam.rs*

FOR PUBLISHER | *ZA IZDAVAČA* *Prof. dr MIOMIR PAVLOVIĆ, predsednik UISKOZAM*

EDITORS | *UREDNICI:* *Dr Miroslav Pavlović, Dr Marijana Pantović Pavlović, Prof. dr Miomir Pavlović*
SCIENTIFIC AREA | *OBLAST:* CORROSION AND MATERIALS PROTECTION **|** *KOROZIJA I ZAŠTITA MATERIJALA*
PAGE LAYOUT | *KOMPJUTERSKA OBRADA I SLOG:* *Dr Marijana Pantović Pavlović*
CIRCULATION | *TIRAŽ:* **200** copies **|** *primeraka*
REPRODUCER | *UMNOŽAVA:* UISKOZAM
PUBLICATION YEAR | *GODINA IZDANJA:* **2024**
ISBN 978-86-82343-31-8

Synthesis : : Materials : : Corrosion : : Environment : : Energy

XXV YuCorr

Analyse : : Discover : : Coat : : Green : : Protect : : Save : : Sustain

May 28-31, 2024, Divčibare, Serbia

Ovaj PDF fajl sadrži elektronsku Knjigu radova prezentovanih u okviru Međunarodne konferencije **XXV YuCorr.** U knjizi su **plavom bojom** obeleženi aktivni linkovi ka pojedinim njenim delovima, iz Sadržaja do naznačenih stranica.

This PDF file contains Proceedings presented on the **XXV YuCorr** International Conference. It can be easily navigated through the book contents by a single click on the appropriate links in Contents (**showed in blue**).

Autori snose punu odgovornost za sadržaj, originalnost, jezik i gramatičku korektnost sopstvenih radova.

Authors bear full responsibility for the content, originality, language and grammatical correctness of their own works.

XXV YUCORR IS ORGANIZED BY
ORGANIZATORI XXV YUCORR-a

SERBIAN SOCIETY OF CORROSION AND MATERIALS PROTECTION

Udruženje Inženjera Srbije za Koroziju i Zaštitu Materijala

INSTITUTE OF CHEMISTRY, TECHNOLOGY AND METALLURGY, UNIVERSITY OF BELGRADE

Institut za Hemiju, Tehnologiju i Metalurgiju, Univerzitet u Beogradu

INSTITUTE OF GENERAL AND PHYSICAL CHEMISTRY, BELGRADE

Institut za Opštu i Fizičku Hemiju

UNION OF ENGINEERS AND TEHNICIANS OF SERBIA, BELGRADE

Savez Inženjera i Tehničara Srbije

ENGINEERING ACADEMY OF SERBIA

Inženjerska Akademija Srbije

XXV YUCORR IS ORGANIZED UNDER THE AUSPICIES OF THE

MINISTRY OF SCIENCE, TECHNOLOGICAL DEVELOPMENT AND INNOVATION OF THE REPUBLIC OF SERBIA

XXV YUCORR JE FINANSIJSKI POMOGLO

MINISTARSTVO NAUKE, TEHNOLOŠKOG RAZVOJA I INOVACIJA REPUBLIKE SRBIJE

SPONSORS | *SPONZORI*

SHERWIN-WILLIAMS | PROTECTIVE & MARINE COATINGS

JADRAN d.o.o., Beograd

INTERNATIONAL SOCIETY OF ELECTROCHEMISTRY, Switzerland

SAVEZ INŽENJERA I TEHNIČARA SRBIJE, Beograd

INŽENJERSKA KOMORA SRBIJE, Beograd

KANSAI HELIOS SRBIJA a.d., Gornji Milanovac

ALFATERM d.o.o., Čačak

FIRESTOP INTERNACIONAL d.o.o., Nova Pazova

SURTEC ČAČAK d.o.o., Čačak

INSTITUT ZA PREVENTIVU d.o.o., Novi Sad

INSTITUT ZA OPŠTU I FIZIČKU HEMIJU, Beograd

Contents

PLENARY LECTURES
PLENARNA PREDAVANJA

Hydrogen Metallurgy for a treatment of bauxite residues-First results on the EURO-TITAN Project

Srecko Stopić[1,*], Nenad Nikolić[2], Dragana Životić[3], Jugoslav Krstić[4], Milena Rosić[5], Vladimir Damjanović[6], Bernd Friedrich[1]

[1] *IME Process Metallurgy and Metal Recycling/RWTH Aachen University, Intzestrasse 3, Aachen, Germany*

[2]*Institute for Mutlidisciplinary Research, University of Belgrade, Kneza Viseslava 1, Belgrade, Serbia*

[3]*Faculty of Mining and Geology, University of Belgrade, Djusina 7, Belgrade, Serbia*

[4]*Institute of Chemistry, Technology and Metallurgy, University of Belgrade, Studentski trg 12-16, Belgrade, Serbia*

[5]*"Vinča" Institute of Nuclear Sciences, National Institute of the Republic of Serbia, University of Belgrade, Mike Petrovića Alasa 12-14, 11351 Vinča, Serbia*

[6]*Alumina d.o.o, Karakaj b.b, 75400 Zvornik, Bosnia and Herzegovina*

[1,*]*sstopic@ime-aachen.de*

Abstract

Hydrogen is the most abundant element in the universe (75 % by mass) and the lightest element (density of 0.00082 g/cm^3). Because of its presence in many different forms such as gaseous hydrogen, its plasma species, water, acid, alkaline, ammonia and hydrocarbons, has high application in different metallurgical unit operations. In this paper, reduction of metallic oxides by hydrogen will be studied. Especially hydrogen reduction of the aluminium residues such as red mud from the Bayer Process will be discussed as first step in production of metallurgical slid residue needed for the recovery of valuable metals such as titanium, rare earth elements and iron.

Keywords: *hydrogen, reduction, metallurgy, recycling, red mud*

Introduction

Hydrogen as a key element in energy transition replacing fossil fuels and their CO_2 emissions was used as a reducing agent instead of carbon [1]. Application of hydrogen in metallurgical operations has gained strong interest in hydrometallurgy and pyrometallurgy of non-ferrous metals [2]. As mentioned by Rodriguez et al. [3] control of hydrogen formation during hydrometallurgical processes such as electrocoagulation and winning electrolysis has a high significance for the metal recovery. Generating green hydrogen efficiently from water and renewable energy requires high-end technology and innovative solutions — like the Silyzer product family from Siemens Energy. Using Proton Exchange Membrane (PEM) electrolysis, the Silyzer is ideally suited for harnessing volatile energy generated from wind and solar [4].

The Bayer Process is the traditional industrial method to produce alumina from bauxite ore. The chemical quality of precipitated aluminum hydroxide, and consequently the final alumina product in the Bayer process directly depends of the level of impurities in a refinery's Bayer liquor. Under optimal reaction parameters (temperature and time) it is possible to remove iron, zinc and copper from Bayer liquor using precipitation agent such as calcium hydroxide with an efficiency of more than 90%, in such a way that the treated solution is still economically usable in the following stages of processing while obtaining different types of aluminum trihydrate [5].

In Europe, alumina refineries operate in Bosnia and Herzegovina (Alumina, Zvornik), France, Hungary, Germany, Greece, Ireland (AAL), Romania (ALUM), Spain and Ukraine, while significant BR deposits from refineries that have stopped their operations (legacy sites) exist in former Yugoslavia (Podgorica, Kidricevo, Mostar, Obrovac), Italy, France (RT), Germany, Hungary and other countries. The current BR production level in the EU is 6.8 million tonnes per year; while the cumulative stockpiled level is a staggering >250 million tonnes (dry matter). The mineralogical structure of bauxite residue, where nearly 80 % consists of three of these phases: cancrinite, sodalite and hematite, as shown in Table 1. [6]

Table 1: Typical mineralogical structure of the bauxite residue (in wt. -%)

Cancrinite [$Na_6Ca_{1.5}Al_6Si_6O_{24}(CO_3)_{1.6}$]:	29.0-33.0
Sodalite [$Na_8(Cl,OH)_2Al_6Si_6O_{24}$]:	16.0-24.0
Hematite [Fe_2O_3]:	27.0-29.0
Boehmite [AlO(OH)]:	5.0-6.0
Gibbsite [$Al(OH)_3$]:	4.0-5.0
Anatase [TiO_2]:	5.0
Andradite [Ca-Fe-Al-Si oxides]:	4.0
Quartz [SiO_2]:	2.0

The bauxite residues contain scandium and gallium (approx. 50-150 ppm) and up to an order of magnitude higher for elements such as: vanadium and rare earths elements (0.05-0.5 %). MYTILINEOS, Greece since 1991 has been pioneering research on BR handling and reuse, focusing initially on massive low value applications such as use as a raw material for geopolymer bricks, cement clinker production, iron production, bricks and tile production, soil remediation (vegetation), extraction of rare earth elements and road substrate.

Due to the generation of large amounts of Bauxite Residue (red mud), an alternative method, called the Pedersen Process was considered in order to prevent the Bauxite Residue generation [7]. In the conventional Pedersen Process, iron in the bauxite is separated in the form of pig iron through a carbothermic smelting-reduction step which has a carbon dioxide emission similar to that during conventional iron production. In order to eliminate the carbon dioxide emission of this step, the focus of their work was to reduce the iron oxides of bauxite ore by hydrogen gas prior to smelting and minimizing the use of solid carbon materials for the reduction. Calcination and reduction of bauxite ore by hydrogen was studied by thermogravimetry method supported by microstructural and phase analysis confirming that the reduction of hematite via magnetite to iron starts at temperatures below 560 °C with slow rate and is faster at higher temperatures. At higher temperatures, i.e., 860, 960, and 1060 °C, the formation of hercynite ($FeAl_2O_4$) retards the complete reduction to metallic iron.

The possibilities to recover rare earths from bauxite residues, which commonly contain only low concentrations of rare-earth elements, but are available in very large volumes and could provide significant amounts of rare earths to European countries are main research subject of the European funded projects (EURARE; REMOVAL, SCALE, REDMUD) in last ten years. The extraction rate of the rare-earth recovery from these industrial waste streams is a part of a comprehensive, zero-waste, “product-centric” valorisation scheme, in which applications are found for the residual fractions that are obtained after removal of not only the rare earths but also other critical metals such as scandium, vanadium and gallium and especially the base elements: aluminium, titanium and iron [8]. EURO-TITAN will study decarbonized technologies for Ti recovery from aluminium and titanium residues in the next 4 years, as shown at Fig.1.

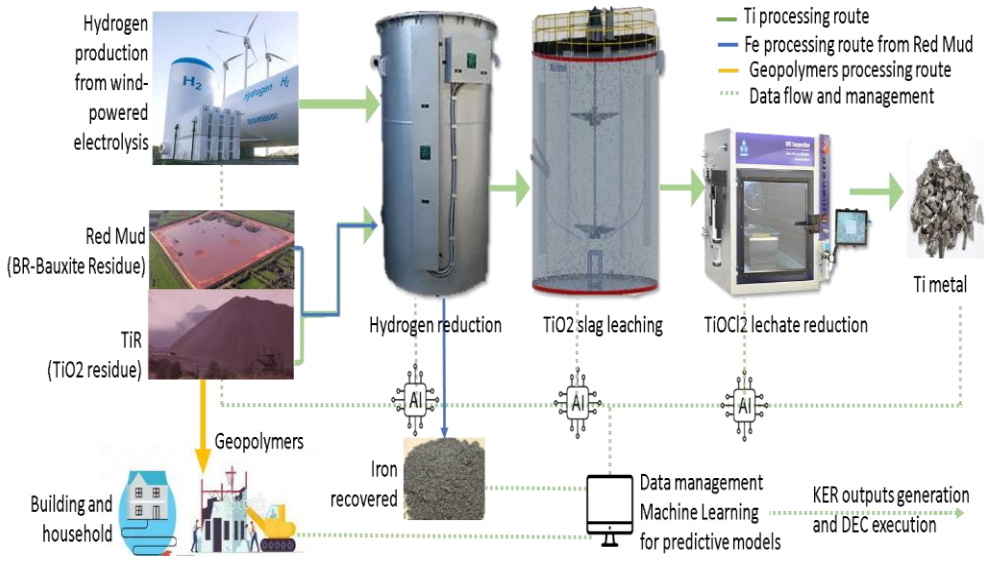

Figure 1. *Euro-Titan Research strategy*

Unfortunately, the extraction of aluminium, iron and titanium from bauxite residue under acid leaching is limited due to insufficient amount of acidic solution from leaching caused by the polymerization of silica [9]. Kinetic studies have demonstrated that at constant temperatures, silica dissolution increases with increasing acid concentration, but it decreases when the temperature is increased and the acid concentration is reduced. This is due to the enhancement in the solubility of monomeric silicic acid formed during acidic leaching. The control mechanisms of silica dissolution have been described according to the shrinking core model by a chemical reaction stage, i.e. silica polymerization, followed by a diffusion stage, because of the silica gel adsorbed on the surface of the particles that limits the metal extraction. Alkan et al [10] studied a recovery of iron, titanium, aluminium, rare earth elements from bauxite residues preventing silica gel formation was performed using dry digestion process with sulphuric acid and hydrogen peroxide. The operational parameters were investigated and the addition of 2.5M hydrogen peroxide into 2.5M sulfuric acid was decided to be the best leaching condition to have favored quartz formation with a suppressed rhomboclase precipitation. Since the leaching reactions mainly controlled by diffusion, no significant increase in the efficiencies were observed after 30 minutes of leaching. While silica gel was not formed in oxidative environment, high titanium extraction from bauxite residue was only achieved when hydrogen peroxide was introduced into the acidic solution.

The combined pyrometallurgical and hydrometallurgical treatment of bauxite residue for the recovery of valuable metals included firstly carbothermic reduction [11]. The reductive smelting of bauxite residue using coke as the reductant between 1500 and 1550°C and acidic to basic fluxes to lower the smelting temperature and the production of conditioned slag. Additional conditioning of the bauxite residue with basic oxygen furnace slag and bottom ash as fluxing agents in the smelting process was performed in order to recover the valuable metals with exclusive use of secondary resources as slag formers [12, 13].

Jovicević-Klug et al. [14] proposed how this red mud can be turned into valuable and sustainable feedstock for ironmaking using fossil-free hydrogen-plasma-based reduction at higher temperatures in electric arc furnace (more than 1600°C), thus mitigating a part of the steel-related carbon dioxide emissions by making it available for the production of several hundred million tonnes of green steel. The process proceeds through rapid liquid-state reduction, chemical partitioning, as well as density-driven and viscosity-driven separation between metal and oxides.

The aim of this work is to offer first information about characterisation of bauxite residues from Alumina, Zvornik and study of hydrogen reduction at temperature below 1000°C. As mentioned this

study is only first part in frame of the EURO-Titan Project (2024-2027) aiming to explain an importance of hydrogen metallurgy in production of green steel.

Thermochemical analysis of hydrogen reduction

Equilibrium calculations were done to identify relevant species and changes in chemical composition during hydrogen reduction at 900°C, as shown at Figure 2. Reduction by hydrogen, even with small ratios of H_2/red mud (kg/kg) lead to reduction of Fe_2O_3 to Fe and CoO and NiO to metallic forms. All these components can be easily recovered by magnetic separation.

Reduction of hematite by hydrogen proceeds in two or three steps, under and above 570 °C, respectively, via magnetite (Fe_3O_4) and wustite (FeO) according to the following equations:

$3Fe_2O_3 + H_2 \rightarrow 2Fe_3O_4 + H_2O$ (1)

$Fe_3O_4 + H_2 \rightarrow 3\ FeO + H_2O$ (2)

$FeO + H_2 \rightarrow Fe + H_2O$ (3)

Pineau et al. [15] found reduction of iron ores with hydrogen leads to compact iron layers that could slow their reduction rate. Additionally thermochemical analysis revaled the formation of Fe_2TiO_4 and $FeAl_2O_4$; what can lead to the formation of a passivation layer in reduction process. The formation of ferrite phases is expected for other elements such as calcium and sodium.

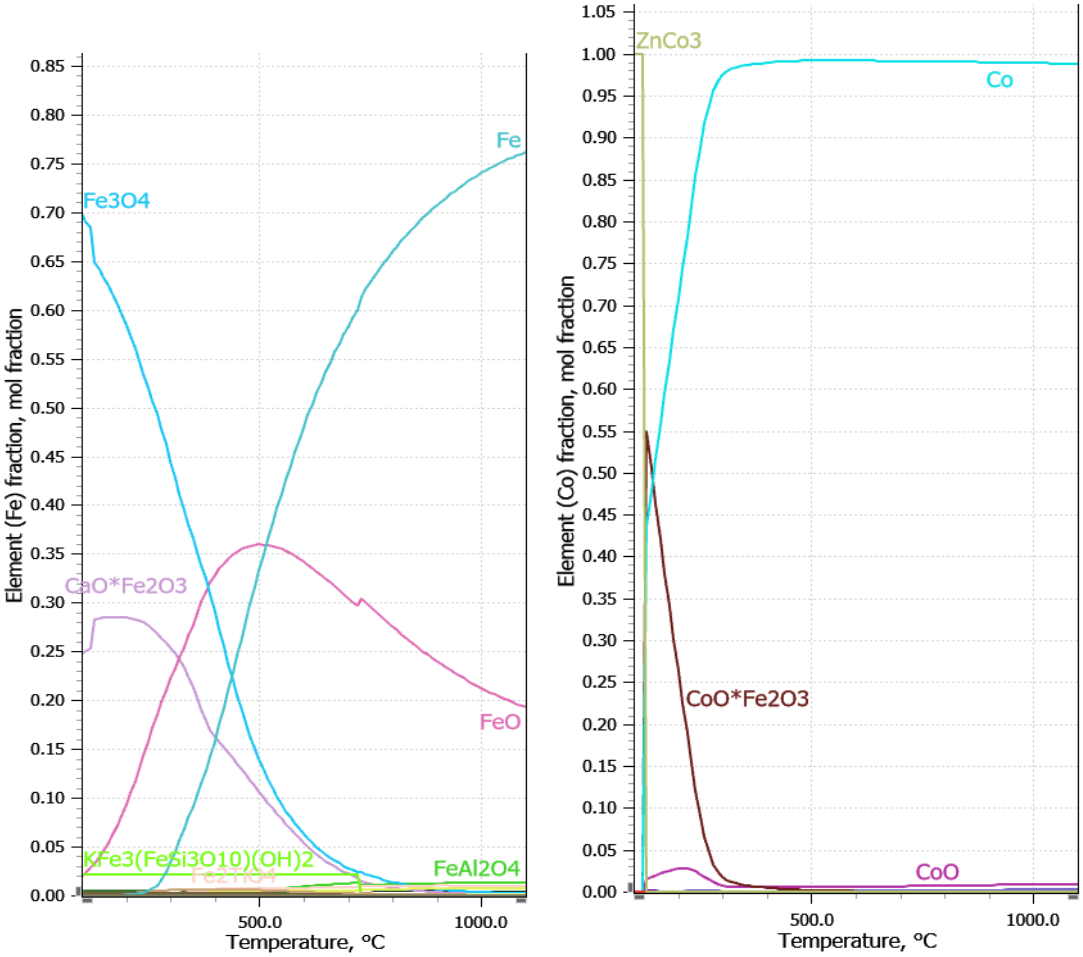

Figure 2. *Thermochemical calculation of reduction of iron oxides and cobalt oxide at 900°C*

Red Mud, Alumina, Zvornik

During the operation of the company Alumina, Zvornik about 19.4 x 10^6 m^3 of red mud suspension was disposed of. Depending on the quality of the bauxite, the amount of completely dry red mud typically ranges from 0.8 to 2 tons of tailings per ton of alumina produced. Accordingly, the amount of red mud that is separated and disposed of at the landfill is about 1.0 - 1.2 tons per ton of Al_2O_3 produced, or approximately 400,000 t per year. The bauxite residue from Alumina was filtrated, washed and dried at 105 °C for 24 h. The chemical composition of red mud is presented in Table 2:

Table 2: Chemical composition of BR, Zvornik

Compounds	%	Compounds	%
Ignition loss at 1000°C	8,32	**Ga_2O_3**	0,225
SiO_2	10,52	**CuO**	0,007
Fe_2O_3	49,29	**K_2O**	0,159
Na_2O	2,45	**Tl_2O_3**	0,088
TiO_2	4,59	**MnO**	0,145
CaO	8,23	**MgO**	0,627
Al_2O_3	12,03	**NiO**	0,034
Ag_2O	0,001	**PbO**	0,019
BaO	0,014	**P_2O_5**	0,930
Cr_2O_3	0,133	**ZnO**	0,016
Sc_2O_3	0,011	**V_2O_5**	0,135
Co_2O_3	0,012	**SrO**	0,075

As shown at Fig.3, XRD-analysis of red mud after found the following phases: hematite, perovskite, cancrinite, ilmenite, calcite, diaspore, gibbsite and hydrogarnet. Iron is present in hematite and ilmenite structure. Titanium is present in perovskite and ilmenite structure, while aluminum is present in structure of cancrinite, diaspore, boehmite, gibbsite and hydrogarnet.

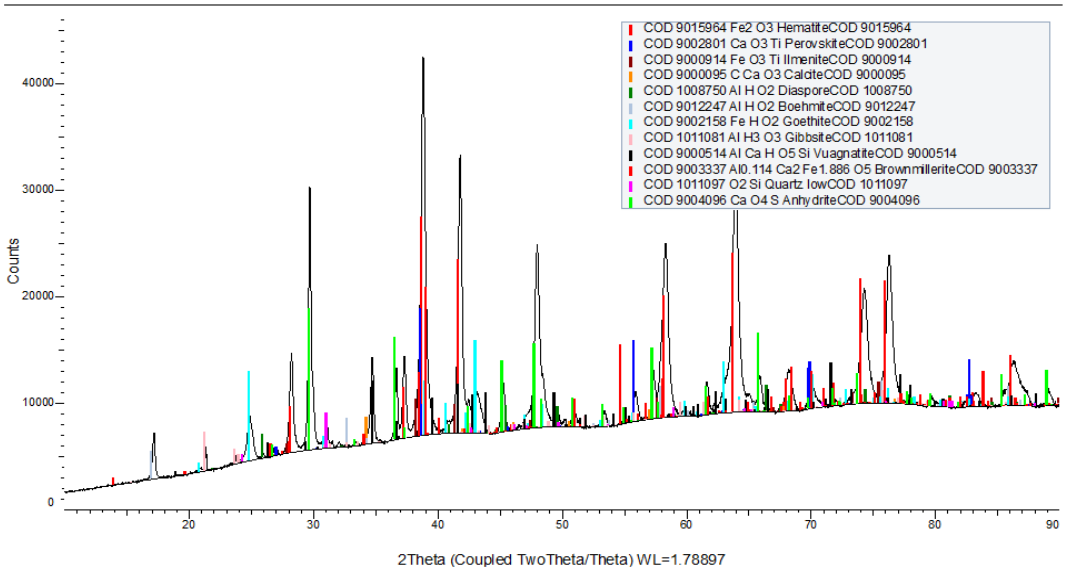

Figure 3. *XRD Analysis of Red mud, Alumina, Zvornik*

The XRD-analysis at Figure 3 has confirmed the presence hematite and other very stable oxides for hydrogen reduction.

Particle size distribution analysis of red mud found very fine particles, as shown at Figure 4. The obtained particle size have the following values ($x_{50,3}$= 4.70 μm and $x_{90,3}$= 5.98 μm).

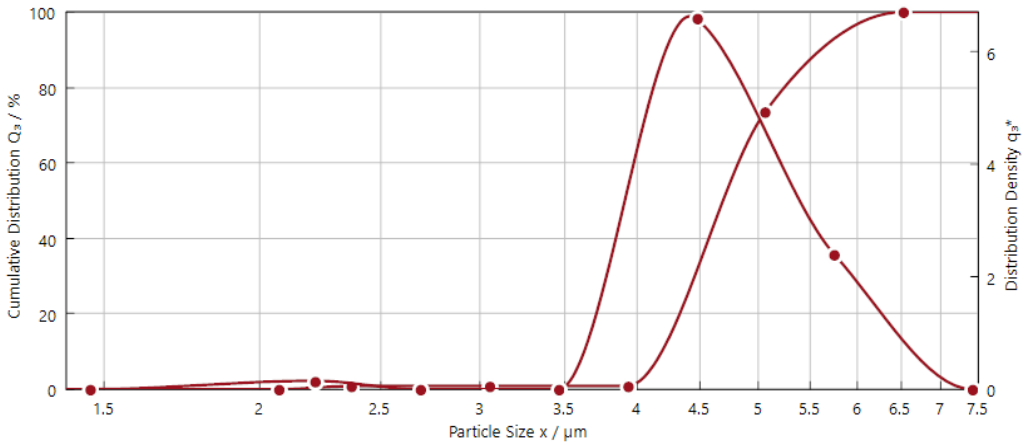

Figure 4: *Particle size of red mud from Alumina Zvornika*

Reduction with hydrogen

Reduction of 1.0 g red mud is performed in small tubular furnace at 700, 800, 900 and 1000 °C at 30 and 60 min using flow rate of 2 l/min of hydrogen and 1l/min of argon. Mass loss of initial sample amounted between 18 and 23 % (as shown in Table 3), what is accorded with an expected total theoretical value of reduction process regarding the mass loss of oxygen from iron oxide, cobalt oxide and nickel oxide through hydrogen reduction (max 15 %) and evaporation in neutral atmosphere (max. 9 %). The obtained particles after hydrogen reduction have magnetic properties, what is very important for the following separation process.

Table 3. Experimental results for hydrogen reduction (constant flow rate: 2l/min H_2, 1 l/min Ar)

Mass loss (%)	700°C	800°C	900°C	1000°C
30 min	18	20	21	23
60 min	21	23	23	-

SEM/EDS analysis of powders

The prepared powders obtained between 700°C and 1000°C have irregular, polygonal form with grain sizes more than 100 μm, as shown at Figure 5.a and 6.a.

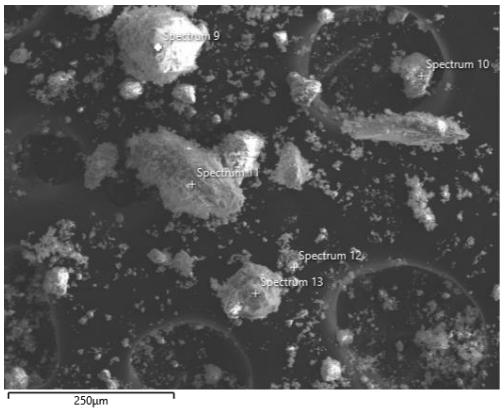

Figure 5.a. *SEM analysis of powders obtained at 700°C*

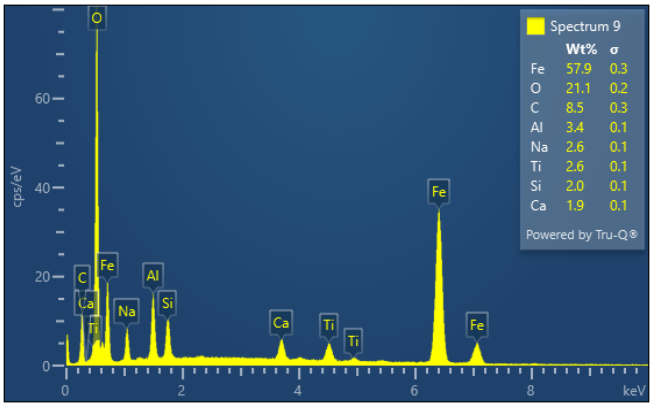

Figure 5.b. *EDS analysis of powders obtained at 700°C*

An increase of temperature from 700°C to increases the content of iron and decrease the content of oxygen as shown at Figure 5a and 5b. The morphological study of the reduced samples of iron oxides by H_2 shows agglomeration of the reaction product at temperatures between 700 and 1000°C.

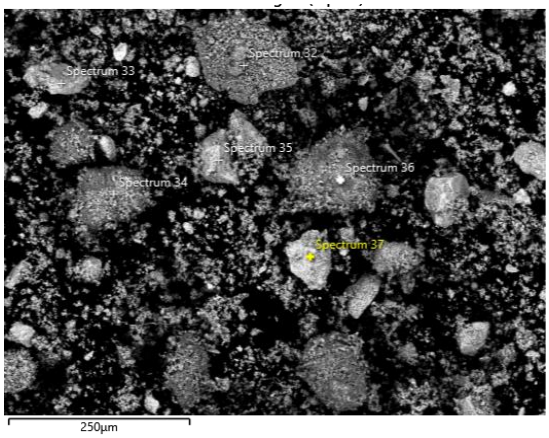

Figure 6.a. *SEM analysis of powder obtained at 900°C by hydrogen reduction of red mud*

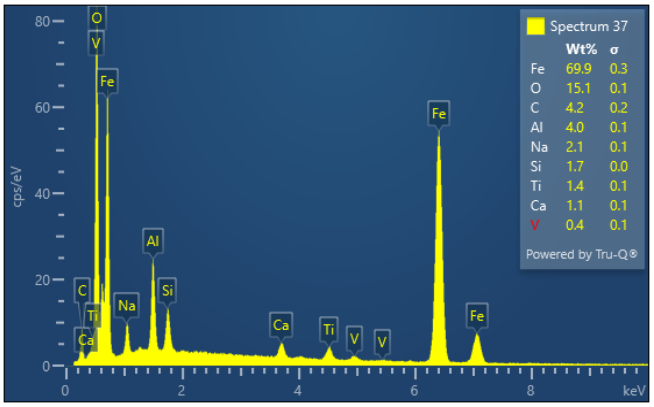

Figure 6.b. *EDS analysis of particles obtained at 900°C by hydrogen reduction of red mud*

An increase of temperature from 700°C to 1000°C increases the content of iron and decrease the content of oxygen as shown at Figure 5b and 6b.

The particle size distribution of reduced red mud revealed an increase of particle size during reduction ($x_{50,3}$= 18,32 µm and $x_{90,3}$= 308,97 µm), as shown at Figure 7.

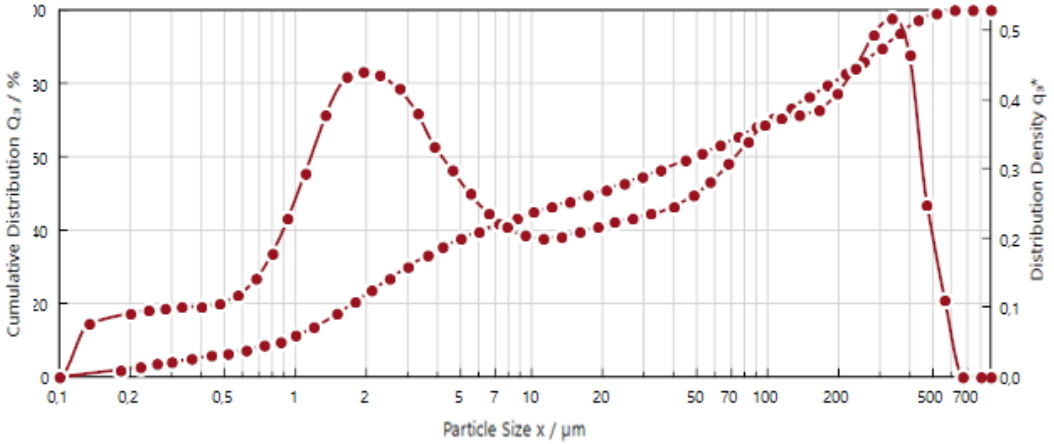

Figure 7*. Particle size distribution of reduced red mud at 900°C*

XRD analysis of reduced powder samples

The reduced red mud powder samples were analysed at room temperature by X-ray powder diffraction techique using the Ultima IV Rigaku diffractometer, equipped with CuK$\alpha_{1,2}$ radiation, using a generator voltage of 40 kV and a generator current of 40 mA. The range of 10–100° 2θ was used for all powder samples in a continuous scan mode with a scanning step size of 0.02° and at a scan rate of 1°/min, using D/TeX Ultra high - speed detector. Glass sample carrier for sample preparation was used. The PDXL2 (Ver. 2.8.4.0) software was used to evaluate the phase composition and identification [16]. All obtained powders were identified using the ICDD database [17].

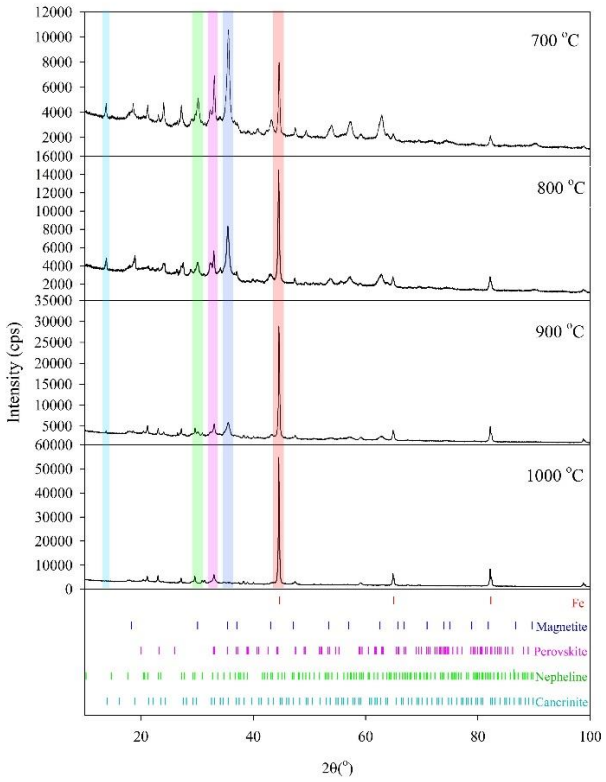

Figure 8. *Diffractograms for the red mud reduced at 700, 800, 900 and 1000 °C. Identified minerals with positions of diffraction maxima are shown in lower part. The position of intensive diffraction maxima which do not overlap with other maxima of other minerals are shown in colored bands and used for comparison in mineral abundance.*

Diffractograms for four red mud samples reduced in hydrogen athmosphere at 700, 800, 900 and 1000 °C are shown in Figure 8. The intensities of diffraction maxima are commented as the proxies for the abundance of mineral phases present. The identified phases are: metallic iron, magnetite, perovskite, nepheline and cancrinite.
Metallic iron apprears as the new phase not present in raw red mud which is characterised with sharp diffraction maxima reflecting the high cristallinity of iron. The intensities of iron diffraction peaks with respect to those of other phases progressively increase with the increase of reduction temperature indicating an increase of iron abundance. At 900 ^{o}C, and especially at 1000 ^{o}C, metallic iron dominates with respect to other phases.
Iron is partly accomodated in magnetite. Magnetite appears as the most abundant phase in sample reduced at 700 ^{o}C. The intensity of magnetite diffraction peaks as well as magnetite content progressive decrease with the increase of reduction temperature. The slight shift in position of diffraction maxima compared to pure Fe_3O_4 may be attributed to the presence of Al, Ti, Ca which is consistent with cetrain amount of those presumablly alloying elements determined by EDS analysis.
The most stiking feature is a progressive increase in metallic iron content accompanied with the decrease in magnetite content with an increase of reduction temperature. Magnetite apprears to be virtually absent in sample reduced at 1000 ^{o}C where only reduced elemental iron dominates.
Of other non-ferrous phases identified are perovskite and nepheline formed during reduction process and not identifiled in raw red mud as well as the residual cancrinite which is authigenic raw red mud mineral. Perovskite as the only Ti-bearing phase appears to be stable in examined range of temperatures (i.e. 700-1000 ^{o}C) inferred from XRD. Nepheline apperas as only newly formed silicate phase stable in examined range of temperatures as well. The striking feature is the observed trend in decrease in residual cancrinite content accompanied with the increase in nepheline content with increase of reduction temperature until complete disapearance of cancrinite at highest reduction temperature. This trend is interpreted as the cancrinite breakdown and transformation into nepheline.

Conclusion

Results of the reduction of iron oxides from red mud with hydrogen in the temperature range of 700–1000 °C leads to the following conclusions:

1. An increase of temperature from 700 °C to 1000 °C leads to reduction of Fe_2O_3 to Fe, but also partial transformation to Fe_3O_4 that is more stable at lower reduction temperatures. The most striking feature inferred from XRD is a progressive increase in metallic iron content accompanied with the decrease in magnetite content with an increase of reduction temperature whereas metallic iron is only identified iron phase at 1000 °C. Similarly, the decrease in residual cancrinite content accompanied with the increase in nepheline content with the increase of reduction temperature is another observed trend in silicate mineralogy.
2. The morphological study of the reduced red mud by hydrogen shows agglomeration of the reaction product at temperatures higher than 700 °C
3. The reduction process leads to increased particle size in comparison to used red mud

Acknowledgements

We would like to thank Dr. Nikola Anastasijević for thermochemical analysis performed in HSC software. This research was funded by European Commission, grant number 101135077 (EURO-TITAN). Part of this research was supported by the funds of the bilateral research project supported by the Ministry of Education, Science and Technological Development of the Republic of Serbia and German Academic Exchange Service (DAAD).

References

1. Stopic, S., Friedrich, B, Formation and application of hydrogen in non-ferrous metallurgy, Military Technical Courier, 2023, 783-796
2. Stopic, S., Ilić, I., Uskoković, D. (1997): Effect of palladium, copper, and nickel additions on the kinetics of nickel-chloride reduction by hydrogen, Metallurgical of Materials of Transaction B. 28, pp. 1241-1248.
3. Rodriguez, J., Stopic, S., Friedrich, B. (2007): Feasibility assessment of electrocoagulation towards a new sustainable wastewater treatment, Environmental Science and Pollution Research, 14, 7, 477-482.
4. Green hydrogen Production, https://www.siemens-energy.com/global/en/home/products-services/product-offerings/hydrogen-solutions.html
5. Damjanovic, V., Kostic, D., Ostojic, Z., Perusic, M., Filipovic, R., Oljaca, Dj., Obrenovic, Z., Micic, V. The Influence of Process Parameters on Removing Iron, Zinc and Copper Impurities from Synthetic Bayer Liquor, TRAVAUX 49, Proceedings of the 38 th International ICSOBA Conference, 16 – 18 November 2020, 325-334
6. Castaldi, P., Silvetti; M., Santona, L., *et al.* (2008): XRD, FTIR, and Thermal Analysis of Bauxite Ore-Processing Waste (Red Mud) Exchanged with Heavy Metals, Clays and Clay Minerals, 56, 4, 461-469
7. Lazou, A., van der Eijk, C, Balomenos, E., Kolbeinsen, L., Safarian, J, (2020): On the Direct Reduction Phenomena of Bauxite Ore Using H_2 Gas in a Fixed Bed Reactor, Journal of Sustainable Metallurgy, pp. 227-238.
8. K. Binnemans, K., Tom Jones, P., Blanpain, B., van Garven, T. Pontikes, Y. (2015): Towards zero-waste valorisation of rare-earth –containing industrial process residues: a critical review, Journal of Cleaner Production, 99, 17-38
9. Rivera, R., Ulenaers, B., Ounoughene, G; Binnemans, K., van Gerven, T., Behaviour of silica during metal recovery from bauxite residue by acidic leaching, International Committee for Study of Bauxite, Alumina & Aluminum, ICSOBA, Hamburg, 02-05.Oktober 2017, 1-9.
10. Alkan, G., Yagmurlu, B., Cakmakoglu, S., Hertel, T., Kaya, S., Gronen, L., Stopic, S., Friedrich, B. (2018): Novel Approach for Enhanced Scandium and Titanium Leaching Efficiency from Bauxite Residue with Suppressed Silica Gel Formation, Nature, Scientific Reports, 8, 5676-5678
11. Xakalashe, B., Friedrich, B, Combined carbothermic reduction of bauxite residue and basic oxygen furnace slag for enhanced recovery of Fe and slag conditioning, 2nd international Bauxite Residue Valorisation and Best Practices Conference (BR2018), Athens (Greece), 7-10 May 2018, 233-240.
12. H. Lucas, G. Alkan, B. Xakalashe, B. Friedrich, Conditioning of bauxite residue with bottom ash in view of recovery of valuable metals: A sustainable approach, 2nd international Bauxite Residue Valorisation and Best Practices Conference (BR2018), Athens (Greece), 7-10 May 2018, 263-270.
13. Yagmurlu, B., Alkan, G., Xakalashe, B., Schier, C., Gronen, L., Koiwa,I., Dittrich, C., Friedrich, B. (2019): Synthesis of scandium phosphate after peroxide assisted leaching of iron depleted bauxite residue (red mud slags), Scientific reports, 9, 11803-11813
14. Jovičević-Klug,M, R. Souza Filho, Springer, H., Adam, C., & Raabe, D., Green steel from red mud through climate-neutral hydrogen plasma reduction. Nature 625, 704-717
15. Pineau, A., Kanari, N., Gaballah, I (2006): Kinetics of reduction of iron oxides by H2 Part I: Low temperature reduction of hematite, Thermochimica Acta 447,) 89–100
16. Rigaku, *PDXL Integrated X-Ray Powder Diffraction Software*. 2011, Rigaku, Tokyo: Japan.
17. *International Crystallographical Database (ICDD)*, N.S. 12 Campus Blvd, PA 19073, USA, Editor. 2012: USA.

Stable non-traditional isotopes as tracers for the identification of contaminant sources

Tea Zuliani[1,2], Majda Nikezić[1,2], Tjaša Žerdoner[1,2],

[1]*Jožef Stefan Institute, Department of Environmental Sciences, Ljubljana, Slovenia*

[2]*Jožef Stefan International Postgraduate School, Ljubljana, Slovenia*

Abstract

The presence of inorganic contaminants in the environment poses a global threat to human health. While natural processes contribute to some of them, human activities like agriculture, industry, and mining generate significant amounts. These contaminants spread through air, water, soil, and organisms. Airborne transport, facilitated by suspended particles like aerosols and dust, as well as water transport, are crucial pathways for redistributing contaminants. These processes can move pollutants from localized sources such as industrial centres or mines to broader environmental areas, impacting ecosystems and human populations.

The application of stable non-traditional isotopes, such as Sr, Pb, Cd, …, has emerged as a powerful tool for tracing the origin of environmental pollutants. Traditional approaches often fall short in discerning complex pollution sources, particularly in regions with a history of mining and industrial activities. This abstract presents a case study demonstrating the efficacy of non-traditional stable isotopes, specifically Pb isotopes, in identifying pollutant sources in the Meža Valley, Slovenia.

The Meža Valley, characterized by its extensive history of mining and smelting of Pb ore, has encountered significant environmental challenges after the closure of mines and smelters over three decades ago. Since 1950, the operation of a Pb recycling facility and battery production has added complexity to the region's pollution dynamics. This study focuses on pinpointing the sources of Pb contamination in the Meža River and PM10 particles within the valley. The isotopic fingerprinting facilitated discrimination between various potential Pb sources, including historical mining activities, traffic, and industrial emissions. The findings indicate distinct isotopic signatures associated with different pollution sources. Integrating these results with spatial and temporal distribution patterns of Pb contamination provides valuable insights into the relative contributions of various emission sources to environmental pollution in the Meža Valley. Such comprehensive source apportionment is pivotal for designing effective pollution mitigation strategies and safeguarding environmental health in regions with complex industrial legacies.

Carbonation of an olivine and slag under high pressure conditions in an autoclave

Srecko Stopic*, Christian Dertmann, Alexander Birich, Bernd Friedrich

IME Process Metallurgy and Metal Recycling/RWTH Aachen University, Intzestrasse 3, Aachen, Germany

[1,]sstopic@ime-aachen.de*

Abstract

Carbonation of magnesium silicate and calcium silicates from olivine and metallurgical slag under high pressure and high temperature was successfully carried out by processing in water in an autoclave from laboratory to scale up conditions. Amorphous silica, magnesite and calcium carbonate, respectively, were the main reaction products in a carbonation of olivine and slag from ferrochromium production under high pressure conditions in an autoclave. Maximal carbonation efficiency was reached for an industrial waste such as a slag from ferrochromium production in an electric arc furnace (EAF), what wass approx. three time higher than a carbonation of olivine under same conditions (T=175°C, P=70 bar). Different experimental parameters were investigated: temperature, time, solid/liquid rate, mixing rate, pressure of carbon dioxide and particle size. In addition, absorption of CO_2 by metallurgical slag and olivine can be a promising technology to reduce gas emissions by storing CO_2 producing valuables products for cement industry.

Keywords: *carbonation, slag, olivine, autoclave,*

Insects as potential plastic waste bio-transformers

Larisa Ilijin

Department of Insect physiology and Biochemistry, Institute for Biological Research "Siniša Stanković", National Institute of the Republic of Serbia, University of Belgrade, Serbia

Abstract

Due to the rapid growth of the human population and increased food consumption, the amount of plastic municipal waste is high and persistent. Polystyrene (PS) and low-density polyethylene (LDPE), deriving from food packaging are the most widely included plastic materials in food processing. PS is a non-biodegradable thermoplastic styrene hydrocarbon polymer, most commonly used in the food industry for protective packaging, and it is a major pollutant of aquatic ecosystems. LDPE is a thermoplastic made from the monomer ethylene widely used as a packaging material and is highly resistant to degradation. It is the main component of plastic carrier bags, greenhouse plastic and kitchen plastic wrap. LDPE microplastic is a significant pollutant of aquatic systems and landfills. The ability of insect species Tenebrio molitor larvae to biodegrade ingested plastics such as PS and LDPE, with the incorporation of waste components into insect biomass without toxic metabolic by-products, has become very attractive. In this metabolic transformation process T. molitor larvae decompose plastic waste to carbon dioxide and water. We have established three self-sustaining laboratory populations of T. molitor reared on wheat bran; wheat bran with added PS, or LDPE in our Department. These populations were recently successfully incorporated the first professional insect breeding initiative in the Republic of Serbia. Insect farming circular systems have multiple benefits, such as waste mitigation and the production of food with higher nutritional value in an environmentally sustainable manner. In our research of the effects of using plastic waste in rearing substrates for these edible insects, different analysis showed no trace of plastic materials in tissues of T. molitor larvae and their frass as well. Also, feeding with plastic did not affect the structure, and composition of chitin (widely applied in medicine, industry, etc.) extracted from their exoskeletons. We did the identification and comparative analysis of the microbiota present in our three self-sustaining laboratory populations of T. molitor larval guts, in the light of microbiological safety and probiotic potential. All our results indicate that T. molitor larvae fed with plastic (PS or LDPE) can be included in the bio-circular economy, and contribute to significant biodegradation of major polluting materials, and to the future development of zero waste insect farming in Serbia.

Analysis of the possibility of applying modern technology for mechanical plastic processing on the Montenegrin coast

Analiza mogućnosti primjene savremene tehnologije za mehaničku obradu plastike na crnogorskom primorju

Jelena Šćepanović[1], Nemanja Radonjić[2]

[1] *University of Montenegro, Faculty of Metallurgy and Technology, Podgorica, Montenegro*

[2] *„Hemosan“ d.o.o. Bar*

Izvod

Plastika spada u grupu najčešće upotrebljivanih vještački proizvedenih materijala. Trend povećanja količine plastike tokom poslednjih decenija, dovodi do potrebe da se njom pravilno upravlja kako bi se izbjegle štetne posledice po životnu sredinu. Ono što ovu vrstu otpada čini problematičnom, jeste činjenica da se većini plastičnih polimera dodaju aditivi kako bi ojačali i postali fleksibilniji. Upravo neki od ovih aditiva produžavaju životni vijek proizvoda, te je tako za razgradnju pojedinih polimera potrebno i do 400 godina.

Obzirom na sveprisutnost ambalaže za hranu i svakodnevnih proizvoda koji imaju široku aplikaciju, plastika je postala nezamjenljiv materijal u mnogim industrijama kao što su građevinarstvo, inženjering, medicina, automobilska kao i vazduhoplovna industrija.

Nažalost, danas je prva asocijacija za riječ plastika zagađenje. Globalno, ogromne količine plastike završe u Svjetske okeane, gdje pod dejstvom atmosferkih prilika dolazi do njihove razgradnje na mirkoplastiku koja je toksična po sve žive organizme. Ovakva činjenica je poražavajuća obzirom da su istraživanja otkrila da se plastika može reciklirati do 7 puta, prije nego što se polimeri degradiraju i izgube svoju vrijednost.

Održivo upravljanje otpadnom plastikom predstavlja jedan od gorućih ekoloških problema u Crnoj Gori. Iako je Zakonom o upravljanju otpadom definisano da se plastika pored ostalih reciklabilnih materijala, odvojeno sakuplja i reciklira, realno stanje nije obećavajuće. Nedovoljno informisana i ekološki osviješćena javnost doprinosi ovakvom stanju, uz neizostavne infrastrukturne i finansijske poteškoće. U pojedinim Primorskim opštinama u kojima se primjenjuju kontejneri za odvojeno prikupljanje reciklabilne suve frakcije (papir, karton, plastika, metal i staklo) zabilježena je neadekvatna selekcija koja dovodi do unakrsne kontaminacije. U radu su predstavljene osnovne vrste i karakteristike plastike, dato je trenutno stanje plastičnog otpada na Crnogorskom primorju, a analizirani su primjeri dobre prakse u zemljama Evropske Unije kada je riječ o upravljanju plastikom. Detaljno je pojašnjen savremeni tehnološki postupak mehaničke reciklaže plastike, gdje kao finalni proizvod nastaje granulat koji se može koristi kao vrijedna sirovina.

Kada je riječ o hijerarhiji upravljanja otpadom, za plastiku, uostalom kao i za ostale kategorije otpada, najpovoljniji scenario je preventivno djelovanje. Uzevši u obzir da je plastika esencijalni materijal koji se sreće na svakom koraku mnogo realnija i prihvatljivija solucija je reciklaža ili ponovna upotreba. U tom smislu mehanička reciklaža plastičnog otpada, kao jedna od mogućih varijanti za tretiranje ove kategorije otpada, predstavlja efikasan sistem, koji omogućava dalju preradu granulata u nove plastične proizvode. Prilikom mehaničkog tretmana plastike poseban akcenat se stavlja na implementaciju mjera koje poboljšavaju efikasnost samog sistema, ovdje se u prvom redu misli na automatizaciju tehnologije sortiranja, ali i primjenu inovativnih tehnologija za prečišćavanje i preradu čime se izbjegava negativan uticaj na životnu sredinu.

Ako je konačni cilj proizvodnja recikliranog granulata, mehanička i hemijska reciklaža su mnogo poželjnije metode obrade plastike u poređenju sa povratom energije putem energetskog iskorišćavanja. Povećanjem kapaciteta reciklaže u razvijenim zemljama, mogu se smanjiti ekološki troškovi koji su procijenjeni na 3,2 milijarde eura godišnje.

Primjenom ove metode reciklaže plastike, dobija se granulat čime se zatvara životni ciklus jednog proizvoda, a u isto vrijeme započinje novi, jer finalni proizvodi reciklaže plastike imaju širok spektar aplikacija. Mogu se koristiti prije svega kao povratni materijal za proizvodnju ambalaže u prehrambenoj industriji, zatim tekstilnoj industriji, industriji transporta, ali i za proizvodnju predmeta široke upotrebe koji zahtijevaju izdržljivost i otpornost na različite vremenske uslove. Na ovaj način se daje doprinos promovisanju cirkularne ekonomije i osnovnih principa održivog dizajna. Osim toga, analizirana je efikasnost paralelne primjene proširene odgovornosti proizvođača i depozitnog sistema vraćanja, dodatno je ponuđen predlog postupka obrade plastičnog otpada na Crnogorskom Primorju, sa najboljom lokacijom za uspostavljanje tehnološke linije u Baru, a na samom kraju je prezentovana mogućnost primjene izdvojenih granulata za proizvodnju potpuno novih ekološki prihvatljivih proizvoda.

Cilj ovih istraživanja je pregled realnog stanja u vezi sa plastičnim otpadom na Crnogorskom primorju, kao i prikaz opisa svjetske prakse kada je riječ o sistemu mehaničkog tretmana plastike, uz mogućnost primjene jedne takve tehnologije u Crnoj Gori, sve sa ciljem promovisanja održivog razvoja, principa cirkularne ekonomije, ali i jačanja privrede otvaranjem novih kompanija koje će se baviti reciklažom plastičnog otpada, što automatski povlači nova radna mjesta i stvara bolje socio-ekonomske uslove za život.

Takođe, cilj istraživanja je i uspješna integracija modela proširene odgovornosti proizvođača (EPR) koji je sastavni dio novog Zakona o upravljanju otpadom. Očekivani benefiti ovakvog modela za životnu sredinu su: smanjenje emisije CO_2, upotreba sekundarnih sirovina u proizvodnji i redukcija upotrebe nereciklabilnih materijala. Istraživanje će takođe biti usmjereno na mogućnost uvođenja Depozitnog sistema naknada (DRS) koji bi u kombinaciji sa EPR doveo do veće motivisanosti građana, a samim tim i efikasnosti sakupljanja plastičnog ambalažnog otpada.

Ključne riječi: *plastični otpad, reciklaža, proširena odgovornost proizvođača, životna sredina, primarna selekcija*

INVITED LECTURES
PREDAVANJA PO POZIVU

Monitoring of electrochemical behaviour of an Au-Ge alloy in an artificial sweat solution

Đenđi Vaštag[1,*], Peter Majerič[2,3], Vojkan Lazić[4], Jovana Marković[4], Rebeka Rudolf [2,3]

[1]*University of Novi Sad, Faculty of Sciences, Novi Sad, Serbia*

[2]*University of Maribor, Faculty of Mechanical Engineering, Slovenia*

[3]*Zlatarna Celje d.o.o., Slovenia*

[4]*School of Dental Medicine, University of Belgrade, Serbia*

**djendji.vastag@dh.uns.ac.rs*

Abstract

Today, people are increasingly exposed for long or short-term contact with different metals or alloys, such as various type of orthopaedic and dental amalgam, implants, or prostheses etc., as well as in the form of various fashion accessories (jewellery, piercings, eyeglass frames, wrist watches, etc.). Contacts between alloys and different types of human electrolytes (sweat, saliva, lymph, blood, etc.) can lead to electrochemical reactions, which on the one hand can change the metals` (alloys) features, and they could also have an impact on human tissue characteristics and properties. Therefore, one of the most important conditions for usage of new materials is their electochemical inertness during the contact with human electrolytes. The aim of this research was to monitor the electrochemical behaviour in artifical sweat solution of a new Au-Ge alloy, as jewellery material. The change of electrochemical behaviour in the function of the exposure time were monitored by using electrochemical methods

Keywords: *Au-Ge alloy; electochemical properties; artifical sweat*

Control of stationary gas emissions in the non-ferrous metals casting process

Snežana Aksentijević[1], Nataša Ćirović[1], Aleksandar Mićić[1], Marija Mihailović[2, *]

[1]*Western Serbia Academy of Applied Studies, Užice Department, Užice, Serbia,*

[2]*Institute of Chemistry, Technology and Metallurgy, Department of Electrochemistry, Belgrade, Serbia*

[*]*marija.mihailovic@ihtm.bg.ac.rs*

Abstract

Copper foundries play a crucial role in industrial manufacturing, producing essential metal for various contemporary applications. However, these foundries are significant sources of gas emissions, contributing to environmental pollution and health risks. This paper investigates the types, sources, and monitoring of gas emissions in Copper Mill Sevojno's foundry, with a focus on sulfur dioxide (SO_2), carbon monoxide (CO), particulate matter (PM), nitrogen oxides (NO_x), volatile organic compounds (VOCs), and metals such as copper, zinc, manganese, tin, lead, nickel, and aluminum. It focuses on the production processes that lead to these emissions and their detrimental effects on air quality, climate change, and human health. Regulatory standards are discussed to underscore the importance of monitoring and controlling emissions. The existing filter plant consists of a coarse filter collector, cyclone batteries, bag filter, and a centrifugal fan. Case study of successful implementation demonstrates the nowadays practical approach. Advanced emission control technologies should be implemented. The paper also looks ahead to future trends in emission control. By addressing these critical issues, the copper foundry industry can move towards a more environmentally responsible and health-conscious operation.

Keywords: *air pollution; waste gas; copper foundry; sustainable foundry practice; environment.*

Levels of As and Pb in soil and *Allium cepa* L. and associated health risk in three Belgrade municipalities

Dragana Pavlović*, Marija Matić, Veljko Perović, Snežana Jarić, Olga Kostić, Miroslava Mitrović, Pavle Pavlović

Department of Ecology, Institute for Biological Research "Siniša Stanković"-National Institute of the Republic of Serbia, University of Belgrade, Bulevar despota Stefana 142, 11000 Belgrade, Serbia

**dragana.pavlovic@ibiss.bg.ac.rs*

Abstract

The health consequences of eating contaminated vegetables for the population are a major problem worldwide. In this study, As and Pb concentrations in soil and in Allium cepa L. (spring onions and onions) from three Belgrade municipalities were determined using an inductively coupled plasma optical emission spectrophotometer (ICP-OES) and possible health risks from onion consumption were assessed. The results showed that As and Pb concentrations in the soil were within the maximum levels proposed by national legislation; the highest concentrations were measured in the soil of Lazarevac. It was found that although A. cepa has a low potential to accumulate As and Pb, this vegetable accumulates As and Pb at levels well above the limits set by the World Health Organisation, so great caution should be exercised when consuming it. The consumption of spring onions could lead to serious health problems over time, especially with regard to the increased As content, although the onions have been shown to be safe for consumption. This study could contribute to a better understanding of the health risks associated with the consumption of vegetables grown near urban and industrial areas.

Keywords: *onion; potentially toxic elements (PTEs); soil; health risk assessment*

Introduction

Environmental pollution by potentially toxic elements (PTEs) and related food safety are a major concern worldwide today [1]. Vegetables are essential for human nutrition and health, especially as a source of vitamins, minerals and fiber, as well as for their biochemical and antioxidant properties [2], which is why it is important to pay attention to their quality. Special attention should be paid to the health control of vegetables grown near industrial facilities, coal mines, thermal power plants and fly ash disposal sites. These anthropogenic activities have been shown to be the main source of pollution by PTEs, which, when released into the soil, are absorbed and accumulated by the edible parts of plants [3]. Unlike some other pollutants, PTEs are non-biodegradable and highly bioaccumulative, can accumulate permanently in tissues and affect various vital parameters of all living organisms [2,4]. It has already been documented that some PTEs such as As and Pb are very toxic to living organisms [3]. Elevated levels of Pb, for example, can lead to problems such as encephalopathy, anemia, vomiting and nausea [5], while long-term exposure to As can cause skin changes, bladder and lung cancer as well as diabetes, lung and cardiovascular diseases [6]. The onion (*Allium cepa* L.) is a globally distributed vegetable, a monocotyledonous plant from the Liliaceae family [4]. It is easy to cultivate and is therefore grown in backyards and other available areas. People all over the world use them as a spice to enhance the taste and smell of food. In addition, onions have medicinal properties such as anti-cancer, antimicrobial, antiviral and antifungal properties [4]. This study argues that anthropogenic activities, such as thermal power plants, can contaminate the food chain and pose significant health risks. Therefore, aims of this study were to (1) determine the presence and content of As and Pb in *Allium cepa* L. (spring onion and onion) and associated garden soils in the vicinity of an open pit mine, thermal power plants and fly ash disposal sites in three

Belgrade municipalities (Lazarevac, Obrenovac and Surčin); (2) assess the efficiency of *A. cepa* to accumulate these elements from the soil as an element transfer factor (TF); (3) assess the risk of As and Pb from onion consumption to human health by calculating the estimated daily intake (EDI), target hazard quotient (THQ) and health risk index (HRI).

Materials and methods

Sample collection and preparation

Sampling was carried out in three municipalities of the City of Belgrade – Surčin (village Jakovo, 20°15'45"E, 44°44'35"N, average altitude 75 m), Lazarevac (village Sokolovo, 20°19'7"E, 44°28'32"N, average altitude 93 m) and in the municipality of Obrenovac (village Krtinska, 44°30'N, 19°58'E, average altitude 80 m). Sampling of *Allium cepa* L. and the associated soil was carried out in spring (spring onion) and autumn (onion) in five randomly selected gardens near the fly ash disposal site of the thermal power plant "Nikola Tesla-A". A paired soil and onion sample was taken from each garden (soil samples from the surface layer at 0-20 cm, onion samples from individual plants, 50 g), Figure 1. The soil and onion samples were kept in a paper envelope and then placed in a polyethylene bag before transportation to the laboratory. In the laboratory, the onion samples were washed with distilled water, cut into smaller pieces and dried at 65°C (Binder, Tuttlingen, Germany) to constant weight. The dried samples were homogenized using a pestle and mortar and then sieved through a 2 mm stainless steel sieve to obtain a fine particle size. The soil samples were dried at 105°C to constant weight, homogenized and sieved through a 0.2 mm stainless steel sieve.

Figure 1. *Sampling of spring onions and onions in the garden near the thermal power plant*

For elemental analysis, 0.3 g of onions were digested in a microwave (CEM, 39 MDS-2000) with a mixture of 9 ml 65% HNO_3 and 3 ml 30% H_2O_2. The 0.3 g of soil was digested with a mixture of 9 ml 36% HCl and 3 ml 65% HNO_3. The final extracts were filtered into 50 mL polyethylene volumetric flasks and then diluted to the mark with deionized water. All samples were analyzed in five replicates, and the results were expressed as mean values with standard deviation (SD). The concentrations of As and Pb in the samples were measured by inductively coupled plasma optical emission spectrometry (ICP-OES) (Spectro Genesis Fee, Spectro-Analytical Instruments GmbH, Kleve, Germany). Quality control was performed with standard reference material (Beach leaves - BCR-100, IRMM, certified by EC-JRC). The recovery values found were within 95-110 % of the certified values for all elements measured. The element concentrations were given in milligrams per kilogram dry weight (mg kg^{-1} d.w.). The detection limits (mg kg^{-1}) for the elements were as follows: As - 0.007 and Pb - 0.002.

Element transfer factor

The soil-to-plant element transfer factor (TF) was calculated as the ratio between the element concentration in the edible parts of the onion and the element concentration in the soil. It helps to assess the potential ability of plants to transfer PTEs from the soil to their edible parts [3]. It was calculated using the following equation:

$$TF = \frac{C_{vegetable}}{C_{soil}} \quad (1)$$

where $C_{vegetable}$ is the element content in the edible part of the plant (mg kg^{-1}) and C_{soil} is the element content in the respective soil (mg kg^{-1}). A transfer factor of more than 1 means that the plant is a potential accumulator of PTEs [3].

Health risk assessment

The potential health risk from vegetable consumption is described by the Target Hazard Quotient - THQ [3,7]. The THQ is a ratio between the calculated estimated daily intake (EDI, mg kg^{-1} day^{-1}) and the reference dose (RfD, mg kg^{-1} day^{-1}). It has been found that there is a chance that non-carcinogenic effects will occur if the THQ is ≥ 1, while it is unlikely that the exposed individual will experience obvious adverse health effects if the THQ is < 1 [3,7]. The EDI and THQ indices for vegetable consumption were calculated as follows:

$$EDI = \frac{C \times IR \times EF \times ED}{BW \times AT} \times 10^{-3} \quad (2)$$

$$THQ = \frac{EDI}{RfD} \quad (3)$$

Where C is the concentration of PTEs in the vegetable samples (mg kg^{-1}), IR is the ingestion rate of the vegetables (30.68 g $person^{-1}$ day^{-1}, [8]), EF is the exposure frequency rate of the vegetables (365 days $year^{-1}$), ED is the exposure duration rate of the vegetables (70 years), BW is the average body weight o fan adult (70 kg) and AT is the average time for non-carcinogenic risks (25550 days) and RfD (reference dose) is the maximum tolerable daily intake of a given PTE (g^{-1} $person^{-1}$ day^{-1}). The RfD values of As and Pb are 0.0003 and 0.0035 [9].

The combined non-carcinogenic risks of more than one PTE were assessed with a hazard risk index (HRI). The HRI is the sum of the THQs of the individual PTE studied [3] and is expressed as follows:

$$HRI = \sum THQ \quad (4)$$

Statistical analysis

The data of this study was analysed by statistical analysis (ANOVA), and the means were separated with a Bonferroni test at a significance level of $p<0.05$ using the Statistica software package (StatSoft In., Tulsa, USA, 2007).

Results and discussion

Concentration As and Pb in soil and Allium cepa L. samples

The results presented in this study show that the concentration of the analyzed elements in the onion soils in both sampling seasons (spring and autumn) was the highest in Lazarevac and differed significantly from their concentration in Obrenovac and Surčin ($p<0.001$, Table 1). The higher As and Pb concentration in Lazarevac compared to the other two sites could be related to the proximity

of the thermal power plant, i.e. the dispersion of ash particles from the ash disposal sites onto agricultural fields, with this ash characterized by elevated levels of various PTEs [10]. However, these concentrations are within the maximum allowable concentrations specified in national legislation [11]. A slight increase in the As content and a decrease in the Pb content during the season were also observed (Table 1).

In contrast to soil, where the Pb concentration was higher compared to the As concentration, this was not the case with spring onions and onions. The As concentration in spring onions was in a wide range of values, e.g. in Surčin below the detection limit, while in Lazarevac and Obrenovac concentrations of 2.28 mg kg^{-1} and 2.44 mg kg^{-1} were measured (Table 1). These concentrations were well above the permissible limit of the WHO/RML standards (0.1 mg kg^{-1}, [2,12]). Lead was only measured in spring onions from Lazarevac (Table 1), where its concentration was above the permissible limit of the WHO/RML standards (0.3 mg kg^{-1}, [2,12]), as for As. In the onions, the As concentration was lower than in the spring onions, and there were no significant differences between the sites (Table 1). Although the As content was lower, it was still well above the permissible limit of the WHO/RML standards (0.1 mg kg^{-1}, [2,12]). In contrast to spring onions, Pb was present in onions from all sites. The content ranged from 0.2 mg kg^{-1} to 0.36 mg kg^{-1}, which corresponds to the permissible levels in Surčin and Obrenovac, while in Lazarevac it was still above the permissible limit of WHO/RML standards (0.3 mg kg^{-1}, [2,12]). Similar to this study, Pb concentrations in onions grown in several Iranian provinces were above the permissible limits of WHO/RML standards [4]. Sackej et al. (2024) also found that the average As and Pb concentrations in onions were above the recommended maximum levels of the WHO/RML standards and that spring onions accumulated more As than onions. They suspected that the increased As content could be due to exhaust fumes from passing vehicles coming into contact with the vegetables grown there, and also to the irrigation water used in cultivation. The constant consumption of vegetables growing in the contaminated areas can be dangerous because it is known that As can cause cardiovascular diseases, peripheral vascular disorders, anemia and reproductive system disorders [7], while Pb has multiple effects on human health and its toxicity disrupts the functions of the digestive, nervous, respiratory and reproductive systems [2].

Table 1. Mean concentration and transfer factor (TF) of As and Pb in soil, spring onion and onion samples

	Soil		**Spring onion**		**TF**	
Locality	**As mg kg^{-1}**	**Pb mg kg^{-1}**	**As mg kg^{-1}**	**Pb mg kg^{-1}**	**As**	**Pb**
Surčin (village Jakovo)	**< DL**^{c}	45.66^{a} ± 9.39	**< DL**^{b}	**< DL**^{b}	-	-
Lazarevac (village Sokolovo)	19.79^{a} ± 1.19	70.3^{b} ± 2.32	2.28^{a} ± 0,53	0.83^{a} ± 0.44	0.12	0.01
Obrenovac (village Krtinka)	4.32^{b} ± 0.56	53.76^{a} ± 1.31	2.44^{a} ± 0.56	**< DL**^{b}	0.56	-
	Soil		**Onion**		**TF**	
Locality	**As mg kg^{-1}**	**Pb mg kg^{-1}**	**As mg kg^{-1}**	**Pb mg kg^{-1}**	**As**	**Pb**
Surčin (village Jakovo)	5.55^{a} ± 0.78	43.83^{a} ± 5.93	0.50^{a} ± 0.19	0.2^{a} ± 0.03	0.09	0.00
Lazarevac (village Sokolovo)	19.83^{b} ± 1.04	63.50^{b} ± 0,84	0.51^{a} ± 0.15	0.36^{b} ± 0.15	0.03	0.01
Obrenovac (village Krtinka)	5.43^{a} ± 1.10	50.83^{a} ± 8.08	0.58^{a} ± 0.16	0.29^{a} ± 0.10	0.11	0.01

(One-way ANOVA - Bonferroni); data represents Mean values with standard deviation (SD) of five replicates (n=5); Means followed by the same letter in column do not differ significantly between sites (P<0.001).

Evaluation of the ability of Allium cepa L. to accumulate As and Pb

The transfer and deposition of PTEs from soil to edible plant parts is the main route by which PTEs enter the food chain [1]. The rate of transfer and accumulation of PTEs in plants depends on various edaphic (soil pH, soil temperature, soil texture, organic matter, cation exchange capacity, etc.) and plant-related factors (physiology, morphology and anatomy of the plant) [3,13,14]. The result of this study shows that spring onions accumulate As to a greater extent than onions, which is not the case for Pb (Table 1). However, the TF values determined for this study were all well below 1, indicating that these vegetables have a low potential to accumulate As and Pb. However, this study has shown that onions absorb As and Pb at levels well above the permissible limits of the WHO/RML standards, so great caution should be exercised when consuming them.

Health risk assessment

The consumption of vegetables is one of the main routes through which PTEs enter the food chain and affect human health, so it is very important to control their concentration to ensure the safety of individual health [4,7]. *A. cepa* (onion) is a common vegetable used worldwide as a spice to improve the taste and smell of food [4]. In this study, the potential health risk from the consumption of spring onions and onions grown in gardens near the thermal power plant and ash disposal sites was assessed by calculating EDI, THQ and HRI (Table 2). The EDI values for As and Pb were below the maximum tolerable daily intake (As-0.13 mg day^{-1}; Pb-0.21 mg day^{-1}, [15]). The THQs for As in samples of spring onions from Lazarevac and Obrenovac were >1, indicating significant health risks. However, the THQs for As in onions and for Pb in spring onions and onions at all sites were <1, indicating no health risk. It was further determined that HRI > 1 for young onions from Lazarevac and Obrenovac, while the HRIs for onions were <1. These results show that only the consumption of spring onions has adverse health effects.

Table 2. Estimated daily intake (EDI), target hazard quotient (THQ) and hazard risk index (HRI) for As and Pb in spring onions and onions in study sites

	Spring onion		**Onion**		**Spring onion**			**Onion**		
	EDI				**THQ**		**HRI**	**THQ**		**HRI**
Locality	**As**	**Pb**	**As**	**Pb**	**As**	**Pb**		**As**	**Pb**	
Surčin (village Jakovo)	< DL	< DL	2.19E-04	8.77E-05	< DL	< DL	< DL	7.30E-01	2.50E-02	7.56E-01
Lazarevac (village Sokolovo)	9.99E-04	3.64E-04	2.24E-04	1.58E-04	**3.33**	1.04E-01	**3.43**	7.45E-01	4.51E-02	7.90E-01
Obrenovac (village Krtinka)	1.07E-03	< DL	2.54E-04	1.27E-04	**3.56**	< DL	**3.56**	8.47E-01	3.63E-02	8.84E-01

* The values in bold indicate significant health risks

Conclusion

The results of the present study show that As and Pb concentrations in soil do not exceed the MAC set by national legislation, with the highest concentrations measured in Lazarevac soil.

A. cepa L. was found to have a low potential to accumulate As and Pb. However, this vegetable accumulates As and Pb in amounts far above the permissible limits of the WHO/RML standards and were significantly higher in the spring onions samples than in the onion samples. From the EDI, THQ and HRI values determined, it can be concluded that the consumption of spring onions could lead to serious health problems over time, especially with regard to the increased As content, although the onions have proven to be safe for consumption.

This study could contribute to a better understanding of the health risks associated with the consumption of vegetables grown near urban and industrial areas.

Acknowledgements

This work was supported by the Ministry of Science, Technological Development and Innovation of the Republic of Serbia, grant no. 451-03-66/2024-03/200007.

References

1. H. R. Gebeyehu, L. D. Bayissa, Levels of heavy metals in soil and vegetables and associated health risks in Mojo area, Ethiopia, *PLoS One*, **15(1)**, e0227883, 2020.
2. L. N. A. Sackey, K. Markin, A. Kwarteng, I. M. Ayitey, P. Kayoung, Presence and levels of potential trace elements in lettuce and spring onion grown in Kumasi, Ghana, *Kuwait J. Sci*., **51(1)**, 100143, 2024.
3. N. Gupta, K. K. Yadav, V. Kumar, S. Krishnan, S. Kumar, Z. D. Nejad, M. A. M. Khan, J. Alam, Evaluating heavy metals contamination in soil and vegetables in the region of North India: Levels, transfer and potential human health risk analysis, *Environ. Toxicol. Phar*., **82**, 103563, 2021.
4. S. Shokri, N. Abdoli, P. Sadighara, A. H. Mahvi, A. Esrafili, M. Gholami, B. Jannat, M. Yousefi, Risk assessment of heavy metals consumption through onion on human health in Iran. *Food Chem. X*., **10(14)**, 100283, 2022.
5. A. Atamaleki, A. Yazdanbakhsh, Y. Fakhri, F. Mahdipour, S. Khodakarim, A. M. Khaneghah, The concentration of potentially toxic elements (PTEs) in the onion and tomato irrigated by wastewater: A systematic review; meta-analysis and health risk assessment, *Food Res. Int*., **125**, 108518, 2019.
6. World Health Organization. (2022, December 7). Arsenic. [Online]. Available: https://www.who.int/news-room/fact-sheets/detail/arsenic
7. N. W. Hu, H. W. Yu, B. L. Deng, B. Hu, G. P. Zhu, X. T. Yang, T. Y. Wang, Y. Zeng, Q. Y. Wang, Levels of heavy metal in soil and vegetable and associated health risk in peri-urban areas across China, *Ecotox. Environ. Safe*., **259**, 115037, 2023.
8. Heigi Library. (2017). Onion Consumption Per Capita in India. [Online]. Available: https: //www.helgilibrary.com/indicators/onion-consumption-per-capita/india/
9. United States Environmental Protection Agency. (2015). Regional Screening Level (RSL) Summary Table. [Online]. Available:
10. https://epa-prgs.ornl.gov/chemicals/download/composite_sl_table_run_NOV2015.pdf
11. R. J. Haynes, Reclamation and revegetation of fly ash disposal sites - Challenges and research needs, *J. Environ. Manage*., **90 (1)**, 43-53, 2009.
12. OGRS. (1994). Regulation about allowable quantities of hazardous and harmful substances in the soil and methods for their investigation. Official Gazette of the Republic of Serbia (Sluzbeni glasnik RS) 23 (in Serbian).
13. Food and Agriculture Organization & World Health Organization. (2016). General standard or contaminants and toxins in food and feed (CODEX STAN 193-1995).
14. M. Pavlović, T. Rakić, D. Pavlović, O. Kostić, S. Jarić, Z. Mataruga, P. Pavlović, M. Mitrović, Seasonal variations of trace element contents in leaves and bark of horse chestnut (*Aesculus hippocastanum* L.) in urban and industrial regions in Serbia, *Arch. Biol. Sci*., **69(2)**, 201-214, 2017.
15. D. Pavlović, M. Pavlović, M. Marković, B. Karadžić, O. Kostić, S. Jarić, M. Mitrović, I. Gržetić, P. Pavlović, Possibilities of assessing trace metal pollution using *Betula pendula* Roth. leaf and bark-experience in Serbia, *J. Serb. Chem. Soc*., **82(6)**, 723-737, 2017.
16. N. Shaheen, N. M. Irfan, I. N. Khan, S. Islam, M. S. Islam, M. K. Ahmed, Presence of heavy metals in fruits and vegetables: health risk implications in Bangladesh. *Chemosphere*, **152**, 431-438, 2016.

Drilling and equipping of new wells due to contamination of the near-well zone by various chemical and mechanical processes on existing wells

Željko Krivačević, Dejan Grgić, Saša Stojanović, Aleksandar Pešić

„Transnafta „ corp., Pančevo, Serbia

Abstract

For the purpose of supplying fuel storage terminal with service water as part of the fire protection system, and due to the long-term pollution of the wellbore zone by various chemical and mechanical processes, new wells were drilled and equipped as the safest method of providing the required amount of water in the continuous process of use.

Fire protection sytem on terminal oil derivatives supply needs a technical water inside fire prtection system and during along used a period of time process destroyed primary and secondary well zones an a different of way chemical and mechanical process, and solved a problem construction new wells and construction all new equipment as the most of security method provide techical water required in continuous use for fire protection systems.

Enhanced Pt@Ni catalysts obtained by galvanic displacement method for successful methanol electrooxidation

Dragana L. Milošević[1,*], Sanja I. Stevanović[2], Dušan V. Tripković[2]

[1] *University of Belgrade - Institute of Chemistry, Technology and Metallurgy - Department of Ecology and Techoeconomic, Njegoševa 12, 11000 Belgrade, Republic of Serbia*

[2] *University of Belgrade - Institute of Chemistry, Technology and Metallurgy - Department of Electrochemistry, Njegoševa 12, 11000 Belgrade, Republic of Serbia*

[*] *dragana.milosevic@ihtm.bg.ac.rs*

Abstract

The successful development of catalysts for the electrooxidation of small organic molecules, such as methanol, requires finding an optimal balance between the catalyst's cost and its activity/stability. Thus far, platinum (Pt) remains one of the best choice for methanol electrooxidation, despite its high costs, limited supply and tendency to poison with carbon monoxide (CO).

In this work, the synergistic effect of the supporting material and annealing temperature in different atmospheres on the performance of the Pt@Ni catalyst was examined. The thin film Pt@Ni catalyst was obtained through spontaneous galvanic displacement by placing a drop of hexachloroplatinic acid onto the Ni support. To mitigate platinum susceptibility to poisoning species such as CO and enhance the catalytic efficiency of Pt@Ni at low potentials in methanol oxidation, the as-prepared catalyst was modified using controlled thermal treatment in a reductive atmosphere containing 5 % H_2 and in an inert atmosphere (N_2). The activity of the catalysts was tested in the methanol oxidation reaction, while the influence of thermal treatment on the surface morphology was monitored using atomic force microscopy (AFM).

Preliminary results have indicated that the galvanic displacement method produces ultra-thin film Pt@Ni catalysts, which were further enhanced through controlled thermal treatment. The catalysts annealed in the inert atmosphere demonstrated superior activity compared to the as prepared and catalyst annealed in the reducing atmosphere.

Keywords: *galvanic displacement; nickel support; thermal treatment; methanol oxidation*

Acknowledgements

This work was financially supported by the Ministry of Science, Technological Development and Innovation of Republic of Serbia (contract no. 451-03-66/2024-03/200026) and the Science Fund of the Republic of Serbia under grant no. 7739802.

POSTER PRESENTATIONS
POSTERSKA SAOPŠTENJA

Efficiency of methylene blue removal and hydrogen production using Au modified TiO_2 under simulated solar and UV radiation

Teodora Vidović[1], Dina Tenji[2], Tamara Ivetić[3], Ivana Jagodić[1], Jovana Cvetić[1], Nemanja Banić[1,*]

[1]*University of Novi Sad, Faculty of Sciences, Department of Chemistry, Biochemistry and Environmental Protection, Trg D. Obradovića 3, 21000 Novi Sad, Serbia,*

[2]*University of Novi Sad, Faculty of Sciences, Department of Biology and Ecology, Laboratory for Ecophysiology and Ecotoxicology - LECOTOX, Trg D. Obradovića 2, 21000 Novi Sad, Serbia*

[3]*University of Novi Sad, Faculty of Sciences, Department of Physics, Trg D. Obradovića 4, 21000 Novi Sad, Serbia*

**nemanja.banic@dh.uns.ac.rs*

Abstract

The increasing focus on energy and environmental concerns has led to significant interest in the advancement of clean and renewable energy sources. The use of photochemical water splitting for hydrogen production has been recognized as a potential replacement for fossil fuels due to the clean, renewable, and eco-friendly nature of solar energy. In addition, the expansion of industry, which involves excessive production, use, and release of chemicals, unavoidably leads to water contamination. As an illustration, organic dyes are in high consumption in several industrial sectors, including textiles, food products, cosmetics, and pharmaceuticals. It is noteworthy that approximately 10-15% of the dyes used in the coloring process eventually find their way into wastewater and finally into aquatic ecosystems. Dyes detected in wastewater have been found to disrupt numerous physiological processes in aquatic organisms, representing a commonly identified environmental issue. Semiconductor-based photocatalytic technologies have promising advantages in terms of cost-effectiveness, efficiency, and environmental sustainability for renewable hydrogen production and water purification. Four Au/TiO_2 materials with different mass ratios of Au to TiO_2 (0.5, 1.0, 2.5, and 5.0%) were synthesized by the photochemical deposition method. Also, the photocatalytic efficiency of these nanopowders for hydrogen production and methylene blue removal under simulated solar (SSR) and UV radiation was investigated. The cytotoxicity of the samples was tested on two mammalian cell lines by MTT assay after 24 h of exposure. Compared with unmodified TiO_2 (8.5 μmol/hg H_2), under SSR, synthesized nanopowders: 0.5%Au/TiO_2 (9.8 μmol/hg H_2), 2.5%Au/TiO_2 (8.9 μmol/hg H_2), and 5.0%Au/TiO_2 (12.9 μmol/hg H_2) show a higher rate in terms of hydrogen generation in a time interval of 300 min. The hydrogen production rate was found to be 1.5 times higher when 5 wt% Au was present in the TiO_2 photocatalyst, compared to unmodified TiO_2. The kinetics of methylene blue removal using the aforementioned photocatalysts were monitored photometrically. Under simulated solar radiation, the 1.0%Au/TiO_2 catalyst proved to be the most efficient, with a photodegradation efficiency of 54.5% after 30 min. In the presence of UV radiation, 0.5%Au/TiO_2 showed the highest photodegradation efficiency, while 79.5% of methylene blue was degraded after 15 min. The dark adsorption efficiency was the highest using 1.0%Au/TiO_2. All the samples obtained from the removal process of methylene blue exhibited lower cytotoxicity compared to the original compound.

Acknowledgements

This study was supported by the Ministry of Science, Technological Development and Innovation of the Republic of Serbia (Grants No. 451-03-66/2024-03/200125 & 451-03-65/2024-03/200125). The authors are especially grateful to the Srbijagas company, which enabled the realization of this research possible by donating a gas chromatograph.

Removal of methylene blue from water using ZnO immobilized on glass spheres in an annular fixed bed photoreactor

Nemanja Banić[1,*], Ivana Jagodić[1], Dina Tenji[2], Teodora Vidović[1]

[1]*University of Novi Sad, Faculty of Sciences, Department of Chemistry, Biochemistry and Environmental Protection, Trg D. Obradovića 3, 21000 Novi Sad, Serbia,*

[2]*University of Novi Sad, Faculty of Sciences, Department of Biology and Ecology, Laboratory for Ecophysiology and Ecotoxicology - LECOTOX, Trg D. Obradovića 2, 21000 Novi Sad, Serbia*

**nemanja.banic@dh.uns.ac.rs*

Abstract

A large number of industries dye their products and consume large amounts of water in these processes. As a result, there is a significant amount of wastewater. Hence, it is imperative to provide suitable treatment for such effluents. Methylene blue (MB), a common cationic dye, frequently occurs in hazardous effluents. Its complex structure renders it resistant to degradation, resulting in persistent pollution. This has prompted the scientific community to effectively develop elimination technologies, known as advanced oxidation processes. Most studies have been carried out using suspended photocatalyst semiconductors. However, post-treatment recovery of photocatalysts is an arduous process due to the size of the catalyst particles in the order of nanometers and the cost involved. Therefore, filtration and resuspension of photocatalyst powder should be avoided, if possible, in a wastewater treatment process. In order to overcome the mentioned problem, the possibility of using an annular fixed bed photoreactor operated in batch-recirculating mode using a newly produced semiconductor/silicone/glass sphere system was studied to carry out MB removal under the influence of UV and simulated solar radiation (SSR). The MB removal kinetics were monitored by UV/Vis spectrophotometry. The MB removal efficiency of glass beads coated with ZnO compared with those coated with TiO_2. The highest removal efficiency was determined for the UV/ZnO/silicone/glass spheres system, where after 180 min, 96.5% of MB was removed. The removal efficiency of methylene blue was examined for the most efficient ZnO/silicone/glass spheres system to highlight the superior performance of the 29 glass spheres used. Air introduction at flow rates up to 5.3 L/min through the column with the coated glass spheres did not affect removal efficiency. Also, for the most efficient ZnO/silicone/glass sphere system, the possibility of reuse was examined five times in a row. The increase in UV radiation intensity from 61.9 to 165 W/m^2 increased MB removal efficiency by 1.57 times.

Acknowledgements

This study is supported by the Ministry of Science, Technological Development and Innovation of the Republic of Serbia (Grants No. 451-03-66/2024-03/200125 & 451-03-65/2024-03/200125).

Development of alternative jet fuels from the aspect of reducing co_2 emissions (fuels for the future) part 2

Božidarka Arsenović

"ORAO" AD for production and repair of Bijeljina; Republic of Serbia; Bosnia and Herzegovina

bokijevmejl@gmail.com

Abstract

Aviation has always been, and remains, a training ground for the demonstration of national, economic, scientific, technological and military prestige in the world. It is reliably known that aviation has a multiple impact on the environment: by polluting the atmosphere, creating noise, disrupting the habitats and flight paths of birds, as well as changing the natural environment due to the construction of infrastructure. The issue of the harmful effects of exhaust gases resulting from the combustion of propellant in aircraft engines, as well as its impact on the atmosphere, is currently being dealt with more thoroughly by certain international aviation organizations, which, among other things, also deal with environmental protection. In the last decades of the twentieth century, the development and use of sustainable alternative jet fuels emerged as a key factor in reducing aviation-related CO_2 emissions. "Refuel Aviation" is an initiative that promotes the use of sustainable fuels, the so-called of SAFs (sustainable aviation fuels) for the decarbonization of air traffic, and represents the obligation of suppliers to increasingly sell sustainable fuels at all airports within the EU. Compared to the CO_2 emission produced during the flight of an airplane with conventional hydrocarbon fuel (kerosene), the use of alternative jet fuels can reduce this emission by up to 80%, depending on the type of raw material used and the method of sustainable fuel production.

The paper gives a brief overview of some of the goals and obligations of the use of alternative jet fuels from the aspect of potential use criteria, as well as progress and further predictions in aviation.

Keywords: *Alternative JET Fuels; impact; development*

Introduction

A little more than a hundred years have passed since the first flight of man by plane. From that time to the present day, aviation has made enormous progress in all spheres of modernization, so aviation can rightly be considered an integral and modern part of society.

Nowadays, the impact of human activity in the technological sphere on environmental warming is considered the most obvious in the case of global warming. The greenhouse effect is a consequence of the accumulation of greenhouse gases in the upper layers of the atmosphere and disruption of the energy balance of received and transferred heat, resulting in an increase in the temperature of the lower layers of the atmosphere and warming of the Earth's surface [1].

According to its chemical composition, conventional hydrocarbon jet fuel, JET A1 is a complex mixture consisting of four basic groups of hydrocarbons: paraffins, naphthenes, aromatics and olefins [1,2]. Their content in the fuel ranges from 98% to 99%, while the rest from 1% to 2% are non-hydrocarbon compounds: sulfur, nitrogen, oxygen and traces of various metals or compounds containing metals. This composition of jet fuels is conditioned by strict requirements for the highest possible thermal power and stability, and the lowest possible formation of soot, which is exactly what paraffin and naphthenic hydrocarbons provide. Gases and particles produced by the combustion of aircraft fuel are: water vapor, H_2O, carbon dioxide, CO_2, nitrogen monoxide, NO, nitrogen dioxide, NO_2 (NO and NO_2 are collectively referred to as NOx), sulfur oxides, SOx and soot [3, 4]. These elements of the fuel combustion process are mostly retained in the part of the troposphere characterized by high humidity and slightly higher temperature, in whose lower layers, the atmosphere is heated, and the warming decreases with height.

According to statistical data on air operations, transported passengers, cargo and mail at airports in Bosnia and Herzegovina (Q1 2019 to 2023), it was confirmed that there was a significant increase in certain indicators in air traffic in Q1 2023 compared to Q1 2022 year (the consequences of Covid 19 are obvious for the year 2021) [5]. In the first quarter of 2023, the number of airport operations shows an increase of 23.1% compared to the same quarter of the previous year, as well as that the number of transported passengers is higher by 68.2% compared to the same quarter of the previous year, Figure 1. The data were processed in accordance with statistical program and standards of the *International Civil Aviation Organization (ICAO)*[1].

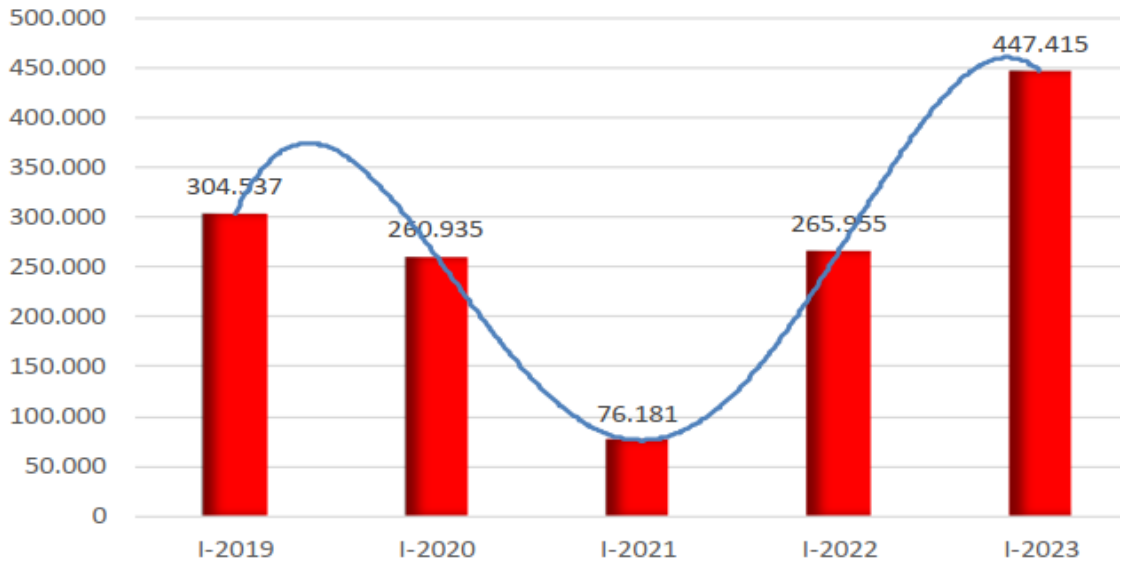

Figure 1. *Graphic representation of the number of transported passengers in air transport for the first quarter from 2019 to 2023 in Bosnia and Herzegovina*

Alternative fuels in air traffic were developed (and are being developed) as a response to the growing emission of harmful substances, which is a consequence of the increasing growth of this type of traffic and the reduction of dependence on fossil fuels.

Legal regulations in the field of emissions of harmful substances

It is known that about 2% of global human-caused CO_2 emissions are caused by air traffic, and of that, 65% of that emission refers to international air traffic.
The level of emissions of harmful substances in air transport was first regulated by an international agreement adopted in 1972 in *Stockholm*, issued by *ICAO (International Civil Aviation Organization)* and later expanded by various additions. This is Annex 16 called "*Environmental Protection*" where emissions of harmful substances are prescribed in *"Volume II"*, while the regulation of noise issues is shown in *"Volume I"*. Later, the agreements were extended to the global level. A significant step in reducing emissions of harmful substances was made in 2005. in *Kyoto*, under the name *Kyoto Protocol*. The protocol required industrial countries listed in *Annex 1* to reduce greenhouse gas emissions. In 2007, an *ICAO* meeting was held at which both developed and developing countries were required to change their policy on reducing emissions of harmful substances and to find stable solutions to the growing problem of emissions and to submit solutions as soon as possible to the UNFCCC *(United Nations Framework Convention on Climate Change).*

[1] All data on the number of passengers, cargo and mail refer to international air traffic, because there is no domestic air traffic in Bosnia and Herzegovina (Statistical Agency of Bosnia and Herzegovina, 2023)

In 2016, the *Paris Agreement* on climate change was reached, the main elements of which are: reduction of emission levels[2]; *transparency of measurement and emission levels; adaptation of countries according to the Paris Agreement; increased cooperation between various sectors related to climate change; greater interest of cities, regions and authorities and giving incentives to developed countries.*
CEAP *(Committee on Aviation Protection)* is in charge of regulating emissions of harmful substances and noise in air transport.
At the CEAP meeting, in *Montreal in February 2016*, under the name *CEAP/10*, new measures were adopted to regulate the emission of harmful substances, noise, operations at airports, insight into the global fossil fuel market and, finally, an incentive for the use of alternative fuels, so that be in global application by 2050. CEAP consists of 24 members and 15 observers. Over 600 experts from different countries participate in its program.
According to the *EAER (European Aviation Environmental Report)* earlier instructions, processes and limitations certified by ICAO, only apply to engines with a thrust greater than 26.7 kN. The LTO *(Loading and Take Off)* process is used to measure the amount of gaseous emissions, Table 1.

Table 1. Display of LTO (Loading and Take Off)

Flight mode	**Thrust, %**	**Time, min**
Takeoff	100	0.7
Climbing	85	2.2
Approach	30	4.9
Transportation	7	26.0

In order to achieve the highest possible speed during the flight process, it is necessary to increase the use of fuel, which requires higher pressure and temperature, which automatically causes higher emissions of harmful gases (NO_X are the most harmful). ICAO takes over the database on harmful emissions from engines from EASA *(European Aviation Security Agency).*
An important step in the control of emissions of harmful substances is the *Clean Sky program,* which, with the help of the latest technology, intends to reduce the negative emissions of air traffic (noise and emissions of harmful gases). The goal of the Clean Sky program is to enable the progress and competence of the European fleet on a global level through its implementation, and it is *financed by Horizon 2020*, and currently has over 5 billion euros for the implementation of the *Clean Sky 2* project. The *Clean Sky* project was launched in 2008 and *Clean Sky 1* was successfully completed. Since 2017, the *Clean Sky 2* project (successor to the 1st project) has been in the implementation phase.
The technological achievements developed during the *Clean Sky 1* project are:
1) smartly fixed aircraft wing;
2) sustainable and "green" engines;
3) "green" regional aircraft;
4) "green" rotorcraft;
5) systems for "green" operation of aircraft operations;
6) ecological design of the aforementioned achievements of *Clean Sky 1* i
7) technological evaluation program.
EU ETS *(Emissions Trading System)* is the largest European organization whose goal is to reduce the emission of harmful substances in air traffic for the prevention of climate change, and it consists of

[2] https://www.nyc.gov/html/dot/downloads/pdf/alternativefuel.pdf, accessed 21.07. in 2023

31 countries. This organization aims to reduce emissions of harmful substances emitted by air carriers with minimal costs, which is a very important factor when using *"green" technologies.*

Greenhouse gas reduction goals

In order to reduce greenhouse gas emissions, in 2007 IATA (International Aviation Transport Association) updated its strategy, the main goal of which is for airplanes to have 0% greenhouse gas emissions by 2050. That strategy consists of four phases:
1) technology improvement and high commitment to low-carbon fuels,
2) improvement of aircraft operations,
3) better infrastructure in airports,
4) economic measures, in order to reach the global market and cover other emissions.
In 2009, IATA set some more goals:
- the limit for the level of CO_2 emissions after 2020,
- improvement of fuel efficiency by 1.5% per year (from 2009 to 2020),
- reduction of CO_2 emissions by 50% by 2050.

In order to achieve the stated goals, in 2016, ICAO launched the CORSIA *(Carbon Offset and Reduction Scheme for International Aviation)* initiative, which is a "scheme" for reducing greenhouse gases at the global level. From 2021 to 2026, voluntary implementation of CORSIA requirements has been approved, and after 2026, these requirements become mandatory. Already 65 countries have accepted the CORSIA requirements, which will affect the reduction of about 80% of CO_2 from 2021 to 2035.
The plan for reducing CO_2 emissions from 2010 to 2040 is shown in Figure 2.

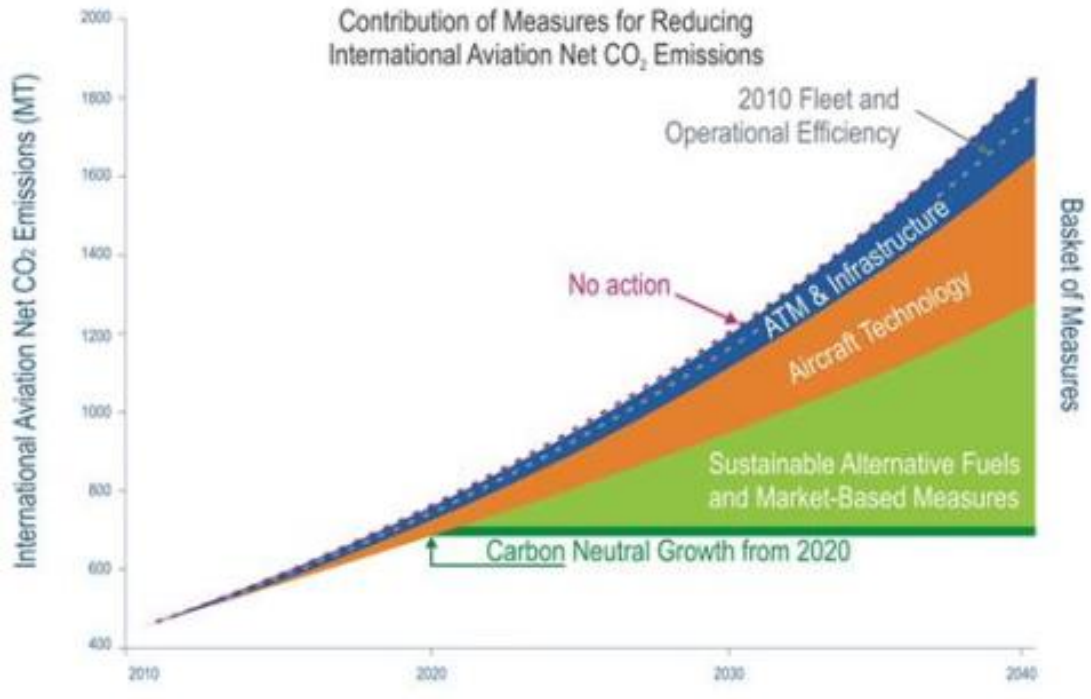

Figure 2. *Graphic representation of the plan to reduce CO_2 emissions until 2040 in air traffic*

Although improvements in aircraft design and in-flight operations can significantly reduce CO_2 emissions, the problem remains the extremely high growth of air traffic globally. As can be seen from Figure 2, a reduction in carbon emissions is expected from 2020, and in order to achieve this, the only close solution so far is *"drop-in" fuel.*

Alternative fuels

Sustainable aviation fuel, SAF

Sustainable Aviation Fuel (Sustainable Aviation SAF) is the main name used by the aviation industry to represent non-conventional aviation fuel.

IATA has accepted this definition, but also accepts other definitions used for these types of fuels such as: alternative fuels, sustainable alternative jet fuels, renewable jet fuels, considering that fuels can also be produced from other non-biological and chemical sources. . A term that is also used is biofuel, but it refers to fuels that are produced from biological resources, most often plant materials. According to the definition accepted by ICAO, an alternative fuel is: "any fuel that has the potential to generate lower carbon emissions than conventional kerosene on a life cycle basis". Also, ICAO uses the definition that alternative fuel is any fuel that is not petroleum-based, which includes liquid fuel from coal, and fuel produced from natural gas, but their production itself emits the same or more harmful substances than is emitted in the production of fuel from petroleum .

By Regulation (EU) 2021/119, the Union established legal obligations to achieve climate neutrality by 2050 at the latest, as well as to reduce net greenhouse gas emissions by 2030 by at least 55% compared to 1990. In order to achieve this, all economic sectors, including the transport sector, must take rapid steps to *decarbonize* [6].

Pursuant to *Amendment 102 - Annex 1*, adopted by the European Parliament on 7 July 2022 (Regulation of the European Parliament and of the Council on ensuring a level playing field for sustainable air transport (COM (2021)0561-C9-0332/2021-2021/0205 COD) the minimum shares of SAFs were determined, including the minimum share of synthetic aviation fuel[3], table 2.

Table 2. Minimum shares of SAFs including the minimum share of synthetic aviation fuel

Aviation fuel available to all aircraft operators in all airports Unions with minimal content of sustainable aviation fuel, SAFs including a minimum content of synthetic aviation fuel	a) From January 1, 2025, a minimum share of SAFs of *2%*, of which a minimum share of synthetic fuels of *0.04%*.
	b) From January 1, 2030, a minimum share of SAFs of *6%*, of which a minimum share of synthetic fuels of *2%*.
	c) From January 1, 2035, a minimum share of SAFs of *20%*, of which a minimum share of synthetic fuels of *5%*.
	d) From January 1, 2040, a minimum share of SAFs of *37%*, of which a minimum share of synthetic fuels of *13%*.
	f) From January 1, 2045, a minimum share of SAFs of *54%*, of which a minimum share of synthetic fuels of *27%*.
	g) From January 1, 2050, a minimum share of SAFs of 85%, of which a minimum share of synthetic fuels of 50%.

Criteria for the potential use of alternative fuels in air traffic

In order for alternative fuels to start being used in air traffic in commercial transport, or in some other type, it is necessary that they meet certain criteria. Apart from the need for an equal or higher energy value than the current aviation fuel [7], and of course, the reduction of greenhouse gas emissions, which is constantly increasing due to the increase in the volume of transport, the main criteria for the potential use of alternative fuels in air transport are [7,8] :

1) characteristics of the fuel itself,

[3] "Synthetic aviation fuels" means hydrogen from renewable sources, electricity from renewable sources or fuels that are renewable fuels of non-biological origin (Regulation of the European Parliament and of the Council on ensuring a level playing field for sustainable air transport, 2022)

2) ecological effects,
3) mass production,
4) economic justification,
5) security of use and compatibility.

The first criterion is that alternative fuels should have the same or better characteristics than hydrocarbon commercial fuels of the kerosene type (JET A-1 and others). This is the reason that air carriers do not have to modify the engine or structure of the aircraft, and that the method of fuel supply does not change. The characteristics of the fuel itself include, among others, the weight of the fuel. Fuels that require larger tanks and are much heavier than currently used fuels are not currently acceptable in air traffic, such as e.g. liquid hydrogen.

Another criterion is environmental effectiveness when using alternative fuels. One of the main goals of using alternative fuels is the reduction of greenhouse gas emissions, and therefore replacing current aviation fuels with some fuel that will have more pronounced emissions of these gases is unacceptable. Figure 3 shows an example of the potential reduction of GHG (greenhouse gases) by using the listed types of biofuels.

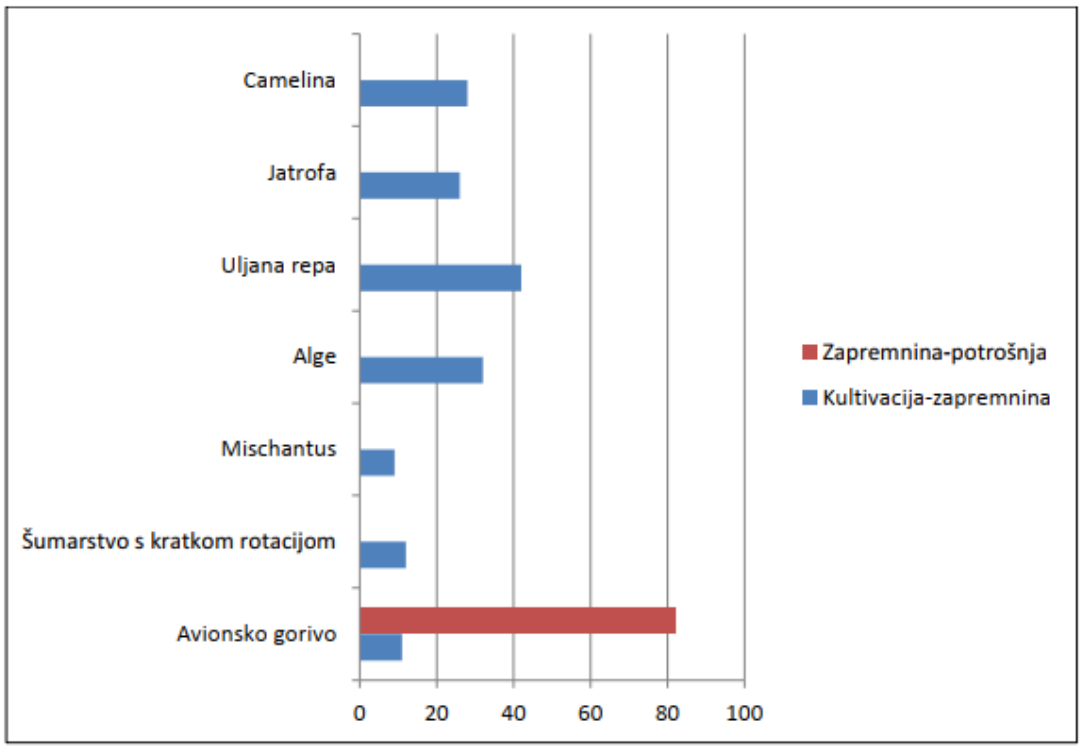

Figure 3. *Potential reduction of greenhouse gases through the use of the listed biofuels, measured in GHG emissions/MJ of fuel*

The third criterion is mass production. If the alternative fuel meets all the criteria, without the possibility of mass production, that fuel is not suitable for use in commercial air traffic. For the use of sustainable alternative fuels in air transport, it is necessary to have large areas intended for the cultivation *of biomass, i.e. raw material that serves as fuel.*

A way to ensure the production of biomass that can meet the needs of commercial traffic is to focus on lands that are not suitable for growing food, plants that do not require pesticides, compost or irrigation and most importantly, that they do not affect the ecological system in which they are located. For example. a plant that is not edible, does not require a large infrastructure or care is *algae*. The mentioned characteristics for biomass production can be fulfilled, but the problem in realizing the production is related to economic justification.

The fourth criterion of economic justification is also the reason why alternative fuels are not yet in global use in air transport.
The fifth criterion is safety of use and compatibility. Fuel that freezes quickly at low temperatures, has a low ignition temperature or is the result of a complicated production process and transport to the aircraft tank itself, is not for use.
Alternative fuels reduce emissions of harmful substances, but they also have disadvantages such as, for example, biodiesel that oxidizes after a long time, and some fuels contain bacteria and fungi (disinfection is necessary constantly).
The goal is that the safety in use tends towards the current aviation fuel or that they are of even better quality. Apart from safety, it is important that the fuel does not significantly affect the structure of the engine, aircraft or the airport infrastructure itself.

Conclusion

Alternative fuels in air transport represent a new generation of fuels. Given that the increase in passenger and freight traffic is increasing, slight modifications aimed at reducing emissions of greenhouse gases and harmful substances cannot cope with such an increase. In addition to having a significant impact on air quality, greenhouse gases also affect global warming, which is one of the most pressing problems today. To prevent such growth, change is needed. The use of hydrocarbon jet fuels of the kerosene type does not make any difference in reducing CO_2 or NOx emissions.
The use of sustainable alternative fuels *(Sustainable Aviation Fuel - SAF)* appears as one of the answers to the reduction of greenhouse gas emissions, primarily CO_2 emissions.
All sustainable alternative fuels must meet certain criteria, starting from ecological and economic justification to safety of application, and most importantly reduced emission of pollutants, and the possibility of sustainable sources of raw materials.
Today, biofuels represent the closest option, and only second and third generation biofuels.
For the sake of easier access to the market, the only close solution so far are *"drop-in" fuels*, where their application will be accompanied by minimal or no modifications to the aircraft and engine construction.

References

1. Arsenović B., Banjac E: "ECOLOGICAL ASPECTS OF AIRCRAFT EXHAUST GASES AFFECT IN SUM OF GREEN-HOUSE ATMOSPHERE GASES"; International Conference on Innovative Technologies; INTECH 2011; BRATISLAVA; SLOVAKIA; (2011)
2. Arsenović B.: "Physico-chemical characteristics of JET A-1 fuel and lubricants for jet engines and their impact on the environment" Innovation and research in the function of technical-technological changes in traffic, ecology and logistics; (p. 39) XIX International Conference, Travnik (2019)
3. Arsenović B.: "Possibility of using renewable energy sources in the Republic of Srpska" Synthesis, 2015. Belgrade (2015)
4. Arsenović B., Janjuš Z., Banjac E.: "Influence of aircraft exhaust gases on the sum of atmospheric greenhouse gases" XIV YUCORR, (2012)
5. Agency for Statistics of Bosnia and Herzegovina, HIV/I, Sarajevo (2023)
6. Amendments of the European Parliament/Annex 1; "Regulation of the European Parliament and of the Council on ensuring a level playing field for sustainable air transport" European Parliament (2022)
7. British Ministry of Defense Standard DEF STAN 91-091/Issue 9, 3 October 2016/Issue 11, 28.October 2019/Issue 14, 07. March 2022. for Turbine, Aviation Kerosene Type, Jet A-1, NATO Code F-35, Joint Service Designation AVTUR.
8. https://www.nyc.gov/html/dot/downloads/pdf/alternativefuel.pdf, accessed 21.07. in 2023

Characterization of coating al applied by phisical vapor phase (pvd) on nickel alloy

Karakterizacija prevlake al nanijete fizičkim postupkom iz parne faze (pvd) na leguru nikla

Danijela Jovičić[1,*], Zorica Ristić[1], Bojana Lukić[1], Stanko Spasojević[1], Marija Mitrović[2], Nebojša Vasiljević[2], Milorad Tomić[2,3]

[1]*"ORAO" AD for production and overhaul of Bijeljina; Republic of Srpska; Bosnia and Herzegovina*

[2]*University of East Sarajevo, Faculty of Technology, Zvornik, Republic of Srpska*

[3]*Engineering academy of Serbia, Kneza Miloša 9/IV, Belgrade, Serbia*

**danijela.matovic@orao.aero*

Abstract

Nickel-based superalloys are often used for the production of aircraft engine parts, which were the subject of this research after surface modification by applying a metal coating. One of the ways to protect the material is the physical application of the coating from the vapor phase, i.e. the PVD (Physical Vapor Deposition) procedure. The aluminum alloy AlSiYFe was chosen for the coating material, which was applied to the nickel alloy by the PVD process. In this way, it is possible to achieve a good connection of the metal coating and the surface of the base material, as well as to improve the exploitation properties of nickel parts intended for work at elevated temperatures. The characterization and properties of the Al coatings applied by the PVD process on the nickel alloy were performed by determining the chemical composition, thickness of the coating, adhesion, and metallographic tests were performed.

Keywords: *nickel alloy; PVD process; Al coating; coating characterization*

Uvod

Savremeni trendovi u razvoju avioindustrije, stalno postavljaju nove zahtjeve u pogledu poboljšanja rada i performansi motora. Istraživanja su uglavnom usmjerena na povećanje mehaničkih i fizičkih osobina metalnih materijala namijenjenih za rad na povišenim temperaturama. Dijelovi motora u procesu eksploatacije izloženi su raznim štetnim djelovanjima kao što su dejstvo atmosfere, agresivnih medija, visoke radne temperature i slično. Legure nikla često se koriste u visokotemperaturnim postrojenjima, jer dobro podnose visoke temperature. Zbog tog svojstva, legure nikla neizbježne su pri izradi turbina avionskih motora, kao i ispusnih ventilima kroz koje prolaze vrući gasovi iz motora. Takođe, ove legure imaju izvanrednu otpornost na koroziju [1,2]. Lopatica turbine predstavlja tipičan primjer uspješnosti primjene niklove superlegure jer treba podnijeti velika naprezanja pri visokim temperaturama koja uzrokuju pucanje, a mora biti otporna i na pojavu mehaničkog i termičkog zamora usljed čestih oscilacija naprezanja pri radnoj temperaturi i čestih temperaturnih promjena [3].

Iako nikl i legure nikla imaju odlične osobine, ponekad je i takve materijale potrebno zaštititi. Jedan od načina poboljšanja eksploatacionih osobina metalnih materijala koji se koriste za izradu dijelova avionskih motora je postupak modifikacije površine nanošenjem metalnih prevlaka. Time se prije svega ostvaruje zaštita metala na visokim temperaturama, a mogu se poboljšati i druge eksploatacione osobine legura [4].

Jedan od postupaka zaštite je fizičko nanošenje prevlaka iz parne faze odnosno PVD (Physical Vapor Deposition) postupak, kojim je moguće nanošenje tankih slojeva različitih materijala na metalne površine. Prevlake na bazi aluminijuma se koriste na dijelovima motora od legura na bazi nikla.

Predviđene su zbog zaštite lopatica od visokotemperaturne gasne korozije, odnosno zaštite od stvaranja sulfidnog ili oksidnog sloja pri visokim temperaturama kao i od kontaktnog trošenja – habanja.
Sadržaj aluminijuma u zaštitnim prevlakama ne treba da bude manji od 28%, a ostali zahtjevi zavise od vrste materijala koji se štiti [5]. Ostali elementi koji doprinose otpornosti prema oksidaciji i koroziji na visokim temperaturama su: tantal, itrijum i lantan. Itrijum je široko zastupljen u višeslojnim premazima tipa NiCrAlY [6,7].
Neki od najviše korištenih metalnih materijala za izradu dijelova avionskih motora su superlegure na bazi nikla, koje su bile predmet ovog istraživanja nakon modifikacije njihovih površina nanošenjem metalnih prevlaka na bazi Al, koji je nanešen na leguru nikla PVD postupkom. Ova kombinacija legura i metalnih prevlaka daje mogućnost da se ostvari dobro spajanje metalne prevlake i površine metala bez pukotina i pora, stabilna disperzno očvrsnuta mikrostruktura prevlake, otpornost na pucanje, te postojanost na interkristalnu koroziju legura sa nanešenim prevlakama.

Proces fizičkog nanošenja prevlaka iz parne faze, pvd postupak

U novije vrijeme velika se pažnja posvećuje razvoju i primjeni postupaka nanošenja prevlaka u parnoj fazi na području izrade mašinskih elemenata i alata u svrhu povećanja njihove otpornosti i trajnosti. Ovim postupcima se nanose stabilne i čvrste veze.
Razlikujemo postupke [8]:

1. hemijskog nanošenja prevlake u parnoj fazi (CVD),
2. fizičkog nanošenja u pranoj fazi (PVD) i
3. plazmom potpomognute postupke hemijskog nanošenja prevlake u parnoj fazi (PACVD).

Postoje različite tehnike fizičkog nanošenja prevlaka iz parne faze i izbor odgovarajuće tehnike zavisi od vrste materijala na koji se nanosi prevlaka, kao i od željenih osobina prevlake. Na uređaju VPM-12M moguće je nanošenje prevlake na uzorak putem isparavanja katoda (target meta) od materijala AlSiYFe u vakuumu, tj. isparavanjem target meta u vakuumu i kondenzaciji njegovih para na površinu uzorka. Na površini prevlaka-uzorak ne dolazi do odvijanja hemijskih reakcija već do fizičkih promjena. Da bi se obezbijedila što ujednačenija prevlaka alati u komori rotiraju oko svoje ose. Veze se pospješuju uvođenjem argona kao reaktivnog gasa. Uređaj ima jednu vakuum komoru u kojoj se proces može vizuelno pratiti preko tri okulara i kontrolisati komandama na PLC ekranu. Uzorke koji se pripremaju za nanošenje prevlake potrebno je očistiti mehanički od bilo kakvih vrsta onečišćenja, a zatim ih je potrebno odmastiti u benzinu i alkoholu pa tretirati destilovanom vodom u ultrazvučnoj kadi. Prvi korak je vakuumiranje komore čime se osigurava inertna sredina i odsustvo hemijskih reakcija u uslovima visokog vakuuma. Uključuju se grijači i vakuum komora se zagrijava do temperature (40-50)°C. Kada je obezbijeđen visok vakuum $9x10^{-5}$mbar i odgovarajuća temperatura prelazi se na čišćenje uzoraka. U vakuum komoru se tada upušta argon protokom (140-150)sccm. U skladu sa tim da je napon veći na uzorcima i reaktivni gas će biti usmjeren ka njima. Istovremeno se uključuju fokusirajući i stabilizirajući kalemi (0,8-1,2)A zbog uspostavljanja elektromagnetnog polja u komori koje olakšava uspostavljanje plazme. Nakon uspostavljanja stacionarnog pritiska u komori, napon se postepeno povećava do vrijednosti (600-700)V kako formiranje plazme i prvih mikrolukova ne bi uticalo na eroziju uzoraka. Ovim postupkom se obezbjeđuje jonsko čišćenje uzoraka i bolji uslovi za vezivanje prevlake za površinu. Vrijednost napona se povećava do 1000V, protok argona do 220sccm a temperatura dostiže vrijednost od 180°C. Kada je proces čišćenja završen prelazi se na pripremu target meta. U ovom ispitivanju su korišćene tri target mete materijala AlSiYFe. Struja na regulatorima elektrolučnig isparivača se podesi na (45-125)A a visoki napon se smanji na 300V. Tada se uključuju elektrolučni isparivači (3-5)minuta što je dovoljno za čišćenje, zasićene meta i predgijavanje. Kada se isključe elektrolučni isparivači struja se podešava na (125-315)A. Nakon pripreme katoda prelazi se na naošenje prevlake. Tada se gasi visok napon i na uzorke dovodi nizak napon. Uključuju se lučni isparivači i njihova struja podesi na (160-

180)A. Izdvojeni atomi sa target meta se kondenzuju na uzorke i grade klice kristalizacije koje rastu i formiraju sloj prevlake. Trajanje procesa nanošenja prevlake zavisi od željene debljine prevlake, a temperatura raste i dostiže vrijednosti (450-500)°C. Kada je proces završen vrši se isključivanje uređaja i ispumpavanje vakuuma. Uzorci ostaju na hlađenju u struji argona i nakon toga se vade iz vakuum komore.
Nakon postupka nanošenja prevlake vrši se i termička obrada. Poznato je da se optimalna mikrostrukturna i mehanička svojstva mnogih materijala, a tako i superlegura, postižu korišćenjem odgovarajuće termičke obrade. Termička odrada, odnosno difuziono žarenje se vrši 2 sata u Ipsen peći (tip „VFC-224-R“) na (1050±10)°C. Uzorci se poslije žarenja hlade 2 sata u vakuumu, a zatim u struji argona do sobne temperature. Nakon završene termičke obrade uzorci su spremni za ispitivanje i korišćenje [9,10,11].

Slika 1. *Uređaj VPM-12M za fizičko nanošenje prevlaka iz parne faze*

Eksperimentalni dio

Postupkom fizičkog nanošenja prevlake iz parne faze (PVD) vrši se modifikacija površina turbinskih lopatica. Pored turbinskih lopatica svaka šarža sadrži i test epruvete na kojima se vrše eksperimentalna ispitivanja prevlake.
Uzorci za ispitivanje:
-šarža br. I: epruveta VELIKA (1 komad dimenzija (7 x 4,93 x 0,09)cm) i epruveta MALA (1 komad dimenzija (3,95 x 0,97 x 0,08)cm);
-šarža br. II: epruveta VELIKA (1 komad dimenzija (7 x 4,94 x 0,09)cm) i epruveta MALA (1 komad dimenzija (3,95 x 0,97 x 0,08)cm).
Ispitivanje hemijskog sastava uzoraka, target meta i prevlake izvršeno je pomoću ručnog XRF analizatora, tip X-MET 8000 Alloy Expert, proizvođač HITACHI (ser. br. 804280).
Ispitivanje adhezije savijanjem je izvršeno uz pomoć alata kojim se uzorci saviju pod uglom od 90°; prečnik trna, tj. prečnik preko koga se vrši savijanje iznosi 12,6 mm.
Metalografsko ispitivanje (metalografski snimak prevlake i debljina prevlake) izvršeno je na metalografskom mikroskopu “Carl Zeiss”, tip Neophot 21 [12].

Rezultati i diskusija

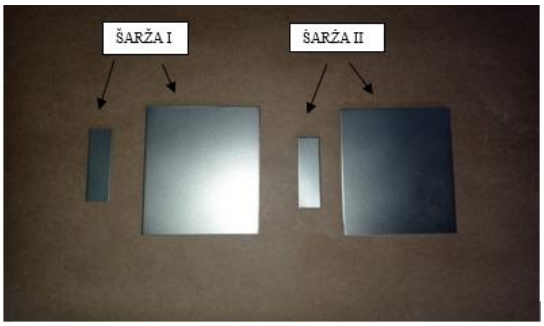

Slika 2. *Izgled uzoraka (epruveta) prije nanošenja prevlake*

Na slici 2. dat je prikaz uzoraka (epruveta) supstrata legure nikla na koju su PVD postupkom nanešene prevlake aluminijuma.
Od svake epruvete isječen je po jedan uzorak za metalografsko ispitivanje. Uzorci su upresovani u bakelitu, a upresak je pripremljen za metalografsko ispitivanje (brušenje, poliranje). Izgled upresaka prikazan je na slici 3.

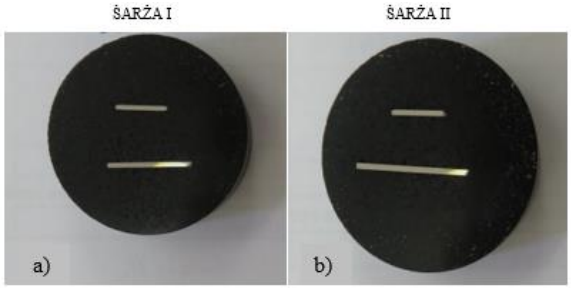

Slika 3. *Izgled upresovanih isječaka malih i velikih epruveta: a) šarža I i b) šarža II*

Vizuelnim pregledom prevlake nisu uočene nedozvoljene greške u vidu: nepokrivenih mjesta, pojava dendritne i sunđeraste strukture prevlake, mjehurovi, odslojavanje, ljuštenje prevlake i dr. Izgled uzoraka (epruveta) sa prevlakom nanešenom PVD postupkom, kao i izgled uzoraka (epruveta) nakon termičke obrade prikazan je na slici 4. Prevlaka je tamno sive boje.

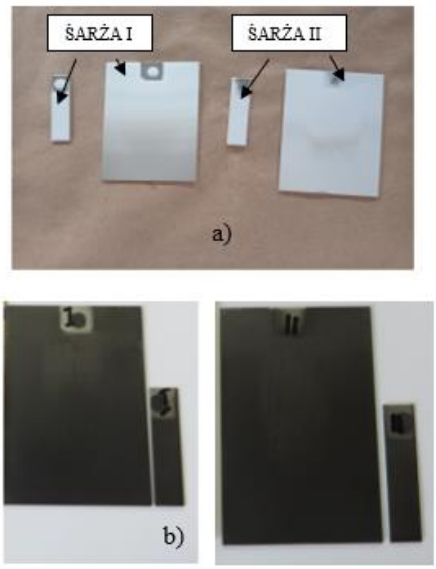

Slika 4. *Izgled uzoraka (epruveta): a) nakon nanošenja prevlake PVD postupkom; b) nakon termičke obrade*

U tabeli 1. prikazani su rezultati ispitivanja hemijskog sastava uzorka (epruvete) prije nanošenja prevlake i hemijski sastav prevlake, kao i rezultati ispitivanja hemijskog sastava metala koji se taloži kao prevlaka PVD postupkom (target meta).

Tabela 1. Hemijski sastav uzorka (epruvete) prije i poslije nanošenja Al prevlake PVD postupkom, kao i metala koji se taloži kao prevlaka (target meta)

Hemijski element	Hemijski sastav % (m/m)		
	Epruveta bez prevlake/osnovni materijal	Nanešena prevlaka	Target meta
Ni	51,40	39,15	-
Cr	18,71	11,18	-
Fe	0,75	0,66	0,81
Co	17,61	13,48	-
Mo	6,95	4,46	-
Ti	2,21	0,89	-
Al	0,35	>28,93	92,05
Mn	0,41	0,07	-
Nb	0,49	-	-
W	0,73	-	-
Si	0,22	1,00	5,05
Cu	0,09	0,11	-
Y	-	-	1,33

Iz rezultata ispitivanja hemijskog sastava epruveta prikazanog u tabeli 1. vidi se da je prevlaka prisutna i da je u toku termičke obrade dio prvlake difundovao u osnovni materijal.
Dobijena vrijednost %Al na epruvetama zadovoljava zahtjev prema kome sadržaj aluminijuma u zaštitnim prevlakama ne treba da bude manji od 28%, naveden u „Programu verifikacionih ispitivanja termozaštitnih prevlaka na lopaticama turbine visokog pritiska DART motora“ [5].
Ispitivanje adhezije savijanjem vršeno je na velikim epruvetama iz šarže 1 i šarže 2, slika 5.

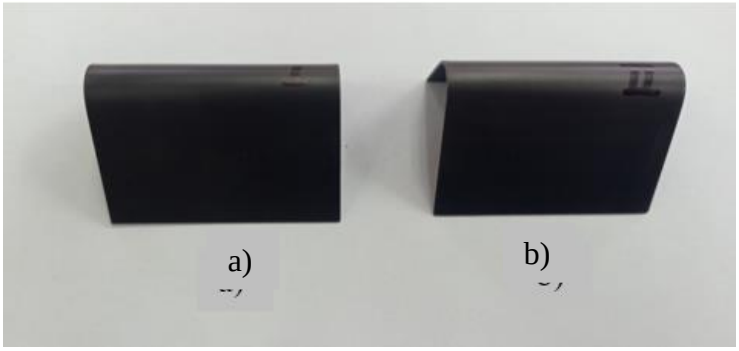

Slika 5. *Izgled savijenih velikih epruveta: a) šarža I i b) šarža II*

Prilikom ispitivanja epruveta na savijanje nije došlo do pucanja prevlake, ljuštenja niti odvajanja iste od osnovnog materijala, što govori da je adhezija prevlake Al na supstratu legure Ni veoma dobra. To dozvoljava i standard DMP 14010 [13].
Metalografski snimak prevlaka nanešenih na epruvete prikazan je na slici 6.

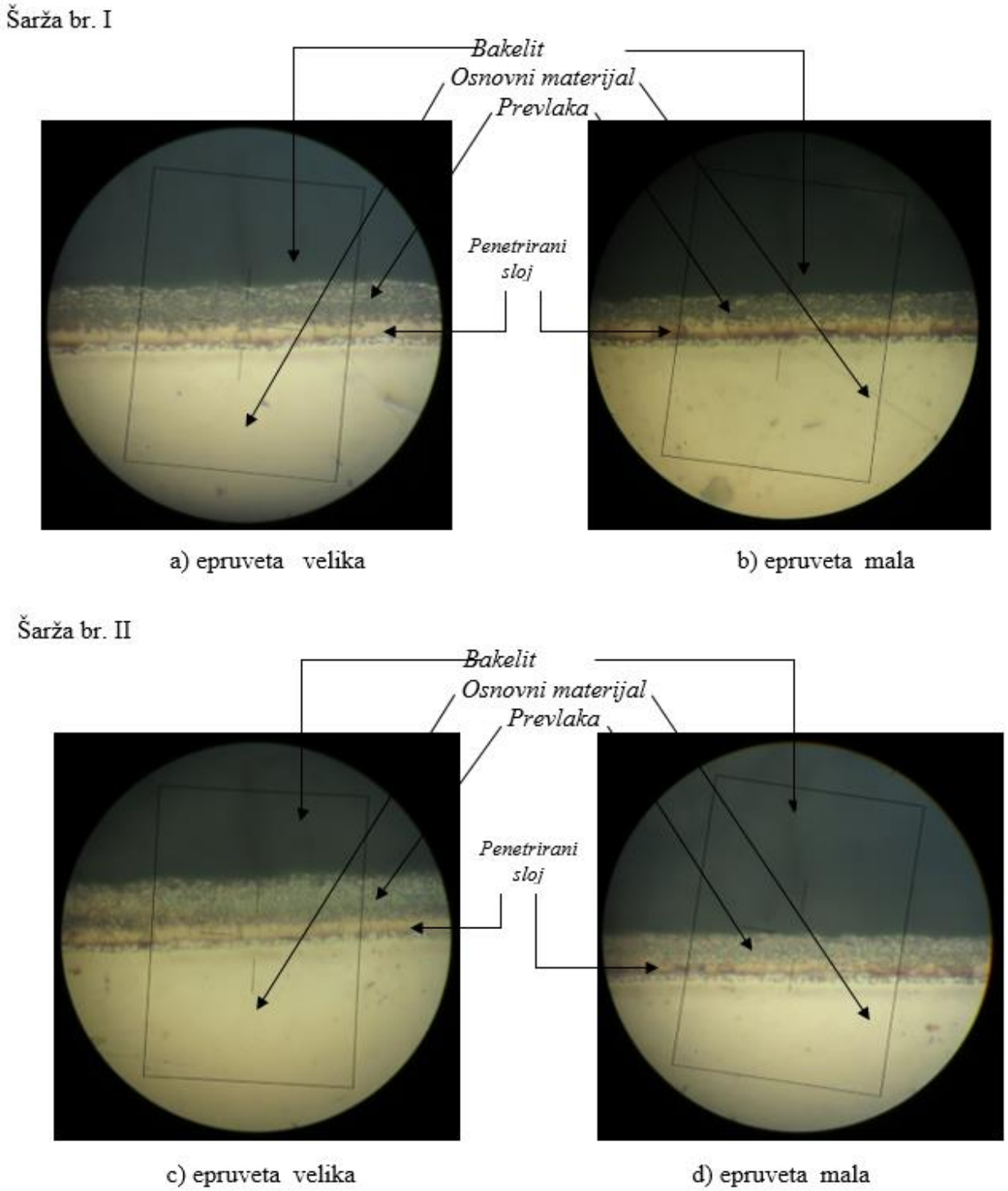

Slika 6. *Metalografski snimak epruveta (uvećanje 400x): a) šarža I, velika epruveta; b) šarža I, mala epruveta; c) šarža II, velika epruveta i d) šarža II, mala epruveta*

Posmatranjem metalografskih snimaka epruveta uočeno je postojanje prevlake, koje se prostire ravnomjerno, i penetriranog sloja na svim posmatranim površinama.

Istovremeno sa posmatranjem prevlake izvršeno je mjerenje njene debljine i debljine penetriranog sloja. Debljina prevlake i debljina penetriranog sloja kod mjerenja mikroskopskom metodom se mjeri pomoću mjerne skale u okularu mikroskopa.
Rezultati mjerenja *debljine prevlake* prikazani su u tabeli 2.

Tabela 2. Rezultati mjerenja debljine prevlake

Šarža	*Epruveta*	*Površina*	*Debljina prevlake (µm)*					*Zahtjev za debljinu prevlake*
			Redni broj mjerenja					
			1	*2*	*3*	*4*	*5*	
I	*Velika*	*1*	*31,3*	*31,3*	*34,4*	*32,8*	*31,3*	*od 20 µm do 38 µm*
	Mala	*1*	*21,9*	*25,0*	*23,4*	*21,9*	*23,4*	
II	*Velika*	*1*	*34,8*	*31,3*	*31,3*	*31,3*	*34,4*	
	Mala	*1*	*23,4*	*25,0*	*25,0*	*26,6*	*23,4*	

Debljina penetriranog sloja na epruvetama kreće se u intervalu (3,1 – 4,7) µm.
Dobijene vrijednosti ukupne debljine prevlake (debljina prevlake + debljina penetriranog sloja) na epruvetama zadovoljavaju zahtjev za debljinu prevlake naveden u „Programu verifikacionih ispitivanja termozaštitnih prevlaka na lopaticama turbine visokog pritiska DART motora“ (od 20 µm do 38 µm).

Zaključak

Postupci fizičkog taloženja prevlake u parnoj fazi ili PVD postupci prate vrlo brz razvoj tehnika i tehnologija te se razvijaju PVD postupci koji uključuju taloženje prevlaka od gotovo svih materijala na niz materijala supstrata. U radu je dat pregled jednog segmenta istraživanja vezan za osvajanje novih materijala i tehnologija za potrebe avioindustrije.
Analizom dobijenih rezultata, može se zaključiti sljedeće:
- prilikom ispitivanja epruveta na savijanje uočeno je da nije došlo do pucanja prevlake, ljuštenja niti odvajanja iste od osnovnog materijala, što je prema standardu DMP 14010 prihvatljivo;
- posmatranjem svih uzoraka epruveta na metalografskom mikroskopu uočeno je postojanje prevlake, koja se prostire ravnomjerno, kao i postojanje penetriranog sloja;
- najmanja debljina prevlake i penetriranog sloja izmjerena je na uzorku male epruvete iz šarže 1 od 21,9 µm, a najveća debljina prevlake i penetriranog sloja izmjerena je na uzorku velike epruvete iz šarže 2 od 34,8 µm;
- debljina penetriranog sloja kreće se u intervalu od 3,1 µm do 4,7 µm;
- dobijene vrijednosti ukupne debljine prevlake (debljina prevlake + debljina penetriranog sloja) na svim epruvetama zadovoljavaju zahtjev za debljinu prevlake naveden u „Programu verifikacionih ispitivanja termozaštitnih prevlaka na lopaticama turbine visokog pritiska DART motora“ (od 20 µm do 38 µm).
Istraživanja su pokazala da je pravilan odabir metalne prevlake i postupka nanošenja na određenu leguru važan segment za primjenu u eksploataciji, pri čemu se mogu ostvariti posebno zahtjevni konstrukcioni ciljevi. Pored svih prednosti PVD postupaka koje su navedene u radu postoji još jedna koja se u današnje vrijeme često spominje, a to je ekološka prihvatljivost. Visoki vakuum, reaktivna plazma te ultračisti gasovi i materijali, koji su osnova za pripremu tankih tvrdih prevlaka kod fizičkih postupaka taloženja u parnoj fazi, predstavljaju temelj ekološki čiste tehnologije. Sa aspekta ekologije ovakav vid zaštite je neuporedivo bolji u odnosu na hemijske ili elektrohemijske procese.

References

1. M. Rimac, M. Oruč, O. Beganović, S. Muhamedagić, Mogućnosti poboljšanja eksplatacionih osobina kod superlegura nanošenjem metalnih prevlaka, International Scientific Conference on Production Engineering , Rim 2011, 1, 145-150.
2. R. Terrence, ASM Handbook, Volume 2, Properties and Selection: Non ferrous Alloys and Special-Purpose materials, ASM International, SAD, 1990.
3. D. Ćorić, T. Filetin, Materijali u zrakoplovstvu, Fakultet strojarstva i brodogradnje, Sveučilište u Zagrebu, 2010.
4. M.G. Hocking , V. Vasantasree, P.S. Siolky, Metallic and Ceramic Coatings High Temperature Properties and Applications, John Willy and sons. INC., New York, 2000.
5. „Program verifikacionih ispitivanja termozaštitnih prevlaka na lopaticama turbine visokog pritiska DART motora“, „ORAO“a.d. Bijeljina, 2022.
6. R. Sunulahpašić, M. Oruč, Superlegure, Univerzitet u Zenici, Metalurško-tehnološki fakultet, 2020, 44.
7. P. Crook, ASM Handbook, Volume 1, Properties and Selection: Irons, Steels, and High Performance Alloys, ASM International, SAD, 1990.
8. T. Filetin, Pregled Razvoja i Primjene Suvremenih Materijala, Hrvatsko društvo za materijale i tribologiju, Zagreb, 2000, 44-46.
9. A. Josipović, Uticaj anodne oksidacije na korozionu postojanost prevlaka niobijuma dobijenih PVD postupkom, Univerzitet u Istočnom Sarajevu, Tehnološki fakultet Zvornik, 14-17, 2023.
10. Tehnička dokumentacija i uputstvo za bezbedan rad, izvodjenje tehnologije depozicije i održavanje opreme VPT-12M, 62-66, 2022.
11. F. Raidenbach, ASM Handbook, Volume 5, Surface Engineering, ASM International, SAD, 1994.
12. Z. Karać, S. Spasojević: „Ispitivanje karakteristika prevlake od aluminijuma (Al) na epruvetama“; M-29/24 „ORAO“a.d. Bijeljina, 2-6, 2024.
13. Standard DMP 14 010, Plasma gun spraying, Snecma, 1980.

Pollutants During Simultaneous Operation Of Plants For The Production Of Concrete-Concrete Base And Plants For The Production Of Asphalt-Asphalt Base

Zagađujuće materije tokom istovremenog rada postrojenja za proizvodnju betona-betonske baze i postrojenja za proizvodnju asfalta-asfaltne baze

D. Vuksanović[1,*], J. Šćepanović[1], D. Radonjić[1]

[1]*University of Montenegro, Faculty of Metallurgy and Technology, Cetinjski put, 81000 Podgorica, Montenegro*

[*]*darkov@ucg.ac.me*

Abstract

The production of concrete and asphalt can lead to certain negative impacts on the environment, depending on the technological process of work, as well as on the location of the location where the process takes place. Impacts that can occur during the operation of concrete and asphalt production plants are emissions of substances into the air, which can cause changes in air quality at the site and in its surroundings.
Air pollution in the atmosphere can be viewed through:
- negative impact on man and his health,
- jeopardizing other elements of the environment (water, soil and other living things).
Emission of pollutants: gases, dust, smoke, etc. into the surrounding space represents its pollution. In this particular case, the sources of air pollution are the concrete production plant, as well as the machines and trucks that service the operation of this plant. Accidental situations can occur due to malfunctioning filters on silos during their filling, which can affect the existing air quality. This impact is temporary and local.
Also, during the operation of the asphalt base, the sources and types of pollutants in the air can be:
- Dryer and aggregate mixing (tower): PM_{10}, CO, SO_2, NO_x, CO_2, VOC, PAH (Point source)
- Emissions from unloading into silos and storage: PM, CO, VOC, PAH (fugitive emissions)
- Asphalt loading and factory circuit: PM, CO, VOC, PAH (fugitive emissions)
- Asphalt heater: CO, SO_2, NO_x (Point source)
- Aggregate storage and dosing: PM_{10}, $PM_{2.5}$ (fugitive emissions)
- Dust emission from roads: PM_{10}, $PM_{2.5}$ (fugitive emissions)
- Emissions of PM particles and gases from transport at the location of the asphalt base.
Keywords: *concrete production; pollutant; environment; air; noise; wastewaters*

Uvod

Prilikom rada postrojenja za proizvodnju betona i postrojenja za proizvodnju asfalta dolazi u određenoj mjeri do emisije zagađujućih materija u vazduh. Emisije zagađujućih materija u vazduh generisane su radom betonske i asfaltne baze, kao i mehanizacije koja radi na otvorenom prostoru, zbog čega se uspostavlja mreža mjernih mjesta u skladu sa Uredbom o uspostavljanju mreže mjernih mjesta za praćenje kvaliteta vazduha („Sl. list CG“, br. 044/10, 013/11, 064/18) [1]. Takođe, za ovo se koriste i: Pravilnik o načinu i uslovima praćenja kvaliteta vazduha („Sl. list CG“, br. 021/11) [2] i Uredba o utvrđivanju vrste zagađujućih materija, graničnih vrijednosti i drugih standarda kvaliteta vazduha („Sl. list CG“, br. 45/08, 25/12) [3].
Tokom rada betonske i asfaltne baze javljaju se suspendovane čestice (PM – Particulate Matter) koje predstavljaju mješavinu prašine, čađi i dima. Ove čestice su suspendovane u vazduhu kao čvrste čestice ili kao tečne kapljice.

Suspendovane čestice predstavljaju jednog od najznačajnijih zagađivača sa veoma štetnim uticajem po ljudsko zdravlje. Zavisno od veličine dijele se na PM_{10} i $PM_{2.5}$ čestice. Ova podjela je zasnovana na veličini čestica, tako da su $PM_{2.5}$ čestice sve one koje su veličine do 2,5 mikrona, dok su PM_{10} čestice sve one čestice veličine do 10 mikrona [4]. Izloženost visokoj koncentraciji suspendovanih čestica dovodi do različitih poremećaja zdravlja, kao što su oboljenja respiratornog sistema, pogoršanje postojećih respiratornih i kardiovaskularnih oboljenja, karcionegeneza [5].
Sumpor dioksid i oksidi azota se javljaju i tokom procesa proizvodnje betona i asfalta.
Najveći izvori sumpor-dioksida nastaju tokom sagorijevanja fosilnih goriva, poput uglja i nafte, dok se manji procenti emisija javljaju u industriji tokom procesa topljenja metala, proizvodnje celuloze i hartije, i u saobraćaju [6]. U prisustvu drugih zagađujućih supstanci sumporni oksidi mogu postati katalizatori hemijskih reakcija u atmosferi, što dovodi do formiranja sekundarnih suspendovanih čestica [7].
Prisustvo NO_2 u vazduhu doprinosi formiranju ozona, suspendovanih čestica i kiselih kiša. U tom smislu, ukupan štetan uticaj oksida azota je teško kvantifikovati i može potencijalno biti obimniji od direktnih negativnih posledica po zdravlje ljudi [8].
Cilj ovog rada je da se kroz proces proizvodnje betona i asfalta pokaže koji svi uticaji mogu biti prisutni, a koji mogu imati negativan uticaj na kvalitet životne sredine prostora u okviru kojeg egzistiraju ovakva postrojenja.

Emisije u vazduh

Betonska baza

U toku tehnološkog procesa, pri radovima zbog vremenske i prostorne dimenzije izvjesne količine mineralne prašine, pogonskog goriva i maziva, gasova i drugih materija mogu dospjeti u vazduh, u vode, deponovati se na okolno zemljište, tj. dospjeti u životnu sredinu. Primijenjenim mjerama zaštite ovaj uticaj se može ograniiti i dovesti u prihvatljive granice.
Prilikom proizvodnje betona mogu se očekivati emisije u vazduh: prašine i polutanata iz energenta (dizel goriva). Navedene emisije nemaju kontinualan karakter i ispuštanje zagađujuih materija u vazduh, u smislu kontinualne industrijske proizvodnje.

Izvori zaprašenosti u zoni pripreme betona i betonskih proizvoda su:
- Doprema cementa, istovar i skladištenje u silos
- Transfer agregata
- Vaganje i doziranje
- Centralni mikser, emisija pri utovaru kamiona
- Transport saobrajnicama

PM čestice, koje se prvenstveno sastoje od cementne prašine, ali uključujući i neke iz emisije agregata, su primarni zagađivači u funkcionisanju betonske baze. Sve emisione tačke osim jedne su fugativne prirode. Jedini tačkasti izvori su transfer cementa u silose, a oni se odvode u fabrički filter od tkanine. Fugativni izvori uključuju prenos agregata, utovar u automikser, saobraćaj vozila i eroziju vjetrom iz skladišta agregata.
U sljedeoj tabeli su dati emisioni faktori za proces proizvodnje betona.

Tabela 1. Emisioni faktori za proces proizvodnje betona

Izvor	**Nekontrolisano**	**Kontrolisano**
	PM_{10}	
Transfer agregata	0,0017	ND*
Istovar cementa u silose	0,24	0,00017
Punjenje mjerne vage	0,0013	ND*
Istovar u automikser	0,078	0,0028

ND* - nije definisano

Količina PM čestica na godišnjem nivou tokom rada betonske baze računa se po formuli:

PM (t/god) = emisioni faktor PM (kg/t) x godišnja proizvodnja (t/god) *x* ***(1 t/1.000 kg)***

1. Transfer agregata

Materija	**EF**	**EF jed.**	**Kapacitet**	**Jedinica**	**Ukupno**	**Jedinica**
PM_{10}-nekontrolisana	0,0017	kg/t	16.200	t	0,027	t/god.
PM_{10}-kontrolisana*	ND	kg/t	0	t	0	t/god.

2. Istovar cementa u silose

Materija	**EF**	**EF jed.**	**Kapacitet**	**Jedinica**	**Ukupno**	**Jedinica**
PM_{10}-nekontrolisana	0,24	kg/t	0	t	0,000	t/god.
PM_{10}-kontrolisana*	0,00017	kg/t	2.250	t	$3,8 \times 10^{-4}$	t/god.

3. Punjenje mjerne vage

Materija	**EF**	**EF jed.**	**Kapacitet**	**Jedinica**	**Ukupno**	**Jedinica**
PM_{10}-nekontrolisana	0,0013	kg/t	16.200	t	0,021	t/god.
PM_{10}-kontrolisana*	ND	kg/t	0	t	0	t/god.

4. Istovar u automikser

Materija	**EF**	**EF jed.**	**Kapacitet**	**Jedinica**	**Ukupno**	**Jedinica**
PM_{10}-nekontrolisana	0,078	kg/t	0	t	0,000	t/god.
PM_{10}-kontrolisana*	0,0028	kg/t	21.600	t	0,06	t/god.

UKUPNO (1 + 2 + 3 + 4) = 0,027 + $3,8 \times 10^{-4}$ + 0,021 + 0,06 = 0,108 t/god

što predstavlja prosječne vrijednosti od 0,004 g/s (računate na 252 radna dana godišnje).

Asfaltna baza

Na kvalitet vazduha u radnoj sredini i u neposrednoj okolini asfaltne baze mogu uticati otpadni gasovi koji nastaju kao produkt sagorijevanja lož ulja, pri istresanju asfalta iz tornja u kamion, zatim

mineralna prašina i vodena para koji se produkuju i emituju u procesu sušenja mineralnog agregata kao i pri skladištenju i manipulaciji filerom.
Pri spaljivanju lož ulja u bubnju za zagrijavanje i sušenje agregata, kao i silosu gotovog asfalta emituju se otpadni dimni gasovi u atmosferu. Otpadni dimni gasovi koji nastaju u postrojenju za sušenje sa sobom nose prašinu, odnosno čvrste čestice koje su preostale nakon filtriranja u filterskom postrojenju.
Količina čestica, u otpadnim dimnim gasovima koje se emituju u atmosferu, zavisi isključivo od ispravnosti filterskog postrojenja i njegovog tekućeg održavanja.
Treba naglasiti da stepen emisije otpadnih dimnih gasova pri sagorijevanju lož ulja zavisi od regulacije sagorijevanja. Prema tome, ukoliko je odnos goriva i vazduha optimalan onda se u atmosferu ispuštaju otpadni dimni gasovi sa zakonski dozvoljenim sadržajem polutanata.
Posebno treba naglasiti da ukoliko temperatura bitumena prelazi 200 ºC postoji mogućnost da se u atmosferu emituju teški ugljovodonici iz postrojenja za miješanje i iz silosa asfalta. Zato je potrebno redovno pratiti ovaj parametar s ciljem sprečavanja zagađivanja atmosfere.
Pri istresanju asfalta iz tornja za proizvodnju izlaze topli gasovi i pare koje nastaju miješanjem sirovina u tornju (mineralnog agregata, kamenog brašna i bitumena).
Kako je bitumen različitog hemijskog sastava, a građen je od viših ugljovodonika i njihovih derivata, to je i sastav gasova i pare koji se ispuštaju u atmosferu, vrlo različit.
Sumpor dioksid (SO_2) nastaje pri sagorijevanju fosilnih goriva, a njegov sadržaj u sagorjelim gasovima zavisi od sadržaja u gorivu i efikasnosti sagorijevanja.
Ugljen monoksid (CO) nastaje nepotpunim sagorijevanjem i veoma je toksičan, a u atmosferi se brzo transformiše u CO_2, čije povećane koncentracije u atmosferi izazivaju efekat staklene bašte.
Ugljen dioksid nastaje kao produkt sagorijevanja, a njegovi ekološki efekti se manifestuju u povećanju tzv. globalnog zagrijavanja.
Azotni oksidi (NO_x) se izražavaju najčešće kao azotni dioksid (NO_2), toksični su, a pri većim koncentracijama i u dužem periodu, kancerogeni.
Pri radu asfaltne baze mogući su određeni ekscesni slučajevi koji mogu uzrokovati povećano zagađenje vazduha, a koji mogu nastati prvenstveno zbog dotrajalosti filterske tkanine. U praksi se može desiti da dođe do oštećenja filterskih vreća i tkanine (što se rijetko dešava) kada bi došlo do povećane emisije, pa se filterske vreće moraju zamijeniti i pogon zaustaviti.
Emisija iz postrojenja asfaltne baze zahtijeva procjenu sledećih kriterijalnih zagađujućih materija-polutanata na lokaciji asfaltne baze:
- Sumpor dioksid (SO_2)
- Ugljen monoksid (CO)
- Azotni oksidi (NO_x)
- Isparljiva organska jedinjenja (VOC);
- Policiklini aromatski ugljovodonici (PAH)
- Ugljen dioksid (CO_2)

Izvori i vrste zagađujućih materija u vazduhu mogu biti:
- Sušara i miješanje agregata (toranj): PM_{10}, CO, SO_2, NO_x, CO_2, VOC, PAH (Tačkasti izvor)
- Emisije istovara u silose i skladištenje: PM, CO, VOC, PAH (difuzne emisije)
- Utovar asfalta i fabrički krug: PM, CO, VOC, PAH (difuzne emisije)
- Grijač asfalta: CO, SO2, NOx (Tačkasti izvor)
- Skladištenje i doziranje agregata: PM_{10}, $PM_{2.5}$ (difuzne emisije)
- Emisija prašine sa saobraćajnica: PM_{10}, $PM_{2.5}$ (difuzne emisije)
- Emisije PM čestica i gasova od transporta na lokaciji asfaltne baze.

Emisioni parametri sistema za otprašivanje

Koncentracija mase u obliku prašine 10 mg/m³
Koncentracija mase u obliku gasa, max
- CO 350 mg/m³
- SO_2 350 mg/m³
- NO_x 350 mg/m³
- C_{uk} 50 mg/m³

Transfer agregata u silose

Materija	EF	EF jed.	Kapacitet	Jedinica	Ukupno	Jedinica
PM_{10}-nekontrolisana	0,0017	kg/t	16.200	t	0,027	t/god.
PM_{10}-kontrolisana*	ND	kg/t	0	t	0	t/god.

što predstavlja godišnje prosječne vrijednosti od 0,0012 g/s (računate na 252 radna dana godišnje).

Sušara i mješalica

Izduvni gasovi iz bubnja za sušenje i vazduh od usisavanja od tornja, odvode se u sistem za otprašivanje filtera, tamo se pročišćavaju i preko dimnjaka se izbacuju u atmosferu.
Emisija od sušenja agregata (Tačkasti izvor)
- emisija prašine: max 10 mg/Nm^3
- kod opterećenja prašinom vlažnog ulaznog gasa od max 250 g/Nm^3

Dimnjak filterskog postrojenja

Garantovana emisija od dobavljača opreme je do 10 mg/m^3.
Ukupna emisija je:
0,02 [g/m^3] * 48 000 [m^3/h] * 42 [sati/godina]/1.000 = 20,16 kg emisija PM godišnje, što predstavlja godišnje prosječne vrijednosti od 9,25x10^{-4} g/s (računate na 252 radna dana godišnje).

Emisioni parametri za nasadni filter bunkera

- Koncentracija mase u obliku prašine 20 mg/m³
- Sa zapreminskom strujom iz toga proizilazi: Struja mase u obliku prašine 0,007 kg/h (punjenje silosa 3 puta godišnje po 20 min = 0,007 kg/god)

Tabela 2. Emisioni faktori za gasove (kg/t) asfaltne baze CO, NO_x, SO_2, VOCs i PAH

Proces	CO	CO_2	NO_x	SO_2	VOCs	PAH
Loženje na lož ulje-sušara i toranj za mješanje	0,2	18,5	0,06	0,044	0,041	5,5x10^{-5}

Emisije gasova iz asfaltne baze

	CO	**CO_2**	**NO_x**	**SO_2**	**VOCs**	**PAH**
Emisioni faktor (kg/t)	0,2	18,5	0,06	0,044	0,041	$5,5x10^{-5}$
Kapacitet (t/god)	10.000					
Ukupno (t/god)	2	185	0,6	0,44	0,41	$5,5x10^{-4}$

što predstavlja godišnje prosječne vrijednosti od (računate na 252 radna dana godišnje):

- CO: 0,091 g/s
- CO_2: 8,49 g/s
- NO_x: 0,027 g/s
- SO_2: 0,02 g/s
- VOCs: 0,018 g/s
- PAH: $2,5x10^{-5}$ g/s

Ukupne emisije od rada asfaltne baze su:

Proces	**PM_{10}**	**CO**	**CO_2**	**NO_x**	**SO_2**	**VOCs**	**PAH**
Transfer agreagata u silose	0,0012						
Dimnjak filterskog postrojenja	$9,25x10^{-4}$	0,091	8,49	0,027	0,02	0,018	$2,5x10^{-5}$
Ukupno (g/s)	**0,0021**	**0,091**	**8,49**	**0,027**	**0,02**	**0,018**	**$2,5x10^{-5}$**

Ukupne emisije zagađujućih materija u vazduhu

Ukupne emisije zagađujućih materija u vazduhu tokom rada betonske i asfaltne baze koje su proračunate i izražene u g/s prikazane su u sljedećoj tabeli.

Tabela 3. Ukupne emisije zagađujućih materija u vazduhu

Izvor	**PM_{10}**	**CO**	**CO_2**	**NO_x**	**SO_2**	**HC**	**VOCs**	**PAH**
Angažovana mehanizacija	0,006	0,952		0,544		0,051		
Betonska baza	0,004							
Asfaltna baza	0,0021	0,091	8,49	0,027	0,02		0,018	$2,5x10^{-5}$
UKUPNO (g/s)	**0,0371**	**1,043**	**8,49**	**0,571**	**0,02**	**0,051**	**0,018**	**$2,5x10^{-5}$**

Imisijske koncentracije zagađujućih materija, proračunate su korišćenjem Gausovog modela difuzije. Proračun je urađen na osnovu sačinjenog računarskog programa čiju osnovu čini Gausov disperzioni model (ISC-3) za slučaj stanja atmosfere koji je izabran na osnovu brzine vjetra i insolacije (dnevni ili noćni uslovi). Rezultati proračuna predstavljaju imisijske koncentracije na površini terena, na datim rastojanjima od mjesta emisije u srednjim atmosferskim uslovima (temperature i vjetra) u toku godine za datu lokaciju.
Proračun imisijskih koncentracija CO, PM_{10} i SO_2, na lokaciji betonske i asfaltne baze dat je u sljedećoj tabeli za različita rastojanja od mjesta emisije (brzina vjetra 3,3 m/s).

Tabela 4. Proračun imisijskih koncentracija CO, PM_{10} čestica i SO_2

Rastojanje od mjesta emisije do mjesta imisije (m)	**Smjer, brzina (m/s)**	**CO (mg/m^3)**	**PM_{10} ($\mu g/m^3$)**	**SO_2 ($\mu g/m^3$)**
25	V=3,3 m/s	4,63	164,83	0,002
50		1,75	62,44	2,21
75		0,86	30,61	4,91
100		0,51	17,99	4,92
150		0,23	8,35	3,44
200		0,13	4,81	2,19
300		0,06	2,19	1,10

Na slikama 1-4 dat je grafički prikaz raspodjele PM_{10} čestica za date uslove.

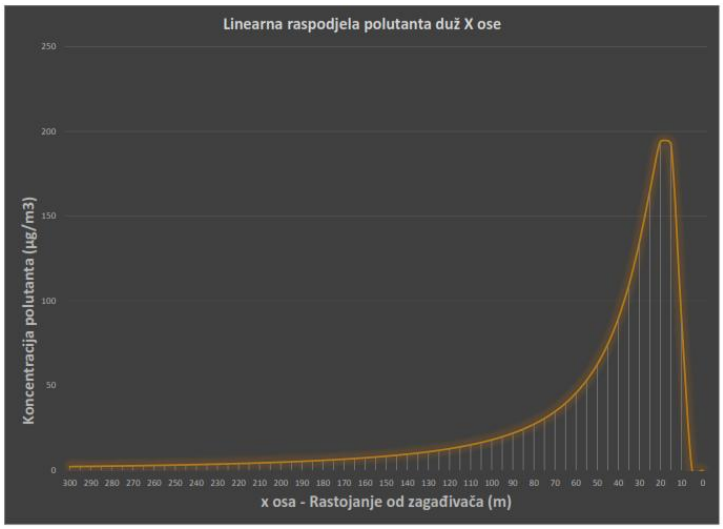

Slika 1. *Linearna raspodjela polutanata PM_{10} čestica duž x ose*

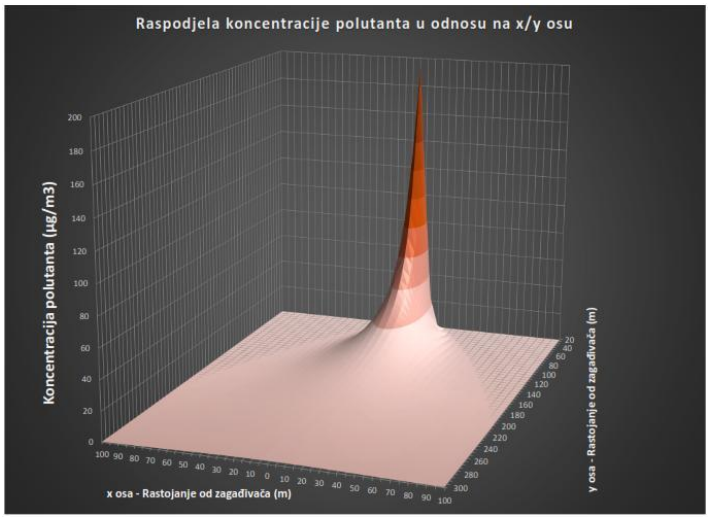

Slika 2. *Prikaz raspodjele koncentracije PM_{10} čestica u odnosu na x/y osu*

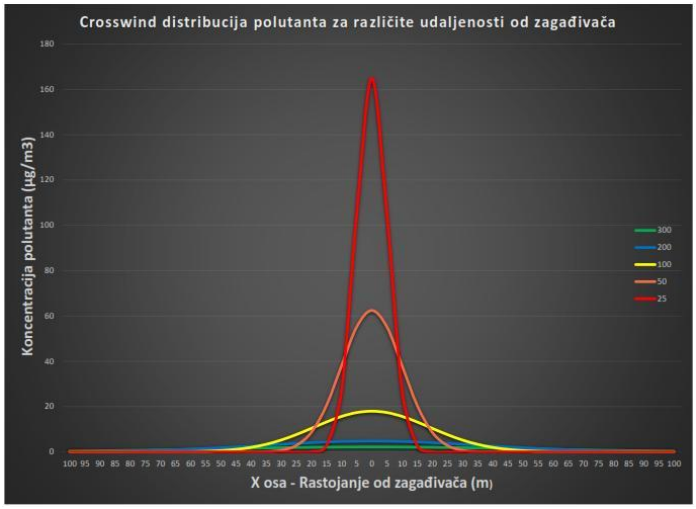

Slika 3. *„Crosswind" distribucija polutanta PM_{10} čestica za različite udaljenosti od zagađivača*

Slika 4. *Raspodjela polutanata PM_{10} čestica na predmetnom prostoru za zadate uslove (pravac vjetra - sjever)*

Slika 5. *Raspodjela polutanata PM_{10} čestica na predmetnom prostoru za zadate uslove (pravac vjetra - istok-jugoistok)*

Zaključak

Na osnovu navedenih podataka i proračuna zagađujućih materija tokom istovremenog rada postrojenja za proizvodnju betona-betonske baze i postrojenja za proizvodnju asfalta-asfaltne baze, može se zaključiti sledeće:

1. Tokom rada postrojenja za proizvodnju betona i asfalta javljaju se emisije zagađujućih materija u vazduh, što može prouzrokovati promjene kvaliteta vazduha na lokaciji njihovog rada i u njenom okruženju.
2. Proizvodnja betona produkuje određene emisije zagađujućih materija u vazduh, prije svega PM čestice, dok se kao zagađujuće materije tokom rada asfaltne baze osim PM čestica javljaju CO, CO_2, NO_x, SO_2, VOCs i PAH-ovi. Ako betonska i asfaltna baza rade u skladu sa normativima koji su za njih propisani, onda su sve emisijske i imisijske vrijednosti zagađujućih materija ispod maksimalno dozvoljenih koncentracija.
3. Iako proračuni dati u radu pokazuju da su emisijske i imisijske koncentracije zagađujućih materija u dozvoljenim granicama, tokom funkcionisanja ovih postrojenja neophodno je vršiti odgovarajući monitoring svih polutanata koji se javljaju, na način što se moraju jasno definisati mjesta i učestalost njihovog mjerenja. Na ovaj način se mogu pratiti svi eventualni propusti u radu betonske i asfaltne baze.

Literatura

1. Uredba o uspostavljanju mreže mjernih mjesta za praćenje kvaliteta vazduha („Sl. list CG“, br. 044/10, 013/11, 064/18).
2. Pravilnik o načinu i uslovima praćenja kvaliteta vazduha („Sl. list CG“, br. 021/11).
3. Uredba o utvrđivanju vrste zagađujućih materija, graničnih vrijednosti i drugih standarda kvaliteta vazduha („Sl. list CG“, br. 45/08, 25/12).
4. Kim K-H, Kabir E, Kabir S. *A review on the human health impact of airborne particulate matter*. Environ Int. 2015;74:136–43.
5. [5] Jimoda LA. *Effects of particulate matter on human health, the ecosystem, climate and materials: A review. Facta universitatis - series*: Working and Living Environmental Protection. 2012;9(1):27–44.
6. Vidaković D. *Višekriterijumska analiza kvaliteta vazduha u urbanim sredinama u zavisnosti od vremenskih faktora. Multicriteria analysis of air quality in urban areas depending on climatic factors* [Internet]. 2013 Oct 29 [cited 2023 August 17]; Available from: http://biblioteka.tfbor.bg.ac.rs/handle/123456789/60
7. Sulphur Dioxide - an overview | ScienceDirect Topics [Internet]. [cited 2023 August 17]. Available from: https://www.sciencedirect.com/topics/earth-and-planetary-sciences/sulphur-dioxide
8. Chen T-M, Gokhale J, Shofer S, Kuschner WG. *Outdoor air pollution: nitrogen dioxide, sulfur dioxide, and carbon monoxide health effects*. Am J Med Sci. 2007;333(4):249–56.

Ecological Characteristics of the Macrophytic Flora of Bardača Wetland

Dijana Ašćerić[1,*], Jelena Vulinović[1], Slađana Petronić[2]

[1]*Faculty of Technology Zvornik, University of East Sarajevo, Zvornik, Bosnia and Herzegovina*

[2]*Faculty of Agriculture, University of East Sarajevo, 71123 East Sarajevo, Bosnia and Herzegovina*

[*]*dijana.asceric97@gmail.com*

Abstract

This paper provides an overview and basic ecological characteristics of the macrophytic flora of the Bardača marsh, including ecological indicator values and the spectrum of life forms. A total of 53 species of macrophytic flora were found through floristic research. Analysis of ecological indices for temperature and humidity indicates the dominance of the belt of mountain mesophilic broad-leaved forests, followed by plants of moist but poorly ventilated habitats, as well as water plants with floating leaves. Regarding soil pH and mineral nitrogen content, the most represented are basifrequent plants and plants of submesotrophic and mesotrophic habitats. Analysis of the light regime indicates the highest number of halflight plants, i.e. plants that mostly thrive in full light but are tolerant to shade as well. Analysis of soil continentality and salinity revealed the dominance of oceanic-suboceanic and suboceanic species, as well as halophob species. Analysis of the biological spectrum of flora found five life forms, with hydrophytes being the most dominant (54.71%), while chamaephytes and therophytes were less represented (1.89%).

Keywords: *macrophytic flora; Bardača; ecological indexs; life forms.*

Introduction

The area of Bardača represents a unique ecosystem of marshes and ponds located in the northeast of Lijevče Polje, bordered by the Sava River to the north, the Brzaja and Vrbas rivers to the east and the Matura River to the west. To the south, in the immediate vicinity, there is the Osorna–Borna–Ljevčanica canal, while to the southwest are the slopes of the Kozara Mountain. Spatially, Bardača covers an area of 2810 hectares (810 hectares of water surface and 2000 hectares of land). The geographical position of the Bardača area is in the center of the moderate zone (45°08'N and 17°25'E), at about 100 meters above sea level, at the foot of Mount Motajica. The marshland ecosystem in which the Bardača fishpond is located is merely a fraction of what was once a huge complex of marshes in northern Bosnia. Until the beginning of the 20th century, what is today's Bardača used to be covered in marshland vegetation with the prevalence of floodplain forests [1]. The first floristic research of the Bardača pond and its surroundings was conducted in the period from 1974 to 1976 within the theme "Flora i vegetacija u području šaranskih ribnjaka sjeverne Bosne", by the scientific advisor of the National Museum of Bosnia and Herzegovina in Sarajevo, dr Željka Bjelčić, and the scientific collaborator of the Institute for the Protection of Cultural Monuments, Natural Wonders and Rarities of Bosnia and Herzegovina, ing Branko Fabijanić [1]. Further research on the Bardača complex is mostly partial and scarce – Nedović&Mejakić (1997) [3] and Šumatić et al. (2001) [4]. Detailed study of the flora and vegetation in the marsh-bar ecosystem of Bardača was carried out in the period from 2002. to 2004. according to the given concept, goals, and tasks of the Project LIFETCY/BIH/041, conducted by Nedović et al. (2004) [5]. Research on the Bardača marsh area continued thereafter, and Kovačević (2005, 2006, 2007) [6-8] was one of the researchers who contributed to a better understanding of this ecosystem, along with Davidović (2007) [9].

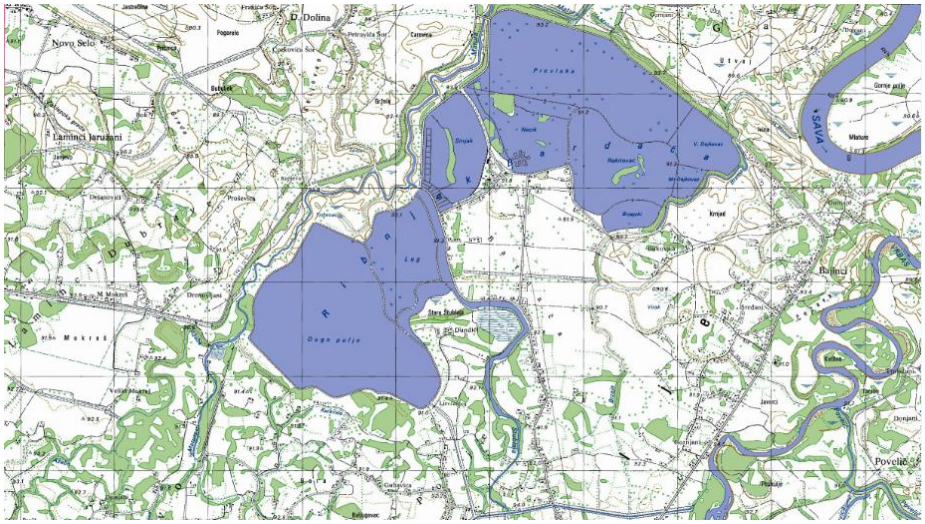

***Figure 1**. The area of Bardača Wetland*

The Bardača marsh was declared a wetland of international importance by the Ramsar Convention on April 12, 2007, due to its exceptional natural values [10]. Already in 1969, the Municipality Assembly of Srbac proposed that this area be declared protected. The Republic Institute for the Protection of Cultural and Natural Monuments of SR Bosnia and Herzegovina issued a Decision on the Protection of Bardača as a special nature reserve in 1969, recognizing its great natural values and sensitive ecosystems, especially in the context of carp production, which was confirmed by the Republic Institute for the Protection of Cultural and Historical Heritage and Natural Heritage of Republika Srpska in 1999. In 2007, the Bardača complex was granted the status of a wetland of international importance under the Ramsar Convention [11]. Researcher Svjetoslav Obratil, studying the Bardača area in 1973, found that it is a unique habitat for shorebirds (178 bird species registered) [12]. According to the Law on Nature Protection of Republika Srpska (Službeni glasnik Republike Srpske, 50/02) [13], in accordance with the proposed amendments to the Law on Nature Protection and the IUCN categorization of protected areas, it is proposed that the Ramsar area of Bardača, together with the Donja Dolina, be declared a protected cultural landscape.

Materials and methods

Floristic research within the Bardača marsh area is presented based on literary data: Davidović (2007) [9], Kovačević (2005) [6], Kovačević et al. (2007) [8]. The names of determined species were adjusted to the nomenclature of Flora Europea, Tuttin et al. (1964-1993) [14]. The floristic analysis of determined taxa includes an ecological analysis, i.e. the affiliation of individual plant species to ecological groups of plants (indicator values) for individual ecological factors, as well as an analysis of life forms. Ecological indexes are given according to Ellenberg [15], concerning individual ecological factors. Indicator values of plant species are presented as indices for basic ecological parameters, namely temperature, moisture, soil reaction, nitrogen supply, light intensity, continentality and salinity. Almost all indicator values are on scales of 1-9, except for humidity, which is on a scale of 1-12 [15]. Data on life forms are given according to Oberdorfer (1979) [16].

Results and Discussion

Through floristic research, 53 plant species were identified in the Bardača marsh. Ecological characteristics were observed through seven main environmental factors; three of them are climatic factors: temperature, light and continentality, as well as three indicators related to soil factors, i.e. humidity, acidity or soil reaction and nitrogen supply. Salinity was also considered. An overview of

the mentioned plant species of the Bardača marsh, as well as their ecological indicator values, is presented in Table 1.

Table 1. Overview and ecological characteristics of the macrophytic flora of the Bardača marsh: TB – temperature, WB – soil moisture, RB – acidity or soil reaction, NB – mineral nitrogen supply, LB – light, KB – continentality, SB – soil salinity.

Plant species	Ecological indicatory values							Life forms
	TB	WB	RB	NB	LB	KB	SB	
1. *Acorus calamus* L.	7	10	7	7	8	5	0	Hyd
2. *Alisma plantago-aquatica* L.	5	10	6	8	7	4	0	Hyd
3. *Caltha palustris* L.	5	9	5	5	7	4	0	H
4. *Carex brizoides* L.	5	7	5	4	6	4	0	G
5. *Carex elata* All.	5	10	6	4	8	2	0	H (Hyd)
6. *Carex flava* L.	5	9	8	4	8	2	0	H
7. *Carex gracilis* L.	5	9	6	4	7	7	0	G (H, Hyd)
8. *Carex pendula* Huds.	6	8	6	5	4	2	0	H
9. *Carex remota* L.	5	8	6	6	4	3	0	H
10. *Carex riparia* Curt.	7	10	7	4	7	3	0	Hyd (H)
11. *Ceratophyllum demersum* L.	7	12	8	8	6	4	0	Hyd
12. *Cirsium palustre* L.	5	8	5	3	7	3	0	H
13. *Deschampsia caespitosa* (L.) P. B.	6	7	6	3	7	5	0	H
14. *Epilobim parviflorum* Schreb.	5	9	7	5	7	3	0	H
15. *Equisetum palustre* L.	4	9	6	3	7	5	0	G
16. *Glyceria fluitans* (L.) R. Br.	5	9	8	5	7	3	0	Hyd
17. *Glyceria maxima* (Hartm.) Hol	5	10	8	7	9	4	0	Hyd
18. *Gratiola officinalis* L.	7	8	7	3	8	5	0	H
19. *Iris pseudacorus* L.	6	9	6	7	7	3	0	Hyd (H)
20. *Juncus articulatus* L.	5	8	6	2	8	3	1	H
21. *Juncus conglomeratus* L.	5	8	5	5	8	7	0	H
22. *Juncus effusus* L.	5	9	6	3	8	3	0	H
23. *Juncus inflexus* L.	5	8	8	4	8	3	1	H
24. *Lemna gibba* L.	6	11	7	8	7	3	0	Hyd
25. *Lemna minor* L.	5	11	7	6	7	3	0	Hyd
26. *Lemna trisulca* L.	5	11	7	6	8	3	0	Hyd
27. *Lycopus europaeus* L.	6	9	6	7	7	5	0	Hyd
28. *Lysimachia nummularia* L.	6	7	8	4	5	4	0	Ch
29. *Lysimachia vulgaris* L.	5	8	6	4	6	5	0	H
30. *Lythrum salicaria* L.	5	9	7	4	7	5	1	H
31. *Mentha aquatica* L.	5	9	7	4	7	3	0	H (Hyd)
32. *Mentha longifolia* (L.) Huds.	5	9	8	8	7	4	0	H
33. *Myriophyllum verticillata* L.	5	9	7	4	7	3	0	Hyd
34. *Myriophyllum spicatum* L.	5	12	8	5	5	4	0	Hyd
35. *Najas marina* L.	7	12	7	6	5	4	1	Hyd
36. *Nuphar lutea* (L.) Sm.	6	11	7	8	8	4	0	Hyd
37. *Nymphaea alba* L.	7	11	7	7	8	3	0	Hyd

38.	*Nymphoides peltata* (Gmel.) Ktze.	8	11	8	7	8	5	0	Hyd
39.	*Petasites hybridus* (L.) Sch.	6	8	7	8	7	2	0	G (H)
40.	*Pedicularis palustris* L.	4	9	6	2	7	3	0	T, H
41.	*Phragmites australis* (Cav.) Trin. ex Steud	5	10	7	5	7	4	1	Hyd, G
42.	*Polygonum amphibium* L.	5	11	7	7	7	4	0	Hyd, H
43.	*Potamogeton crispus* L.	5	12	7	6	6	3	1	Hyd
44.	*Potamogeton fluitans* Roth.	6	12	7	6	6	5	0	Hyd
45.	*Potamogeton gramineus* L.	4	12	7	3	8	4	0	Hyd
46.	*Potamogeton natans* L.	4	12	7	4	6	5	0	Hyd
47.	*Ranunculus repens* L.	5	8	6	6	6	4	1	H
48.	*Salvinia natans* (L.) Allioni	8	11	7	7	7	5	0	Hyd
49.	*Sium latifolium* L.	6	10	7	8	7	4	0	Hyd
50.	*Spirodela polyrrhiza* (L.) Schl.	6	11	7	7	7	5	0	Hyd
51.	*Trapa natans* L.	7	11	6	8	8	5	0	Hyd
52.	*Urticularia vulgaris* L.	6	12	7	5	7	5	0	Hyd
53.	*Wolffia arrhiza* (L.) Wimm.	6	11	7	5	8	7	0	Hyd

Analyzing the ecological characteristics of the macrophytic flora in the Bardača marsh (Table 2), it can be concluded that, besides taxonomic, ecological diversity is also pronounced.

Table 2. The average values of ecologic indexes of flora in the Bardača marsh

Ind. val.	**Ecological indexes**													
	TB		**WB**		**RB**		**NB**		**LB**		**KB**		**SB**	
	№	%	№	%	№	%	№	%	№	%	№	%	№	%
0	-	-	-	-	-	-	-	-	-	-	-	-	46	86,79
1	0	-	0	-	0	-	0	-	0	-	0	-	7	13,21
2	0	-	0	-	0	-	2	3,78	0	-	4	7,55	0	-
3	0	-	0	-	0	-	6	11,32	0	-	17	32,08	0	-
4	4	7,55	0	-	0	-	12	22,64	2	3,77	15	28,30	0	-
5	27	50,94	0	-	4	7,55	9	16,98	3	5,66	14	26,41	0	-
6	13	24,53	0	-	15	28,30	7	13,21	7	13,21	0	-	0	-
7	7	13,21	3	5,66	25	47,17	9	16,98	25	47,17	3	5,66	0	-
8	2	3,77	10	18,87	9	16,98	8	15,09	15	28,30	0	-	0	-
9	0	-	14	26,42	0	-	0	-	1	1,89	0	-	0	-
10	-	-	7	13,21	-	-	-	-	-	-	-	-	-	-
11	-	-	11	20,75	-	-	-	-	-	-	-	-	-	-
12	-	-	8	15,09	-	-	-	-	-	-	-	-	-	-
Σ	53	100,00	53	100,00	53	100,00	53	100,00	53	100,00	53	100,00	53	100,00
$\bar{x}$	5,55		9,70		6,74		5,36		6,96		3,96		0,13	

Analyzing the ecological index for temperature, we conclude that the marsh is dominated by the montane mesophilous broad-leaved forest belt (TB_5–50.94%, 27 plants). To a lesser extent, there is representation of the submontane broad leaved forest belt (TB_6–24.53%, 13 plants), while the thermophilous forest or woodland belt (TB_7–13.21%, 7 plants), montane needle-leaved forest or taiga belt (TB_4–7.55%, 4 plants), and submediterranean woodland and grassland belt (TB_8–3.77%, 2 plants) are even less represented.

Analyzing the ecological index for soil moisture, we find that the most represented are plants of wet, not well aerated soils (WB_9–26.42%, 14 plants), followed by water plants with floating of partly seergent leaves (WB_{11}–20.75%, 11 plants), plants of moist soils tolerating short floods (WB_8–18.87%, 10 plants), water plants, most wholly submersed in water (WB_{12}–15.09%, 8 plants), while the least represented are plants of frequently flooded soils (WB_{10}–13.21%, 7 plants) and plants of moist soils not drying out and well aerated (WB_7–5.66%, 3 plants).
Analyzing the ecological index for acidity or soil reaction, it can be observed that dominate basifrequent plants, mostly on basic soils (RB_7–47.17%, 25 plants), slightly less represented are wide-tolerant plants, mostly found on neutral soils, but also on acidic and basic ones (RB_6–28.30%, 15 plants), as well as plants of basiphilous sites (RB_8–16.98%, 9 plants). The smallest percentage is occupied by plants of slightly acid soils (RB_5–7.55%, 4 plants).
Regarding the mineral nitrogen content in the soil, plants of submesotrophic habitats dominate (NB_4–22.64%, 12 plants), followed by plants of mesotrophic habitats and plants on soils rich in mineral nitrogen ($NB_{5,7}$–16.98%, 9 plants). To a lesser extent, there are indicator plants of nitrogen on fertilized soils (NB_8–15.09%, 8 plants) and plants of moderately nutrient rich habitats (NB_6–13.21%, 7 plants). The fewest plants belong to moderately oligotrophic habitats (NB_3–11.32%, 6 plants) and plants of habitats very poor in nitrogen (NB_2–3.78%, 2 plants).
Analyzing the ecological index for light regime, we conclude that the most represented are halflight plants, mostly living in full light but also shadow tolerants (LB_7–47.17%, 25 plants). A smaller percentage is occupied by light plants whose photosynthetic minimum is above 40% relative light intensity (LB_8–28.30%, 15 plants), as well as halfshadow-halflight plants, whose photosynthetic minimum is 10-40% relative light intensity (LB_6–13.21%, 7 plants). Only a few percent are taken up by halfshadow plants receiving more than 10% but less than 100% relative light intensity (LB_5–5.66%, 3 plants) and shadow-halfshadow plants whose photosynthetic minimum is 5-10% relative light intensity (LB_4–3.77%, 2 plants). One plant of full light of open habitats was found, which does not receive less than 50% relative light intensity (LB_9–1.89%).
Regarding continentality, we found that oceanic-suboceanic species are the most represented (KB_3–32.08%, 17 plants), followed by suboceanic species (KB_4–28.30%, 15 plants) and an intermediate type of plants with a slightly suboceanic-subcontinental character (KB_5–26.41%, 14 plants). Oceanic species are the least represented (KB_2–7.55%, 4 plants), as well as continental-subcontinental species (KB_7–5.66%, 3 plants).
Analyzing the ecological index for soil salinity, we concluded that as many as 46 plants (SB_0–86.79%) belong to halophob species not occurring in salty or alkalic soils, while only 7 plants (SB_1–13.21%) are plants that tolerate salt but mostly live on non-saline soils.

Table 3. Spectrum of life forms in flora in the Bardača marsh

Life form	№ of species	%
Hydrophytes (Hyd)	29	54,71
Geophytes (G)	4	7,55
Hemicryptophytes (H)	18	33,96
Chamaephytes (Ch)	1	1,89
Therophytes (T)	1	1,89
Σ	53	100,00

Through the analysis of the biological spectrum of flora, five life forms were found. Hydrophytes (Hyd) are the most dominant, accounting for 54.71% (29 species) of the total number of found plants. A significant percentage belongs to hemicryptophytes (H) (33.96%; 18 species), while geophytes account for 7.55% (4 species). Only one plant belongs to chamaephytes and therophytes (1.89%).

Conclusion

The research provides an overview of the macrophytic flora and its ecological characteristics in the Bardača marsh, encompassing ecological indicator values and life form spectra. A total of 53 macrophytic flora species were identified. Analysis of ecological indices for temperature and moisture indicates a dominance of montane mesophilous broad-leaved forest belt, alongside plants from wet, not well aerated soils and water plants with floating leaves. Soil pH and mineral nitrogen content predominantly favor basifrequent plants and those from submesotrophic and mesotrophic habitats. Light regime analysis reveals a prevalence of halflight plants. Regarding continentality and salinity, the most represented are oceanic-suboceanic and halophob species. The marsh exhibits a diverse ecological spectrum, emphasizing the need for conservation efforts to protect its unique biodiversity.

References

1. T. Maksimović, S. Lolić, B. Kukavica, Seasonal Changes in the Content of Photosynthetic Pigments of Dominant Macrophytes in the Bardača Fishpond Area, *Ekológia*, **39(3)**, 201–213, 2020.
2. S. Obratil, Ekološki pristup utvrđivanju štetnosti ihtiofagnih ptica u ribnjacima Bardača, *Glasnik Zemaljskog muzeja Bosne i Hercegovine u Sarajevu*, 19–20, 139–256, 1980.
3. B. Nedović,V. Mejakić, Ekologija i prostorna distribucija makrofita u močvarno-barskom ekosistemu Bardače, *Ecologica, posebno izdanje 4*, Beograd – Banjaluka, 1997.
4. N. Šumatić, Lj. Toplić, D. Pavlović-Muratspahić, Zajednica Polygono-Bidentetum tripartitae (W. Koch 26) Lohm. 50 na Bardači, *Zbornik radova Naučnog skupa „Zasavica 2001"*, 122-128, 2001.
5. B. Nedović, R. Lakušić, Z. Kovačević, B. Marković, „Raznoliki živi svijet", in *Život u močvari (Life in wetland)*, Ž. Šarić, Č. Maksimović, M. Stanković, D. Butler, Eds. Laktaši, Urbanistički zavod RS a. d., Grafomark, 2004, 88-97.
6. Z. Kovačević, *Vaskularna flora i akvatična vegetacija Bardače*, Magistarska teza, Poljoprivredni fakultet, Univerzitet u Banjaluci, 2005.
7. Z. Kovačević, M. Kojić, Ekološke i fitogeografske karakteristike hidrofita kompleksa Bardača, *Agroznanje*, **7(3)**, 35-46, 2006.
8. Z. Kovačević, N. Šumatić, S. Stojanović, M. Kojić, Makrofitska flora kompleksa Bardača, *Glasnik Republičkog zavoda za zaštitu prirode Crne Gore*, **31**, 2007.
9. B. Davidović, *Distribucija i diverzitet makrofitske flore ribnjaka Bardače*, Magistarska teza, Prirodno-matematički fakultet, Univerzitet u Banjaluci, 2007.
10. Ramsar Sites Information Service. Bardaca Wetland [Online]. Available: https://rsis.ramsar.org/ris/1658
11. CIN. Database of protected areas [Online]. Available: https://cin.ba/en/baza-zasticenih-podrucja/
12. D. Crnić-Babić, O. Pušić-Babić, Međunarodno pravna zaštita močvarnih staništa u Bosni i Hercegovini, *Сварог*, **1(7)**, 2013.
13. Službeni glasnik Republike Srpske 50/02
14. T. G. Tutin, V. H. Heywood, N. A. Burges, D. M. Moore, D. H. Valentine, S. M. Walters, D. A. Webb, *Flora Europaea*, Berkeley, California Botanical Society, 1964-1980.
15. A. Borhidi, *Social behavior types of the Hungarian flora, its naturalness and relative ecological indicator values*, Janus Pannonicus Tudományegyetem Növénytani Tanszék, Pécs, 1993.
16. E. Oberdorfer, *Pflanzensoziologische Exkursionsflora fiir Siiddeutschland*, Eugen Ulmer, Stuttgart, 1979.

Selected thiazole derivative as copper corrosion inhibitor in acidic solution

Đenđi Vaštag[1,*], Suzana Apostolov[1], Gorana Mrđan[1], Borko Matijević[1]

[1]*University of Novi Sad, Faculty of Sciences, Novi Sad, Serbia*

[*]*djendji.vastag@dh.uns.ac.rs*

Abstract

Copper, as one of the most important non-ferrous metals, is widely used in various parts of the industry. Copper has good corrosion properties in wide range of pH, but in acidic solution (pH< 5) copper corrosion takes place rapidly. Among many ways of copper corrosion protection, in acidic media the application of inhibitors is one of the most widely used methods. In this paper possibility of corrosion protection of copper was investigated in acidic media using inhibitors. Inhibitor properties of 5-(4`-aminobenzylidene)-2,4-dioxotetrahydro-1,3-thiazole, (ABDT) was tested on copper corrosion in acidic sulfate contains solution (0.1 moldm^{-3} Na_2SO_4, pH=3), using potentiostatic polarization measurements and electrochemical impedance spectroscopy (EIS). It was found that in given experimental condition ABDT derivative acts as cathodic inhibitor on copper corrosion, whereby the efficiency of the inhibitor depended on using concentration. The obtained results indicate that investigated thiazole derivate exerts inhibiting properties against copper corrosion during the adsorption on the metal surface following the mechanism of Langmuir isotherm.

Keywords: *copper;corrosion;thiazole deivatives*

Solar-Driven Photocatalytic Degradation of the Fluoroquinolone Antibiotic Ciprofloxacin Employing ZnO Nanoparticles Synthesized Using Green Tea Extract

Dušica Jovanović[1,*], Nina Finčur[1], Sanja Panić[2], Vesna Despotović[1], Sabolč Bognar[1], Daniela Šojić Merkulov[1]

[1] *University of Novi Sad Faculty of Sciences, Department of Chemistry, Biochemistry and Environmental Protection, Trg Dositeja Obradovića 3, 21000 Novi Sad, Serbia*

[2] *University of Novi Sad, Faculty of Technology Novi Sad, Bulevar Cara Lazara 1, 21000 Novi Sad, Serbia*

[*] *dusica.jovanovic@dh.uns.ac.rs*

Abstract

Ciprofloxacin (CIP), a broad-spectrum fluoroquinolone antibiotic, is a popular choice for treating infectious diseases in human and veterinary medicine. As organic micropollutants, fluoroquinolone antibiotics have swiftly become a major concern due to their potential calamitous impact on the aquatic ecosystems, and human health in the long run. Since safe and clean water is the ultimate endgame, the possible solution is the green and eco-friendly advanced oxidation process known as photocatalysis. This process relies on the generation of various reactive species (mainly HO•), that can degrade and sometimes even entirely mineralize the pollutant molecules to products that exhibit less environmental harm than the initial compounds. In this study, ZnO nanoparticles, synthesized using green tea extract, were employed in the removal of CIP from the aqueous medium utilizing simulated sunlight. The influence of the catalyst loading and initial substrate concentration on CIP removal efficiency was studied (optimal conditions: 0.5 mg/cm^3 and 0.05 mmol/dm^3). Moreover, the maximum solubility of CIP (0.041418 g/dm^3) was investigated in water as the solvent of interest. Finally, ZnO catalyst was doped with iron, whrereby its photocatalytic activity was enchanced.

Keywords: *ciprofloxacin; photocatalysis; ZnO; green tea extract*

Acknowledgements

This research was supported by the Science Fund of the Republic of Serbia (Grant No. 7747845, *In situ* pollutants removal from waters by sustainable green nanotechnologies – CleanNanoCatalyze) and the Ministry of Science, Technological Development and Innovation of the Republic of Serbia (Grant No. 451-03-66/2024-03/200125 and 451-03-65/2024-03/200125).

Opportunities for the application of coordination compounds of cobalt for the synthesis of multivalent oxide (Co_3O_4)

Enisa Selimović[1,*], Vladimir Panić[1–3]

[1] *State University in Novi Pazar, Department of Natural Sciences and Mathematics, Vuka Karadžića 9, Novi Pazar, Serbia*

[2] *Institute of Chemistry, Technology, and Metallurgy, National Institute of the Republic of Serbia, Department of Electrochemistry, University of Belgrade, Njegoševa 12, Belgrade, Serbia*

[3] *ICTM Center of excellence for of environmental chemistry and engineering, University of Belgrade, Belgrade, Serbia*

[*] *eselimovic@np.ac.rs*

Abstract

The aim of this paper is to present an overview of literature data on the synthesis of cobalt oxide nanoparticles Co_3O_4 by the method of thermal decomposition of coordination compounds. Six different coordination compounds played the role of precursors. The paper describes a pathway from precursor synthesis to transformation into cobalt oxide nanoparticles Co_3O_4 .The performance of the resulting nanoparticles was compared to nanoparticles obtained by other methods and from different types of precursors. In addition, the compared literature data are useful, in terms of both simplicity and cost-effectiveness and the ecological acceptability of the thermal decomposition method.
Keywords: *complexes; oxides; nanoparticles Co_3O_4; thermal decomposition; electrocatalysts.*

Introduction

Cobalt-mixed-oxide Co_3O_4 is non-toxic and hence considered a material with promising multiple applications. The increasing consumption of energy requires innovative sources and innovative devices for chemical energy conversion and storage. In addition to batteries, a potential source can also be a supercapacitor whose properties depend on the material of the electrode. Therefore, it is important to synthesize or discover an electrochemically-active material with adequate characteristics for a supercapacitor that meets modern trends [1]. Modified Co_3O_4, or more precisely, Co_3O_4/graphene nanocomposite, is one such material [2].

By electrolysis of water from renewable energy sources, environmentally friendly hydrogen is produced, which represents a promising path towards achieving a carbon-neutral economy [3–5]. Cobalt-mixed-oxide Co_3O_4 can be used as a catalytically active anodic component for electrolysis under alkaline conditions as an alternative to expensive precious metals.

In recent years, there has been a lot of research of economically more efficient electrocatalysts for oxygen evolution reaction (OER). Transition metals and their oxides have shown a good relationship between stability, and OER activity. Cobalt oxides obtained by different methods also belong to this group of these oxides [6–8]. The need for a simple synthetic method of producing pure Co_3O_4 oxide nanoparticles without the use of organic surfactants has become increasingly important [9]. One possible pathway implies the use of coordination compounds, *i.e*. Co complexes as precursors. Cobalt oxide nanoparticles were used to create a metal oxide-based electrode with improved properties. They can be synthesized using thermal decomposition of appropriate coordination compounds [10]. This method has attracted interest due to its advantages. Namely, the path was simple, without additional purification steps, and the obtained product had an expected stoichiometry [11]. The intermediates, produced while the precursors break down thermally, serve as protective agents and play an important role in creation of nanoparticles with distinctive morphologies, which is another benefit [12].

The literature data presented below illustrate that the topic is current and that complex compounds can be suitable potential precursors.
This paper presents the preparation of cobalt oxide nanoparticles (*N*) from six different complex compounds (*C*) that were used as precursors.

From coordination compounds to cobalt oxide nanoparticles Co_3O_4

Synthesis of complexes

Synthesis of complex C1

Complex *C1*, $[Co(C_6H_5COO)_2(N_2H_4)_2]$ (cobalt benzoate dihydrazinate), was synthesized according to the protocol published by Thangavelu *et al.* (2011) [9]. The complex was prepared by mixing an aqueous solution of *cobalt(II)-nitrate hexahydrate* (0.01 mol) and an aqueous solution of *hydrazinium benzoate* (0.02 mol) *in-situ* with constant stirring. The synthesized complex is stable in air and insoluble in water. The formation of the cobalt complex precursor can be represented by the equation:
$Co(NO_3)_2 \cdot 6H_2O + 2C_6H_5COON_2H_5 \rightarrow [Co(C_6H_5COO)_2(N_2H_4)_2] + 2HNO_3 + 6H_2O$

Synthesis of complex C2

Dinuclear complex *C2*, $[(NH_3)_5Co(O_2)Co(NH_3)_5](NO_3)_4$, was synthesized according to the protocol published by Parry, 1970 [13]. The dinuclear complex was prepared starting from an aqueous solution of *cobalt(II)-nitrate hexahydrate*, by dissolving 5 g in 100 mL of water (0.017 mol) and subsequent filtering. Aqueous *ammonia* solution (15 M, 25 mL) was then added, and the mixture was cooled to 5–15 °C. An oxygen flow (1000 mL/min, *i.e.*, fast current) is passed through the mixture for one hour, stirring with a magnetic stirrer. Oxygen can be replaced with air, in which case a longer procedure (2–3 h) at 0–5 °C is recommended. Then 5 mL of aqueous sodium nitrate solution (0.024 mol) is added. Oxygen (or air) is passed through the solution for another hour, and the mixture is cooled in ice towards the end of this period. The dark brown crystals are collected on a glass filter and washed with a small amount of 15 M aqueous ammonia and then with ethanol.

Synthesis of complex C3

The precursor in the form of the complex compound *C3* was synthesized by a procedure developed by Meghdadi *et al.* (2016) [14]. They first synthesized the ligand H2bqbenzo (*bqbenzo*$^{2-}$ {3,4-bis(2-quinolinecarboxamido)benzo-phenone), which is then complexed with cobalt. 1**.**57 g (0,003 mol) of the ligand *H2bqbenzo* was dissolved in 50 mL of chloroform. The solution was added dropwise to the solution obtained by dissolving 0.747 g (0.003 mol) of *cobalt(II) acetate tetrahydrate* in 50 mL of methanol. The resulting red solution was left at room temperature for 4 days to give the red crystals of the complex $[Co^{II}(bqbenzo)]$. The crystals were isolated by filtration, washed with cold methanol, and dried in vacuum.

Synthesis of complex C4

The precursor in the form of the complex compound *C4*, was also synthesized by a procedure developed by Meghdadi *et al*. (2016) [14]. They first synthesized the ligand H2bqb (*bqb*$^{2-}$ {bis(2-quinolinecarboxamido)-1,2-benzen}) which is then complexed with cobalt. 1**.**26 g (0,003 mol) of the ligand *H2bqb* was dissolved in 50 mL of chloroform. The solution was added dropwise to the solution obtained by dissolving 0.747 g (0.003 mol) of *cobalt(II) acetate tetrahydrate* in 50 mL of methanol. The resulting orange-red solution was left at room temperature for 4 days to give the orange-red crystals of the complex $[Co^{II}(bqb)]$. The crystals were isolated by filtration, washed with cold methanol and dried in vacuum. Nanoparticles *N4*, Co_3O_4 are obtained by thermal decomposition of the synthesized complex.

Synthesis of complex C5

Complex *C5*, [Co(HDSH-2H)(H_2O)$_2$], 2,5-hexanedione bis(salicyloylhydrazone) cobalt (II) complex, was synthesized according to the protocol published by Jeragh *et al.* (2014) [15]. The complex was prepared by mixing a solution of the ligand *HDSH*, *(2,5-hexanedione bis(salicyloylhydrazone)* (3 mmol), dissolved in 20 mL of absolute ethanol, and a solution of the metal salt *cobalt(II)-chloride hexahydrate* (3 mmol) in 30 mL of absolute ethanol. The mixture was intensively stirred on a hot plate under reflux for 2–4 h. After completion of the reaction, the precipitate was filtered off, washed with ethanol and diethyl ether, and finally dried. After completion of the reaction, the precipitate was filtered off, washed with ethanol, diethyl ether and finally dried.

Synthesis of complex C6

Complex *C6*, [Co(ADH)(H_2O)Cl_2].2H_2O, as adipic acid dihydrazide cobalt (II) complex, was synthesized according to the protocol published by Jeragh *et al.* (2014) [16]. A mixture of the ligand *ADH* (adipic acid dihydrazide) (1 mmol), dissolved in 30 mL of absolute ethanol, and the metallic salt of *cobalt(II)-chloride hexahydrate* (2 mmol), dissolved in 20 mL of absolute ethanol, was heated under reflux in a water bath for 2–4 h.

Synthesis of Co_3O_4 nanoparticles

Synthesis of nanoparticles N1

Co_3O_4 nanoparticles *N1* were synthesized according to the protocol published by Thangavelu *et al.* (2011) [9]. After being moved to a spotless silicon crucible, the complex *C1* was heated first slowly over a low flame and then intensely. The complex was transferred to a clean silica crucible and gently heated with a low flame, then strongly heated. During heating, the complex completely disintegrated, giving nanoparticles Co_3O_4. The formation of cobalt oxide can be represented by the equations:

a) $[Co(C_6H_5COO)_2(N_2H_4)_2] + 16O_2 \rightarrow CoO + 2N_2H_4 + 14CO_2 + 5H_2O$

b) $6CoO + O_2 \rightarrow 2Co_3O_4$

The nanoparticles are characterized by Raman, XRD (X-ray diffraction), SEM (scanning electron microscopy) and TEM (transmission electron microscopy). The advantage of using the complex as a precursor, in this case, is to obtain fine particles of *N1*, cobalt oxide, of high purity after the distribution of metal ions in the 3D coordination sphere.

TEM analysis confirmed almost uniform Co_3O_4 nanoparticles with an average particle size of about 20 nm, whereby the problem of agglomeration was successfully overcome. The TEM image suggests that this preparation method is appropriate for producing smaller-sized Co_3O_4 nanoparticles and that it successfully tackles the problem of agglomeration.

Synthesis of nanoparticles N2

Nanoparticles *N2* was synthesized according to the protocol published by Goudarzi *et al.* (2014) [17].The resulting powder (0.01 mol) of the *C2* as dinuclear Co(III) complex, was thermally treated at 500 °C in air. The temperature rise was 30 °C per min until the set temperature value was reached. Thermal treatment at 500 °C lasts 3 h and cooling is carried out at room temperature. As a result of heating, a black nanocomposite based on Co_3O_4 is formed.. The nanoparticles are characterized by XRD, FT-IR (Fourier-transform infrared spectroscopy), SEM and TEM.

The diameter of *N2* nanoparticles was calculated according to Scherrer's formula and was 25–30 nm. SEM analysis confirmed that *N2* particles have fairly uniform spherical dimensions and tend to form agglomerates which can grow further when treated at a temperature of 600 °C. TEM analysis confirmed the spherical shape of the particles, the presence of dense agglomerates, and their uneven distribution (10–15 nm). The advantage of the proposed method of thermal decomposition of the

complex for obtaining nanoparticle Co_3O_4 is that it is simple and economically feasible, without extreme conditions, which is also suitable for mass production.

Synthesis of nanoparticles N3 and N4

Nanoparticles *N3* and *N4* were synthesized by thermal decomposition of complexes *C3* and *C4*, respectively, according to the same method developed by Meghdadi *et al*. (2016) [14]. The calcination temperature for each complex was determined based on the results of TG-DTA/vide infra (thermogravimetric/differential thermal analysis). Each cobalt complex was ground and placed in a pre-dried ceramic crucible. The crucibles were heated in a furnace at 500 °C for 2 h in the presence of air. The samples were then cooled to room temperature, and the black Co_3O_4 nanocrystals were collected and characterized by FT-IR, XRD, and field emission scanning electron microscopy (FE-SEM).

The catalytic activity of nanoparticles of *N3* and *N4* was also studied by LSV (Linear sweep voltammetry) and Tafel plot in 1 M KOH at room temperature. The results showed that, compared to the conventional Pt/C 10 wt. % Pt catalyst, both *N3* and *N4* cobalt oxides, showed improved OER activity in alkaline medium. However, *N3* nanoparticles have more acceptable activity and stability during OER.

Synthesis of nanoparticles N5 and N6

Nanoparticles *N5* and *N6* were obtained by autocatalytic decomposition of precursors, according to the procedure used by Madkour *et al*. (2016) [18]. The obtained precursors *C5* and *C6* in the form of complex compounds were dried and transferred to two silicon dioxide crucibles and then heated to 550 °C in air atmosphere for about 60 min, with a heating rate of 15 °C/min in accordance with the thermal behavior of the precursor. The complete decomposition of the precursor complexes led to the formation of the oxide nanoparticles, which were cooled to room temperature. After that, they are well ground and stored.

SEM analysis showed that the morphology of nanoparticles *N5* and *N6* depends on the geometry of the precursor. As the geometry changed from octahedral to square pyramidal, the morphology varied from hemispherical aggregations to pyramidal. One of the advantages of this method is that by controlling the geometry of the complex compound precursor, the morphology of cobalt oxide nanoparticles can be controlled. Photocatalytic activity measurements showed the superior efficiency of the synthesized nanoparticles, and the relationship between morphology and photo efficiency was established.

Conclusion

The method of thermal decomposition of complex compounds seems very interesting because the results showed that in this way, starting from various complex compounds as precursors, nanoparticles of cobalt oxide with better performance can be obtained, such as high purity, pronounced OER activity in an alkaline environment and stability during OER, controlled particle morphology and better photocatalytic activity. Also, uniform nanoparticles can be obtained from suitable precursors with controllable agglomeration. In addition, the advantage of the thermal decomposition method is reflected in a simple way, without the use of special instruments, large financial investments and without extreme reaction conditions that are often not environmentally acceptable.

In future research, the authors of this paper will use new complex compounds as precursors to obtain nanoparticles Co_3O_4 to reach better and controlled oxide characteristics.

Acknowledgements

Authors wish to acknowledge the support of the Science Fund of the Republic of Serbia PROJECT NUMBER 6666, Renewal of the Waste Oxygen-Evolving anodes from Hydrometallurgy and their improved Activity for Hydrogen Economy, Wastewater and Soil Remediation - OxyRePair.

References

1. A. Soam, C. Mahender, R. Kumar, M. Singh, Power performance of BFO–graphene composite electrodes based supercapacitor, *Mater. Res. Express* , **6**, 025054, 2019.
2. R. Lakra, R. Kumar, P. K. Sahoo, D. Sharma, Dhirendranath Thatoi a, A. Soam, Facile synthesis of cobalt oxide and graphene nanosheets, nanocomposite for aqueous supercapacitor application, *Carbon Trends*, **7**, 100144, 2022.
3. O. Bic Ková, P. Straka, Production of hydrogen from renewable resources and its effectiveness, *International Journal of Hydrogen Energy*, **37**, 11563–11578, 2012.
4. H. Ishaq, I. Dincer, C. Crawford, A review on hydrogen production and utilization: Challenges and opportunities, *International Journal of Hydrogen Energy*, **47**, 26238-26264, 2022.
5. P. J. Megía, A. J. Vizcaíno, J. A. Calles, A. Carrero, Hydrogen Production Technologies: From Fossil Fuels toward Renewable Sources. A Mini Review, *Energy Fuels*, **35**(20), 16403–16415, 2021.
6. N. H. Chou, P. N. Ross, A. T. Bell, T. D. Tilley, Comparison of cobalt-based nanoparticles as electrocatalysts for water oxidation, *ChemSusChem*, **4**, 1566–1569, 2011.
7. T. Maiyalagan, K. A. Jarvis, S. Therese, P. J. Ferreira, A. Manthiram, Spinel-type lithium 316 cobalt oxide as a bifunctional electrocatalyst for the oxygen evolution and oxygen 317 reduction reactions, Nat. Commun., **5**(3949), 1–8, 2014.
8. N. Suzuki, T. Horie, G. Kitahara, M. Murase, K. Shinozaki, Y. Morimoto, Novel noble-metal-free electrocatalyst for oxygen evo-lution reaction in acidic and alkaline media, *Electrocatalysis*, **7**, 115–120, 2016.
9. K. Thangavelu, K. Parameswari, K. Kuppusamy, Y. Haldorai, A simple and facile method to synthesize Co_3O_4 nanoparticles from metal benzoate dihydrazinate complex as a precursor, *Mater. Lett.*,**65**, 1482–1484, 2011.
10. R. K. Gupta, A. K. Sinha, B. N. Raja Sekhar, A. K. Srivastava, G. Singh, S. K. Deb, Synthesis and characterization of various phases of cobalt oxide nanoparticles using inorganic precursor, *Appl. Phys. A Mater. Sci. Process*, **103**, 13–19, 2011.
11. A. T. Kelly, I. Rusakova, T. Ould-Ely, C. Hofmann, A. Lüttge, K. H. Whitmire, Iron Phosphide Nanostructures Produced from a Single-Source Organometallic Precursor: Nanorods, Bundles, Crosses, and Spherulites, *Nano Letters*, **7**, 2920-2925, 2007.
12. R. Gaur, P. Jeevanandam, Effect of anions on the morphology of CdS nanoparticles prepared via thermal decomposition of different cadmium thiourea complexes in a solvent and in the solid state, New Journal of Chemistry, **39**, 9442-9453, 2015.
13. R. W. Parry, Inorganic Syntheses, McGraw-Hill Book Company, 1970, Vol. XII.
14. S. Meghdadi, M. Amirnasr, M. Zhiani, F. Jallili, M. Jari, M.Kiani, Facile Synthesis of Cobalt Oxide Nanoparticles by Thermal Decomposition of Cobalt(II) Carboxamide Complexes: Application as Oxygen Evolution Reaction Electrocatalyst in Alkaline Water Electrolysis, *Electrocatalysis*, **8**, 122-131, 2016.
15. B. Jeragh, A. A. El-Asmy, Spectroscopic and structural study of some 2,5-hexanedione bis(salicyloylhydrazone) complexes: Crystal structures of its Ni(II) and Cu(II) complexes and N-(2,5-dimethyl-1H-pyrrol-1-yl)-2-hydroxy-benzamide, *Spectrochimica Acta Part A: Molecular and Biomolecular Spectroscopy*, **129**, 307-313, 2014.
16. B. Jeragh, A. A. El-Asmy, Structure and spectroscopic studies of homo-and heterometallic complexes of adipic acid dihydrazide, *Spectrochimica Acta Part A: Molecular and Biomolecular Spectroscopy*, **125**, 25-35, 2014.
17. M. Goudarzi, M. Bazarganipour, M. Salavati-Niasari, Synthesis, characterization and degradation of organic dye over Co_3O_4 nano-particles prepared from new binuclear complex precursors, *RSC Adv*., **4**, 46517–46520, 2014.

18. M. Madkoura, Y. K. Abdel-Monemb, F. Al Sagheera, Controlled synthesis of NiO and Co_3O_4 nanoparticles from different coordinated precursors: The impact of precursor's geometry on the nanoparticles characteristics, *Industrial & Engineering Chemistry Research*, **55**(50), 12733–12741, 2016.

Distribution of essential and potentially essential elements in wild fruit from the Pešter Plateau in the Republic of Serbia

Enisa Selimović[1,*], Bojana Veljković[1], Aleksandra Pavlović[2], Emilija Pecev-Marinković[2]

[1]*State University in Novi Pazar, Department of Natural Sciences and Mathematics, Vuka Karadžića 9, Novi Pazar, Serbia*

[2]*Department of Chemistry, Faculty of Sciences and Mathematics, University of Niš, Višegradska 33, P.O.Box 224, 18000 Niš, Serbia*

[*]*eselimovic@np.ac.rs*

Abstract

The aim of this work was to determine the content of essential and potentially essential elements in selected samples of wild fruits from the Pešter Plateau in the Republic of Serbia. The wild fruit is used as food and drugs in traditional medicine on the Pešter Plateau. Five samples of wild fruit were collected from three locations. In this work three species of fruits were studied : common juniper, blackthorn, and blueberry. The content of six potentially essential elements (B, Co, Mn, Ni, Si and V) and five essential elements (Cu, Fe, Cr, Zn and Se) were determined. In most cases, the results showed that the content of microelements in fruit is affected by the type of samples, but not by the location where they were collected. The average contents of essential microelements are decreasing in the following order: Fe > Zn > Cu > Cr > Se, for all species. The average contents of potentially essential trace elements decrease in the following order: Mn > Si > B > Ni > V > Co, in common juniper and blueberry, and Si > B > Mn > Ni > Co > V in blackthorn samples. The obtained data can supplement and clarify the data available in the literature as well as the database on the chemical composition of foods.

Keywords*: wild berries; elements; ICP OES; Pešter Plateau.*

Introduction

The Pešter Plateau, in a narrower sense, is the highest plateau on the Balkan Peninsula and among the highest in Europe. The Pešter field, with an area of 63 square kilometers at 1,150 m above sea level, is a unique oasis of nature. That part has been declared a nature reserve and is under special protection [1]**.** The main resources of the Pešter Plateau are the still-preserved natural environment (lush pastures, meadows, forests, and clean water) that enables the production of healthy food.

For that reason, nowadays, there is an emerging interest in the international community in consuming many underutilized wild food plants, with a linkage between agriculture, nutrition, and health [2].

Berries and related species occupy a very important place in people's daily diets because of their high content of vitamins, minerals, polysaccharides, essential oils, and phytochemical substances, and especially because of their antioxidant protection [3]. In addition to organic compounds, various minerals and trace metals are present in the fruits [4,5]. Metals may be naturally present in the fruits or may enter the fruit as a result of human activities such as industrial or agricultural processes. They can have both beneficial and harmful effects on human health [6]. Trace elements play an important role in the functioning of the human body. They mainly act as cofactors for various enzymatic systems (generally redox-active metals) or possess regulatory activity [7].

Juniper berries (*J. communis L.)*, nowadays, the cones and their essential oils are recognized by the European Pharmacopoeia and are pharmaceutical raw materials. Nowadays, the cones of *J. communis* and their essential oils are recognized by the Official Pharmacopoeias of Austria and Switzerland, as well as the European Pharmacopoeia. The strong antibacterial, antifungal, antiviral, antioxidant, and antiinflammatory properties are characteristic of the essential oil of *J. communis* cones; therefore, it is used in contemporary pharmacy for healing colds or as a bacterial and fungal antiseptic [8,9].

Blackthorn (*Prunus spinosa L.),* despite being widespread in Spain, it is ethnobotanic use is best known in Navarra, where infusions of its branches are used in the treatment of hypertension [10] and its macerated fruits for gastrointestinal disturbances and in the preparation of a type of schnapps called 'pacharan [11].
Blueberry (*Vaccinium myrtillus L.*) is one of the most popular wild-harvested fruits in many North American countries, traditionally used as a healthy food as well as in folk medicine. Headaches, fever, eye problems, diarrhea, and other problems have all apparently been eased or cured by various vaccines [12].
The content of six potentially essential elements and five essential elements were determined by the Inductively Coupled Plasma Optical Emission Spectrometry method (ICP OES).

Experimental

Material

The 65% nitric acid (Merck, Germany) and 30% hydrogen peroxide (Fluka, Switzerland) were used for sample preparation. All glassware was soaked in 10% HNO_3 for at least 12 hours and rinsed with ultrapure distilled water. All plastic containers were rinsed with 20% v/v HNO_3 and rinsed with ultrapure (0.05 µS cm^{-1}) deionized water (MicroMed high purity water system, TKA Wasseraufbereitungssysteme GmbH) before use. All chemicals were of analytical grade. Before analysis, the fruit samples were stored in a freezer at -18°C. The corresponding geographic data for each location are listed in Table 1, and the map of the study area, indicating the locations of selected species, is presented in Figure 1.

Table 1. Geographic data on the locations of studied wild fruits from the Pešter Plateau

No. Samples	Species	Latin name	Location	Geographic coordinates		Altitudes (m)
				Longitude	Latitude	
J1	Common juniper	*Juniperus communis*	Zari	42°56'	19°55'	1200
J2	Common juniper	*Juniperus communis*	Gonje	43°20'	19°50'	1250
B2	Wild Blueberry	*Vaccinium myrtillus*	Gonje	43°20'	19°50'	1250
B3	Wild Blueberry	*Vaccinium myrtillus*	Javor	43°25'	20°10'	1519
P3	Blackthorn	*Prunus spinosa*	Javor	43°25'	20°10'	1519

Figure 1. *Location of the studied species*

Methods

For complete mineralization of frozen fruit samples, 2 g were weighed and mixed with 5 mL of concentrated nitric acid and 1 mL of 30% hydrogen peroxide. The contents were transferred to the microwave oven. The temperature program was as follows: heating up to 180 °C for 10 min, then constant heating at the same temperature for 15 min [6]. After cooling, the samples were filtered through quantitative filter paper and diluted with 0.5% HNO_3 to a volume of 25 mL. Until the beginning of the analysis, the samples were stored in plastic vials at 4 °C. A blind test was prepared in an identical way. The inductively coupled plasma atomic emission spectrometer (Thermo Scientific, Cambridge, UK) was an iCAP 6000 series

Results and discussion

Element contents of fruits differed according to fruit variety and type. The average data (concentration ± SD) of eleven selected elements obtained as a result of testing the concentration of micro- (in μg g^{-1}) and macro (in mg g^{-1}) elements in wild and domestic fruits from the Pešter Plateau using ICP OES are shown in Table 2 and 3.

Table 2. Essential microelement contents (μg g^{-1}) in wild fruit samples from the Pešter Plateau

No.	Samples	Cu	Samples	Fe	Samples	Cr
1	J2	3.683±0.092	J2	27.58±0.98	J2	2.730±0.063
2	J1	3.50±0.13	P3	17.894±1.081	J1	2.258±0.012
3	P3	2.34±0.15	J1	14.74±0.57	P3	0.714±0.017
4	B2	1.706±0.015	B2	5.103±0.036	B3	0.394±0.074
5	B3	1.359±0.014	B3	3.43±0.11	B2	0.312±0.030
No.	Samples	Zn	Samples	Se		
1	J2	18.37±0.64	B3	0.319±0.005		
2	J1	13.98±0.55	B2	0.279±0.006		
3	P3	4.910±0.086	J2	0.1321±0.0001		
4	B2	4.21±0.07	J1	0.119±0.007		
5	B3	1.853±0.024	P3	0.035±0.014		

J2/J1 = *Common juniper; P3= Blackthorn;B2/B3 = Wild Blueberry;*

Table 3. Potentially essential microelement contents (μg g^{-1}) in wild fruit samples from the Pešter Plateau

No.	Samples	B	Samples	Co	Samples	Mn
1	J2	28.23±2.34	J2	0.674±0.013	J1	108.55±10.77
2	J1	26.43±1.25	J1	0.520±0.014	B2	62.56±0.49
3	P3	9.690±1.076	P3	0.051±0.002	J2	35.73±0.59
4	B2	2.750±0.084	B2	0.036±0.007	B3	19.94±1.38
5	B3	1.379±0.069	B3	0.023±0.004	P3	7.62±0.48
No.	Samples	Ni	Samples	Si	Samples	V
1	J1	9.60±0.32	J2	59.37±0.48	J1	1.511±0.035
2	J2	4.03±0.17	J1	49.34±0.13	J2	0.95±0.017
3	P3	1.10±0.33	P3	35.79±0.25	P3	0.520±0.075
4	B2	0.899±0.014	B2	10.42±0.15	B2	0.407±0.007
5	B3	0.53±0.01	B3	8.89±0.34	B3	0.2245±0.0007

J2/J1 = *Common juniper; P3= Blackthorn;B2/B3 = Wild Blueberry;*

The results (Table 2 and 3) of the analysis of **common juniper** samples showed values (μg g^{-1}) for microelements: Fe (14.74-27.58) > Zn (13.98-18.37) > Cu (3.50-3.683) > Cr (2.258-2.730) > Se (0.119-0.1321), and: Mn (35.73-108.55) > Si (49.34-59.37) > B (26.43-28.23) > Ni (4.03-9.60) > V (0.95-1.511) > Co (0.520-0.674). It is a very interesting fact that of all examined species, common juniper samples contain the highest amounts of almost all microelements, except Se.
In Lithuania, a multielement analysis of Juniperus communis needles, but not of fruits, was performed at fourteen locations. Samples were analyzed by atomic absorption spectrophotometry [13]. At certain doses, Oxycedrus fruits and leaves extracts were given in streptozotocin (STZ) - induced diabetic rats. The results showed that fruit and leaf extracts reduce blood glucose levels. Increasing zinc levels is also associated with protecting tissues from free radicals [14].
The results (Table 2 and 3) of the examined **blackthorn** in this work showed values (μg g^{-1}) for microelements:: Fe 17.894 > Zn 4.910 > Cu 2.34 > Cr 0.714 > Se 0.035, and: Si 35.79 > B 9.690 > Mn 7.62 > Ni 1.10 > Co 0.051 > V 0.520.
According to literature data, the content of microelements (Zn, Mn, Fe, Cu, and Ni) in thorn from southeastern Serbia, from five locations, was determined by Atomic Absorption Spectroscopy (AAS) [15]. The content of trace elements in the thorn was in the range of Zn (2.82–18.48), Mn (2.22-25.21), Fe (123.8–292.1), Cu (2.57–10, 38), and Ni neither was detected [15]. The values of Fe and Cu in the literature data are higher compared to our results, while the value of Mn is in the range shown.
Also, the content of six microelements (mg kg^{-1}): B (26.99), Cr (2.28), Fe (16.18), Mn (4.58), Ni (1.22), V (3, 01)) of blackthorn growing in Turkey were detected [16]. The content of microelements agrees with the literature data, or their content is less than the data available in the literature. The determined values of Mn and Fe are higher in the blackthorn sample presented in this work.
The contents (μg g^{-1}) of microelements (Table 2 and 3) for the analyzed **wild blueberry** were found in the range of: Fe (3.43 -5.103) > Zn (1.853-4.21) > Cu (1.359-1.706) > Cr (0.312-0.394) > Se (0.279-0.319), and Mn (19.94-62.56) > Si (8.89-10.42) > B (1.379-2.750) > Ni (0.53-0.899) > V (0.2245-0.407) > Co (0.023-0.036). Wild blueberries on the Pešter Plateau contain more essential elements, Cr and Cu, and potentially essential Mn, compared to the results of element content in wild and cultivated fruit grown in central Poland [17]. Zinc concentrations are lower or on par with the compared data. Blueberry samples from Poland showed the following results: wild: Cr (0.023-0.174), Cu (0.24-0.41), Fe (5.31-12.7), Mn (5.82-29.0), Zn (3.83-6.07); cultivated: Cr (0.014-0.033), Cu (0.28-0.32), Fe (5.44-10.70), Mn (2.94-4.47), Zn (2.95-3.79) [17]. It is a very interesting fact that of all examined species, blueberry samples contain the least amounts of almost all microelements.

Conclusion

The results showed that common juniper is significantly richer in almost all microelements, except for selenium, compared to wild blueberries and blackthorn. Wild blueberries contain the smallest amount of tested microelements. In most cases, sample type has a more dominant influence on micronutrient content than location where the samples were collected. Also, if comparing the samples of the same species, it was observed that the location is a more important factor. The obtained data on the content of essential and potentially essential microelements in wild fruits that grow on the Pešter Plateau in Serbia can supplement and clarify the available data in the literature and the database on the chemical composition of foods.

Acknowledgements

The authors gratefully acknowledge financial support from State University of Novi Pazar, Novi Pazar, Republic Serbia.

References

1. "Službeni glasnik RS" br. 114/2015-3; Uredba Vlade Republike Srbije o proglašenju Specijalnog rezervata prirode "Peštersko polje")
2. J. Ganry, Will fruits and vegetables now be part of the international agenda? *Fruits*, **68 (1)**, 1–2, 2013.
3. S. H. Nile and S. W. Park, Edible berries: bioactive components and their effect on human health, *Nutrition*, **30,** 134–144, 2014.
4. A. Venketeshwer Rao, D. M. SnydSSer, J. Agric. *Food Chem*., **58**, 3871–3883, 2010.
5. A. V. Pavlović, D.Č. Dabić, N.M. Momirović, B.P. Dojčinović, D. M. Milojković-Opsenica, Ž. Lj. Tešić, M. M. Natić, J. Agric, *Food Chem*., **61**, 4188–4194, 2013.
6. M. Nikolić, A. Pavlović, S. Mitić, S. Tošić, E. Pecev-Marinković, M. Đorđević and R. Micić, Optimization and validation of an inductively coupled atomic emission spectrometry method for macro- and trace element determination in berry fruit samples, *Analytical Method*, **8 (24)**, 4844-4852, 2016.
7. C. G. Fraga, Relevance, essentiality and toxicity of trace elements in human health, *Mol Asp Med***, 26**, 235–244, 2005.
8. N. Filipowicz, M. Kaminski, J. Kurienda, M. Asztemborska, J. R. Ochocka, Antibacterial and antifungal activity of juniper berry oil and its selected components, *Phytother. Res*., **17**, 227–231, 2003.
9. S. Pepeljnjak, I. Kosalec, Z. Kalodera, N. Blaževic, Antimicrobial activity of juniper berry essential oil (Juniperus communis L., Cupressaceae), *Acta Pharm*., **55**, 417–422, 2005.
10. M. I. Calvo, & R. Y. Cavero, Medicinal plants used for cardiovascular diseases in Navarra and their validation from Officinal sources, *Journal of Ethnopharmacology*, **157**, 268–273, 2014.
11. M. I. Calvo, S. Akerreta, & R. Y. Cavero, The pharmacological validation of medicinal plants used for digestive problems in Navarra, Spain, *European Journal of Integrative Medicine*, **5**, 537–546, 2013.
12. A. Karlsons, A. Osvalde, G. Čekstere, J. Pormale, Research on the mineral composition of cultivated and wild blueberries and cranberries, *Agronomy Research*, **16(2)**, 454-463, 2018.
13. L. Jocienė, E. Krokaitė, T. Rekašius, R. Vilčinskas, A. Judžentienė, V. Marozas, and E. Kupčinskienė, Ionomic Parameters of Populations of Common Juniper (Juniperus communis L.) Depending on the Habitat Type, *Plants*, **12(4)**, 961, 2023.
14. N. Orhana, A. Berkkanb, D.D. Orhana, M. Aslana, and F. Erguna, Effects of Juniperus oxycedrus ssp. oxycedrus on tissue lipid peroxidation, trace elements (Cu, Zn, Fe) and blood glucose levels in experimental diabetes, *Journal of Ethnopharmacology*, **133(2)**, 759–764, 2011.
15. S. S. Randjelovic D. A. Kostic, G. S. Stojanovic, S. S. Mitic, M. N. Mitic, B. B. Arsic, A. N. Pavlovic, Metals content of soil, leaves and wild fruit from Serbia, *Central European Journal of Chemistry*, **12(11),** 1144-1151, 2014.
16. T. Markoglu, D. Arslan, M. Ozcan, H. Hacıseferogulları, Proximate composition and technological properties of fresh blackthorn (Prunus spinosa L. subsp dasyphylla), *Journal of Food Engineering*, **68,** 137–142, 2005.
17. P. Dróżdż, V. Šėžienė, & K. Pyrzynska, Mineral Composition of Wild and Cultivated Blueberries, *Biol Trace Elem Res*,**181(1),** 173-177, 2018.

Corrosion of oil and gas pipelines with special reference to high-frequency welded pipes

Snežana Joksić[1*], Jovana Živić[1] , Živče Šarkoćević[1], Marija Matejić[1]

[1] *University of Pristina with temporary settled in Kosovska Mitrovica, Faculty of Technical Science, Knjaza Miloša, br.7, 38220, Kosovska Mitrovica , Serbia*

[*]*snezana.joksic@pr.ac.rs*

Abstract

In this paper, an overview of the most common problems caused by pipeline corrosion in the oil and gas industry is given. Corrosion is a chemical process that leads to the degradation of metals, which can lead to serious consequences when it comes to the oil industry. When metal, i.e. steel (from which oil and gas transport pipes are made) is found in a chemically aggressive environment, it leads to serious consequences that can threaten the operation of the entire system. Corrosion most often occurs in H_2S (hydrogen sulfide) and CO_2 (carbon dioxide) environments, which in these cases can be predicted, prevented or controlled. However, if it is other types of corrosion, such as stress corrosion, which in most cases cannot be easily removed, then serious and catastrophic pipeline failures occur. Depending on the mechanism of formation and the environment in which it occurs, stress corrosion cracking has a large number of subgroups. It occurs in a combination of stress and a chemically aggressive environment, which lead to the appearance of a crack that is difficult to predict. In the oil and gas industry, pipes are most often made by high-frequency welding without additional material. Welding, which leads to inhomogeneity of the material, is a source for the initiation and propagation of cracks in the material, that is, it leads to stress corrosion cracking or hydrogen embrittlement. Given that corrosion problems represent a major economic challenge in the oil and gas industry, it is necessary to prescribe regular controls and prevention of corrosion in pipelines.

Keywords: *corrosion; oil and gas industry; hydrogen sulphide; carbon dioxide; stress corrosion cracking; high-frequency welding.*

Introduction

Corrosion is a chemical and/or electrochemical reaction between any given material, usually a metal, and its surrounding environment which eventually leads to degradation of the material and its properties [1]. Corrosion is considered to be the main cause of failure in the oil and gas production process, particularly in the transport system. Over the last decades, these corrosion failures have led to concerns about energy security, reduced production rates, financial losses and environmental contamination [1,2]. Due to the development of fields in deeper offshore wells with higher pressure, temperature, and higher levels of hydrogen sulfide, carbon dioxide, and chloride, corrosion costs are increasing.

Corrosion in the modern society is one of the outstanding challenging problems in the industry. Most industrial designs can never be made without taking into consideration the effect of corrosion on the life span of the equipment. Recent industrial catastrophes have it that many industries have lost several billions of dollars as a result of corrosion. Reports around the world have confirmed that some oil companies had their pipeline ruptured due to corrosion and that oil spillages are experienced which no doubt created environmental pollution; in addition, resources are lost in cleaning up this environmental mess, and finally, large-scale ecological damage resulted from corrosion effects [3].

Corrosion occurs in almost all stages of oil manipulation, during exploitation, transportation and processing in industrial plants. In engineering practice related to the exploitation and processing of oil, industrial equipment, installations and plants are subject to a high degree of corrosion due to

difficult working conditions, as well as due to exposure to corrosion agents 2. Corrosion can lead to structural damage, expensive repairs, product contamination, environmental damage, risk to personnel, and loss of public confidence [4]. Stress corrosion, corrosion fatigue, and corrosion erosion are major problems in the aquatic environment. In order to initiate any type of corrosion under mechanical load, in addition to an aggressive environment, an external load is also a significant factor [5].

Controlling and monitoring corrosion in oil and gas pipelines is essential for continuous production and maintenance of normal pipeline operation [6]. There are different types of corrosion, which occur depending on many factors, such as: environment, pipe material, temperature , pressure etc. The following types of corrosion are distinguished in the oil industry:

- General corrosion (the most common type), characterized by a chemical or electrochemical reaction;
- Localized corrosion (pitting corrosion, corrosion in gaps, corrosion under coatings or coatings);
- Galvanic corrosion;
- Stress corrosion (there are different types of stress corrosion, ie a wide range of subgroups);
- Intergranular corrosion;
- High temperature corrosion etc [7].

Internal corrosion in pipelines is influenced by temperature, corrosive gases (CO_2 and H_2S) content, water chemistry, flow velocity, oil or water wetting and composition, sulphate reducing bacteria and surface condition of the steel. Any change in any of these parameters could influence the corrosion rate considerably because it would affect the properties/integrity of the corrosion products that form on the metal surface.

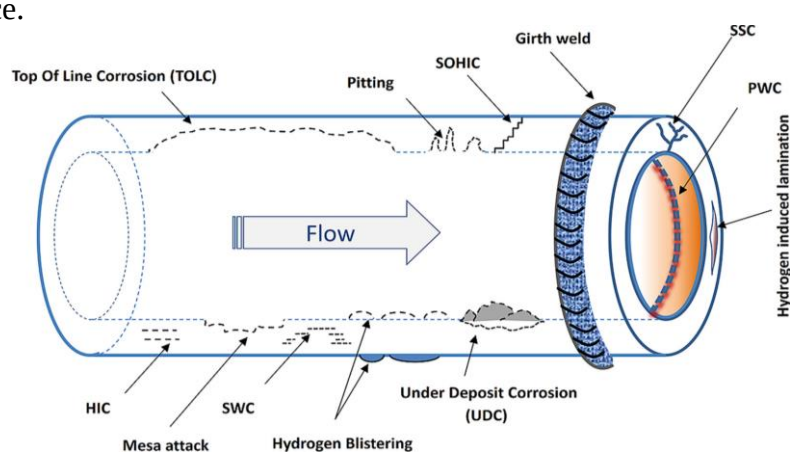

Figure 1. *Presentation of different types of corrosion [8]*

Recently, the challenges of internal corrosion has been a great concern to the oil and gas pipelines due to the increase in water cut over time and most of the previously oil wetted pipelines surface have now become water wetted leading to electrochemical (corrosion) process, and also due to the increasing bacterial activity in the production system [9].

Corrosion due to the presence of CO_2

In addition to numerous researches that have been carried out so far, the corrosion of low-carbon steel in aqueous CO_2 solutions is still a significant problem. When considering the use of low carbon steels, it is necessary to calculate the general CO_2 corrosion rate [6,10].

In the oil industry, together with oil and gas, CO_2 is produced, which dissolves in water. The dissolution of CO_2 in water leads to a decrease in the pH value, i.e. an increase in acidity by the formation of carbonic acid. Such an acidic environment is a source of corrosion of metal surfaces that

are in direct contact with water, that is, until the appearance of CO_2 or "sweet" corrosion. Water injection into a crude oil reservoir is used to bring the oil to the surface. During exploitation, the amount of water increases, which leads to a greater presence of CO_2, and therefore to a greater risk of corrosion [11]. Factors affecting CO_2 corrosion are: partial pressure, temperature, speed and pH value [12]. There are different mechanisms of this type of corrosion, but each of them consists of carbonic acid and bicarbonate ions obtained by dissolving CO_2 in water [13]. The most well-known mechanism of CO_2 corrosion is:

$$H_2CO_3 + e^- \rightarrow H + HCO_3 \quad (1)$$

$$2H \rightarrow H_2 \quad (2)$$

With iron that reacts:

$$Fe \rightarrow Fe^{2+} + 2e^- \quad (3)$$

And it is obtained:

$$CO_2 + H_2O + Fe \rightarrow FeCO_3\,(\text{iron carbonate}) + H_2 \quad (4)$$

Therefore, CO_2 corrosion leads to the formation of $FeCO_3$ (siderite) corrosion product which can represent a protective layer depending on environmental conditions. It has been experimentally determined that the rate of corrosion is significantly affected by the pH value. In conditions of reduced water pH, there is an increase in corrosivity, which leads to pitting corrosion [14]. An increased pH value leads to a decrease in the solubility of $FeCO_3$, which means that it leads to a higher rate of precipitation and the formation of a protective film. Temperature has a significant effect on the formation of the $FeCO_3$ layer. With increasing temperature, the rate of $FeCO_3$ deposition also increases. However, at low pH values and high temperatures, the corrosion rate increases [15]. Another important factor is the chemical composition of the water. If there is a large percentage of chloride ions in the water that are in direct contact with the metal in a CO_2 environment, the process of localized and pitting corrosion will be accelerated [16]. The greatest danger from this type of corrosion is when the temperature reaches the dew point. Then the CO_2 dissolves in the condensed water and forms carbonic acid. Corrosion products then form a brittle film on the pipe surfaces, through which electrolytes reach the metal. According to research, the maximum rate of CO_2 corrosion occurs at temperatures between 60°C and 90°C [17].

CO_2 corrosion of carbon steels in the petroleum industry has been widely investigated. However, corrosion testing at high temperatures (over 100 °C) has not yet been investigated due to the complexity and influencing factors [18]. It is estimated that about 60% of failures and damages in the oil industry can be attributed to CO_2-induced corrosion, and that this type of corrosion is inevitable while carbon steel is used to manufacture drilling, storage and transportation equipment [19]. Although there are other alloys that are resistant to this type of corrosion, carbon steel is still the most cost-effective construction material [20]. The simultaneous presence of CO_2 and H_2S in fluids leads to the formation of an aggressive environment that can lead to serious consequences when it comes to corrosion [21].

Corrosion due to the presence of H_2S

Researchers state that corrosion caused by H_2S has not been sufficiently studied in laboratory conditions due to the difficulty of testing [21]. The primary problem with H_2S hydrogen, which is an aggressive and very dangerous gas, which causes embrittlement of metals (hydrogen embrittlement). Fluids with a high level of H_2S are called acidic, that is, this type of corrosion is called "sour" corrosion. NACE defines H_2S levels above 0.05 psi partial pressure as acidic conditions. Acidic corrosion can have different forms, most often it leads to the appearance of pitting corrosion [22].

H_2S (hydrogen sulfide) occurs naturally in crude oil and natural gas by bacterial decomposition of organic matter [23].
If the ratio of the partial pressures of CO_2 and H_2S, or PCO_2/PH_2S is less than 20, it is acid corrosion, between 20 and 500 it refers to sweet-acid corrosion and a ratio greater than 500 indicates purely sweet corrosion. Constructions of distribution systems, tanks and pipelines are susceptible to acid corrosion [24]. Hydrogen sulphide can have different effects, such as: mass loss due to corrosion, pitting corrosion or initiation of stress cracks. The basic forms of corrosion in the H2S environment are: general corrosion, pitting corrosion and hydrogen embrittlement, as a result of which bubbles or cracks appear on the metal surface [25,26].
Corrosion in pipelines containing H_2S can occur through a number of different mechanisms. First, H_2S gas dissolves in water and thus leads to the creation of an acidic environment. Upon dissolution, it goes through ionization, creating H^+ hydrogen and HS^- (bisulphide). High values of partial pressures of H_2S lead to an increase in corrosion because they lead to a decrease in their pH values. High-strength steels used in pipelines form a protective FeS film that acts as a barrier [27]. The ionization process and formation of H^+ hydrogen and bisulfide are shown in equations (5) and (6):

$$H_2S \rightleftharpoons H^+ + HS^- \quad (5)$$

$$HS^- \rightleftharpoons H^+ + S^{2-} \quad (6)$$

The presence of hydrogen in steel depends on the microstructure, type of material and stress distribution. Diffusion of hydrogen into the metal, which remains in a solid solution in the crystal structure, reduces the ductility and deformability of the metal, that is, a phenomenon called hydrogen embrittlement occurs. That is, if the metal is brittle due to the presence of hydrogen and is exposed to tensile stresses, then a phenomenon called HIC (hydrogen embrittlement) occurs. There is a case when cracks appear in the material in the presence of H_2S and the effect of stress, and this phenomenon is called SSC (stress corrosion). The main factors influencing the increase of SSC are pH value, H_2S concentration and temperature [28]. Due to the presence of H_2S, microbiological damage (MIC) can also occur by bacteria that reduce sulfates present in water and create H_2S as a byproduct [29].

Corrosion due to the presence of O_2

In addition to CO_2 and H_2S, the danger of accelerated corrosion development is also the presence of oxygen O_2. The presence of oxygen leads to an accelerated development of corrosion when it comes to both sweet and salt corrosion. Oxygen is not available at depths above 100 m, but penetration through vents, pumps, etc. may occur. O_2 is a strong oxidant and leads to accelerated corrosion development even when present in small amounts. Also, the presence of O_2 in environments exposed to the effect of CO_2 under high pressure leads to the destruction of the $FeCO_3$ layer, which is a form of corrosion protection under certain conditions. In the event that O_2 reacts with H2S, elemental sulfur appears, which increases the risk of localized corrosion under the deposit. Also, it can change the structure of the FeC layer, and thus lead to a reduction in corrosion protection. [29,30,31]. When oxygen reacts with metal in the air, the process is called chemical or dry corrosion. It is caused by the formation of an oxide layer on the surface of the metal, which prevents further corrosion and is called passivation [32].

Stress corrosion cracking

Stress corrosion cracking (SCC - Stress Corrosion Cracking) is a form of material degradation under the influence of stress and corrosion. Stress corrosion occurs due to the effect of tensile stresses (mainly internal), which are the result of residual stresses due to cold deformation or welding in an

environment of elevated temperature, pressure and dangerous solutions containing H_2S, chlorides of alkali and alkaline earth metals, etc. Depending on the environment in which it occurs and the mechanism of formation, stress corrosion has a large number of subgroups, such as SSC (Sulphide Stress Corrosion) - stress corrosion due to the action of H_2S [33].
A large amount of hydrogen sulfide in oil wells leads to brittleness of the material, which easily leads to the initiation of cracks and fatigue due to corrosion and is a source for the occurrence of SSC stress corrosion cracking. This type of corrosion is characteristic in the oil and gas industry [34]. When sulfur is absorbed on the surface of the metal, it slows down the recombination of hydrogen, resulting in the penetration of hydrogen into the metal along the grain boundary. In this way, hydrogen penetrates inside the gaps and increases the pressure inside them, which leads to the appearance of cracks. Stress corrosion occurs in places where hydrogen accumulates intensively and in places with high stress. It was found that the greatest effect of SSC on metal surfaces is at room temperatures. Crack formation in stress corrosion can be caused by one mechanism, e.g. anodic reactions, and crack propagation takes place by another mechanism such as hydrogen embrittlement [35,36].
SSC is not the most common type of corrosion that occurs in pipes in the oil industry, however its consequences lead to catastrophic fractures and occurs without any indication or warning. Therefore, special attention must be paid to this type of corrosion when choosing materials. However, carbon steel is still the most commonly used material for making pipes, not only because of its price, but also because of its availability [30].
H_2S can be present in the gas phase, dissolved in the exact phase, with or without the presence of hydrocarbons. With the presence of hydrocarbons, the appearance of SSC is delayed due to compounds in hydrocarbons that protect the metal surface [37].
It has been found that there are a large number of factors that influence and contribute to SSC, such as material properties (chemical composition, microstructure, alloying elements, heat treatment, welding), environment (soil, temperature, humidity, microorganisms, CO_2), type of stress (pressure, tension, residual stresses) and the appearance of the corroded surface (appearance of corrosion pits, pit geometry, passive film formation), etc. [38].
There are two types of cracks that appear due to SSC: intercrystalline and transcrystalline cracks, which are related to the pH value. A high pH value (greater than 9) is associated with intercrystalline cracks, while a lower pH value (less than 6) is associated with transcrystalline cracks [39]. One of the biggest problems is the way to detect and identify SSC corrosion, given that it occurs suddenly and leads to major accidents. One of the most common solutions is regular control and monitoring of pipelines. In addition, high-frequency surface coils and eddy current testing are used to detect and monitor stress corrosion in pipelines. However, no solution has yet been found for timely detection of this type of corrosion [40].

Corrosion resistance of welded pipe joints by high-frequency welding

High frequency welding is often used in the oil and gas industry to weld pipes. This type of welding does not require additional material, provides high productivity and can be used for pipes of different dimensions. The demand for welded pipes of high reliability and strength, good quality, as well as high resistance to corrosion is necessary because such pipes are intended for work in difficult conditions such as the oil industry. This is achieved by choosing the optimal welding parameters and procedures, controlling all technological operations during production and testing the resistance and deformation of the welded joint and the base material [41,42,43].
Voltage during high-frequency welding is generated by HF contact or HF induction across the edges of the pipe opening to the point of closure (joint). With the help of voltage, current passes along the edges of the joint, which leads to rapid heating of the metal. The edges heated in this way are joined under pressure with the help of welding rollers, removing all the impurities of the welded element,

while the extrusion of material should be as little as possible, especially from the inside of the pipe [44-47].
Corrosion of welded pipes by high-frequency welding can lead to hydrogen embrittlement or stress corrosion cracking, which lead to crack initiation and propagation, leading to structural failure and fracture. As a result of mechanical, structural and electrochemical inhomogeneity, welded joints have a reduced resistance to corrosion, and therefore a shorter life span. Therefore, in addition to the aggressive environment in which the pipes are located, one of the biggest problems is defects in the welded joint. One of the main causes of the short life of the pipe is the corrosion of the inner wall in the area of the welded joint [48].
In class J55 steels, each element has a key role, low contents of P and S (less than 0.01%), the addition of Cu and Cr can improve the corrosion resistance of the steel [49]. Pipeline specifications are determined by the API 5CT standard, which prescribes the dimensions of pipes and joints and mechanical characteristics, while the most common failures of pipelines are the cause of insufficient resistance to corrosion and formation, propagation of cracks and poor welded joints. There are different methods for estimating the service life of corroded surfaces, but the biggest problem is that corrosion can occur on the outside or inside of the pipe, under different loads and environmental conditions. Therefore, it is necessary to take into account a large number of factors that influence the development of corrosion, which makes this examination complex [50].
In the work [51], experimental and numerical methods were used to test the integrity and lifetime of pipes made by the high-frequency welding process. Pipes made of new and exploited material (API J55) were tested. The results obtained show that corrosion does not affect the tensile properties and impact toughness, but that it affects the fracture toughness and fatigue crack growth rate, which leads to an increased risk of static fracture. The cracks are oriented in the axial direction, perpendicular to the direction of the tensile stress [52].
Table 1 shows the results of X-ray diffractometric analysis for API J55 pipes. X-ray diffractometric analysis (XRD) was carried out to detect the phases present and determine the crystallographic parameters in the samples. In order for this analysis to be carried out successfully, the samples had to be ground beforehand, i.e. turned into a fine powder. Figure 2 shows the device for XDR analysis.

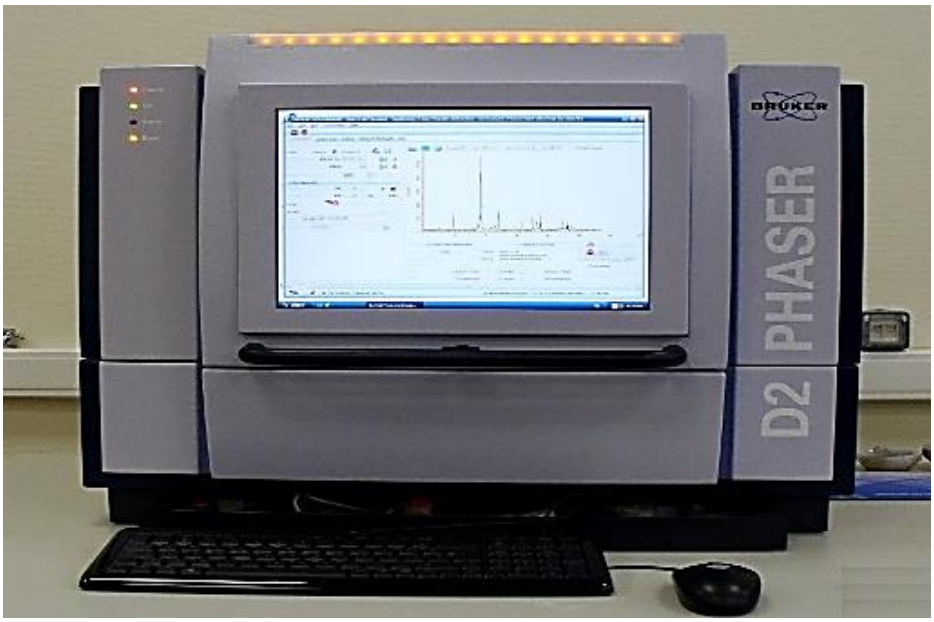

Figure 2. *Device for XRD analysis*

After obtaining diffractograms that were composed of different peaks, the next step is data processing.

Table 1. Results of XRD analysis.

The sequence number	Detected compounds	Chemical formulas
1.	Aluminium Nickel	$(Al_3Ni_2)_{0.4}$
2.	Iron Silicon	$Fe_{0.9}Si_{0.1}$
3.	Copper Iron	$Fe_{0.5}Cu_{0.5}$
4.	Iron Nickel	Fe_7Ni_3
5.	Iron Manganese	$(Fe_{24}Mn)_{0.08}$
6.	Iron Phosphide	$Fe_{0.96}P_{0.04}$
7.	Chromium Iron	$(Cr_{0.2}Fe_{0.8})$
8.	Silicon Chromium Iron	$CrFe_8Si$
9.	Iron Molybdenum	$(Fe_{24}Mo)_{0.08}$
10.	Iron Phosphorus Sulfide	$Fe_2(P_2S_6)$

Based on the XRD analysis, it is concluded that ten different phases, i.e. compounds, occur in the examined sample. What is common to each recognized phase is that it is basically iron with very small concentrations of Ni, Si, Cu, Al, Mn, P, Cr, S and Mo. The results obtained by XRD analysis confirm the chemical composition of the API J55 steel sample itself, Table 2.

Table 2. Chemical composition of API J55 steel, mas.% [50]

	C	Si	Mn	P	S	Cr	Ni	Mo	V	Cu	Al	*Ceq*
Material J55	0,29	0,23	0,96	0,013	0,022	0,1	0,06	0,023	0,003	0,13	0,025	0,49

Methods of control and prevention of corrosion

Control and inspection of pipelines is performed at all stages of the pipeline's life cycle. In the case of new pipelines, it is necessary that all technical requirements are in accordance with the regulations. After the production of pipes, it is necessary that they undergo all destructive and non-destructive tests. Then regular control of pipelines is required, especially if it is about pipelines that have been in operation for many years. The control is carried out in a period of one to five years, depending on the working conditions. Pipeline inspections include the following: measurement of pipe dimensions and thickness, concentration of pipe connections, supports, corrosion on contact surfaces of concrete and steel [53].

The fact is that unprotected pipelines corrode regardless of whether they are in the ground, out of the ground, or in water. NACE prescribes several preventive methods of corrosion protection: cathodic protection, coatings and linings, corrosion inhibitors and material selection [54]. Cathodic protection is a method of protecting pipes from corrosion using direct current. Used for pipes that are in the ground or water. Cathodic polarization in the electrolytic medium reduces or completely stops the corrosion process [55].

Internal corrosion control in the oil industry is most often carried out using corrosion inhibitors. Corrosion inhibitors are chemical substances that are added to a solution and are effective when added in small amounts. Inhibitors are usually divided into natural and synthetic. One of the main problems with inhibitors is that synthetic inhibitors are environmentally toxic and can harm plants and animals.

That is why natural ("green") inhibitors have been used more and more lately. Harmful chemical substances that are added to synthetic inhibitors have led to the prescription of strict international laws for the use of ecological, ie. green inhibitors [56].
Natural inhibitors are obtained from plants and minerals (salicylic acid, vegetable oils, tannins) and they are environmentally friendly and biodegradable. However, they have limited use, as they cannot prevent corrosion in aggressive environments. Synthetic inhibitors are amine salts, phosphates and nitrites. They have high efficiency by forming a protective film on the metal surface and reacting with corrosive substances [57]. Organic inhibitors have cathodic-anodic protection or absorption effect [58]. Hydrophobic corrosion inhibitors are also used in the oil and gas industry, which form a permanent protective layer [59].
The method of corrosion protection with linings and coatings is a passive type of protection. The basic function of the coating is to act as a barrier on the metal surface against moisture, electrolytes and corrosive gases. Depending on the application, there can be internal and external coatings. External coatings provide protection against seawater, soil and moisture, while internal coatings provide protection against fluids inside the pipe and improve flow. Instead of coatings, plastic or polyethylene coatings are used for corrosion protection, however there is a risk that corrosive substances will get behind the coating and thus lead to even greater corrosion [52,60].

References

1. D. A. Jones, “The technology and evaluation of corrosion, ” in *Principles and Prevention of Corrosion*, 1992, 1-35.
2. G. H. Koch et al., *Corrosion cost and preventive strategies in the United States*. VA, McLean, 2002.
3. B. O. Oyelami, A. A. Asere, Mathematical modelling: An application to corrosion in a petroleum industry. NMC Proceedings Workshop on Environment. National Mathematical Centre, 2011.
4. V. Garcia-Arriaga et al., H2S and O2 influence on the corrosion of carbon steel immersed in a solution containing 3M diethanolamine, *Corrosion Science*, **52(7)**, 2268-2279, 2010.
5. D. Martínez et al., Amine type inhibitor effect on corrosion–erosion wear in oil gas pipes, *Wear*, **267(1-4)**, 255-258, 2009.
6. L. Smith, Control of corrosion in oil and gas production tubing, *British Corrosion Journal*., **34(4)**, 247-253, 1999.
7. V. Pilić, *Innovative approach to risk assessment and inspection methodology for pressure equipment*, Ph.D. dissertation, Mechanical Engineering, University of Novi Sad, Faculty of Technical Sciences, Novi Sad, 2022.
8. M. Askari, M. Aliofkhazraei, S. Afroukhteh, A comprehensive review on internal corrosion and cracking of oil and gas pipelines, *Journal of Natural Gas Science and Engineering*, **71**, 2019.
9. Y. Garsany et al., Quantifying the AcetateEnhanced Corrosion of Carbon Steel in Oilfi eld Brines, *Corrosion*, **60(12)**, 1155–1167, 2004.
10. I. Lj. Jevremovic, *Use of organic inhibitors for mitigation of mild steel corrosion in the presence of CO_2*, Ph.D. dissertation, Faculty of Technology and Metallurgy, University of Belgrade.
11. Ž. Šarkoćević et al., Corrosion resistance of welded pipes in oil wells, *Material protection*, **54(1)**, 57-63, 2013.
12. K. Tamalmani, H. Husin, Review on Corrosion Inhibitors for Oil and Gas Corrosion Issues, *Applied Sciences.*, **10(10)**, 2020.
13. L. T. Popoola et al., Corrosion problems during oil and gas production and its mitigation, *International Journal of Industrial Chemistry*, **4(1)**, 1-13, 2013.
14. Z. Bošković et al., *The basics of hydrocarbon exploitation*, Faculty of Mining, Geology and Civil Engineering, Tuzla, Copygraf, 2016.
15. M. Koteeswaran, *CO_2 and H_2S Corrosion in Oil Pipelines*, Master Thesis, Dept. Environmental Tehnology, University of Stavanger, Faculty of Mathematics and Natural Science, Stavanger.
16. F. Pessu, *Investigation of pitting corrosion of carbon steel in sweet and sour oilfield corrosion conditions : a parametric study*, Ph.D. dissertation, School of Mechanical engineering, The University of Leeds.

17. A. S. Tyusenkov, O. A. Nasibullina, Corrosion of tubing of oil fields, *IOP Conference Series: Materials Science and Engineering*, **687(6)**, 2019.
18. T. Tanupabrungsun, B. Brown, S. Nesic, Effect of pH on CO_2 Corrosion of Mild Steel at Elevated Temperatures, Corrosion., 2013.
19. I. B. Obot et al., Modified-polyaspartic acid derivatives as effective corrosion inhibitor for C1018 steel in 3.5% NaCl saturated CO_2 brine solution, *Journal of the Taiwan Institute of Chemical Engineers*, **135(5)**, 2022.
20. A. Kahyarian, M. Achour, S. Nesic, "CO_2 corrosion of mild steel, " in *Trends in Oil and Gas Corrosion Research and Technologies*, A. M. El-Sherik, Woodhead Publishing, 2017, 149-190.
21. C. A. Silva, Corrosion in multiphase-flow pipelines: the impact on the oil and gas industry, Ph.D. dissertation, Polytechnic School, University of Sao Paulo.
22. K. Nalli, "Corrosion and Its Mitigation in the Oil and Gas Industries, " in *Process Plant Equipment: Operation, Control, and Reliability*, M. D. Holloway, C. Nwaoha, O. A. Onyewuenyi, Wiley, 2012, 81-105.
23. K. Mohammed, Drilling and Casing Pipes Corrosion Investigation in Water Based Drilling Mud of Iraqi Oil Fields Environment, *Journal of Mechanical Engineering Research and Developments*, **44(8)**, 232-240, 2021.
24. G. Mubarak et al., Internal corrosion in oil and gas wells during casings and tubing: Challenges and opportunities of corrosion inhibitors, *Journal of the Taiwan Institute of Chemical Engineers*, **150**, 2023.
25. M. L. Martin, P. Sofronis, Hydrogen-Induced Cracking and Blistering in Steels: A Review, *Journal of Natural Gas Science and Engineering*, **101**, 2022.
26. A. Groysman, Corrosion problems and solutions in oil, gas, refining and petrochemical industry, Koroze a ochrana materiálu, **61(3)**, 100-117, 2017.
27. M. Vakili, P. Koutník, J. Kohout, Addressing Hydrogen Sulfide Corrosion in Oil and Gas Industries: A Sustainable Perspective, *Sustainability*, **16(4)**, 2024.
28. M. Ziomek-Moroz, Environmentally Assisted Cracking of Drill Pipes in Deep Drilling Oil and Natural Gas Wells, *Journal of Materials Engineering and Performance*, **21(6)**, 1061-1069, 2012.
29. Y.T. Al-Janabi, "An Overview of Corrosion in Oil and Gas Industry: Upstream, Midstream, and Downstream Sectors, " in *Corrosion Inhibitors in the Oil and Gas Industry*, V. S. Saji, S. A. Umoren, Wiley, 2020, 1-39.
30. N. R. Rosli, *The Effect of Oxygen in Sweet Corrosion of Carbon Steel for Enhanced Oil Recovery*, Ph.D. dissertation, The Faculty of the Russ College of Engineering and Technology, Ohio University.
31. M. Kirby et al. (2024, Mart 21). Unintended Introduction of Oxygen into Gas Export Systems as a Result of the Use of Flare Gas Recovery Systems [Online]. Available: https://www.qa3.co.uk/images/pdfs/Unintentional_Introduction_of_Oxygen_into_Gas_Export_Systems.pdf
32. O. S. I. Fayomi, I. G. Akande, S. Odigie, Economic Impact of Corrosion in Oil Sectors and Prevention: An Overview, *Journal of Physics*, **1378(2)**, 2019.
33. M. Horvat, I. Samardžić, V. Kondić, Stress corrosion cracking, *Tehnički glasnik*, **5(2)**, 103-109, 2011.
34. D.E.P. Klenam, et al., Corrosion resistant materials in high-pressure high-temperature oil wells: An overview and potential application of complex concentrated alloys**,** *Engineering Failure Analysis*, **157(1)**, 2024.
35. M.D.H.C. Peiris, L.W.L. Perera, G.I.P. De Silva, Study of the Effect of Sulphide Stress Corrosion on the Load Bearing Capability of API 5L Grade B Steel used in Petroleum Pipelines, *Engineer Journal of the Institution of Engineers Sri Lanka*, **53(2)**, 13-21, 2020.
36. B.V. Jegdić, B.M. Bobić, A.B. Alil, Stress corrosion cracking of metals and alloys and their welded joints, part i: conditions of stress corrosion cracking occurence, *Welding and welded structures*, **57(1)**, 35-41, 2012.
37. T. E. Perez, Corrosion in the Oil and Gas Industry: An Increasing Challenge for Materials, *Scholarly Journal*, **65(8)**, 1033-1042, 2013.
38. C. Subramanian, Sulfide Stress Cracking of column overhead pipe to flange fitting joints in a petroleum industry, *Materials Today Communications*, **37(2)**, 2023.
39. Y. F. Cheng, *Stress Corrosion Cracking of Pipelines*, Wiley, Canada, 2013.

40. A. Contreras, "Assessment of Stress Corrosion Cracking on Pipeline Steels Weldments Used in the Petroleum Industry by Slow Strain Rate Tests, " in Arc Welding, W. Sudnik, InTech, 2011, 127-150.
41. M. Hussain et al., Review of Prediction of Stress Corrosion Cracking in Gas Pipelines Using Machine Learning, *Machines*, **12(1)**, 2024.
42. P. Yan et al., Tackling the Toughness of Steel Pipes Produced by High Frequency Induction Welding and Heat–Treatment, *Materials Science and Engineering*, **528(29)**, 8492-8499, 2011.
43. P. Simion, Controlling and Monitoring of Welding Parameters for Micro-Alloyed Steel Pipes Produced by High Frequency Electric Welding, *Advanced Materials Research*, **1036**, 464-469, 2014.
44. Ž. Šarkoćević et al., Mechanical properties of welded pipes made by high-frequency welding process from steel API J55, *Welding and welded structures*, **55(4)**, 137-142, 2010.
45. K. Mansouri, A. Abboudi, H. Djebaili, Vickers Hardness Test of Steel Pipes Welded by High Frequency Induction, *Journal of Nano- and Electronic Physics*, **14(1)**, 01013-1-01013-4, 2022.
46. S. Cvetovski, Investigation properties of high frequency welded steel pipes for natural gas transportation made of X60 steel, *Welding and welded structures*, **62(2)**, 53-64, 2017.
47. Ž. Šarkoćević et al., Fabrication of high strength seam welded steel tubes and quality indicator testing, *Integrity and lifetime of constructions*, **8(2)**, 81-98, 2008.
48. Lyudmila Nyrkova et al., Stress corrosion resistance of welded joints of low-alloy pipe steel produced by high frequency welding, *Zastita Materijala*, **61(4)**, 328-338, 2020.
49. Z. Chen, X. Chen, T. Zhou, Microstructure and Mechanical Properties of J55ERW Steel Pipe Processed by On-Line Spray Water Cooling, *Metals*, **7(4)**, 2017.
50. A. Sedmak et al., Remaining strength of API J55 steel casing pipes damaged by corrosion, *International Journal of Pressure Vessels and Piping*, **188**, 2020.
51. A. Sedmak et al., Corrosion effects on structural integrity and life of oil rig drill pipes, *Chemical Industry*, **76(3)**, 167-177, 2022.
52. R. R. Fessler (2024, Mart 28). Pipeline Corrosion - Final Report [Online]. Available: https://www.phmsa.dot.gov/pipeline/hazardous-liquid-integrity-management/pipeline-corrosion-final-report
53. S. Petronić et al., Inspection of pipelines in operation and analysis of the causes of failure, *Process technology*, **30(1)**, 32-29, 2018.
54. T. Nagalakshmi, A. Sivasakthi, Corrosion Control, Prevention and Mitigation in Oil & Gas Industry, *International Journal of Innovative Technology and Exploring Engineering*, **9(2)**, 1568-1572, 2019.
55. S. Stankov, Regulation of operation and monitoring of stations for cathodic protection, *Protection of materials*, **53(1)**, 73-81, 2012.
56. M. Rehioui, "Controlling Corrosion Using Non-Toxic Corrosion Inhibitors", in *Introduction to Corrosion - Basics and Advances*, A. Singh, IntechOpen, 2023.
57. A. Al-Amiery, R. W. Isahak, W. K. Al-Azzawi, Corrosion Inhibitors: Natural and Synthetic Organic Inhibitors, *Lubricants*, **11(4)**, 2023.
58. P. D. Desai et al., Corrosion inhibitors for carbon steel: A review, Vietnam Journal of Chemistry, **61(1)**, 15-42, 2023.
59. J. Brzeszcz, A. Turkiewicz, Corrosion inhibitors – application in oil industry, *Nafta-Gaz*, **71(2)**, 67-75, 2015.
60. V. A. Solovyeva, K. H. Almuhammadi, O.Badeghaish, Current Downhole Corrosion Control Solutions and Trends in the Oil and Gas Industry: A Review, *Materials*, **16(5)**, 2023.

Biocompatibility Testing of Zein/Hydroxyapatite Composite Coatings on Titanium Substrate

Katarina Đ. Božić[1,2,*], Miroslav M. Pavlović[1,2], Đorđe N. Veljović[3], Marijana R. Pantović Pavlović[1,2]

[1] *Institute of Chemistry, Technology and Metallurgy, National Institute of the Republic of Serbia, Department of Electrochemistry, University of Belgrade, Belgrade, Serbia*

[2] *Center of Excellence in Environmental Chemistry and Engineering, Institute of Chemistry, Technology and Metallurgy, Belgrade, Serbia*

[3] *Faculty of Technology and Metallurgy, University of Belgrade, Belgrade, Serbia*

[*]*katarina.bozic@ihtm.bg.ac.rs*

Abstract

The combination of hydroxyapatite with biopolymers like zein holds great promise for enhancing the properties of bone implants. Hydroxyapatite provides structural similarity with bone minerals, facilitating integration with natural bone tissue, while zein adds further benefits such as biodegradability, biocompatibility, and even potential antibacterial activity. By incorporating zein onto the surface of hydroxyapatite coatings, the implant becomes more compatible with the body's tissues, reducing the risk of rejection or adverse reactions. Additionally, the controlled biodegradability of zein allows for gradual replacement by natural bone tissue over time, promoting long-term stability and integration of the implant.

This paper presents an investigation into the biocompatibility of zein/titanium dioxide (zein/TiO_2), hydroxyapatite/zein/titanium dioxide (HAp/zein/TiO_2) and strontium-doped hydroxyapatite/zein/titanium dioxide (Sr-HAp/zein/TiO_2) composite coatings which obtained by in-situ anodization/anaphoretic deposition process. The biocompatibility of all prepared coatings was assessed by measuring cell viability through the MTT test using two different fibroblast cell lines: L929 and MRC-5. The results indicated an increase in the number of viable cells in all tested samples. The highest percentage of survival of healthy L929 and MRC-5 cells was observed with the zein/TiO_2 coating. This suggests that zein is not only non-cytotoxic but also enhances cell proliferation, differentiation, and cell viability when present in the coatings. The morphology and adhesion of cells on the surface were analysed using SEM.

Biocompatibility testing confirmed that the coatings are safe for use in both orthopedic and dental applications.

Keywords: *in situ synthesis; cytotoxicity; MTT assay; cell poliferation*

Development of novel photocatalytic coating based on illite clay/TiO_2 composite

Vojo Jovanov[1,*], Snežana Vučetić[2], Biljana Angjusheva[1], Jonjaua Ranogajec[2], Emilija Fidanchevski[1]

[1] *Ss. Cyril and Methodius, University in Skopje, Faculty of Technology and Metallurgy, Ruger Bosković 16, 1000 Skopje, Republic of North Macedonia*

[2] *University of Novi Sad, Faculty of Technology, bul. Cara Lazara 1, 21000 Novi Sad, Serbia*

[*] *vojo@tmf.ukim.edu.mk*

Abstract

Natural clays have attracted great attention in regard to synthesis of clay-based photocatalysts, due to their layer structure, large specific surface area and remarkable adsorption capacity.
The aim of this work was to develop photocatalytic coating based on titanium-dioxide and illite clay. TiO_2 (Degussa Company) was used as the active component while illite clay acts as a support. In order to initiate the interaction between the active component and the support, TiO_2 in content of 3 and 10wt% was impregnated by mechanical activation in atritor and planetary mill. The developed illite clay/TiO_2 suspensions were applied and investigated on three types of substrates: non-porous (glass), porous (clay roofing tile) and highly porous (clay–fly ash composite). The system illite clay/10wt% TiO_2 impregnated in atritor mill showed better characteristics in the aspect of grain size, morphology, photocatalytic efficiency and durability of coatings.
Photocatalytic efficiency of the developed coating was assessed by photodegradation of the model pollutant Rodamin B performed before and after durability tests.
The investigation showed that photocatalytic activity of the illite clay/TiO_2 coating generally depends on impregnation conditions and applied TiO_2 content.
Keywords: *TiO_2, clay, photocatalysis, photocatalytic coatings, composite materials*

Acknowledgements

The investigation was supported by Ministry of Science, Technological Development and Innovation of Republic of Serbia (Contract No. 451-03-65/2024-03/ 200134)

Comparative Study of Activation Energy and Desulfurization Efficiency of Coal in Graphite and Dimensionally Stable Anode (DSA) Electrodes

Katarina R. Pantović Spajić[1,*], Marijana R. Pantović Pavlović[2], Srećko Stopić[3], Đorđe V. Gjumišev[2], Branislav Marković[1], Miroslav M. Pavlović[2], Ksenija Stojanović[4]

[1]*Institute for Technology of Nuclear and Other Mineral Raw Materials, Belgrade, Serbia*

[2]*University of Belgrade, Institute of Chemistry, Technology and Metallurgy, National Institute of Republic of Serbia, Belgrade, Serbia*

[3]*Process Metallurgy and Metal Recycling, RWTH Aachen University, Aachen, Germany*

[4]*University of Belgrade, Faculty of Chemistry, Belgrade, Serbia*

[*]*k.pantovic@itnms.ac.rs*

Abstract

This study investigates the electrochemical desulfurization of sulfur-rich subbituminous coal (6.96 wt.%) from the Bogovina Basin using graphite and dimensionally stable anode (DSA) electrodes. The objective was to evaluate and compare the efficacy of these electrodes under varying thermal conditions to determine the optimal operational parameters that balance desulfurization efficiency with energy consumption. Electrochemical assessments were conducted through linear sweep voltammetry (LSV) to derive polarization curves and calculate activation energies, reflecting the intrinsic energy barriers of the desulfurization reactions. These tests were performed across a temperature range from 30°C to 70°C, providing insight into the thermally activated nature of these processes. The results demonstrated that the DSA electrodes outperformed the graphite electrodes in several key areas. Notably, DSA electrodes exhibited higher current densities at equivalent temperatures and potentials, indicating a more robust electrochemical activity conducive to higher desulfurization rates. Moreover, activation energy analysis revealed that DSA electrodes operate with significantly lower energy barriers, facilitating easier and more efficient reaction initiations. Energy consumption metrics were critical in evaluating the operational costs associated with each electrode type. The DSA electrodes were found to consume less energy per kilogram of sulfur removed, particularly at an optimal temperature of 50°C, which was identified as the most energy-efficient operational point. At this temperature, the DSA electrodes achieved peak desulfurization efficiency with the most favorable balance between energy input and desulfurization output. The study substantiates the superiority of DSA electrodes over traditional graphite electrodes for coal desulfurization processes, particularly at the optimal operational temperature of 50°C. The findings highlight significant potential for enhancing the sustainability and cost-effectiveness of coal desulfurization technologies, suggesting a paradigm shift towards the adoption of DSA electrodes in industrial applications to achieve more efficient and environmentally friendly outcomes.

Keywords: *electrochemical desulfurization; subbituminous coal; dimensionally stable anode (DSA); graphite electrodes; optimal temperature; energy efficiency*

Efficacy of Novel Hybrid Coating on Titanium Substrates in Targeting Cancerous Cells

Marijana R. Pantović Pavlović[1,*], Evelina A. Herendija[2], Miloš M. Lazarević[3], Nenad L. Ignjatović[4], Miroslav M. Pavlović[1,*]

[1]*Institute of Chemistry, Technology and Metallurgy, Department of Electrochemistry, Belgrade, Serbia*

[2]*University of Belgrade, Multidisciplinary PhD Studies, Belgrade, Serbia*

[3]*School of Dental Medicine, University of Belgrade, Belgrade, Serbia*

[4]*Institute of Technical Science of the Serbian Academy of Sciences and Arts, Belgrade, Serbia*

[*]*m.pantovic@ihtm.bg.ac.rs*

Abstract

This study investigates the anti-cancer properties of a novel composite coating comprising amorphous calcium phosphate (ACP), chitosan oligosaccharide lactate, and germanium (Ge) on titanium (Ti) substrates. The coating was applied using an in situ anodization/anaphoretic deposition process. The primary focus is on the germanium layer's effectiveness in targeting and eliminating cancerous cells. Experimental analysis included MTT assays and flow cytometry to evaluate cytotoxicity and cellular uptake, respectively. MTT assays were conducted on SCC-25 cancer cell lines and dental pulp stem cells (DPSC) over 1, 3, and 7 days. Results indicated a significant reduction in SCC-25 cell viability, particularly notable with the germanium-enhanced coating, which drastically reduced the number of cancerous cells. In contrast, DPSC showed minimal cytotoxic effects, demonstrating the selective nature of the coating. Flow cytometry further confirmed these findings, revealing that the germanium coating was effective in reducing cancer cell viability without significant penetration into healthy cells. This study suggests that germanium-coated Ti substrates with ACP and chitosan oligosaccharide lactate are highly effective in targeting cancer cells while preserving healthy cells, making this composite coating a promising candidate for anti-cancer therapies. Future research will focus on optimizing the coating process and expanding in vivo studies to further validate these findings.

Keywords: *Germanium; Titanium substrate; SCC-25 Cancer cells; Dental Pulp Stem Cells (DPSC); Cytotoxicity; MTT assay; Flow cytometry.*

Innovative Multimetal Multivalent Oxides for Sustainable Energy Solutions: Emphasizing Oxygen Evolution Reactions

Miroslav Pavlović[1,*], Katarina Đ. Božić[1], Srećko Stopić[2], Alexander Birich[2], Bernd Friedrich[2], Marija M. Jonović[3], Marijana R. Pantović Pavlović[1]

[1]*Institute of Chemistry, Technology and Metallurgy, Department of Electrochemistry, Belgrade, Serbia*

[2]*Process Metallurgy and Metal Recycling, RWTH Aachen University, Aachen, Germany*

[3]*Mining and Metallurgy Institute Bor, Bor, Serbia*

[*]*miroslav.pavlovic@ihtm.bg.ac.rs*

Abstract

This paper explores the synthesis and characterization of potential catalysts for oxygen evolution reactions (OER) using rare earth elements (REEs) such as Ce, Y and Yb, in combination with transition metals Co and Ir. Utilizing the ultrasonic spray pyrolysis (USP) synthesis method, multivalent oxides were produced from metal salt precursors, demonstrating promising catalytic properties for OER. The research encompasses various experimental techniques including microwave synthesis, IrO_2 deposition, and a range of electrochemical analyses (XRD, SEM/EDS, CV, LSV, PEIS, C-DC) to evaluate the performance of these multivalent oxides. Additionally, the study highlights the critical role of REEs in advanced technology manufacturing and investigates the potential of coal fly ash (CFA) as a resource for REE recovery, promoting circular economy principles and sustainable resource management. The research emphasizes the importance of local extractive technologies to reduce transportation costs and environmental impacts, thereby enhancing regional resource independence and sustainability. This study aims to provide valuable insights into the development of efficient catalysts for oxygen evolution reactions, supporting the transition towards more sustainable energy storage and conversion technologies. The findings reveal the superior catalytic activity of the synthesized multivalent oxides compared to conventional catalysts, underscoring their potential for practical applications in rechargeable metal-air batteries and fuel cells.

Keywords: *Oxygen Evolution Reactions; Rare Earth Elements; Ultrasonic Spray Pyrolysis; Coal Fly Ash; Sustainable Resource Management*

Voltammetric evaluation of essential oils antioxidative properties

Bojana Radojković, Milica Košević, Marija Mihailović*

Institute of Chemistry, Technology and Metallurgy, Department of Electrochemistry, Belgrade, Serbia

**marija.mihailovic@ihtm.bg.ac.rs*

Abstract

Antioxidant activity of Achillea millefolium (yarrow), Melisssa officinalis (lemon balm), Calendula officinalis (Marygold) was examined using essential oils obtained by dry extraction method, without using standard solvents. It is discussed in the light of the overall plant capability to act antioxidative. Antioxidant activity encompasses different mechanisms, what is the reason to employ various assays to assess these properties. Since the evaluation may be very complex, the fast and accurate electrochemical test for assessment the overall plant antioxidant capability is presented in this paper. It must be noted that the measured current shows the contribution of all compounds in the plant extract, revealing their synergetic effect. Systematic determination of anodic current peaks and the oxidation potentials enables the classification of investigated plants according to their antioxidant properties. Since each plant extract is composed of numerous different compounds, the voltammetric method is fast and reliable way of essential oils antioxidative properties evaluation.

Keywords: *Achillea millefolium; Melisssa officinalis; Calendula officinalis; anodic peak, antioxidative potential.*

Microwave-assisted polyol synthesis of Pt/MXene catalyst for the methanol oxidation reaction

Sanja Stevanović[1*], Dragana Milošević[1], Marija Pergal[1], Ivan Pešić[1], Dušan Tripković[1], Lazar Rakočević[2], Vesna Maksimović[2]

[1] *University of Belgrade - Institute of Chemistry, Technology and Metallurgy, Njegoševa 12, 11000 Belgrade, Serbia*

[2] *University of Belgrade - Vinča Institute of Nuclear Sciences, Mike Petrovića Alasa 12-14, 11351 Vinča-Belgrade, Serbia*

[*]*sanjas@ihtm.bg.ac.rs*

Abstract

Recent years indicate a significant increase in interest in MXene-based composite hybrid nanostructures because of their potential uses as catalyst supports for enhanced electrochemical performance in direct alcohol fuel cells. MXenes are a new family of 2D materials with the general formula of $M_{n+1}X_nT_n$, where M represents transition metals, X represents C/N and T represents chemical functional groups such as –OH, -O, and –F groups on the MXene surface. They possess high specific surface area, good resistance to electrochemical corrosion, strong interaction with metal support i.e. large redox-active surface area, exceptional mechanical properties, rich surface chemistries and enhanced electrical conductivity. All these qualities make them good candidates as catalyst support material for anode processes in fuel cells. In this study, we present an approach for successfully synthesizing platinum nanocatalysts with MXenes as support. Toward this goal, Pt/MXene catalyst will be synthesised by the microwave-assisted polyol method. The electrochemical behavior of the synthesized catalyst was investigated by cyclic voltammetry, the electro-oxidation of adsorbed CO, and the chronoamperometry method. The physicochemical properties of prepared catalysts were characterized by X-ray diffraction (XRD) and X-ray Photoelectron Spectroscopy (XPS). The high catalytic activity of the Pt/MX catalyst for the methanol electrooxidation reaction and good electrochemical stability was achieved thanks to thoroughly balanced conditions during the microwave synthesis, as well as by choosing MXene as the catalyst support.

Keywords: *platinum; MXenes; methanol electrooxidation; microwave-assisted polyol synthesis*

Acknowledgments

This work was financially supported by the Ministry of Science, Technological Development and Innovation of the Republic of Serbia (contract no. 451-03-66/2024-03/200026) and the Science Fund of the Republic of Serbia under grant no. 7739802.

References

1. M. R. Lukatskaya, O. Mashtalir, at all., Cation intercalation and high volumetric capacitance of two-dimensional titanium carbide." *Science* **341**, 1502-1505, 2013.
2. I. M. Chirica, A. G. Mirea, S. Neat¸ M. Florea, M. W. Barsoum, F. Neat, Applications of MAX phases and MXenes as catalysts, *J. Mater. Chem. A*, **9**, 19589-19612, 2021.
3. Z. Li, L. Yu, C. Milligan, T. Ma, L. Zhou, Y. Cui, Z. Qi, N. Libretto, B. Xu, J. Luo, E. Shi, Z. Wu, H. Xin, W. N. Delgass, J. T. Miller and Y. Wu, Two-dimensional transition metal carbides as supports for tuning the chemistry of catalytic nanoparticles, *Nat. Commun.*, **9**, 5258, 2018.
4. J. Zhu, L. Xia, R. Yu, R. Lu, J. Li, R. He, Y. Wu, W. Zhang, X. Hong, W. Chen, Y. Zhao, L. Zhou, L. Mai, Z. Wang, Ultrahigh Stable Methanol Oxidation Enabled by a High Hydroxyl Concentration on Pt Clusters/MXene Interfaces, J. Am. Chem. Soc. **144 (34)**, 15529-15538, 2022.

CuPd alloy formation by Cu electrodeposition from a deep eutectic solvent

Nataša M. Petrović[1], Nebojša D. Nikolić[1,*], Vladimir D. Jović[2], Tanja S. Barudžija[3], Silvana Dimitrijević[4], Jovan N. Jovićević[1], Vesna S. Cvetković[1]

[1] *Department of Electrochemistry, Institute of Chemistry, Technology and Metallurgy, University of Belgrade, Njegoševa 12, 11000 Belgrade, Serbia*

[2] *Institute for Multidisciplinary Research, University of Belgrade, Kneza Višeslava 1, 11030 Belgrade, Serbia*

[3] *Institute for Nuclear Sciences Vinča, University of Belgrade, P.O.Box 522, 11001 Belgrade, Serbia*

[4] *Mining and Metallurgy Institute, Zeleni bulevar 35, 19210 Bor, Serbia*

[*] *nnikolic@ihtm.bg.ac.rs*

Abstract

Electrodeposition of copper from an eutectic mixture based on choline chloride and ethylene glycol containing copper(II) chloride salt at 50 °C was investigated. It was shown that electrochemical reduction process of Cu(II) proceeds via two steps, Cu(II) → Cu(I) and Cu(I) → Cu(0). Electrodeposits were obtained by potentiostatic electrolysis and analyzed by scanning electron microscope (SEM) and Energy-dispersive X-ray spectroscopy (EDS). SEM results showed that the electrodeposited Cu on Pd was relatively uniform and smooth, with Cu grains of approximately 1 μm. EDS analysis of the Pd electrode surface after Cu electrodeposition revealed that Cu is dominating in the deposit. The presence of CuPd alloy, along with metallic Cu on the Pd surface is confirmed by X-ray diffraction (XRD).

Keywords: *copper electrodeposition; deep eutectic solvent; copper/palladium alloys; morphology.*

Introduction

Due to their improved catalytic performance compared to pure Pd and their application in hydrogen capture and storage, a strong interest in electrodeposited CuPd alloys has recently increased [1]. Different techniques, such as sputtering and electroless deposition, have been used to deposit PdCu alloys [1,2]. To date, CuPd alloys have been electrodeposited mainly from aqueous electrolytes [3,4]. However, interest in the development of non-aqueous electrolytes which can be used on an industrial scale, when aqueous media are not suitable for copper electrodeposition, placed special interest on deep eutectic solvents (DESs). DESs are structurally similar to ionic liquids (ILs) in that both have low vapor pressure and low flammability, but unlike ILs, they are biodegradable, non-toxic and inexpensive [5]. In addition, DESs can facilitate redox reactions and electrodeposition of a wide range of metals [6]. Promising results obtained for Cu electrodepositions from DES resulted in electrodeposition of Cu alloys on platinum or gold from chlorine-based DESs, ChCl/urea, and ChCl/EG with $CuCl_2$ added [7,8]. It was found that because of the high chloride concentration in DESs, the complexation of copper ions and the electrodeposition kinetic is different than in the aqueous electrolytes [7,8]. The comparison of Cu electrodeposition from chloride aqueous electrolytes and DESs with $CuCl_2$ added on a GC electrode was also performed [2,6,7]. Those experimental results showed that the systems behave in the same way, with the exception that in DES systems a higher temperature and higher Cu(II) concentrations are required to achieve a current density comparable to that in aqueous electrolytes [2]. There are no detailed electrochemical studies in the literature related to the electrochemical Cu electrodeposition onto Pd and CuPd alloys formation from choline chloride ethylene glycol (ChCl:EG) electrolyte with $CuCl_2$ added as a source

of Cu(II) ions. In this work, we investigated copper electrodeposition onto Pd electrode from ChCl:EG electrolyte at 50°C. The main task was to achieve a better understanding of the electrochemical behavior of Cu(II) in this electrolyte and to accomplish electrodeposition of CuPd alloys.

Experimental

The electrolyte was prepared by mixing choline chloride (≥98%, $HOC_2H_4N(CH_3)_3Cl$) and ethylene glycol (99.8%, ethane-1,2-diol) at a 1:2 molar ratio. The mixture was then placed onto a hot plate at 40 °C until a homogeneous, colorless liquid was formed. $CuCl_2 \cdot 2H_2O$ (99.0 %, Merck) was added to make the electrolyte with copper ions concentration of 0.1 M. The electrolyte was stirred again until all of the salt had been completely dissolved. A three electrode electrochemical cell configuration was employed, in which Pd (Pd, 99.999% Sigma Aldrich; wires or plates) was used as a working electrode, reference electrode was made from a Cu rod (99.99%, Thermo Fisher Scientific, UK, diameter ø =4 mm), a Cu rod (diameter ø = 6 mm) with an active surface area of 1.5 cm^2 in the electrolyte, was used as a counter electrode. The details of the electrochemical cell set up and procedure of the electrodes preparation have already been reported elsewhere [9]. All experiments were performed at 50 °C. The electrochemical measurements: cyclic voltammetry (CV, using various scan rates in the range of 2–20 mV/s), square vawe voltammetry (SWV), chronoamperometry, potentiodynamic and open-circuit potential chronopotentiometry, were controlled by an potentiostat/galvanostat Interface 1010 E (Gamry Instruments, Warminster, PA, US). Cu electrodeposition was performed by applying constant potentials to the Pd cathode in the electrolytes containing Cu(II) ions. The structure analysis of the deposit was revealed by X-ray diffraction (XRD), employing a SmartLab® X-ray diffractometer (Rigaku Co., Tokyo, Japan). The morphology and composition of CuPd deposits were explored using a scanning electron microscope (JOEL JSM-IT300LV), equipped with an energy-dispersive X-ray spectroscopy (EDS) Oxford Instruments X-MAX^N and AZtec version 3.1 software.

Results and Discussion

CV and SWV were used to attain a better understanding of the nature of the electrode reaction involved in Cu(II) → Cu(0) redox transition. The CVs recorded for 0.1 M Cu(II) at a Pd electrode in ChCl:EG at 50 °C are shown in Fig. 1. a). The CVs show that there are two distinct pairs, A/A' and B/B', of reduction/oxidation current waves that can be associated with Cu(II) ⇄ Cu(I) and Cu(I) ⇄ Cu(0) redox transitions, respectively. The reduction process in the potential range of 0.600 V and 0.900 V vs. Cu indicates that Cu(II) is reduced to Cu(I), followed by the reduction from Cu(I) → Cu(0) at around − 0.100 V vs. Cu. The latter process leads to metallic copper deposition with a characteristic stripping response on the anodic scan (B'). These indicate that Cu deposition and dissolution processes occur in two well-separated steps with the intermediate formation of Cu(I). This type of behavior has been observed previously since a high concentration of chloride in ethaline (ChCl:EG) stabilizes Cu(I) through complexation [6,8,9]. To obtain a clearer picture of this behavior, SWV was also recorded at a Pd electrode, as a more sensitive technique than CV. Figure 1.b). shows a SWVs recorded at a step potential of 1 mV and different frequencies from 0.800 V to − 0.300 V on Pd electrode at 50 °C. The SWV results shows two distinct peaks A and B at around 0.600 V and – 0.100 V, which correspond to the reduction of Cu(II) and Cu(I), respectively. As can be seen from Fig. 1. b), the SWV results are consistent with the results obtained from CVs in Fig. 1. a) and allow more evident identification for the Cu electrodeposition process. In general, the electrochemical behavior of Cu(II) species observed in these voltammograms is similar to those reported in details for glassy carbon or Pt working electrodes [6,8,9].

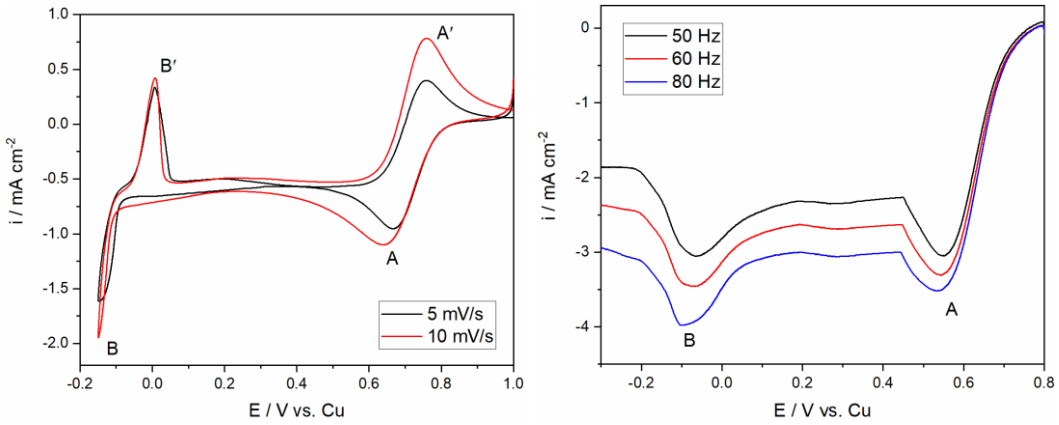

a) b)

Figure 1. *a) Cyclic voltammograms of Pd working electrode in ChCl:EG (1:2 molar ratio) electrolyte containing 0.1 M Cu(II). The CVs started from initial potential E_i towards cathodic end potential E_c = − 0.175 V vs. Cu with different scan rates; b) SWV obtained with different frequencies on Pd cathode; pulse height 25 mV; potential step 1 mV; T=50 °C.*

The microstructure of the deposit was investigated by SEM analysis, while the elemental composition of the electrodeposits produced on Pd was determined by EDS analysis, as shown in Figure 2. The Cu deposit obtained on Pd was uniform, relatively smooth and porous, Fig. 2. a). The EDS results of the Cu electrodeposit onto Pd revealed that only Cu was detected on the substate surface area, Fig. 2. b). The presence of almost 100 % Cu (Spectrum 1; Fig. 2. b.) proved the formation of compact Cu deposit on the entire Pd substrate.

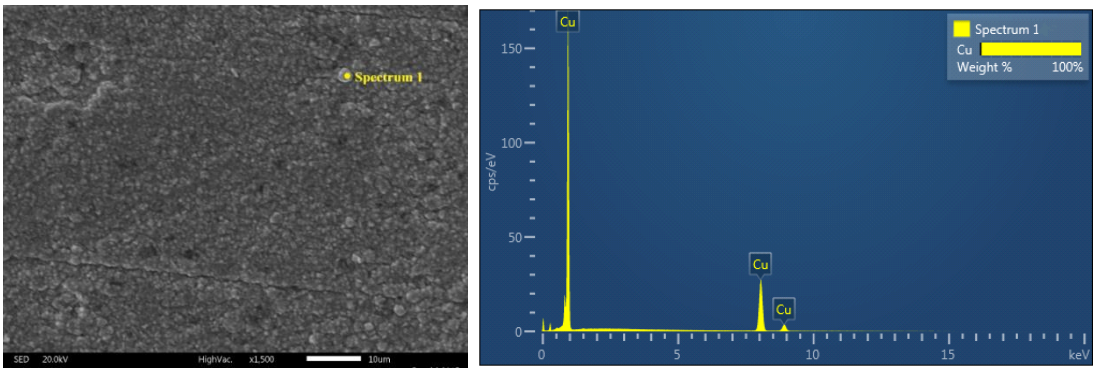

a) b)

Figure 2. *a) The SEM micrographs of deposits obtained by Cu electrodeposition in an overpotential region (– 0.100 V vs. Cu) and b) EDS analysis of the deposit; electrolyte 0.1 M Cu(II) - ChCl:EG (1:2 molar ratio), working electrode Pd, deposition time 120 min.*

The results of XRD analysis of the sample formed by electrodeposition of Cu onto Pd cathode in a potentiostatic mode from 0.1 M Cu(II) - ChCl:EG showed that in the addition to the prominent peaks (2θ = 43.317º, 50.449º and 74.125º) belonging to Cu metal [JCPDS No. 01-085-1326], the characteristic peak which belongs to face-centered cubic CuPd was identified at 2θ = 41.424 º [JCPDS No.00-048-1551], Fig. 3. The formation of CuPd alloy is expected, since the Cu atom is smaller than Pd, which allows the Cu atoms to enter the Pd crystal and generate an fcc PdCu intermetallic. The electrodeposited Cu was found to remain on the surface due to Cu segregation and low constant loading in Pd with insertion of Cu [10]. This could explain why the surface area is quite compact after $Cu_{(s)}$, has reached 50 at.% in the intermetallic.

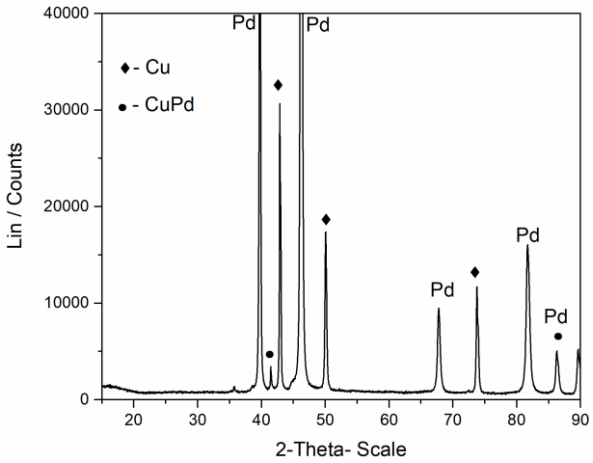

Figure 3. *X-ray diffraction analysis of the deposit obtained by Cu electrodeposition in potentiostatic mode (deposition potential – 0.100 V vs. Cu) from ChCl:EG (1:2 molar ratio) electrolyte containing 0.1 M Cu(II), working temperature 50 ºC, deposition time120 min.*

Conclusion

Copper electrodeposition from Cu(II) on Pd in 0.1 M Cu(II) - ChCl:EG electrolyte (1:2 ratio of choline chloride and ethylene glycol), at 50 ºC, on a Pd electrode was investigated. The experiments performed show that Cu(II) electroreduction to Cu metal proceeds via two steps, Cu(II) → Cu(I) and Cu(I) → Cu(0), through the formation of an intermediate Cu(I) species. Cu was electrodeposited from 0.1 M Cu(II) - ChCl:EG in potentiostatic mode and SEM analysis of the deposit revealed that the electrodeposited Cu on Pd is relatively uniform and smooth. EDS analysis showed that Cu was predominantly present in the deposit. The formation of surface CuPd alloy was confirmed by X-ray diffraction. The incorporation of Cu into Pd substrate by Cu solid state interdiffusion leads to the formation of compact surface area after Cu(s), reaches 50 at.% in the intermetallic.

Acknowledgements

This work was supported by the Ministry of Science, Technological Development and Innovation of the Republic of Serbia (Contract No: 451-03-66/2024-03/200026).

References

1. L.-S. Jou, J.-K. Chang, T.-J. Twhang, I.-W. Sun, Electrodeposition of Palladium–Copper Films from 1-Ethyl-3-methylimidazolium Chloride–Tetrafluoroborate Ionic Liquid on Indium Tin Oxide Electrodes, *J. Electrochem. Soc.,* **156**, D193–D197, 2009. https://doi.org/10.1149/1.3106144.
2. P. Sebastián, E. Vallés, E. Gómez, Copper electrodeposition in a deep eutectic solvent. First stages analysis considering Cu(I) stabilization in chloride media, *Electrochim. Acta*., **123**, 285–295, 2014. https://doi.org/10.1016/j.electacta.2014.01.062.
3. C. Milhano, D. Pletcher, The electrodeposition and electrocatalytic properties of copper-palladium alloys, *J. Electroanal. Chem*., **614**, 24–30, 2008. https://doi.org/10.1016/j.jelechem.2007.11.001.
4. F. Gobal, R. Arab, A preliminary study of the electro-catalytic reduction of oxygen on Cu-Pd alloys in alkaline solution, *J. Electroanal. Chem*., **647**, 66–73, 2010. https://doi.org/10.1016/j.jelechem.2010.05.009.
5. K. Salimiyan, D. Saberi, Choline Chloride/Urea as an Eco-Friendly Deep Eutectic Solvent for TCT-Mediated Amide Coupling at Room Temperature, *ChemistrySelect*., **4**, 3985–3989, 2019. https://doi.org/10.1002/slct.201804066.
6. M.B. Vukmirovic, R.R. Adzic, R. Akolkar, Copper Electrodeposition from Deep Eutectic Solvents—Voltammetric Studies Providing Insights into the Role of Substrate: Platinum vs Glassy Carbon, *J. Phys. Chem. B.,* **124**, 5465–5475, 2020. https://doi.org/10.1021/acs.jpcb.0c02735.

7. T. Geng, S.J. Zeller, L.A. Kibler, M.U. Ceblin, T. Jacob, Electrodeposition of Cu onto Au(111) from Deep Eutectic Solvents: Molar Ratio of Salt and Hydrogen Bond Donor, *ChemElectroChem.*, **9**, e202101283, 2022. https://doi.org/10.1002/celc.202101283.
8. A.P. Abbott, K. El Ttaib, G. Frisch, K.J. McKenzie, K.S. Ryder, Electrodeposition of copper composites from deep eutectic solvents based on choline chloride, Phys. *Chem. Chem. Phys.*, **11**, 4269–4277, 2009. https://doi.org/10.1039/b817881j.
9. V.S. Cvetković, V.D. Jović, N.D. Nikolić, T.S. Barudžija, S. Dimitrijević, J.N. Jovićević, Electrodeposition of copper on glassy carbon and palladium from choline chloride - ethylene glycol deep eutectic solvent, *J. Electroanal. Chem.*, **958**, 18161, 2024. https://doi.org/10.1016/j.jelechem.2024.118161.
10. F. Fouda-Onana, S. Bah, O. Savadogo, Palladium–copper alloys as catalysts for the oxygen reduction reaction in an acidic media I: Correlation between the ORR kinetic parameters and intrinsic physical properties of the alloys, *J. Electroanal. Chem.*, **636**, 1–9, 2009. https://doi.org/10.1016/j.jelechem.2009.06.023.

Designing of the Shape of Zinc particles by Variation of Electrolysis Conditions

Nebojša D. Nikolić[1,*], Jelena D. Lović[1], Nikola Vuković[2], Sanja I. Stevanović[1]

[1]*University of Belgrade, ICTM–Department of Electrochemistry, Njegoševa 12, Belgrade, Serbia*

[2]*Institute for Technology of Nuclear and Other Mineral Raw Materials, Belgrade, Serbia*

[*]*nnikolic@ihtm.bg.ac.rs*

Abstract

Zinc-air batteries belong to the group of green and sustainable energy storage systems, and as such, they attract a huge attention of both academic and technological communities. For this system, the alkaline electrolytes of zinc with high concentrations of ZnO and KOH are used. Morphology of zinc electrodeposits is characterized by the scanning electron microscopy (SEM) technique, and it was found that it depended on an overpotential of the electrodeposition with a strong contribution of a length of the electrodeposition time on the final shape. Variety of morphological shapes was observed: irregular and regular grains including those hexagonal shape were predominately formed at the overpotential belonging to the plateau of the limiting diffusion current density. The compact both regular and irregular dendrites were formed at this overpotential with the longer electrodeposition time. The 2D (two-dimensional) and 3D (three-dimensional) dendrites were formed at overpotentials outside the plateau of the limiting diffusion current density, in the zone of the rapid growth of the current density with the increase of the overpotential. In this zone, hydrogen evolution reaction as the second reaction to Zn electrolysis at high overpotentials started to take place. It is manifested by the appearance of craters on the surface of the electrode, which originate from detached hydrogen bubbles. All morpholical forms were explained and discussed applying the basic laws of electrocrystallization.

Keywords: *zinc; electrolysis; morphology; SEM; dendrites; hydrogen.*

Acknowledgement

This work was financially supported by MSTDI of RS (Grant No. 451-03-66/2024-03/200026) and Science Fund of RS (Grant No. AdCatFC: 7739802).

Evaluation of the phytoremediation potential of Tilia tomentosa Moench. for Cu, Pb and Zn on green areas in Belgrade

Natalija Radulović[1*], Olga Kostić[1], Olivera Košanin[2], Dragana Pavlović[1], Dimitrije Sekulić[1], Milica Jonjev[1], Miroslava Mitrović[1], Pavle Pavlović[1]

[1]*Institute for Biological Research 'Siniša Stanković' - National Institute of the Republic of Serbia, University of Belgrade, Department of Ecology, Belgrade, Serbia,*

[2]*Faculty of Forestry, University of Belgrade, Belgrade, Serbia*

[*]*natalija.radulovic@ibiss.bg.ac.rs*

Abstract

Linden trees are one of the most popular tree species in European cities and also in Serbia, often used for planting on green areas (parks and tree lines) in Belgrade. In this study, individuals of silver linden Tilia tomentosa Moench. in the tree line (Bulevar Nikola Tesla) and city park (Park Ušće) in Belgrade were selected and the concentration of potentially toxic elements (PTEs) Cu, Pb and Zn in roots and leaves and in the soil (0-10cm and 10-30cm) under each individual as well as in the natural habitat on Fruška Gora mountain (control) were collected. To evaluate the potential of the selected species for phytoremediation (phytoextraction and phytostabilisation of PTEs), the bioaccumulation of roots and leaves (BCF_{root} and BCF_{leaf}), and translocation factors (TF) were calculated. Site-dependent variations were observed for all analysed parameters. In the soil samples, the concentrations of Cu, Pb and Zn were above the average values for European soils only at urban sites (17.3 mg kg^{-1}, 32 mg kg^{-1} and 68.1 mg kg^{-1}, respectively) and in the critical range for plants for Zn (>70 mg kg^{-1}) and for Cu (>60 mg kg^{-1}) only in the tree line, while the concentration of Pb was above the MAC. A high correlation was found for the concentration of all tested elements in the soil and in the roots, and only for Zn in the leaves. Nevertheless, the levels of Cu and Pb in the roots and Cu in the leaves were within the normal range for plant tissues (5-30 mg kg^{-1}, 5-10 mg kg^{-1}) at all sites analysed, while Zn was in deficit (<20 mg kg^{-1}). By analysing the bioconcentration and translocation factors for the measured elements, it was found that T. tomentosa has the potential for their phytostabilisation (BCF_{root}<1, BCF_{leaf}<1, TF>1). These findings could be of great importance in the planning of sustainable management of urban areas.

Keywords: *phytoremediation; linden tree; city parks; tree lines; heavy metal accumulation; bioconcentration and translocation*

Assessment of As and Pb in *Solanum tuberosum* L. from urban areas of Belgrade and potential dietary health risk for the population

Marija Matić*, Dragana Pavlović, Veljko Perović, Olga Kostić, Snežana Jarić, Miroslava Mitrović, Pavle Pavlović

Department of Ecology, Institute for Biological Research "Siniša Stanković", National Institute of the Republic of Serbia, University of Belgrade, Bulevar despota Stefana 142, 11000 Belgrade, Serbia

**marija.pavlovic@ibiss.bg.ac.rs*

Abstract

Vegetable crops are one of the most important foods in the human diet and understanding their ability to accumulate toxic concentrations of hazardous elements can help reduce potential risks to human health. Solanum tuberosum L. is considered the most important non-cereal crop in the world and one of the most important foods in the diet, therefore it is particularly important to identify the potential health risks of consuming vegetables that may be grown in the immediate vicinity of coal mines and thermal power plants. Samples of S. tuberosum and associated soils were taken in the area of the municipalities of Lazarevac (village of Sokolovo) and Obrenovac (village of Krtinka) and Surčin (village of Jakovo) to determine the As and Pb content and to assess the potential human health risk associated with dietary exposure from consumption of the investigated crop. The results obtained showed that the content of non-essential and toxic elements As and Pb was within the range considered normal in plant tissues and below the MAC for dried vegetables under national legislation of the Republic of Serbia. Arsenic was not measured in the tubers of S. tuberosum in 2013, but was measured in the 2014 harvest, while the Pb concentration showed a decreasing trend between the two sampling seasons. The calculation of the non-carcinogenic risk showed that the target hazard quotient and the hazard risk index for S. tuberosum from 2014 exceeded the provisional maximum tolerable daily intake, as the values were >1. These results show that consumption of the 2014 harvest from the investigated sampling sites posed a health risk to humans and urge caution when growing S. tuberosum at the sampling sites.

Keywords: *Solanum tuberosum; potentially toxic elements; non-carcinogenic risk; urban pollution*

Introduction

Urban expansion increases anthropogenic activities and alters urban biogeochemistry, including contamination with potentially toxic trace elements (PTEs). As a result, soil structures and processes are altered, making them more susceptible to surface contamination and exposing people to contaminated food [1]. Furthermore, many mining areas and industrial regions are so heavily contaminated that the risk to human health is of great concern [2]. Potentially toxic elements can pose dangerous health risks to all living organisms, as they tend to accumulate and transfer in the soil with irrigation water and many other sources [3], which is why growing urban vegetables in polluted areas of cities is a major hazard and of great concern for public health [4].

Accumulation of PTEs in soils, vegetables and food crops (especially those that are not essential for plant growth, such as As and Pb) above the Food and Agriculture Organisation (FAO)/World Health Organisation [5] threshold can lead to nerve, cardiovascular, kidney, bone and neurological damage, among other things [1,6]. The consumption of vegetables contaminated with Pb has multiple effects on human health, for example, the continuous consumption of contaminated vegetables can lead to disorders of the functions of the digestive, nervous, respiratory and reproductive systems, as well as bone weakness, as it prevents enzymes from carrying out their normal activities [7]. As for As, it is

known to cause cardiovascular disease, peripheral circulatory disorders, anemia and disorders of the reproductive system [8].
Previous studies have shown that oral ingestion of contaminated food is the most common route by which toxic substances enter the human body, compared to inhalation and dermal contact [9-11]. Techniques such as the estimated daily intake of elements (EDI) and probabilistic risk assessment models have been used in the assessment of exposure risk and toxic concentrations of PTEs in humans [1]. Considering that vegetable crops are one of the most important foods in the human diet, understanding their ability to accumulate toxic concentrations of hazardous elements can help reduce potential risks to human health [12]
In this context, this research focuses on the assessment of arsenic (As) and lead (Pb) concentrations in the tubers of *Solanum tuberosum* L., the most common and widespread vegetable species, and associated soils in the vicinity of a pit mine, a thermal power plant and a fly ash disposal sites in three Belgrade municipalities (Lazarevac, Obrenovac and Surčin). The second objective was to investigate the potential human health risk associated with dietary exposure from consumption of the studied crop by calculating the estimated daily intake (EDI), the target hazard quotient (THQ) and the health risk index (HRI) for the studied elements.

Materials and methods

Species description

Solanum tuberosum L., commonly known as the white potato, is considered the most important non-cereal crop in the world and is the fourth largest crop after wheat, maize and rice. It is an annual plant from the nightshade family (Solanaceae), which is cultivated for its starchy, edible tubers. The potato is native to the Peruvian-Bolivian Andes and is one of the most important food plants in the world. There are several varieties, some of which have highly pigmented flesh in colors other than white, including yellow, beige, orange, red, brown, purple and blue [13, 14]. The tubers of *S. tuberosum* are a rich source of starch and glycoalkaloids, are easily digestible and provide vitamin C, protein, thiamine and niacin.

Figure 1. *Stem, flower and tuber of Solanum tuberosum*

The compound leaves are spirally arranged; each leaf is 20–30 cm long and consists of a terminal leaflet and two to four pairs of leaflets. The white, lavender or purple flowers have five fused petals and yellow stamens. The fruit is a small poisonous berry with numerous seeds. All green parts of the potato plant are inedible as they contain a poison called solanine. The stems extend underground in structures called stolons. The ends of the stolons can greatly enlarge and form a few to more than 20 tubers of different shapes and sizes, usually weighing up to 300 g. The buds sprout to form clones of the parent plant, allowing growers to vegetatively propagate the desired traits. The most important form of commercial propagation is vegetative propagation. Potatoes can either be harvested mature when the tubers are fully grown and/or the plant has dried out in around June.

Sample collection and preparation

Sampling was carried out in three Belgrade municipalities – Surčin (village Jakovo, 44°30' N, 19°58' E), Lazarevac (village Sokolovo 44°28' N, 20º19' E) and Obrenovac (village Krtinka 44°44' N, 20°15' E). In each of the three villages, three sampling sites (gardens) were randomly selected for plant and soil sampling. All selected gardens are located near the fly ash disposal site of the thermal power plant "Nikola Tesla-A". The tubers of *S. tuberosum* were sampled in a quantity of about 1 kg. The tubers were first graded using a grater, then dried for 10 days at room temperature and finally in a drying chamber (Binder, Tuttlingen, Germany) to a constant weight. The associated soil was also sampled at three individual sampling points and then mixed to a composite sample according to a harmonized sampling regime at a depth of 0-20 cm. Soil samples were dried to a constant mass and homogenized.

Element concentrations and statistical analysis

The concentrations of selected elements in *S. tuberosum* were measured after wet digestion according to USEPA 3052 method, using concentrated nitric acid and hydrogen peroxide. The concentrations were measured using the optical emission spectrometry method for simultaneous multielemental analysis (ICP - OES, Spectro Genesis). Beech leaves (BCR - 100) were used as reference material to validate the analytical procedure and for quality control of the laboratory protocol. The analysis was carried out in six replicates (n=6). The detection limits for As were 0.007 mg kg^{-1} and for Pb 0.002 mg kg^{-1}. The element content in the soil was determined in the same way as for the plant material, namely according to USEPA method 3050 using aqua regia, followed by a validation of the analytical procedure using the standard reference material (Loam soil - ERM - CC141). The detection limits were identical to those of the plant material.

The data of this study were analysed using a statistical analysis (ANOVA) and the means were separated with a Bonferroni test at a significance level of $p<0.05$ using the Statistica software package (StatSoft In., Tulsa, USA, 2014).

Health risk assessment (non-carcinogenic risk-NCR)

The estimated daily intake of elements (EDI) and the target hazard quotient (THQ) are necessary procedures to calculate the NCR of PTEs to humans [3,8]. The EDI of PTEs is proportional to their concentration in the edible parts of vegetables and to the amount of the corresponding vegetables consumed, and it has been calculated using equation (1):

$$EDI = \frac{C \times IR \times EF \times ED}{BW \times AT} \times 10^{-3} \quad (1)$$

Where C is the concentration of PTEs in vegetable samples (mg kg^{-1}), IR is the ingestion rate of the vegetables, in this case tubers of *S. tuberosum* (93 g $person^{-1}$ day^{-1}, [15]; although it is very ungrateful to speak of global average consumption of potatoes, as these figures vary between 50-800 g per person per day depending on the region of the world), EF is the exposure frequency rate of the vegetables (365 days $year^{-1}$), ED is the exposure duration rate of the vegetables (70 years), BW is the average adult body weight (70 kg), and AT is the average time for non-carcinogenic risks (25550 days) and RfD (reference dose) is the maximum tolerable daily intake of a specific PTE (g^{-1} $person^{-1}$ day^{-1}). The RfD values of As and Pb are 0.0003 and 0.0035 [16].

The THQ is a ratio between the calculated estimated daily intake (EDI, mg kg^{-1} day^{-1}) and the reference dose (RfD, mg kg^{-1} day^{-1}). If the THQ is ≥ 1, there is a possibility that non-carcinogenic effects will occur, while if the THQ is < 1, it is unlikely that the exposed person will experience obvious health damage [3,8]. THQ was calculated using equation (2):

$$THQ = \frac{EDI}{RfD} \quad (2)$$

The combined non-carcinogenic risks of more than one PTE were assessed with a hazard risk index (HRI). The HRI is the sum of the THQs of the individual PTEs investigated [3] and is expressed by equation (3):

$$HRI = \sum THQ \quad (3)$$

Results and discussion

Arsenic and lead content in S. tuberosom tubers and associated soil

Arsenic content was below the detection limit in both *S. tuberosum* tubers and associated soil at all sampling sites in 2013, except in Lazarevac soil (3.19 mg kg^{-1}), so no statistical analysis was performed between sites. In contrast, the As content in *S. tuberosum* in 2014 ranged from 0.59 mg kg^{-1} in Obrenovac to 0.76 mg kg^{-1} in Lazarevac (Table 1), which is why there were no statistically significant differences between sampling sites.

Table 1. Difference in As and Pb content between sampling sites in *S. tuberosum* and associated soil in 2013 and 2014

2013			***S.tuberosum***				**Soil**	
As (mg kg^{-1})	av ± st dev	Surčin	Lazarevac	Obrenovac	av ± st dev	Surčin	Lazarevac	Obrenovac
Surčin	<DL	/			<DL	/	***	ns
Lazarevac	<DL		/		3.19±0.90	***	/	***
Obrenovac	<DL			/	<DL	ns	***	/
Pb (mg kg^{-1})								
Surčin	2.56±0.24	/	ns	*	56.24±6.71	/	*	**
Lazarevac	2.58±0.63	ns	/	*	71.45±10.11	*	/	ns
Obrenovac	1.74±0.42	*	*	/	74.43±3.23	**	ns	/
2014			***S.tuberosum***				**Soil**	
As (mg kg^{-1})	av ± st dev	Surčin	Lazarevac	Obrenovac	av ± st dev	Surčin	Lazarevac	Obrenovac
Surčin	0.74±0.13	/	ns	ns	5.85±0.67	/	***	ns
Lazarevac	0.76±0.11	ns	/	ns	19.23±1.04	***	/	***
Obrenovac	0.59±0.14	ns	ns	/	5.23±1.25	ns	***	/
Pb (mg kg^{-1})								
Surčin	0.50±0.11	/	ns	ns	42.64±3.83	/	***	ns
Lazarevac	0.69±0.21	ns	/	ns	64.21±0.71	***	/	**
Obrenovac	0.65±0.11	ns	ns	/	51.23±7.88	ns	**	/

ANOVA, n=5, *p<0,05, **p<0,01, ***p<0,001, ns-no statistical significance

The normal As content in plant tissues is in the range of 1-1.7 mg kg^{-1} [17], and all values determined do not exceed the MAC prescribed by the legal regulations for dried vegetables (1 mg kg^{-1};[18]). It is assumed that plants take up As passively with the water flow, but literature data show that the highest concentrations are always found in old leaves and roots. As for soils, the As content at the Lazarevac sampling site was higher than the average values for world soils (4.4-8.4 mg kg^{-1}), while higher values than the background concentrations for world soils (5 mg kg^{-1}) were measured at all sampling sites. However, the results of the analysis of the As content were below the MAC value prescribed by the national regulation (25 mg kg^{-1}) at all sampling sites [19]. The Pb content in *S. tuberosum* tubers in 2013 was in the range of 1.74-2.58 mg kg^{-1}, while in 2014 it fluctuated in a narrow range of 0.50-0.76 mg kg-1, and no statistically significant differences were found between sampling sites, with the content decreasing between the two sampling years (Table 1). All results for Pb content in *S. tuberosum* were below the MAC for dried vegetables (3 mg kg^{-1}, national regulation) and within the range considered normal for plant tissue [17]. Lead is known to be an element with low mobility and the ability to bind to the cell walls of roots, which is why its translocation to other plant tissues is negligible. The variation in Pb content of plants is highly influenced by environmental factors and when plants are grown in uncontaminated sites, the content is relatively stable. Since the

uptake of Pb by the roots is passive, the uptake rate from the soil is low [20]. The Pb content in soil ranged from 56.24 mg kg^{-1} in Surčin to 74.43 mg kg^{-1} in Obrenovac in 2013, with statistically significant differences ($p<0.01$) determined between these two sampling sites, while in 2014 it ranged from 42.64 mg kg^{-1} in Surčin to 64.21 mg kg^{-1} in Lazarevac, with a decrease in Pb content between the two seasons. All results for Pb content in soils were below the MAC (maximum allowable concentrations in soils for agricultural purposes) of 375 mg kg^{-1} and the MAC for soils (100 mg kg^{-1} , [19]). Arsenic and Pb are non-essential and extremely toxic elements, but a mitigating circumstance is their characteristic of being less mobile and most frequently absorbed on fine soil particles, organic matter and amorphous oxides [17], so *S. tuberosum* from the studied sites is unlikely to accumulate in concentrations that may cause adverse effects when consumed. Its presence in the soil is related to the possible use of pesticides containing As and Pb [21].

Non-carcinogenic risks (NCR)

The estimated daily intake (EDI), the target hazard quotient (THQ) and the hazard risk index (HRI) for two tested elements are shown in Table 2.

Table 2. Estimated daily intake (EDI), target hazard quotient (THQ), and hazard risk index (HRI) for As and Pb in *S. tuberosum*

	***S. tuberosum* harvest 2013**		***S. tuberosum* harvest 2014**		***S. tuberosum* harvest 2013**			***S. tuberosum* harvest 2014**		
Sampling site	**EDI**				**THQ**		**HRI**	**THQ**		**HRI**
	As	**Pb**	**As**	**Pb**	**As**	**Pb**		**As**	**Pb**	
Surčin	<DL	3,40E-03	9,80E-04	6,60E-04	< DL	9,71E-01	9,72E-01	3,28	1,90E-01	3,47
Lazarevac	<DL	3,42E-03	1,01E-03	9,20E-04	< DL	9,77E-01	9,79E-01	3,36	2,62E-01	3,62
Obrenovac	<DL	2,31E-03	7,80E-04	8,60E-04	< DL	6,60E-01	6,60E-01	2,61	2,47E-01	2,86

The EDI was determined based on the mean element concentration accumulated in *S. tuberosum*, ingestion rate, the exposure duration, the exposure frequency, the average body weight and the average time. The THQ represents the ratio between the calculated dose of a pollutant and an oral reference dose [3,8]. As can be seen from the results, the THQ for As in *S. tuberosum* was higher than 1 in 2014, indicating a serious health risk associated with its consumption. The Hazard Risk Index (HRI) estimates the cumulative effects of ingestion of various PTEs through consumption, and as it was >1 at all sampling sites, it indicates that the consumption of potatoes from these sampling sites may pose a health risk to the population.

Conclusion

The results obtained showed that the content of non-essential and toxic elements As and Pb was within the range considered normal in plant tissues and below the MAC for dried vegetables under national legislation of the Republic of Serbia (<1 mg kg^{-1} for As and <3 mg kg^{-1} for Pb). Arsenic was not measured in the tubers of *S. tuberosum* in 2013, but was measured in the 2014 harvest, while the Pb concentration showed a decreasing trend between the two sampling seasons. The As content in the examined soils was above the background value for global soils (5 mg kg^{-1}), but below the MAC (<25 mg kg^{-1}), as was the Pb content (<100 mg kg^{-1}), with concentrations decreasing significantly between the two seasons.

Lazarevac proved to be the most polluted sampling site, where the highest concentrations of As and Pb were measured in *S. tuberosum* and the associated soil.
The calculation of the non-carcinogenic risk showed that the target hazard quotient and the hazard risk index for *S. tuberosum* from 2014 exceeded the provisional maximum tolerable daily intake, as the values were >1. These results show that the consumption of the 2014 harvest from the investigated sampling sites posed a health risk to humans.
To better understand the potential health and contamination risks for vegetable production in the vicinity of major pollutants, the bioavailability of potentially toxic elements, their forms and the plant-available fractions of these elements need to be determined in future studies.

Acknowledgements

This work was supported by the Ministry of Science, Technological Development and Innovation of the Republic of Serbia, grant no. 451-03-66/2024-03/200007.

References

1. J. I. Nwachukwu, L. J. Clarke, E. Symeonakis, F. Q. Brearley, Assessment of human exposure to food crops contaminated with lead and cadmium in Owerri, South-eastern Nigeria, *J. Trace Elem. Miner*., **2**, 100037, 2022.
2. L. Chen, S. Zhou, Y. Shi, C. Wang, B. Li, Y. Li, S. Wu, *Sci. Total Environ*., **615**, 141-149, 2018.
3. N. Gupta, K. K. Yadav, V. Kumar, S. Krishnan, S. Kumar, Z. D. Nejad, M. A. M. Khan, J. Alam, Evaluating heavy metals contamination in soil and vegetables in the region of North India: Levels, transfer and potential human health risk analysis, *Environ. Toxicol. Phar*., **82**, 103563, 2021.
4. C. O. Ogunkunle, R. A. Obidele, N. O. Ayoola, G. O. Okunlola, A. B. Rufai, O. A. Olatunji, A. T. Adetunji, M. A. Jimoh, Potential toxic elements in market vegetables from urban areas of southwest Nigeria: Concentration levels and probabilistic potential dietary health risk among the population, *J. Trace Elem. Miner*., **1**, 100004, 2022.
5. Food and Agriculture Organization & World Health Organization. (2016). General standard or contaminants and toxins in food and feed (CODEX STAN 193-1995).
6. X. S. Luo, S. Yu, Y. G. Zhu, X. D. Li, Trace metal contamination in urban soils of China, *Sci. Total Environ*., **421**, 17-30, 2012.
7. L. N. A. Sackey, K. Markin, A. Kwarteng, I. M. Ayitey, P. Kayoung, Presence and levels of potential trace elements in lettuce and spring onion grown in Kumasi, Ghana, *Kuwait J. Sci*., **51(1)**, 100143, 2024.
8. N. W. Hu, H. W. Yu, B. L. Deng, B. Hu, G. P. Zhu, X. T. Yang, T. Y. Wang, Y. Zeng, Q. Y. Wang, Levels of heavy metal in soil and vegetable and associated health risk in peri-urban areas across China, *Ecotox. Environ. Safe*., **259**, 115037, 2023.
9. G. Nabulo, S. D. Young, C. R. Black, Assessing risk to human health from tropical leafy vegetables grown on contaminated urban soils, *Sci. Total Environ*., **408(22)**, 5338-5351, 2010.
10. G. J. Wagner, Accumulation of cadmium in crop plants and its consequences to human health, *Adv. Agron*., **51**, 173-212, 1993.
11. J. A Ryan, H. R. Pahren, J. B. Lucas, Controlling cadmium in the human food chain: a review and rationale based on health effects, *Environ. Res*. **28(2)**, 251-302, 1982.
12. X. Luo, B. Ren, A. S. Hursthouse, F. Jiang, R. J. Deng, *Environ. Geochem. Health*, **42**, 1965-1976, 2020.
13. R. do Nascimento, M. da Rochaalves, N. Hargreaves Noguera, D. C. Lima, M. R. Marostica Junior, "Cereal grains and vegetables", in Natural plant produsts in inflammatory bowel diseases, R. do Nascimento, A. Paula, et. al., Eds. Academic Press, 2023, 103-172.
14. P. Saar-Reismaa, K. Kotkas, V. Rosenberg, M. Kulp, M. Kuhtinskaja, M. Vaher, Analysis of Total Phenols, Sugars, and Mineral Elements in Colored Tubers of *Solanum tuberosum* L. *Foods, 9*, 1862, 2020.
15. G. Burgos, T. Z. Felde, C. Andre, S. Kubow, "The Potato and Its Contribution to the Human Diet and Health", in *The Potato Crop*, H. Campos, O. Ortiz, Eds. Switzerland, Springer, 2020, 37-75.
16. United States Environmental Protection Agency. (2015). Regional Screening Level (RSL) Summary Table. [Online]. Available: https://epa-prgs.ornl.gov/chemicals/download/composite_sl_table_run_NOV2015.pdf

17. A. Kabata-Pendias, H. Pendias, *Trace elements in soils and plants*. CRC Press, Boca Raton, FL, 2001.
18. National Regulations on the quantities of pesticides, metals, metalloids and other toxic substances, chemotherapy drugs, anabolics and other substances that can be found in foodstuffs: FRY 5/1992-67, 11/1992-151 (amend.), 32/2002-2, RS 25/2010-16 (other regulations), RS 28/2011-9 (other regulations) Official Gazette RS, no. 23/94).
19. OGRS (1994). Regulation about allowable quantities of hazardous and harmful substances in the soil and methods for their investigation. Official Gazette of the Republic of Serbia, 23, 1994. (in Serbian).
20. A. Kabata-Pendias, A. B. Mukherjee, *Trace elements from soil to human*. Springer Berlin Heidelberg, New York, 2007.
21. M. B. McBride, Arsenic and lead uptake by vegetable crops grown on Historically contaminated orchard soils, *Appl. Environ. Soil Sci*., **283472**, 2013.

Estimation of enzyme affinity of chemically bonded Glucose Oxidase onto polyaniline-based enzyme electrode

Branimir Jugović[1] , Zorica Knežević-Jugović[2], Milica Gvozdenović[2,*]

[1] *Institute of Technical Science, SASA, Knez Mihajlova 35, 11 000 Belgrade, Serbia*

[2] *Faculty of Technology and Metallurgy,University of Belgrade, Karnegijeva 4, 11120 Belgrade, Serbia*

[*] *popovic@tmf.bg.ac.rs*

Abstract

The enzyme electrode (EE) was formed by immobilizing Glucose Oxidase by chemical bonding and establishing peptide bonds onto a polyaniline based electrode (PE). The PE was formed electrochemically,using galvanostatic co-polymerization of aniline and m-aminobenzoic acid from an acidic aqueous electrolyte composed of 0.2 mol dm $^{-3}$ monomers in equal amounts at a constant current density of 2.0 mA cm $^{-2}$. The EE response to different concentrations of glucose was evaluated from chronopotentiometric experiments recorded at 10 µA cm $^{-2}$, in phosphate buffer at pH 6.8. The dependence of the potentials of EE on glucose concentrations has the shape of a typical rectangular hyperbola, characteristic of Michaelis-Menten enzyme kinetics with the linearity range of the response wider than that of the cross-linked EE. From the Lineweaver-Burk linearization, the estimated value of the apparent Michaelis-Menten constant was 0.50 mmol dm $^{-3}$, which is a greater value than for cross-linked enzyme, revealing the slight loss of the activity, as expected for chemical bonding, but still much lower than the value for the free enzyme, indicating high affinity of the chemically bonded enzyme into polyaniline-based electrode material. However, EE obtained by chemical bonding showed much better storage stability compared to the cross-linked EE, which is a good base for analytical applications.

Keywords: *enzime electrode, Glucose Oxidase, chemical imobilization, enzyme affinity*

Electrochemical polymerization of pyrrole on mild steel from p-toluensulfonic acid electrolyte

Milica Gvozdenović[1,*], Tijana Kovač[2], Branimir *Jugović3*, Bojan Jokić[4], Enis Džunuzović[1]

[1] *Faculty of Technology and Metallurgy,University of Belgrade, Karnegijeva 4, 11120 Belgrade, Serbia*

[2] *Innovation Center of the Faculty of Technology and Metallurgy in Belgrade, Karnegijeva 4, 11120 Belgrade, Serbia*

[3] *Institute of Technical Science, SASA, Knez Mihajlova 35, 11 000 Belgrade, Serbia*

[4] *Faculty of Applied Arts, University of Arts in Belgrade, Kralja Petra 4, 11000 Belgrade, Serbia*

[*] *popovic@tmf.bg.ac.rs*

Abstract

Conditions for electrochemical synthesis of polypyrrole on mild steel were investigated in an aqueous electrolyte containing different concentrations of p-toluenesulfonic acid in the range of 0.05 - 0.3 mol dm^{-3} without and with the addition of 0.2 mol dm^{-3} pyrrole, aiming to estimate the composition of the electrolyte and polymerization current density, necessary for achieving the formation of uniforme and adherent polypyrrole. The optimal concentration of p-toluensulfonic acid of 0.1 mol dm^{-3},was chosen based on recorded anodic polarization curves. To estimate the current density for the electrochemical polymerization of pyrrole, chronopotentiometric curves of mild steel at different constat current densities, were recorded in 0.1 mol dm^{-3} p-toluenesulfonic acid and 0.2 mol dm $^{-3}$ pyrrole. It was shown that deposition of polypyrrole was achieved with an induction period which was lower comparing to the resuts obtained in oxalic acid, as the most popular electrolyte for electrochemical synthesis of polypyrrole on steel. The protection efficiency based on polarization curves of mild steel and mild steel with electrochemically formed p-toluensulfonic acid doped polypyrrole in 3% NaCl was around oko 90 % which is higher than the value obtained for p-toluensulfonic acid doped polyaniline.

Keywords: *polypyrrole, p-toluenesulfonic acid, electrochemical polymerization, protection efficiency*

Optimization of Process Parameters for Assessing the Inhibitory Potential of Dandelion Root Extract in NaCl Solution

Nebojša Vasiljević[1,*], Marija Mitrović[1], R.F. Godec[2], Jovan Vujić[3], Milorad Tomić[1,4]

[1] *University of East Sarajevo, Faculty of Technology, 75400 Zvornik, Republic of Srpska*

[2] *University of Maribor, Faculty of Chemistry and Chemical Engineering, Slovenia*

[3]*Jugoinspekt Beograd a.d., Breograd, Srbija*

[4]*Enginering academy of Serbia, Serbia*

[*]*nebojsa.vasiljevic@tfzv.ues.rs.ba*

Abstract

This paper explores the impact of steel type, inhibitor concentration, and time on the effectiveness of dandelion root extract as an inhibitor in a 3% NaCl solution. Two distinct steel types with known compositions were utilized, and the inhibitory efficiency was assessed over intervals of 2, 4, 6, 24, and 48 hours. Dandelion root extract, acquired via the Soxlet method with 96% ethanol, was subsequently diluted (at concentrations of 0.5 g/l, 1.0 g/l, and 1.5 g/l) in the 3% NaCl solution. Experimental data were optimized using MINITAB 21 software. The paramount parameter of the inhibitory efficiency pertains to the concentration of dandelion in 3% NaCl solution, with discernibly profound effects, whereas time exhibit nominal impact, given the expeditious attainment of beneficial outcomes within a mere two-hour interval. Furthermore, a heightened efficieny in inhibition is noted for Steel type 1.

Keywords: *corrosion; dandelion roots; optimization; inhibitor*

Introduction

Metal corrosion, governed by thermodynamic principles, is an unavoidable occurrence leading to the conversion of pure metals into more stable thermodynamic forms [1]. This natural process poses significant challenges, particularly in industrial settings where metals used in equipment and structures are highly susceptible to corrosion, resulting in substantial damage to material performance [2]. To address this threat, numerous corrosion prevention methods have been developed, including coatings, corrosion inhibitors, sacrificial anodes, and corrosion-resistant alloys [3], [4], [5], [6]. These methods aim to mitigate the economic, material conservation, and safety impacts of corrosion across various engineering applications. One effective strategy to combat corrosion is the use of corrosion inhibitors. These substances, due to their low cost, ease of fabrication, and convenience in operation, are widely employed in industrial settings [7].

Traditional corrosion inhibitors, while effective, often contain toxic chemicals harmful to human and ecological health. With increasing awareness of environmental protection, there has been a growing interest in greener alternatives [8]. Green corrosion inhibitors, focusing on non-toxic, eco-friendly processes and utilizing renewable materials at low cost, have gained prominence [9], [10]. Recent studies have shown promising results utilizing plant extract-based green corrosion inhibitors, which are biocompatible, biodegradable, and cost-effective [11], [12], [13].

Green chemistry principles advocate for the development of eco-friendly chemicals to minimize the discharge of hazardous materials into the environment. Natural plant extracts, with their rich chemical constituents such as polyphenols, flavonoids, tannins, alkaloids, and polysaccharides, possess the potential to inhibit metal corrosion effectively [14], [15]. These extracts, derived from various parts of plants, offer a renewable and cost-effective solution to corrosion challenges, making them an attractive avenue for further research and application in environmental corrosion inhibition [16], [17].

In this study, a novel bio-based extract has been examined to prevent corrosion of steel in aggressive NaCl environments. This extract was sourced from dandelion roots (*Taraxacum officinale*), a compound utilized in traditional medicine and modern pharmaceutical formulations [18]. *Taraxacum officinale* is renowned for its antioxidant properties, attributed to its high polyphenol content, including sesquiterpene lactones, phenylpropanoids, triterpenoid saponins, and polysaccharides [19], [20]. Many of these compounds contain heteroatoms such as nitrogen and oxygen, as well as multiple bonds in their molecular structures, which may facilitate the adsorption onto the surface of metal.

Experimental

To determine the inhibitory effect of dandelion root extracts in a 3% NaCl solution, two steel samples of known composition were utilized, each with dimensions of 31x31mm. The samples underwent chemical preparation of their surfaces before testing the corrosion rate. All experiments were conducted indoors at room temperature.

The steel samples were first degreased using detergent, followed by rinsing with running and distilled water. They were then subjected to chemical degreasing at 80-90°C for 20 minutes. After another round of rinsing, the samples underwent etching in 20% H_2SO_4 at 60-70°C for 1 minute. Post-etching, the samples were rinsed again and dried using 96% ethanol for expedited drying. After a 5-minute drying period, the initial mass of each sample was measured. Subsequently, the sample surfaces were activated in 20% H_2SO_4 at 60-70°C for 2 seconds. Following another round of rinsing, the samples were immersed in either uninhibited or inhibited solutions for intervals of 2, 4, 6, 24, and 48 hours.

The inhibition extracts were prepared by Soxlet extraction of dandelion roots using 96% ethanol, and the dry matter content (dandelion content) in the extract was determined by evaporation. After that, 3% NaCl solutions with 0.5 g/l, 1.0 g/l, and 1.5 g/l of dandelion were prepared with the obtained dandelion extract.

From the measured mass loss of the steel samples in the solutions, corrosion rate (Km^-), depth corrosion indicator (π), and inhibitor efficiency (degree of inhibitor protection, z) were calculated.

Experimental data were fitted to a second-order polynomial model to obtain the regression coefficients. The generalized second-order polynomial model is as follows:

$$Y = a_0 + \sum a_i X_i + \sum a_{ii} X_i^2 + \sum a_{ij} X_i X_j \quad (1)$$

In the developed model, Y denotes the experimental response, with a_0 being a constant, and a_i, a_{ii}, and a_{ij} representing the coefficients of the linear, quadratic, and interactive regression models, respectively. X_i and X_j stand for independent variables in coded values.

The adequacy of the model was evaluated using the coefficient of determination (R^2) and p-values obtained from analysis of variance (ANOVA). Regression analysis and contour plots were employed to illustrate the influence of independent variables on the response.

Results and Discusion

Table 1 displays the impact of process parameters on corrosion rate (Km^-), depth corrosion indicator (π), and inhibitor efficiency (z).

Table 1. Influence of steel type, inhibitor concentration and time on output variables

Input			Output			Input			Output		
Steel type	Inhibitor concentration [g/l]	Time [h]	Corrosion rate Km$^-$ [g/m^{2}h]	Depth corrosion indicator π [mm/year]	Inhibitor efficiency z [%]	Steel type	Inhibitor concentration [g/l]	Time [h]	Corrosion rate Km$^-$ [g/m^{2}h]	Depth corrosion indicator π [mm/year]	Inhibitor efficiency z [%]
1	0	2	0.2577	0.3135	0.00	2	0	2	0.2051	0.2379	0.00
1	0	4	0.2448	0.2978	0.00	2	0	4	0.1923	0.0624	74.99
1	0	6	0.2663	0.3240	0.00	2	0	6	0.1966	0.0648	79.98
1	0	24	0.2556	0.3110	0.00	2	0	24	0.1944	0.0519	78.28
1	0	48	0.2567	0.3123	0.00	2	0	48	0.1955	0.0597	74.74
1	0.5	2	0.1804	0.2195	30.00	2	0.5	2	0.0513	0.0611	74.32
1	0.5	4	0.1675	0.2038	31.58	2	0.5	4	0.0385	0.0936	62.51
1	0.5	6	0.1718	0.2090	35.47	2	0.5	6	0.0427	0.0780	66.67
1	0.5	24	0.1675	0.2038	34.47	2	0.5	24	0.0491	0.0727	69.58
1	0.5	48	0.1718	0.2090	33.07	2	0.5	48	0.0502	0.0754	68.11
1	1	2	0.1031	0.1254	59.99	2	1	2	0.0769	0.0793	66.65
1	1	4	0.1160	0.1411	52.61	2	1	4	0.0641	0.0624	74.99
1	1	6	0.1117	0.1359	58.05	2	1	6	0.0598	0.0780	66.67
1	1	24	0.1095	0.1332	57.16	2	1	24	0.0620	0.0624	73.91
1	1	48	0.1085	0.1320	57.73	2	1	48	0.0652	0.0727	69.24
1	1.5	2	0.0515	0.0627	80.01	2	1.5	2	0.0513	0.0741	68.85
1	1.5	4	0.0387	0.0471	84.19	2	1.5	4	0.0641	0.2379	0.00
1	1.5	6	0.0429	0.0522	83.89	2	1.5	6	0.0513	0.0624	74.99
1	1.5	24	0.0387	0.0471	84.86	2	1.5	24	0.0598	0.0648	79.98
1	1.5	48	0.0376	0.0457	85.35	2	1.5	48	0.0609	0.0519	78.28

To assess the impact of process parameters on the output, ANOVA analysis was employed alongside the evaluation of the resultant models.

Experimental data for each measurement variable were fitted into a quadratic model. For each member of the regression model, F-value and p-value were calculated. With a confidence level set at 95%, any p-value exceeding 0.05 was deemed not statistically significant.

Table 2 presents the ANOVA outcomes detailing the influence of input parameters on corrosion rate (Km-), inhibitor efficiency (z), and depth corrosion indicator (π).

Table 2. Results of ANOVA analysis

Source	DF[a]	Corrosion rate Km$^-$ [g/m^{2}h]				Depth corrosion indicator π [mm/year]				Inhibitor efficiency z [%]			
		Adj SS[b]	Adj MS[c]	F-value	P-value[d]	Adj SS	Adj MS	F-val.	P-val.	Adj SS	Adj MS	F-val.	P-val.
Regresion	8	0.208313	0.026039	38.76	0.001	0.307230	0.038404	41.34	0.001	34080.8	4260.10	24.39	0.001
Steel type (A)	1	0.027290	0.027290	40.62	0.001	0.039042	0.039042	42.02	0.001	1299.1	1299.09	7.44	0.010
Inhibitor conc. (B)	1	0.058155	0.058155	86.57	0.001	0.084693	0.084693	91.16	0.001	9316.0	9316.00	53.33	0.001
Time (C)	1	0.000053	0.000053	0.08	0.780	0.000083	0.000083	0.09	0.768	8.7	8.67	0.05	0.825
BB	1	0.015769	0.015769	23.47	0.000	0.022491	0.022491	24.21	0.001	3880.9	3880.90	22.22	0.001
CC	1	0.000032	0.000032	0.05	0.829	0.000061	0.000061	0.07	0.800	2.5	2.53	0.01	0.905
AB	1	0.011735	0.011735	17.47	0.001	0.017029	0.017029	18.33	0.001	661.2	661.24	3.79	0.061
AC	1	0.000025	0.000025	0.04	0.849	0.000016	0.000016	0.02	0.897	11.6	11.61	0.07	0.798
BC	1	0.000001	0.000001	0.00	0.975	0.000000	0.000000	0.00	0.997	0.2	0.20	0.00	0.973
Error	31	0.020826	0.000672			0.028801	0.000929			5415.6	174.70		
Total	39	0.229139				0.336031				39496.4			
Coefficients of determination		R^2 = 0.9091 Adjusted R^2 = 0.8857 Predicted R^2 = 0.8510				R^2 = 0.9143 Adjusted R^2 = 0.8922 Predicted R^2 = 0.8578				R^2 = 0.8629 Adjusted R^2 = 0.8275 Predicted R^2 = 0.7747			

[a] – Degree of Fredom

[b] – Adjusted sum of square

[c] – Adjusted mean square

[d] - $p<0.05$ indicates statistical significance

Note: Terms: AA (square of steel type) cannot be evaluated and were eliminated from the model.

The R^2 values for corrosion rate, depth corrosion indicator, and inhibitor efficiency were found to be 0.9091, 0.9143, and 0.8629, respectively. These values indicate that the variability in response was well accounted for by the generated model, explaining 90.91% of corrosion rate variation, 91.43% of depth corrosion indicator variation, and 86.29% of inhibitor efficiency variation.

Adjusted R^2 serves as a corrected measure for R^2, considering only the terms in the model significantly affecting responses. For corrosion rate, depth corrosion indicator, and inhibitor efficiency, the Adjusted R^2 values were 0.8857, 0.8922, and 0.8275, respectively. These values closely mirror the R^2 values, implying that the proposed models adequately explain variations after excluding members with p-values greater than 0.05.

Predicted R^2 assesses the regression model's predictive capability. The Predicted R^2 values for corrosion rate, depth corrosion indicator, and inhibitor efficiency were 0.8510, 0.8578, and 0.7747, respectively. The disparity between Adjusted R^2 and Predicted R^2 for all output variables was less than 0.2, indicating the obtained model offers reliable predictions for new observations.

Figure 1 illustrates Pareto diagrams depicting the corrosion rate, depth corrosion indicator, and inhibitor efficiency.

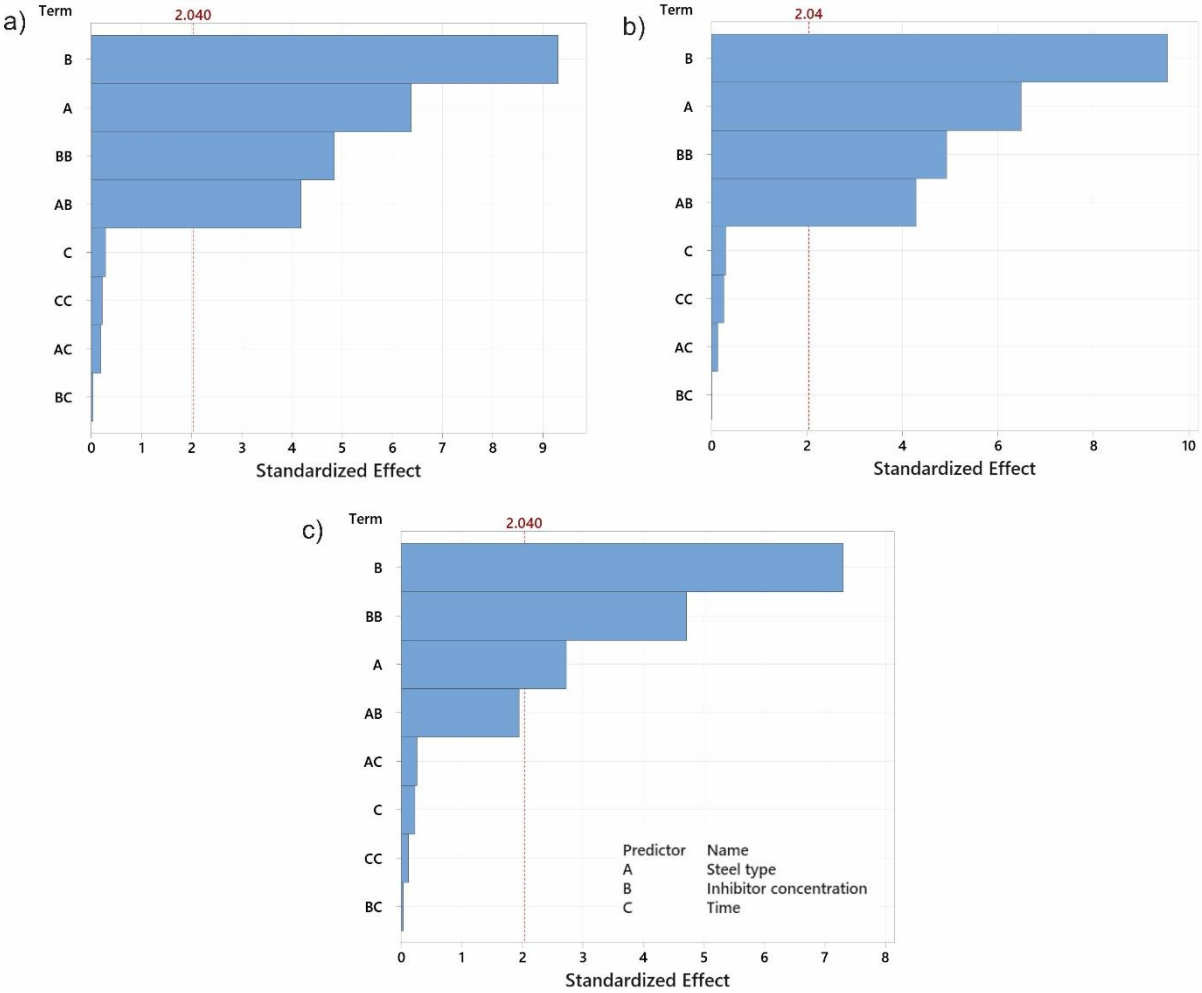

Figure 1. *Pareto diagrams for a) corrosion rate, c) depth corrosion indicator and c) inhibitor efficiency*

Upon analyzing the p-values from Table 2 alongside the Pareto diagram (Figure 1a), it was concluded that the corrosion rate is influenced by the following parameters: inhibitor concentration (B), steel type (A), the square of inhibitor concentration (BB), and the interaction between steel type and inhibitor concentration (AB). Parameters with p-values exceeding 0.05 can be disregarded from abbreviated regression equation.

Additionally, upon examining Figure 1a and Figure 1b, it becomes evident that the Pareto diagrams for the corrosion rate and depth corrosion indicator are nearly identical. This similarity suggests that the input factors exert an equal impact on both outputs.

Lastly, the examination of Table 2 and the Pareto diagram in Figure 1c revealed that the most influential parameters affecting inhibitor efficiency are inhibitor concentration (B), the square of inhibitor concentration (BB), and steel type (A). Although the mutual interaction of steel type and inhibitor concentration (AB) has a p-value slightly above 0.05, it will be retained in the abbreviated regression equation. Other factors with p-values greater than 0.05 can be omitted.

After excluding insignificant elements, the abbreviated regression equations for all outputs took the following form:

$$\text{Corrosion rate } (Km^{-}) = 0.3734 - 0.1008\,A - 0.3212\,B + 0.0794\,BB + 0.0613\,AB \quad (2)$$

$$\text{Depth corrosion indicator } (\pi) = 0.4521 - 0.1206\,A - 0.3876\,B + 0.0949\,BB + 0.0738\,AB \quad (3)$$

$$\text{Inhibitor efficiency } (z) = -30.40 + 22.00\,A + 128.60\,B - 39.40\,BB - 14.55\,AB \quad (4)$$

To assess the impact of process parameters on the output value, contour diagrams were constructed for the steel type (A) and inhibitor concentration (B), as well as for the inhibitor concentration (B) and time (C). However, the contour diagram depicting the influence of steel type and time on the output was not generated, as it is dependent on the preceding diagrams based on the number of degrees of freedom.

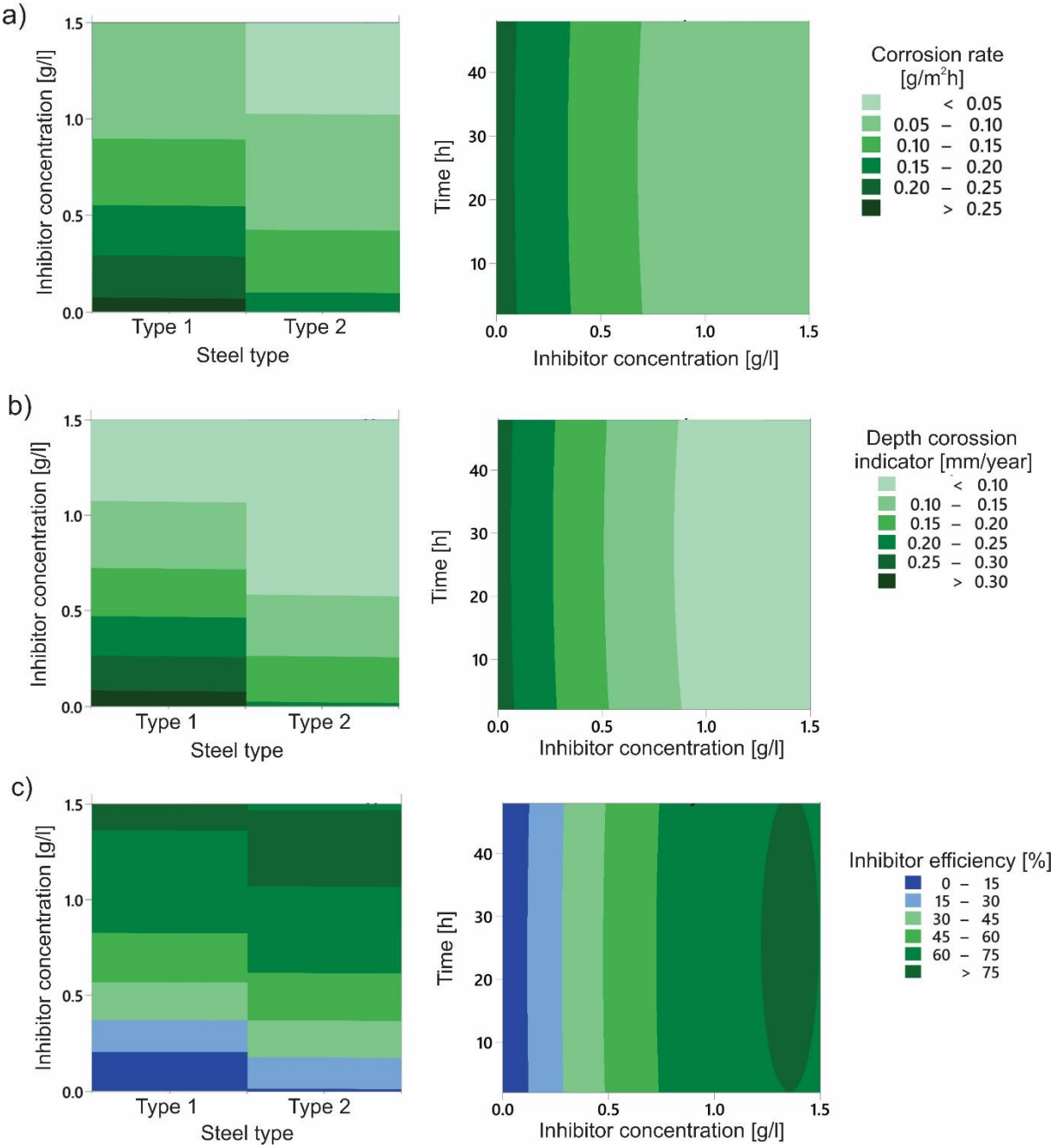

Figure 2. Contour diagrams for: a) corrosion rate, b) depth corrosion indicator and c) inhibitor efficiency

Figure 2a illustrates that in a pure 3% NaCl solution (without inhibitor addition), Steel type 2 (S2) demonstrates significantly greater corrosion resistance, with a mass loss (corrosion rate) ranging between 0.15-0.20 g/m^{2}h, whereas Steel type 1 (S1) exhibits a higher mass loss exceeding 0.25 g/m^{2}h. Moreover, it is evident that inhibitor concentration notably influences the reduction of mass loss, while the mass loss remains relatively stable over time. Additionally, optimal inhibitor concentrations for S1 fall within the range of 0.9-1.5 g/l, resulting in mass losses between 0.05-0.1 g/m^{2}h. For S2, mass loss below 0.05 g/m^{2}h is attained at inhibitor concentrations of 1.0-1.5 g/l.

The findings depicted in Figure 2b largely mirror those in Figure 2a. Specifically, for Steel type 1 (S1), it is evident that with inhibitor concentrations exceeding 1.1 g/l, the depth corrosion indicator falls below 0.1 mm/year, whereas in the absence of inhibitors, the depth corrosion indicator surpasses 0.3 mm/year. Similarly, for Steel type 2 (S2), inhibitor concentrations ranging from 0.6-1.5 g/l result

in a depth corrosion indicator of less than 0.1 mm/year, while without inhibitors, the depth corrosion indicator for S2 in 3% NaCl measures between 0.2-0.25 mm/year.
From Figure 2c, it is evident that for Steel type 1 (S1), a protective factor (inhibitor efficiency) exceeding 75% is achieved with an inhibitor concentration surpassing 1.4 g/l. Conversely, for Steel type 2 (S2), a protective factor greater than 75% is attained at inhibitor concentrations ranging from 1.1-1.5 g/l. Notably, the exposure time of the steel to the corrosion environment does not affect inhibitor efficiency; in other words, the inhibitor efficiency remains constant over time for specific inhibitor concentrations. However, variations in inhibitor concentration in 3% NaCl significantly influence the inhibitor efficiency of both steels (S1 and S2). Steel S2 exhibits higher corrosion resistance (greater propensity for self-passivation) in 3% NaCl compared to S1, resulting in a lesser protective effect from the utilized inhibitor. Nonetheless, the obtained results demonstrate the successful use of dandelion root extract in protecting both types of steel.

Conclusion

This study explores the impact of steel type, inhibitor concentration, and time on the inhibitory effect of dandelion root extract in a 3% NaCl solution, employing MINITAB 21 for statistical analysis. The high R2 values for corrosion rate, inhibitor efficiency, and depth corrosion indicator suggest that the model effectively accounts for response variability. Furthermore, the Adjusted R2 and Predicted R2 values closely align with R2, indicating the models' robustness in explaining various variations and making reliable predictions even after excluding members with p-values exceeding 0.05. By optimizing various process parameters, it was established that dandelion root extract serves as an effective corrosion inhibitor, notably decreasing the corrosion rate for both types of steel. Despite this, the inhibition effect is more pronounced in steel S1. In the absence of inhibitors, steel S1 exhibits superior corrosion resistance compared to steel S2 in a 3% NaCl solution; however, with inhibitor inclusion, the reduction in mass loss is notably more significant in steel S1. Attaining an inhibitor efficiency exceeding 75% in both steel types necessitates an inhibitor concentration surpassing 1.4 g/l. The most substantial effect on reducing the corrosion process of steel in 3% NaCl is attributed to inhibitor concentration, followed by the type of steel, with time exerting the least influence on corrosion rate. These findings underscore the successful application of dandelion root extract as a corrosion inhibitor for the specified and similar steels.

References

1. S. Wan, H. Chen, T. Zhang, B. Liao, X. Guo, Anti-corrosion mechanism of parsley extract and synergistic iodide as novel corrosion inhibitors for carbon Steel-Q235 in acidic medium by electrochemical, XPS and DFT methods, Front. Bioeng. Biotechnol., 9, 815953, 2021.
2. M. Ridjošić, M. Tomić, R. Godec-Fuchs, M. Pavlović, Sage extract as an inhibitor of steel and copper corrosion, Zaštita materijala, 58(4), 475–486, 2017.
3. A. A. Nazeer, M. Madkour, Potential use of smart coatings for corrosion protection of metals and alloys: A review," J. Mol. Liq., 253, 11–22, 2018.
4. S. Wan, H. Chen, X. Ma., L. Chen, K. Lei, B. Liao, Z. Dong, X. Guo, Anticorrosive reinforcement of waterborne epoxy coating on Q235 steel using NZ/BNNS nanocomposites, Prog. Org. Coat., 59, 106410, 2021.
5. S. Z. Salleh, A. H. Yusoff, Siti Koriah Zakaria, M. Taib, A. Abu Seman, M. N. Masri, M. Mohamad, S. Mamat, Sharizal Ahmad Sobri, Arlina Ali, P. Teo, Plant extracts as green corrosion inhibitor for ferrous metal alloys: A review, J. Clean. Prod., 304, 127030, 2021.
6. Y. Cao, D. Zheng, F. Zhang, J. Pan, C. Lin, Layered double hydroxide (LDH) for multi-functionalized corrosion protection of metals: A review, J. Mater. Sci. Technol., 102, 232–263, 2022.
7. Q.H. Zhang, B.S. Hou, Y.Y. Li, G.Y. Zhu, Y. Lei, X. Wang, H.F. Liu, G.A. Zhang, Dextran derivatives as highly efficient green corrosion inhibitors for carbon steel in CO2-saturated oilfield produced water: Experimental and theoretical approaches, Chem. Eng. J., 424, 130519, 2021.

8. M. Alimohammadi, M. Ghaderi, A. Ramazani S.A, M. Mahdavian, Falcaria vulgaris leaves extract as an eco-friendly corrosion inhibitor for mild steel in hydrochloric acid media, Sci. Rep., 13, 3737, 2023.
9. M. Tomić, V. Mićić, L. Mlađenović, R. Fuchs-Godec, M. Pavlović, Đ. Vaštag, Common Sage Extract as an Inhibitor of Steel Corrosion in 3% NaCl, Int. J. Innov. Res. Sci. Eng. Technol., 3, 2278-2299, 2014.
10. M. V. Tomić, M. G. Pavlović, M. Jotanović, R. Fuchs-Godec, Protection of copper and its alloys using corrosion inhibitor-Literature review, Quality of Life, 1, 72-89, 2010.
11. H. Hassannejad, A. Nouri, Sunflower seed hull extract as a novel green corrosion inhibitor for mild steel in HCl solution, J. Mol. Liq., 254, 377-382, 2018.
12. L. L. Liao, S. Mo, H. Q. Luo, N. B. Li, Corrosion protection for mild steel by extract from the waste of lychee fruit in HCl solution: Experimental and theoretical studies, J. Colloid. Interface Sci., 520, 41-49, 2018.
13. M. Ghaderi, A. R. Saadatabadi, M. Mahdavian, S. A. Haddadi, pH-Sensitive polydopamine–La (III) complex decorated on carbon nanofiber toward on-demand release functioning of epoxy anti-corrosion coating, Langmuir, 38, 11707–11723, 2022.
14. E. E. Oguzie, A. I. Onuchukwu, P. C. Okafor, E. E. Ebenso, Corrosion inhibition and adsorption behaviour of Ocimum basilicum extract on aluminium, Pigm. Resin. Technol., 35(2), 63-70, 2006.
15. H. Hassannejad, A. Barati, A. Nouri, The use of nanoemulsion-based strategies to improve corrosion inhibition efficiency of Thyme-based inhibitor, J. Mol. Liq., 296, 112110, 2019.
16. N. A. Abd Aziz, R. Hasham, M. R. Sarmidi, S. H. Suhaimi, M. K. H. Idris, A review on extraction techniques and therapeutic value of polar bioactives from Asian medicinal herbs: Case study on Orthosiphon aristatus, Eurycoma longifolia and Andrographis paniculata, Saudi Pharm. J., 29(2), 143-165, 2021.
17. E. A. Noor, Potential of aqueous extract of Hibiscus sabdariffa leaves for inhibiting the corrosion of aluminum in alkaline solutions, J. Appl. Electrochem., 39(9), 1465-1475, 2009.
18. B. Lis, B. Olas, Pro-health activity of dandelion (Taraxacum officinale L.) and its food products – history and present, J. of Funct. Foods, 59, 40-48, 2019.
19. E. Yarnell, K. Abascal, Dandelion (Taraxacum officinale and T. mongolicum), Integr. Clin. Med., 8(2), 35-38, 2009.
20. W. Biel, A. Jaroszewska, E. Łysoń, A. Telesiński, The chemical composition and antioxidant properties of common dandelion leaves compared with sea buckthorn, Can. J. Plant Sci., 97(6), 1165-1172, 2017.

Recycling honey bee drone brood

Ponovna upotreba trutovskog legla medonosne pčele

Nenad M. Zarić[1, 2 *], Miloš Petrović[3], Ratko Pavlović[4]

[1] *University of Belgrade – Faculty of Biology, Studentski trg 12-16, Belgrade, Serbia*

[2] *University of Natural Resources and Life Sciences (BOKU), Department of Agrobiotechnology (IFA-Tulln), Institute of Bioanalytics and Agro-Metabolomics, Konrad-Lorenzstr 20, Tulln, Austria*

[3] *University of Novi Sad, Faculty of Agriculture, Trg Dositeja Obradovića 8, 21102 Novi Sad, Serbia*

[4] *University of Belgrade – Faculty of Chemistry, Department of Biochemistry, Studentski trg 12-16, Belgrade, Serbia*

[*]*nenad.zaric@bio.bg.ac.rs; nenad.zaric@boku.ac.at*

Abstract

Due to the need for sustainable food sources, scientists are increasingly turning to insects as a good source of protein and minerals. Until now, many insects have been proposed as good sources of nutrients for animal and human consumption. One of them is Tenebrio molitor. In this paper, we compared the mineral composition of Tenebrio flour with flour obtained from the brood of bee drones, which until now have not been approved as animal feed. We have shown that 1.5 kg of drone brood can yield 200 g of flour. Although the mineral composition is different, both types of insects are suitable to compensate for deficiencies in mineral needs. Drone brood is removed from the hive as a form of green control against varroa and are generally thrown away. We suggest that they can be used as a diet rich in minerals and proteins.

Keywords: *honey bees; arsenic; pollution; ICPMS; Apis mellifera*

Uvod

U potrazi za održivim i hranljivim izvorima hrane, istraživanje alternativnih izvora proteina postaje sve važnije poslednjih godina [1]. Među ovim alternativama, insekti su se pojavili kao rešenje koje obećava zbog svog nutritivnog sastava, efikasnog korišćenja resursa i minimalnog ekološkog otiska [2]. Iako je mnogo pažnje posvećeno proteinima koje insekata sadrže, njihov mineralni sastav je podjednako važan i treba ga istražiti [3].

Larve *Tenebrio molitor* se već koriste kao hrana, kako kod životinja, tako i kod ljudi [4,5]. Pored toga što imaju visok sadržaj proteina, ovi insekti imaju niz minerala koji su važni za ljudsko zdravlje, uključujući kalcijum, magnezijum, cink, gvožđe i selen [6]. Na sadržaj minerala mogu uticati faktori kao što su ishrana, uslovi uzgoja i razvojni stadijum, što ih čini raznovrsnim kandidatima za zadovoljavanje specifičnih nutritivnih potreba [7].

Mineralni sastav insekata koji se koriste u ishrani je od posebnog značaja u kontekstu globalnih problema ishrane (Bukkens, 2005). Sa neuhranjenošću i nedostatkom mikronutrijenata koji pogađaju milione ljudi širom sveta, posebno u ranjivoj populaciji, potreba za dostupnim izvorima hrane bogatim hranljivim materijama je hitnija nego ikad [9]. Insekti nude odličnu priliku za rešavanje ovih izazova jer obezbeđuju održiv i biodostupan izvor esencijalnih minerala [10]. Štaviše, ekološka održivost uzgoja insekata dodaje još jedan sloj njihovoj ulozi u ishrani ljudi [11]. U poređenju sa konvencionalnim uzgojem stoke, uzgoj insekata zahteva manje resursa i emituje manje gasova staklene bašte, što ga čini ekološki prihvatljivijom opcijom[12]. Dok se svet bori sa pitanjima klimatskih promena, gubitka biodiverziteta i oskudice resursa, uvođenje sistema ishrane zasnovanih na insektima predstavlja pragmatičan pristup.

Uprkos potencijalnim prednostima upotreba insekata kao izvora minerala ima i neke prepreke [9]. Kulturološki stavovi, pravni okviri i tehnološke barijere utiču na integraciju insekata u svakodnevnu ishranu [13]. Prevazilaženje ovih izazova zahteva međusektorsku saradnju između vlade, industrije, akademske zajednice i civilnog društva kako bi se promovisale inovacije, podigla svest i razvile politike podrške i infrastrukture [14].
Do sada se brašno Tenebria već koristilo u ljudskoj ishrani. Ovaj rad ima za cilj da istraži potencijal trutovskog legla i uporedi ga sa larvama Tenebrio kao održivih izvora hrane za ljudsku ishranu. Ispitujući njihov mineralni sastav, cilj nam je da rasvetlimo ulogu minerala dobijenih od insekata u rešavanju globalnih izazova u pogledu hrane i održivosti.

Materijal i metode

Uzgoj trutovskog legla, Tenebria i priprema brašna

U pet pčelinjih društava sakupljeno je ukupno 1,50 kg zatvorenog trutovskog. Larve i lutke su pregledane na prisustvo varoe. Da bi se uklonio vosak, trutovsko leglo je prokuvano u 4,5 litara vode. Čim je voda počela da ključa, ova smeša procеđena. Postupak je ponovljen još jednom sa 3 litra vode. Kao rezultat, dobili smo kuvane larve i lutke, koje su osušene i samlevene.
Ciklus uzgoja larvi Tenebrio je počeo sa odraslim jedinkama starim 10 dana. Odrasle jedinke su ostavljene na odabranoj mešavini 7 dana da se pare i polažu jaja. Posle sedam dana, odrasle jedinke su uklonjene, a jajima je omogućeno da završe embriogenezu i da se novorođene larve izlegnu. Ciklus uzgoja je trajao 90 dana. Larve stare 90 dana su prosijane iz supstrata za hranu i stavljene u čistu posudu da umru od gladi. Ova procedura je trajala 24 sata i korišćena je radi uklanjanje preostalog izmeta iz digestivnog trakta. Preostali izmet je odbačen, a larve su prvo isprane pod tekućom vodom, a zatim su prokuvane. Nakon toga su osušene i mlevene u brašno.

Priprema i analiza uzoraka

Približno 100 mg liofilizovanih i homogenizovanih uzoraka brašnara Tenebria i brašna trutovskog legla je podvrgnuto mirkotalasnoj digestiji ultraCLAVE IV mikrotalasnom digestivnom sistemu (MLS GmbH, Leutkirch, Nemačka) uz korišćenje 5 mL koncentrovane HNO_3. Svaka digestija je praćena sa tri slepe probe (5 mL konc. HNO_3) i tri referentna materijala BOVM-1 “Goveđi mišićni prah” (NRC, Kanada). Nakon digestije, uzorci su razblaženi ultra čistom vodom do krajnje zapremine od 50 mL (10% (v/v) azotne kiseline). Koncentracije elemenata su određene primenom ICPMS (Agilent ICPMS 7700k, Valdbronn, Nemačka). Korišćena je eksterna kalibraciona kriva sa šest tačaka i četiri opsega koncentracije. Kalibraciona kriva je napravljena u 10% HNO_3 da bi odgovarala matriksu uzorka. Kontrola kvaliteta je postignuta kontinuiranim dodavanjem Be, Ge, In i Lu. Efikasnost ekstrakcije je procenjena podvrgavanjem BOVM-1 referentnog materijala kroz isti proces digestije kao i uzorci.

Rezultati i diskusija

Od oko 1,5 kg trutovskog legla dobijeno je 1130 g kuvanih larvi i lutki, što je rezultiralo sa 300 g suve mase larvi i lutki trutova. Iz ovih podataka možemo proceniti da dobijeno brašno čini oko 20% prvobitne mase zatvorenog trutovskog legla koje je izvađeno iz košnice.
Poređenje elemenata između trutovskog i Tenebrio brašna je pokazalo statistički značajne razlike prema ANOVA testu. Brašno trutova je imalo veće koncentracije Ca, Al, Rb, Sr, Cr, Ag, Sb, Pb, Li i Co. Tenebrio brašno je imalo veće koncentracije P, S, K, Na, Mg, Fe, Cu, Zn, Mn, Ni, As, Se, Mo, Cd. Nije bilo razlike za B, Ba i Sn. Najzastupljeniji elementi su S, P, K, Mg, Ca i Na, koji čine 98,96% ukupne količine elemenata u trutovskom brašnu i 99,11% od ukupne količine elemenata u brašnu Tenebrio.

Trutovsko leglo i larve Tenebrio su bogati izvori proteina, esencijalnih aminokiselina, vitamina i minerala. Uporedne analize njihovog nutritivnog profila pokazuju da obe vrste insekata nude izbalansiran spektar hranljivih materija, što ih čini pogodnim kandidatima za ljudsku ishranu. Pored toga, njihov nizak sadržaj masti i visoka konverzija proteina u hranu za životinje i ljude naglašavaju njihovu nutritivnu vrednost.

Za razliku od konvencionalnog stočarstva, uzgoj insekata zahteva znatno manje resursa kao što su zemlja, voda i stočna hrana. Trutovsko leglo i larve Tenebrio imaju efikasnu konverziju hrane i mogu se uzgajati sa organskim otpadom, smanjujući zagađenje i potrošnju resursa. Svodeći emisiju gasova staklene bašte i korišćenje zemljišta, uzgoj insekata pruža održivu alternativu konvencionalnim metodama proizvodnje proteina i minerala doprinoseći globalnim naporima za ublažavanje klimatskih promena i očuvanje biodiverziteta.

Pored svega navedenog proizvodnja trutovskog brašna može pružiti dodatnu korist pčelarima time što se istovremeno bore i protiv varoe. Naime varoa se najviše razmnožava upravo na larvama trutova. Njeno prisustvo u trutovskom leglu je 7-8 puta veće nego u leglu pčela radilica. Zbog toga se uklanjanje trutovskog legla i njegovo pretvaranje u bračno koje bi se koristilo za životinjsku i ljudsku ishranu smatra duplo korisnim.

Zaključak

Brašno Tenebria se već koristi u ishrani životinja i ljudi. U ovom radu smo pokazali kako se mineralni sastav brašna Tenebria i trutova razlikuje. Međutim, iako je njihov mineralni sastav različit oba brašna su bogata mineralima i proteinima i pogodna su za životinjsku i ljudsku upotrebu. Pčelari su do sada iz košnica vadili trutovsko leglo, kao vid borbe protiv varoe i bacali ga. Mi predlažemo da se umesto bacanja ova leglo iskoristi kao hrana za životinje ili ljude, čime bi se ostvarila dodatna dobit za pčelare i pomoglo se održivom korišćenju prirodnih resursa.

Zahvalnica

Zahvaljujem se Ministarstvu nauke, tehnološkog razvoja i inovacija (ugovor br. 451-03-66/2024-03/ 200178). Univerzitetu u Grazu i prof. Walteru Goessleru i njegovim saradnicima, kao i Austrijskom fondu za nauku (FWF).

Reference

1. Rumpold, B.A.; Schlüter, O.K. Nutritional Composition and Safety Aspects of Edible Insects. Mol Nutr Food Res 2013, 57, 802–823, doi:https://doi.org/10.1002/mnfr.201200735.
2. van Huis, A. Potential of Insects as Food and Feed in Assuring Food Security. Annu Rev Entomol 2013, 58, 563–583, doi:https://doi.org/10.1146/annurev-ento-120811-153704.
3. Nowak, V.; Persijn, D.; Rittenschober, D.; Charrondiere, U.R. Review of Food Composition Data for Edible Insects. Food Chem 2016, 193, 39–46, doi:https://doi.org/10.1016/j.foodchem.2014.10.114.
4. Pavlović, R.; Dojnov, B.; Šokarda Slavić, M.; Pavlović, M.; Slomo, K.; Ristović, M.; Vujčić, Z. In Pursuit of the Ultimate Pollen Substitute (Insect Larvae) for Honey Bee (Apis Mellifera) Feed. J Apic Res 2023, 62, 1007–1016, doi:10.1080/00218839.2022.2080950.
5. Kotsou, K.; Chatzimitakos, T.; Athanasiadis, V.; Bozinou, E.; Athanassiou, C.G.; Lalas, S.I. Innovative Applications of Tenebrio Molitor Larvae in Food Product Development: A Comprehensive Review. Foods 2023, 12.
6. Payne, C.L.R.; Scarborough, P.; Rayner, M.; Nonaka, K. A Systematic Review of Nutrient Composition Data Available for Twelve Commercially Available Edible Insects, and Comparison with Reference Values. Trends Food Sci Technol 2016, 47, 69–77, doi:https://doi.org/10.1016/j.tifs.2015.10.012.
7. Jajić, I.; Popović, A.; Urošević, M.; Krstović, S.; Petrović, M.; Guljaš, D. Chemical Composition of Mealworm Larvae (Tenebrio Molitor) Reared in Serbia. Contemporary Agriculture 2019, 68, 23–27, doi:doi:10.2478/contagri-2019-0005.

8. Bukkens, S.G.F. Insects in the Human Diet: Nutritional Aspects. In; Science Publishers, Inc.: Enfield; pp. 545–577.
9. Food and Agriculture Organization (FAO) The State of Food Security and Nutrition in the World 2023; FAO; IFAD; UNICEF; WFP; WHO;, 2023;
10. Huis, A.; Van Itterbeeck, J.; Klunder, H.; Mertens, E.; Halloran, A.; Muir, G.; Vantomme, P. EDIBLE INSECTS Future Prospects Fo Food and Feed Security; 2013; Vol. 171; ISBN 978-92-5-107595-1.
11. Oonincx, D.G.A.B.; de Boer, I.J.M. Environmental Impact of the Production of Mealworms as a Protein Source for Humans – A Life Cycle Assessment. PLoS One 2012, 7, e51145-.
12. van Huis, A. Insects as Food and Feed, a New Emerging Agricultural Sector: A Review. J Insects Food Feed 2020, 6, 27–44, doi:https://doi.org/10.3920/JIFF2019.0017.
13. Looy, H.; Dunkel, F. V; Wood, J.R. How Then Shall We Eat? Insect-Eating Attitudes and Sustainable Foodways. Agric Human Values 2014, 31, 131–141, doi:10.1007/s10460-013-9450-x.
14. Durst, P.B.; FAO Regional Office for Asia and the Pacific. Forest Insects as Food : Humans Bite Back : Proceedings of a Workshop on Asia-Pacific Resources and Their Potential for Development, 19-21 February 2008, Chiang Mai, Thailand; Food and Agriculture Organization of the United Nations, Regional Office for Asia and the Pacific, 2010; ISBN 9789251064887.

Monitoring of arsenic in the environment using honey bees

Praćenje arsena u životnoj sredini pomoću medonosne pčele

Nenad M. Zarić[1,2,*]

[1] *University of Belgrade – Faculty of Biology, Studentski trg 12-16, Belgrade, Serbia*

[2] *University of Natural Resources and Life Sciences (BOKU), Department of Agrobiotechnology (IFA-Tulln), Institute of Bioanalytics and Agro-Metabolomics, Konrad-Lorenzstr 20, Tulln, Austria*

[*]*nenad.zaric@bio.bg.ac.rs; nenad.zaric@boku.ac.at*

Abstract

Arsenic is a metalloid found in air, water, soil and living organisms, so in the entire environment. It can be of natural or anthropogenic origin. Arsenic can reach humans through the food chain.. Considering that it is very toxic, its constant monitoring in the environment is necessary. In this work, honey bees were used to monitor arsenic concentrations in the environment. Bee samples were taken in a rural environment without industry (Mesić), an industrial city (Pančevo), the area around thermal power plants Kostolac (TEK) and an urban environment with intense traffic (Belgrade). Sampling was carried out in 2014 and 2019. It was found that the highest concentrations are in the vicinity of thermal power plants and Belgrade, while the lowest are in Mesić and Pančevo. The burning of fossil fuels is one of the main anthropogenic sources of arsenic, which explains these findings. Between the two sampling periods, there was a decrease in arsenic concentrations at all locations. This reduction is drastic in Mesić and Pančevo, while in Belgrade and TEK there was a smaller drop in concentrations.

Keywords: *honey bees; arsenic; pollution; ICPMS; Apis mellifera*

Uvod

Arsen (As) je metaloid koji se prirodno pojavljuje u životnoj sredini i 54. je najzastupljeniji element u Zemljinoj kori [1]. Može se pojaviti u različitim oblicima u vazduhu, vodi, zemljištu i živim organizmima [2,3]. U atmosferi, arsen može biti prisutan u obliku čestica (PM) ili u gasovitom stanju. Njegovo poreklo u površinskim slojevima zemljištima i u vodi je prvenstveno iz prirodnih litogenih izvora, pri čemu je glavni izvor geotermalna voda [4]. Ljudske aktivnosti kao što su rudarstvo, industrija stakla i keramike, proizvodnja pigmenata i elektronika, kao i upotreba pesticida, herbicida, đubriva i životinjskog stajnjaka u poljoprivredi doprinose zagađenju zemljišta i vode arsenom [5-7]. Arsen može ući u lanac ishrane insekata, životinja i ljudi direktno preko vazduha ili vode, ili indirektno kroz zemljište akumulirajući se u biljkama koje se konzumiraju kao hrana. Biljke preuzimaju elemente iz tla putem korena i prenose ih u nadzemne delove, uključujući polen [8,9]. Polen se koristi kao indikator zagađenosti zemljišta i vazduha, posebno arsenom [10]. Međutim, zagađenje otkriveno u polenu odražava samo ograničenu površinu oko same biljke koja je stacionarni organizam.

Medonosne pčele (*Apis mellifera*) igraju važnu ulogu kao socijalni insekti koji žive u kolonijama (društvima). Većinu društva čine ženke - pčele radilice, koje nakon tri nedelje postaju izletnice i odgovorne su za sakupljanje vode i hrane [11]. U potrazi za resursima, izletnice tokom leta pokrivaju oko 7 km^2 [12]. Tokom leta, medonosne pčele akumuliraju čestice iz vazduha na svojim dlakavim telima, dok ih voda koja se koristi za piće ili hlađenje košnice izlaže zagađivačima [13]. Pčele izletnice sakupljaju polen i nektar sa cveća, pa je zagađenje koje se nalazi u pčelama odraz zagađenja vazduha, vode, zemljišta i flore.

U ovom istraživanju koristili smo medonosne pčele kako bismo pratili zagađenje životne sredine arsenom na različitim lokacijama, ali i tokom vremena.

Materijal i metode

Lokacije uzorkovanja

Uzorci su sakupljani sa više različitih lokacija u Srbiji.
Mesić – selo na obroncima Vršačkih planina. Okruženo je šumom i poljoprivrednim zemljištem. U neposrednoj blizini nema industrijskih izvora zagađenja.
Pančevo - Poznat je kao industrijski grad. U gradu se nalazi fabrike za proizvodnju đubriva, petrohemijska industrija i rafinerija nafte.
TEK – Region u kome se nalaze dve termoelektrane, Kostolac A i B. Pored toga u neposrednoj blizini je i otvoreni rudnik uglja Drmno, kao i pepelište koje se nalazi između ove dve elektrane.
Beograd – Glavni grad Srbije koji karakteriše intenzivan saobraćaj. Uzorkovane su pčele koje se nalaze u neposrednoj blizini autoputa.

Uzorkovanje

Uzorci su sakupljani tokom 2014. i 2019. godine. Žive pčele su sakupljene sa spoljašnjeg rama na kojem se nalazi med i polen, ali na kojem nema legla. Smatra se da su ovo pčele izletnice i da su one bile u dodiru sa spoljašnjom sredinom [14]. Sa svake lokacije uzorci su uzeti iz minimum 2 košnice. Oko 50 – 100 pčela je uzeto po košnici. Pčele su odnesene u laboratoriju gde su zamrznute na -20 °C.

Priprema i analiza uzoraka

Uzorci su osušeni do konstante mase. Nakon toga su homogenizovani. Oko 100 mg uzorka je podvrgunto mikrotalasnoj digestiji uz pomoć HNO_3. Potom su uzorci razblaženi ultračistom vodom (18.2 MΩ*cm) do konačne zapremine od 10% *v*/v HNO_3.
Ukupne koncentracije arsena su merene korišćenjem ICPMS uređaja. Kontrola kvaliteta je rađena merenjem slepih proba, sertifikovanog referentnog materijala, kao i konstantnim dodavanjem internih standarda.

Rezultati i diskusija

Kao što se može uočiti u Tabeli 1. tokom 2014. godine najniža koncentracija arsena je zabeležena u Mesiću, praćeno Pančevom i Beogradom, dok je najviša koncentracija zabeležena u okolini termoelektrana Kostolac. Tokom 2019. godine ostaje ovaj trend, sa malim razlikama. I dalje su najviše koncentracije zabeležene u okolini termoelektrana Kostolac, zatim u Beogradu, Mesiću, a najniže koncentracije su zabeležene u Pančevu.

Tabela 1. Koncentracije arsena u pčelama sa različitih lokacija tokom 2014. i 2019. godine izražene u $\mu g\ kg^{-1}$

Lokacija	2014	2019
Mesić	195	41
Pančevo	206	29
TEK	400	367
Beograd	280	213

Poređenje 2014. i 2019. godine nam pokazuje da su se koncentracije arsena na svim lokacijama smanjile. Do drastičnog smanjenja je došlo u Mesiću i Pančevu, dok je do nešto manjeg došlo u Beogradu i okolini termoelektrana. Moguće je da su tokom 2014. godine duvali vetrovi koji su zagađenje iz Beograda i regiona termoelektrana duvali prema Pančevu i Mesiću. Tokom kampanje uzorkovanja 2019. verovatno nije bilo ovih vetrova stoga su koncentracije arsena na lokacijama Mesić i Pančevo drastično smanjene. Ovo nam pokazuje da poljoprivredna aktivnost u okolini Mesića

nema značajniji uticaj na koncentraciju arsnea u životnoj sredini. Takođem petrohemijska industrija, kao i proizvodnja goriva u rafineriji nafte izgleda ne oslobađa veće količine arsena ili su u međuvremenu urađena unapređenja proizvodnog procesa koja drastično utiču na smanjenje zagađenja životne sredine toksičnim metalima.
Termoelektrane Kostolac A i B koriste ugalj kao gorivo. Poznato je da je spaljivanje uglja jedan od najznačajnihij antropogenih izvora arsena [15]. Stoga je očekivano da njegova koncentracija u neposrednoj blizini termoelektrana koje rade na ugalj bude povišena. Drugi veoma značajni antropogeni izvor arsena je sagorevanje ulja i goriva za automobile [15]. Beograd je milionski grad sa veoma intenzivnim saobraćajem. Pčele koje smo uzorkovali se nalate u neposrednoj blizini autoputa i samim tim sakupljaju svo zagađenje koje potiče iz saobraćaja, uključujući i arsen.

Conclusion

Medonosna pčela se pokazala kao dobar biomonitor zagađenja životne sredine arsenom. Tokom ovog istraživanja ustanovljeno je da su se koncentracije arsena na svim lokacijama smanjile između 2014. i 2019. godine. Najveće smanjenje je uočeno u Pančevu.
Najviše koncentracije arsena su uočene u regionu termoelektrana Kostolac A i B, a zatim u Beogradu. Ovo je prepisano spaljivanju uglja i goriva kao dva glavna antropogenih izvora arsena.

Acknowledgements

Zahvaljujem se Ministarstvu nauke, tehnološkog razvoja i inovacija (ugovor br. 451-03-66/2024-03/ 200178). Univerzitetu u Grazu i prof. Walteru Goessleru i njegovim saradnicima. Austrijskom fondu za nauku FWF i njihovom ESPRIT programu (ESP 428-B).

References

1. Cullen, W.R., 2008. Is Arsenic an Aphrodisiac?: The Sociochemistry of an Element. *Royal Society of Chemistry*.
2. Hughes, M.F., Beck, B.D., Chen, Y., Lewis, A.S., Thomas, D.J., 2011. Arsenic exposure and toxicology: a historical perspective. *Toxicol. Sci.* 123 (2), 305–332.
3. Tanda, S., Gingl, K., Li˘cbinský, R., Hegrova, ´ J., Goessler, W., 2020. Occurrence, seasonal variation, and size resolved distribution of arsenic species in atmospheric particulate matter in an Urban Area in Southeastern Austria. *Environ. Sci. Technol.* 54 (9), 5532–5539.
4. Baba, A., Sozbilir, ¨ H., 2012. Source of arsenic based on geological and hydrogeochemical properties of geothermal systems in Western Turkey. *Chem. Geol.* 334, 364–377.
5. Leonard, A.,1991. Arsenic. In S. M. M. Ernest, A. Manfred, I. Milan (Ed.), *Elements and their Compounds in the Environment: Occurrence, Analysis and Biological Relevance* (2nd, Compl ed., pp. 751–773). Wiley-VCH.
6. Ran, H., Guo, Z., Yi, L., Xiao, X., Zhang, L., Hu, Z., Li, C., Zhang, Y., 2021. Pollution characteristics and source identification of soil metal(loid)s at an abandoned arsenic containing mine. *Chin. J. Hazard. Mater.* 413, 125382
7. Jiang, Q.Q., Singh, B.R., 1994. Effect of different forms and sources of arsenic on crop yield and arsenic concentration. *Water Air Soil Pollut.* 74 (3), 321–343
8. Negri, I., Mavris, C., Di Prisco, G., Caprio, E., Pellecchia, M., 2015. Honey bees (Apis mellifera, L.) as active samplers of airborne particulate matter. *PLoS ONE* 10 (7), e0132491.
9. Smith, K.E., Weis, D., Chauvel, C., Moulin, S., 2020. Honey maps the Pb fallout from the 2019 fire at Notre-Dame Cathedral, Paris: a geochemical perspective. *Environ. Sci. Technol. Lett.*7(10), 753-759.
10. Alvarez-Ayuso, ´ E., Abad-Valle, P., 2017. Trace element levels in an area impacted by old mining operations and their relationship with beehive products. *Sci. Total Environ*. 599–600, 671–678.
11. Huang, Z.Y., Robinson, G.E., 1996. Regulation of honey bee division of labor by colony age demography. *Behav. Ecol. Sociobiol*. 39 (3), 147–158.

12. Perugini, M., Manera, M., Grotta, L., Abete, M.C., Tarasco, R., Amorena, M., 2011. Heavy metal (Hg, Cr, Cd, and Pb) contamination in urban areas and wildlife reserves: Honeybees as bioindicators. *Biol. Trace Elem. Res.* 140 (2), 170–176.
13. Zari´c, N.M., Ilijevi´c, K., Stanisavljevi´c, L., Gr˘zeti´c, I., 2017. Use of honeybees (Apis mellifera L.) as bioindicators for assessment and source appointment of metal pollution. *Environ. Sci. Pollut. Res*. 24 (33), 25828–25838.
14. van der Steen, J., Cornelissen, B., Blacqui`ere, T., Pijnenburg, J.E.M.L., Severijnen, M., 2016. Think regionally, act locally: metals in honeybee workers in the Netherlands (surveillance study 2008). *Environ. Monit. Assess.* 188 (8)
15. Manoli, E., Voutsa, D., Samara, C., 2002. Chemical characterization and source identification/apportionment of fine and coarse air particles in Thessaloniki, Greece. *Atmos. Environ*. 36 (6), 949–961.

Improvement of the corrosion-inhibiting properties of the hydrophobic layer through the addition of eugenol

Regina Fuchs–Godec[1,*], Marija Riđošić[2], Milorad. V. Tomić[2]

[1]*Faculty of Chemistry and Chemical Engineering, University of Maribor,Smetanova 17, Maribor*

[2]*Faculty of Technology Zvornik, University of Eastern Sarajevo, Karakaj bb, Republic of Srpska*

[*]*regina.fuchs@um.si*

Abstract

The inhibitory effect of eugenol incorporated into a hydrophobic protective layer for corrosion protection of copper in 3.5% NaCl was evaluated by electrochemical polarization methods and electrochemical impedance spectroscopy. The electrochemical data show that the corrosion resistance increases significantly and the stability of the protective layer also increases when eugenol is added in an amount greater than 1.0 wt%. This is confirmed by the high value of the inhibition efficiency, which remains high and above 90% even after three days of immersion in the selected corrosion medium.

Keywords: *Copper; NaCl; Hydrophobic layers; Eugenol*

Introduction

Corrosion of copper manifests itself in various forms, including tarnishing, pitting and erosion, each of which is influenced by environmental factors such as moisture, oxygen, pollutants and pH levels. Understanding the electrochemical processes involved in copper corrosion is critical to developing effective protection strategies. Factors such as alloy composition, surface finish and exposure conditions have a major influence on the corrosion resistance of copper-based materials.

The green approach to corrosion prevention emphasizes the use of environmentally friendly materials, processes, and technologies to inhibit or mitigate corrosion without compromising performance. Biodegradable inhibitors derived from natural sources, such as plant extracts and organic compounds, offer effective alternatives to conventional chemical inhibitors. These eco-friendly inhibitors exhibit corrosion inhibiting properties while minimizing toxicity and environmental footprint. Eugenol, a natural compound found in clove oil, has attracted attention as a potential corrosion inhibitor for copper due to its favorable properties. Research suggests that eugenol has promising corrosion-inhibiting properties, especially in acidic environments where copper corrosion is common. Studies have shown that eugenol forms a protective film on the copper surface that effectively prevents corrosion by acting as a barrier between the metal surface and corrosive substances. It is believed that the film formed by eugenol contains complex organic compounds that adhere strongly to the copper surface and hinder the progression of corrosion reactions. In addition, the inhibitory effect of eugenol on copper corrosion is attributed to its ability to adsorb to the metal surface, thus reducing the availability of active sites for the initiation of corrosion. This adsorption process is influenced by factors such as the concentration, temperature and pH of the solution, which can affect the effectiveness of eugenol as an anti- corrosion agent. In addition, eugenol is beneficial as a corrosion inhibitor because it is environmentally friendly and derived from natural sources. Its biodegradability and low toxicity make it an attractive alternative to synthetic inhibitors, which meets the growing demand for environmentally sustainable corrosion protection strategies [1-3].

The present study is an extension of our previous work [4-6], in which we investigated the stability and effectiveness of the hydrophobic layer thus prepared on copper and copper alloys in a simulated solution of acidic urban rain (pH = 5) and stainless steel in 3.0 % of NaCl and in a simulated solution of acidic urban rain (pH = 3) at 25 °C. The etched sheets were immersed at room temperature for about one hour in a 0.05 M ethanolic solution of stearic acid SA ($CH_3(CH_2)_{16}COOH$) with and

without the addition of different concentrations of vitamin E to form the self-assembling layer. The results obtained in terms of the inhibitory effect were fascinated, so it was obvious to extend these studies. This simple chemical method for producing a superhydrophobic surface on Cu was also used in the present study. The only difference was that the vitamin E was replaced by Eugenol (EUG). The immersion time was constant at two hour, as was the concentration of stearic acid at c = 0.05 M (M = mol L^{-1}). The chosen concentration of added EUG was constant; c = 1.0 and 2.0 wt%. Since we were also interested in the durability of the hydrophobic coating on the copper surface in 3.5 % of NaCl at 25 °C over time, we performed EIS measurements after prolonged exposure to a corrosive medium, namely after 1h, 5h, 15h and after 1d and 3 days of exposure (Figure 3), while polarization measurements were performed after 1 hour and after 3 days of exposure from the first immersion of the sample with a modified surface.
For this purpose, two different electrochemical methods were used, namely classical potentiodynamic measurement and electrochemical impedance spectroscopy (EIS).

Experimental

A conventional three-electrode configuration was used for the potentiodynamic investigations. All potentials were measured against a saturated calomel electrode (SCE), and the counter electrode consisted of Pt. The potentiodynamic current-potential curves were recorded by automatically changing the electrode potential from -0.6 to 0.05 V (for copper) with a sampling rate of 1 mVs-1. The SCE was immersed in a Luggin capillary placed as close as possible to the working electrode. Polarisation diagrams were generated from the results of the experiments 1 hour after immersion of the working electrode in the solution to allow stabilisation of the steady-state potential. Impedance spectra were determined at constant open-circuit potential (OCP) in the frequency range from 100 kHz to 5 mHz with 10 points per decade and an amplitude of 10 mV (peak-to-peak) of the excitation signal. Nyquist and polarisation diagrams were generated from the results of these experiments one hour after immersion of the working electrode in the solution to allow stabilisation of the steady-state potential (three replicate measurements were performed).
All the experiments were carried out at 25°C ±1°C. The measurements were performed using the Solartron 1287 Electrochemical interface and with a Gamry 600™ potentiostat/galvanostat controlled by electrochemical program, respectively. Data were collected and analysed using CorrView, CorrWare, Zplot and ZView software, developed by Scribner Associates, Inc. The test specimens were fixed within a PTFE holder, and the geometric area of the electrode exposed to the electrolyte was 0.785 cm2. Before etching, the metal surface was abraded successively using a circulating device under a stream of water and SiC papers of grades 1000, 1200 and 2400. Etching was carried out in aqueous solutions of 10% HNO3 for 1 min and then washed in deionised water. After etching the samples were cleaned ultrasonically in a bath of Milli-Q water, washed with ethanol, rinsed several times with distilled water, and finally dried using hot air. Subsequently, the etched sheets were immersed within 0.05 mol/L ethanolic solution of SA with, and without the addition of Eugenol at room temperature, for about one hour..

Results and discussion

Figures 1 shows polarisation curves for bare and modified copper surfaces with hydrophobic properties in 1 hour and after 3 days of immersion in 3.5% solution of NaCl.

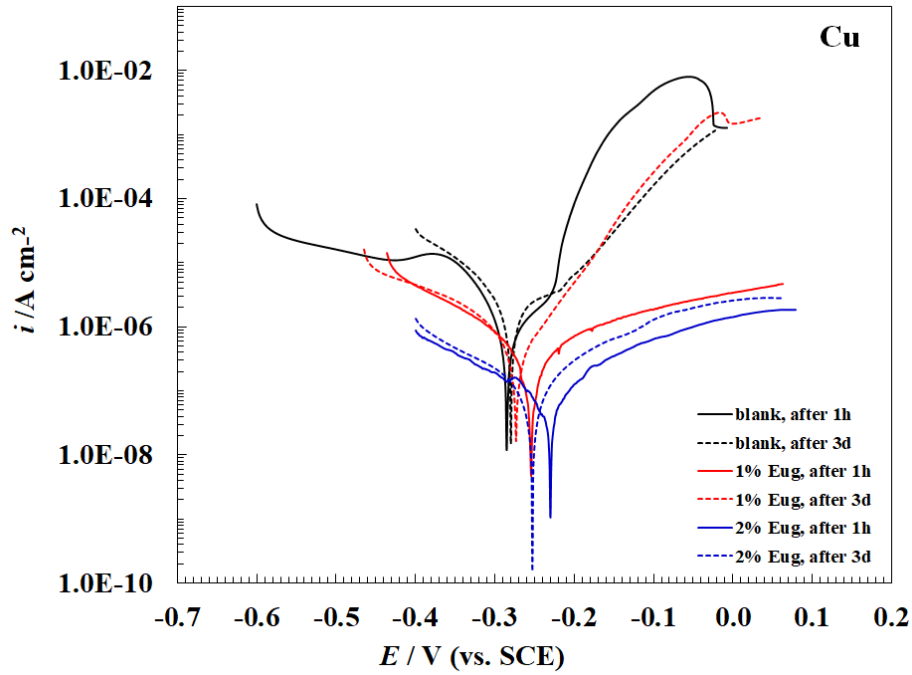

Figure 1. *Potentiodynamic polarisation curves (1 mVs^{-1}) of pure Cu for bare and modified surfaces in the 3.5% NaCl at 25ºC, after 1h, and 3 days duration test. (The modified surfaces were prepared by immersion of Cu in 0.05 M stearic acid in ethanol with and without the addition of 1% and 2% Eugenol).*

Table 1. Kinetic parameters for corrosion of Cu obtained from potentiodynamic polarisation curves for the bare and modified surfaces in the 3.5% NaCl at 25ºC, after 1h, and 3 days duration test.

Corrosive media 3.5% NaCl	i_{corr} (μA cm^{-2})	E_{corr} (V/SCE)	R_p (kΩ cm^2)	R (mm y^{-1})	$\%\eta_{i_{corr}}$	$\%\eta_{R_p}$
bare surface Cu						
1 h	1.635	-0.280		1.90E-02		
3 days	2.891	-0.281		3.36E-02		
modified surface 0.05 M SA + 1.0 w% EUG						
1h	0.739	-0.263	21.98	8.60E-03	54.80	66.92
3 days	0.375	-0.273	29.98	4.36E-03	77.06	75.75
modified surface 0.05 M SA + 2.0 w% EUG						
1h	0.151	-0.231	50.89	1.76E-03	90.76	85.71
3 days	0.098	-0.262	69.76	1.14E-03	94.01	89.57

Compared to the bare copper surface, the modified copper surface showed a decrease in current density mainly in the anodic directions (Fig.1), while the reduction of the cathode current density is not as pronounced or only minima. Reduction of the corrosion current was noticeable up to a two order of magnitude lower i_{corr} was observed for the chosen 'mixture' with respect to the blank solution. The stability of the protective layer is increased by the addition of eugenol. By increasing the eugenol content from 1 % to 2 %, the polarisation resistance has more than doubled.

Based on the results obtained from electrochemical measurements, which show that the stability of the self-assembled hydrophobic layer increased during the exposure of the samples for up to 3 days,

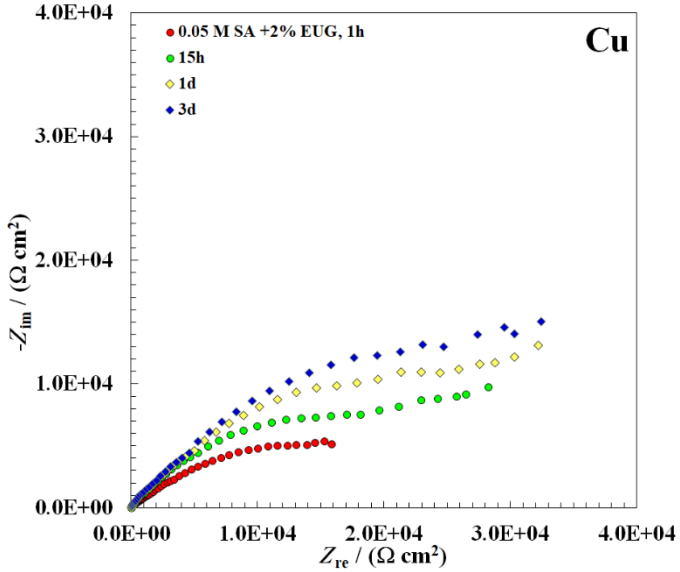

we can assume a synergistic effect between star acid and eugenol. This is reflected in the formation of a more robust and cohesive protective layer on the metal surface than when either inhibitor is used alone. This barrier prevents the diffusion of corrosive substances to the metal surface and thus reduces the corrosion rate. In addition, the combination of stearic acid and eugenol can also improve the stability and durability of the protective film formed on the metal surface. This extended film stability increases the long-term corrosion protection provided by the inhibitor mixture.

EIS measurements

The corrosion behaviour of the samples in corrosive electrolyte was investigated by EIS measurements. The corrosion resistance of the as-prepared hydrophobic surfaces were further investigated using the EIS diagrams. Figure 2 shows Nyquist diagrams of pure copper for bare and modified surfaces prepared after 1, 15 hours and after 1 and 3 days immersion test at open-circuit potential in 3.5% NaCl solution. The results obtained by EIS confirm to a certain extent the interpretation mentioned above (polarisation measurements).

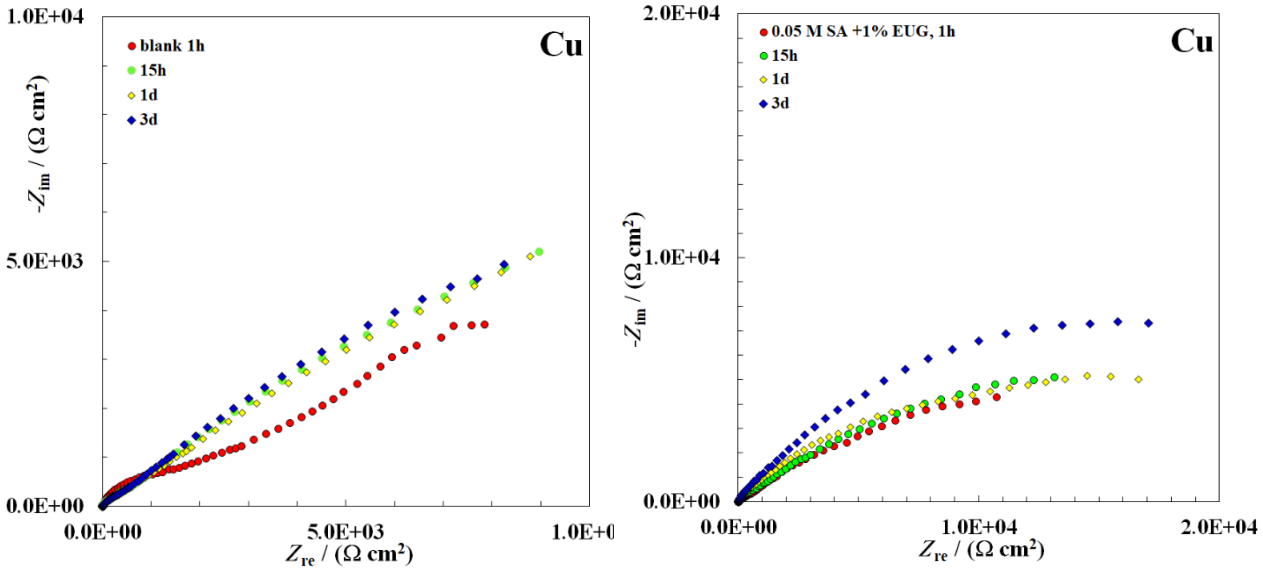

Figure 2. *EIS Nyquist plots for pure Cu samples for bare and modified surfaces prepared after 1and 15 hours and after 1 and 3 days immersion test at open-circuit potential in 3.5% NaCl solution.*

Conclusion

When stearic acid is used in combination with eugenol as a corrosion inhibitor, their synergistic effect enhances the overall inhibitive properties. Stearic acid is a long-chain fatty acid with a carboxylic acid functional group (-COOH). When combined with eugenol, which contains a phenolic hydroxyl group (-OH), the two compounds can interact in several ways to inhibit corrosion, especially with a synergistic effect, manifested in an increase in the stability and robustness of the self-assembled hydrophobic layer on the surface of copper, which was used as a test material.
The inhibition efficiency in the formation of a hydrophobic layer by the addition of 1.0 wt.% eugenol reached 55 % after 1 hour of immersion in 3.5 % NaCl and increased to 77 % after 3 days of immersion. With the addition of 2.0 wt.% eugenol, the value increases and reaches 85 % after 1 h immersion in the selected corrosion medium and more than 90 % after 3 days of immersion.

Acknowledgements

This work was financially supported by Slovenian Research Agency under research project “Physico-Chemical Processes on the Surface Layers and Application of Nanoparticles” (P2-0006).

References

1. R. C. Nascimentob , M. J. O. C. Guimarãesa , S. L. D. C. Brasilc , S. H. R. Barra, Green Eugenol Oligomers as Corrosion Inhibitors for Carbon Steel in 1M HCl, *Mater. Res.*, doi.org/10.1590/1980-5373-MR-2022-0012, 2022.
2. E. Azzouyahar, A. Abu-Obaid4, M. El Hajji , L. Bazzi , M. Belkhaouda , A. Lamiri1 , R. Salghi, S. J., M. Essahli, Plants extract as green corrosion inhibitors: The case of eugenol from Clove, *Der Pharma Chemica*, **8(2)**, 467-475, 2016.
3. A. Acidi, A.Sedik, A. Rizi, R. Bouasla, K. O. Rachedi, et al., Examination of the main chemical components of essential oil of Syzygium aromaticum as a corrosion inhibitor on the mild steel in 0.5 M HCl medium, *Journal of Molecular Liquids*, **391**, **B,** 123423, 2023.
4. R. Fuchs-Godec, Flower-like superhydrophobic surfaces fabricated on stainless steel as a barrier against corrosion in simulated acid rain. *Materials*. 2022, **15(20)**, 1996-1944, 2022.
5. R. Fuchs-Godec, G. Zerjav, Corrosion resistance of high-level-hydrophobic layers in combination with Vitamin E – (a-tocopherol) as green inhibitor, *Corros. Sci.*, **97**, 7-16, 2015.
6. R. Fuchs-Godec, A synergistic effect between stearic acid and (+)-α-tocopherol as a green inhibitor on ferritic stainless steel corrosion inhibition in 3.0% NaCl solution. *Coatings.* 2021, **11 (8)**, 1-21, 2021.

Examining the Potential of Deep Eutectic Solvents for Eco-Friendly Extraction of Bioactive Compounds from Peels of *Allium cepa* L.

Maša Islamčević Razboršek[1*], Regina Fuchs-Godec[1], Sabina Begić[2]

[1] *University of Maribor, Faculty of Chemistry and Chemical Engineering, Smetanova 17, 2000 Maribor, Slovenia*

[2] *University of Sarajevo, Faculty of Science, Bosnia and Herzegovina*

[*]*masa.islamcevic@um.si*

Abstract

In this study, the extraction efficiency of deep eutectic solvents (DES) for the isolation of bioactive compounds from onion peels, in particular the Slovenian onion variety "Ptujski lük" (Allium cepa L.), was investigated. DES formulations were synthesized based on choline chloride as hydrogen bond acceptor (HBA) and various hydrogen bond donors (HBD) including propane-1,2-diol, acetic acid, lactic acid, fructose and butane-1,4-diol. Comparative analyzes were performed with 70% ethanol, 70% methanol and water extractions. The phytochemical profiles of the extracts were analyzed spectrophotometrically (TPC, ABTS, FRAP, DPPH) and chromatographically (HPLC-UV). Protocatechuic acid, quercetin, quercetin-3,4'-diglucoside and quercetin-3-β-D-glucoside were identified in all extracts. Water extraction showed the highest efficiency for protocatechuic acid (4.3 mg/g dry weight (DW)), while 70% methanol yielded the highest levels of quercetin and quercetin-3,4'-diglucoside (4.2 mg/g DW and 8.5 mg/g DW, respectively). Among the DES solvents, choline chloride with acetic acid proved to be the most effective (protocatechuic acid, 1.5 mg/g DW; quercetin, 1.7 mg/g DW and quercetin-3,4'-diglucoside 4.4 mg/g DW). DES extracts showed comparable antioxidant activity to alcoholic extracts, especially those with acetic or lactic acid as donors. This study underlines the potential of using environmentally friendly, sustainable DES solvents for the extraction of health-promoting compounds from waste materials such as onion peels. The environmentally friendly DES extraction method offers a promising alternative to conventional organic solvents and addresses the need for sustainable use of agro-industrial waste.

Keywords: *deep eutectic solvents (DES), antioxidant tests, onion peels, HPLC-UV, LC-MS, phenolic compounds*

Introduction

The advancement of analytical chemistry plays a central role in various sustainability efforts, ranging from waste reduction to safer chemical processes to improved energy efficiency. This symbiotic relationship between analytical chemistry and sustainability is underscored by the use of instrumental methods, automation and minimization techniques, all of which contribute to a more sustainable approach within this scientific discipline. The search for alternative solvents is an important step towards the use of more environmentally friendly methods. The main goal in this process should not only be to replace them, but to take the added advantage of the different properties of these solvents to improve the selectivity, sensitivity and reliability of the analysis and shorten its duration [1].

A burgeoning trend in analytical chemistry is the use of environmentally friendly alternatives, in particular deep eutectic solvents (DES), which represent a sustainable replacement for conventional organic solvents. These DES, synthesized from hydrogen bond acceptors (HBA) such as choline chloride and hydrogen bond donors (HBD) such as propane-1,2-diol, acetic acid, lactic acid, fructose and butane-1,4-diol, represent a promising avenue for environmentally friendly analytical methods [2][3].

In the search for more environmentally friendly solvents, the extraction of bioactive compounds from natural sources has attracted considerable attention. Among these sources, onion (*Allium cepa* L.)

stands out as a reservoir of functional food ingredients, especially flavonols such as quercetin and its derivatives. The indigenous Slovenian onion variety "Ptujski lük" with its special morphological and sensory properties is an interesting topic for analytical chemistry. Exploiting the potential of onion extracts, especially through innovative extraction methods such as ultrasound-assisted extraction (UAE) with DES solvents in combination with centrifugation, offers a way to unlock the bioactive potential of this plant resource [4][5][6].

Due to the increase in global onion production, waste generation is increasing (500000 tons of onion waste per year), but at the same time the disposal of onion waste poses certain problems as it cannot be used as animal feed due to its specific aroma, composting is limited due to its high susceptibility to white rot growth and incineration of onion waste can lead to excessive costs. DES can help to solve this problem as they allow us to extract bioactive compounds from onion peels. DES are an innovative material that has great potential for many chemical processes, but we need to develop sustainable processes for their production and use to ensure their safe and beneficial use for future generations [4][7].

Antioxidants occur naturally in plants, animals and microorganisms or can be synthesized from chemical substances. Higher plants are a rich source of natural antioxidants such as tocopherols and polyphenols, which are mainly found in spices, herbs, fruits and vegetables. In addition, by-products from the food and agricultural industries like onion peels, are a rich source of antioxidants. Methods and tools for measuring antioxidant activity have evolved enormously over the last few decades. Early methods measured the effectiveness of antioxidants against the formation of certain types of oxidation products and were therefore based on the measurement of lipid oxidation. Today, various chemical tests and highly sensitive and automated technologies are used for evaluation of antioxidant activity. Methods for measuring antioxidant activity differ in terms of the type of oxidation substrates, oxidizing agents, reaction mechanisms and conditions, technology and interpretation of results [8].

In this context, our study aims to investigate the quantitative and qualitative aspects of the bioactive compounds present in onion extracts using a comprehensive analytical approach. By using high performance liquid chromatography (HPLC) in conjunction with UV detection and liquid chromatography with mass spectrometry (LC-MS), we seek to identify and quantify key compounds such as protocatechuic acid, quercetin, quercetin-3,4'-diglucoside and quercetin-3-β-D-glucoside. In addition, we endeavor to evaluate the antioxidant efficiency of onion extracts using established assays such as ABTS, FRAP, DPPH and total phenolic content (TPC). Through a systematic comparison of extraction solvents, including conventional 70% ethanol, 70% methanol and water, as well as DES based on choline chloride as HBA and various HBDs (propane-1,2-diol, acetic acid, lactic acid, fructose and butane-1,4-diol), we aim to identify the most efficient solvent system for the extraction of bioactive compounds with high antioxidant activity.

Materials and methods

Samples and chemicals

Slovenian onion variety "Ptujski lük was obtained on the Slovenian market. Dry samples were ground in the electric blender for 1 min, and kept in the dark place before analysis. All chemicals used were of analytical grade.

Preparation of eutectic liquids

Five selected deep eutectic solvents (DES): choline chloride:1,2-propanediol (DES1, molar ratio1:2), choline chloride:acetic acid (DES2, molar ratio 1:2), choline chloride:lactic acid (DES3, molar ratio of 1:2), choline chloride:fructose:water (DES4, 2:1:1) and choline chloride: butane-1,4-diol (DES5, molar ratio 1:2) were prepared according to the heating and stirring method previously described [9].

Ultrasound assisted extraction (UAE)

For comparison, UAE was performed with 70 % ethanol, 70 % methanol and water as well as with different DES solvents according to our previously published work [10]. Briefly, 500 mg of the ground onion peels were weighed into a 50 mL conical centrifuge tube and 10 mL of the respective solvent was added. The mixture was sonicated at an elevated temperature of 40 °C for 30 minutes. After centrifugation at 10,000 rpm for 15 minutes, the clear supernatant was transferred to a 25 mL glass flask and the extraction was repeated a second time with another 10 mL of the respective solvent. The supernatants were combined in the 25 mL volumetric flask and additionally pooled with the solvent up to the mark.

Analytical procedures to evaluate the antioxidant efficacy of onion extracts

Total phenolic content (TPC)

Total phenolic content (TPC) was determined by the standard spectrophotometric method, described in our previously published work [9]. Absorbance at 765 nm was measured and results were expressed as mg gallic acid equivalent per g dry weight (mg GA/g DW).

ABTS radical scavenging assay

The radical scavenging capacity of the onion peels extracts, expressed as mg Trolox equivalent per gram dry weight (mg TE/g DW), was determined using the standard ABTS assay [9]. The scavenging effect, expressed in %, was calculated using the following equation (1):

$$Scavenging\ effect\ \% = \frac{AB - AA}{AB} \times 100\ \% \qquad (1)$$

where: AB represents the absorbance of the mixture of ABTS•+ and EtOH (blank value), while AA represents the absorbance of the mixture of ABTS•+ and extracts/Trolox solution.

FRAP assay

The antioxidant capacity of the extracts, expressed as mg Fe^{2+} ion equivalent per gram dry weight (mg Fe^{2+}/g DW), was determined by a standard method [9]. The absorbances were measured at 593 nm against FRAP reagent as blank.

DPPH assay

Firstly, a DPPH radical solution with a mass concentration of 40 mg/L was prepared. This solution was needed for the further preparation of all samples, including for the calibration curve solutions. The calibration curve solutions were prepared in the concentration range from 0.1 mmol/L to 5.0 mmol/L from the Trolox stock solution (10 mmol/L in 96% ethanol). The Trolox reagent is used as a standard for measuring the antioxidant capacity. Before starting the absorbance measurement, the zero point was calibrated with methanol at a wavelength of 517 nm.

To prepare the calibration curve and samples, 4.950 mL of the DPPH radical solution and 50 µL of ethanol (control solution) or 50 µL of Trolox or 50 µL the properly diluted sample (1:1 or 1:5 with water) were pipetted into a 5 mL plastic microcentrifuge with stopper. The solutions thus prepared were first shaken for a few seconds with a vortex mixer, then left in a dark room for 30 minutes and finally their absorbances were measured at 517 nm.

Equation 2 was used to calculate the percentage of inhibition:

$$\%\ inhibition = \frac{A_0 - A_1}{A_0} \times 100\ \% \qquad (2)$$

where: where A_0 is the absorbance of the control solution and A_1 is the absorbance in the presence of Trolox or samples in DPPH solution.

Quantification of individual phenolic compounds by high performance liquid chromatography with UV detection (HPLC-UV) and liquid chromatography with MS detection (LC-MS)

For the chromatographic analysis of the phenolic compounds in the onion peel extracts, the previously developed and validated HPLC-UV method was applied [9]. In brief, a Varian (ProStar) HPLC-UV system was used for the identification and quantification of protocatechuic acid, quercetin and quercetin-3-β-D-glucoside. In addition, quercetin-3,4'-diglucoside was identified using a Vanquish Flex UHPLC LC-MS instrument equipped with a TSQ Quantis Triple Quadrupole Mass Spectrometer (Thermo Scientific). in both cases an Eclipse XDB-C18 column (150 mm×4.6 mm i.d., 5 µm; Agilent) was used to separate the compounds. The mobile phase consisted of acetonitrile (eluent A) and water with 1 % (v/v) acetic acid (eluent B) using a gradient elution (0-1 min 100 % B, 1-5 min 100-90 % B, 5-30 min 90-59 % B, 30-31 min 100 %) at room temperature (RT) and a flow rate of 1 mL/min. The absorption wavelength of the HPLC-UV was set to 280 nm. The LC-MS analysis conditions were as follows:

- negative ion spray voltage: 3 000 V,
- Sheath gas: 6.57 l/min,
- Auxiliary gas: 7.97 l/min,
- Sweep gas: 13.37 l/min,
- Temperature of the ion transfer tube: 350 °C and
- Evaporator temperature: 400 °C

Calibration curves of external standards (protocatechuic acid, quercetin, quercetin-3,4'-diglucoside and quercetin-3-β-D-glucoside) in 80 % MeOH in the concentration range from 1 mg/L to 200 mg/L were prepared.

Protocatechuic acid, quercetin and quercetin-3-β-D-glucoside were confirmed by an external standard method using the HPLC-UV system, while quercetin-3,4'-diglucoside was identified by LC-MS. All compounds were quantitatively evaluated by the calibration curve method and HPLC-UV analysis.

Results

The results of the study are divided into two main groups: the results of the HPLC-UV and LC-MS analysis and the results of the antioxidant tests.

Results of the HPLC-UV and LC-MS analyses

The linearity of the method was confirmed by determining the squared correlation coefficient (R^2) and the quality coefficient (*QC*). The method is linear if $R^2 \geq 0.99$ and $QC \leq 5\%$. In addition, the upper and lower limits of the 95 % confidence interval were determined. The masses of the bioactive components in the onion peels were calculated from the calibration curves and the contents were given in mg/g dry weight (DW).

Protocatechuic Acid

The linearity was confirmed by a linear correlation coefficient (R^2 = 0.9997) and the quality coefficient (*QC* = 1.7%). The most successful extraction of protocatechuic acid was obtained with deionized water (4.3 mg/g DW), followed by 70% ethanol (3.5 mg/g DW) and 70% methanol (3.4 mg/g DW). Among the DES solvents tested, the most successful extraction was achieved when acetic acid was used as HBD (DES 2) (1.5 mg/g DW). More detailed data for protocatechuic acid are shown in Table 1.

Table 1. Protocatechuic acid content in onion peels as a function of the extraction solvents used

Extraction solvent	mg of protocatechuic acid /1 g onion peels
MeOH	3.4
EtOH	3.5
H_2O	4.3
DES_1	1.2
DES_2	1.5
DES_3	1.3
DES_4	0.5
DES_5	1.2

Quercetin

The linearity was confirmed by a linear correlation coefficient (R^2 = 0.9998) and the quality coefficient (QC = 1.6%). The most successful extraction of quercetin was obtained with 70% methanol (4.2 mg/g DW), followed by 70% ethanol (3.4 mg/g DW) and the worst results were obtained with deionized water (0.3 mg/g DW). Among the DES solvents tested, the most successful extraction was again achieved when acetic acid was used as HBD (DES 2) (1.7 mg/g DW). More detailed data for quercetin are shown in Table 2.

Table 2. Quercetin content in onion peels as a function of the extraction solvents used

Extraction solvent	mg of quercetin /1 g onion peels
MeOH	4.2
EtOH	3.4
H_2O	0.3
DES_1	1.3
DES_2	1.7
DES_3	1.3
DES_4	0.7
DES_5	1.3

Quercetin-3-β-D-glucoside

The linearity was confirmed by a linear correlation coefficient (R^2 = 0.9998) and the quality coefficient (QC = 1.7%). The concentrations of quercetin-3-β-D-glucoside was below the limit of quantification (≤ 0.1 mg/g DW) in all extracts, therefore the comparison within the extractions with different solvents was not meaningful.

Quercetin-3,4‘-diglucoside

The linearity was confirmed by a linear correlation coefficient (R^2 = 0.9998) and the quality coefficient (QC = 1.7%). The most successful extraction of quercetin-3,4‘-diglucoside was obtained with 70% methanol (8.5 mg/g DW), followed by 70% ethanol (6.0 mg/g DW) and deionized water (2.9 mg/g DW). Among the DES solvents tested, the most successful extraction was again achieved when acetic acid was used as HBD (DES 2) (1.4 mg/g DW). More detailed data for quercetin-3,4‘-diglucoside are shown in Table 3.

Table 3. Quercetin-3,4‘-diglucoside content in onion peels as a function of the extraction solvents used

Extraction solvent	mg of quercetin-3,4‘-diglucoside/1 g onion peels
MeOH	8.5
EtOH	6.0
H_2O	2.9
DES_1	3.3
DES_2	4.4
DES_3	4.3
DES_4	2.2
DES_5	3.1

The total phenolic content (TPC)

Total phenolic compounds were determined by the Folin-Ciocalteau method and the TPC results were expressed as milligrams of gallic acid equivalents per gram of dry weight (mg GA g^{-1} DW). Results are presented in Table 4.

Table 4. The total phenolic content in different onion peel extracts

Extraction solvent	Concentration [mg GA/1 g DW]
MeOH	45.61
EtOH	45.48
H_2O	17.06
DES_1	35.69
DES_2	44.32
DES_3	41.63
DES_4	58.91
DES_5	37.58

When analyzing the antioxidant activity of onion peel extracts using the TPC test, the results clearly show that the extractions using alcohols or DES solvents had comparable antioxidant activity, while the worst results were obtained with water. Interestingly, DES 4 (HBD is fructose) proved to be the most effective solvent (58.91 mg GA g^{-1} DW). We believe that this is a false positive test. The false-positive result of the TPC test in the case of the solvent DES4 can be explained by the structural formula of fructose, which contains higher number of OH groups compared to other solvents or HBDs used. The TPC test is non-specific and is based on the reaction of phenols or polyphenolic compounds with the Folin–Ciocalteu reagent, in which electron transfer takes place. In the structure of phenols or polyphenolic compounds, there are a larger number of –OH compounds, therefore, according to the results of HPLC analysis, we can claim that in the case of DES4, the hydroxyl groups of fructose have reacted in the reaction and this is the reason for the false positive results.

ABTS antioxidant assay

The antioxidant activity of the onion peel extracts was also evaluated by ABTS test. The antioxidant activity of extracts was expressed as miligrams of Trolox equivalents per gram of dry weight material (mg Trolox g^{-1} DW). The results are presented in Table 5.

Table 5. Antioxidant activity of onion peel extracts determined by ABTS test

Extraction solvent	Concentration [mg Trolox/1 g DW]
MeOH	46.15
EtOH	45.50
H_2O	21.66
DES_1	43.92
DES_2	49.60
DES_3	44.96
DES_4	34.43
DES_5	45.49

The results of the ABTS test, which are shown in Table 5, do not show any significant differences depending on the extraction solvent used. The antioxidant activity also does not differ significantly when comparing the extracts obtained with 70% methanol or ethanol with extracts in which DES solvents were used. The extracts obtained with DES2 solvent using acetic acid as HBD were found to be the most effective and again, the water extracts showed the lowest antioxidant capacity.

DPPH antioxidant assay

The antioxidant activity of the onion peel extracts was additionaly evaluated by DPPH test. The antioxidant activity of extracts was expressed as miligrams of Trolox equivalents per gram of dry weight material (mg Trolox g^{-1} DW). The results are presented in Table 6.

Table 6. Antioxidant activity of onion peel extracts determined by DPPH test

Extraction solvent	Concentration [mg Trolox/1 g DW]
MeOH	61.70
EtOH	51.71
H_2O	27.25
DES_1	37.06
DES_2	37.76
DES_3	39.82
DES_4	33.34
DES_5	44.75

The results of the DPPH antioxidativity test shown in Table 6 correspond to a certain extent with the results of the ABTS test. In the DPPH test, the alcoholic extracts show better antioxidant efficiency than the extracts obtained with DES solvents or with water.

FRAP antioxidant assay

The antioxidant activity of the extracts was finally determined by the FRAP spectrophotometric method. The final results were given in mg of Fe^{2+} ions per 1 g of dry onion peels. The results are presented in Table 7.

Table 7. Antioxidant activity of onion peel extracts determined by FRAP test

Extraction solvent	Concentration [mg Fe^{2+}/1 g DW]
MeOH	104.72
EtOH	106.75
H_2O	49.78
DES_1	99.73
DES_2	96.43
DES_3	168.29
DES_4	67.28
DES_5	89.03

The results are similar to those previously reported for the ABTS and DPPH antioxidant activity assays. The most suitable solvent was DES3 where lactic acid was used as HBD. Water extracts showed the lowest antioxidant activity. Other results follow the above trend.

Conclusion

nvironmental pollution is one of the biggest problems of modern times. The food industry also contributes to pollution, as several million tons of food and food waste are thrown away every year. Food waste and by-products include peels, shells, seeds, leaves and other by-products that can be inedible for us. Onion peels are also part of the agro-industrial residues. As these by-products are produced in large quantities, solutions are being sought to recycle and reuse them. It has been shown that such residues can contain a large quantity of compounds with high bioactivity. For example, they contain polysaccharides, proteins, carbohydrates, polyphenolic compounds, etc. Waste can therefore represent renewable natural resources for us, the advantages of which lie in their availability, cost-effectiveness, sustainability and, of course, their environmental friendliness.

The main result of the master thesis was the optimization of the environmentally friendly and sustainable extraction of bioactive compounds from onion peels with the aim of replacing conventional organic solvents with a more environmentally friendly alternative or the use of deep eutectic solvents. Using DES solvents, we extracted various phenolic compounds from onion peels grown in Slovenia (Ptujski lük) and compared the yield of these solvents with the yield obtained using conventional organic solvents and water. All extracts were analyzed chromatographically using the HPLC-UV or LC-MS method. We confirmed the presence of protocatechuic acid, quercetin and its glucoside derivatives, quercetin-3-β-D-glucoside and quercetin-3,4'-diglucoside. The antioxidant activity of all extracts was determined using various antioxidant assays (ABTS, DPPH, FRAP, TPC). In the extraction of protocatechuic acid from onion peels, deionized water proved to be the most effective, but in the antioxidant tests we found that extracts with water contributed the least to antioxidant activity.

Quercetin, quercetin-3-β-D-glucoside and quercetin-3,4'-diglucoside, were maximally extracted with 70% methanol and 70% ethanol. Among the DES solvents, the two solvents in which choline chloride was combined with acetic and lactic acid were found to be the best, followed by the choline chloride solvents in combination with propane-1,2-diol and butane-1,4-diol. The antioxidant activity of extracts with DES solvents is usually close to the antioxidant activity of alcohol extracts.

From the above observations, we can conclude that it is useful to interpret the results in such a way that we combine the results obtained with HPLC analysis and antioxidant tests, since the results of HPLC analysis alone do not give us enough information; especially when we cannot qualitatively and quantitatively evaluate all the extracted compounds. And if we intend to use waste due to the high content of bioactive compounds and not just the reuse of certain compounds, we decide on solvents

that provide us with an extract with the highest antioxidant activity in addition to a successful extraction. At he end we can conclude that DES solvents are the green solvents of our future.

Acknowledgements

This research was supported by funds from the Scientific Research Cooperation between the Republic of Slovenia and Bosnia and Herzegovina (BI-BA/24-25-028), founded by the Slovenian Research and Innovation Agency (ARIS). The authors also gratefully acknowledge financial support from the ARIS program P2-0006.

References

1. M. Koel and M. Kaljurand, "Application of the principles of green chemistry in analytical chemistry," *Pure Appl. Chem.*, **vol. 78**, **no. 11**, pp. 1993–2002, 2006, doi: 10.1351/pac200678111993.
2. A. Paiva, R. Craveiro, I. Aroso, M. Martins, R. L. Reis, and A. R. C. Duarte, "Natural deep eutectic solvents - Solvents for the 21st century," *ACS Sustain. Chem. Eng.*, **vol. 2**, **no. 5**, pp. 1063–1071, 2014, doi: 10.1021/sc500096j.
3. A. K. Dwamena, "Recent advances in hydrophobic deep eutectic solvents for extraction," *Separations*, **vol. 6**, **no. 1**, 2019, doi: 10.3390/separations6010009.
4. A. Mandura, "Onion Solid Waste as a Potential Source of Functional Food Ingredients 1," **vol. 15**, **no. 3**, pp. 7–13, 2020.
5. "Ptujski luk." Accessed: May 11, 2024. [Online]. Available: https://www.travel-slovenia.si/slo/ptujski-luk/
6. "O luku." Accessed: May 11, 2024. [Online]. Available: https://zelena-tocka.si/ptujski-luk/o-luku/
7. R. Celano *et al.*, "Onion peel: Turning a food waste into a resource," *Antioxidants*, **vol. 10**, **no. 2**, pp. 1–18, 2021, doi: 10.3390/antiox10020304.
8. F. Shahidi and Y. Zhong, "Measurement of antioxidant activity," *J. Funct. Foods*, **vol. 18**, pp. 757–781, 2015, doi: 10.1016/j.jff.2015.01.047.
9. M. Ivanović, P. Krajnc, A. Mlinarič, and M. I. Razboršek, "Natural Deep Eutectic Solvent-Based Matrix Solid Phase Dispersion (MSPD) Extraction for Determination of Bioactive Compounds from Sandy Everlasting (Helichrysum arenarium L.): A Case of Stability Study," *Plants*, **vol. 11**, **no. 24**, 2022, doi: 10.3390/plants11243468.

Electrodeposition and characterization of smart selfhealing composite Zn-Co-RE coatings

Marija Mitrović[1*], Aleksandra Mijatović [2], Anđela Simović[3], Miroslav Pavlović[3], Regina Fuchs Godec[4], Milorad Tomić[1,5],Miomir Pavlović[1,5], Jelena Bajat[2]

[1]*University of East Sarajevo, Faculty of Technology, Zvornik, Republic of Srpska*

[2]*Faculty of Technology and Metallurgy, University of Belgrade, Serbia*

[3]*Institute of Chemistry, Technology and Metallurgy, narional Institute of the Republic of Serbia*

[4]*University of Maribor, Faculty of Chemistry and Chemical Engineering, Maribor, Slovenia*

[5]*Engineering academy of Serbia, Kneza Miloša 9/IV, Belgrade, Serbia*

[*]*marija.ridjosic@tfzv.ues.rs.ba*

Abstract

Incorporation of Rare earth elements (RE), which are known as good corrosion inhibitors, could be promising for extending a useful life of metallic coatings. In this work electrodeposited Zn-Co-RE composite coatings (RE=La, Sm, Y) were studied with the aim of defining the optimal parameters for obtaining the coatings with improved corrosion stability. The coatings were deposited galvanostatically, at different current densities, from chloride electrolyte at 25 °C. The chemical content of composite coatings was determined by energy dispersive X-ray analysis (EDS), morphology by scanning electron microscopy (SEM) and corrosion stability by electrochemical impedance spectroscopy (EIS). It was shown that deposition is of anomalous type. Zn-Co-Sm coatings contain K that forms a water soluble complex with Sm that easily dissolves leaving a porous coating of a poor corrosion stability. Since small deposition current density favors greater Sm, as well as K, incorporation, coatings obtained at greater current density showed better corrosion stability with short self-healing effect. Contrary, Zn-Co-Y coatings deposited at smaller current densities, with greater Y amount, exhibited excellent selfhealing effect with considerable increase in impedance values.

Keywords: *smart coatings, selfhealing, corrosion, electrodeposition*

Acknowledgements

This research was financially supported by the Ministry of Science, Technological Development and Innovation of the Republic of Serbia (Grant No. 451-03-65/2024-03/200135) and by the Ministry of Scientific and Technological Development and Higher Education of the Republic of Srpska (Grant No. 19.032/431-1-34/23)

Application of ZnO nanomaterials based on green tea leaf extract for enhanced photocatalytic degradation of tembotrione

Szabolcs Bognár[1,*], Vesna Despotović[1], Sanja Panić[2], Nina Finčur[1], Dušica Jovanović[1], Predrag Putnik[3], Daniela Šojić Merkulov[1]

[1] *University of Novi Sad Faculty of Sciences, Department of Chemistry, Biochemistry and Environmental Protection, Trg Dositeja Obradovića 3, 21000 Novi Sad, Serbia*

[2] *University of Novi Sad, Faculty of Technology, Bulevar Cara Lazara 1, 21000 Novi Sad, Serbia*

[3] *University North, Department of Food Technology, Trg dr. Žarka Dolinara 1, 48000 Koprivnica, Croatia*

[*] *sabolc.bognar@dh.uns.ac.rs*

Abstract

The application of advanced oxidation processes, such as photocatalytic degradation, makes it possible to remove persistent pollutants from water. The aim of this study was to investigate the activity of newly synthesized ZnO nanomaterials based on green tea leaf extract, in the photocatalytic degradation of tembotrione (TEM). The effect of synthesis approach on the photocatalytic activity of ZnO was examined and the highest photocatalytic activity was achieved in the system where the new material was prepared using zinc nitrate precoursor in water solution. Then, the effect of catalyst loading, initial pH, and TEM initial concetration on the photocatalytic efficiency was also investigated. All experiments were carried out using simulated solar irradiation (SSI). The highest removal rate was observed in the case of $\gamma = 0.5$ mg/cm^3, when 97% of TEM was degraded, after 60 min of SSI. Regarding the findings about the initial pH, it can be highlighted that the pH did not have significant effect on the TEM degradation efficiency. On the other hand, studying the influence of initial substrate concetration, it can be noted that the degradation efficiency of TEM decreased by increasing the initial substrate concentration.

Keywords: *Water purification; tembotrione; heterogeneous photocatalysis; nanotechnology; green synthesis, green tea leaf extract*

Acknowledgement

The research was funded by the Science Fund of the Republic of Serbia (In situ pollutants removal from waters by sustainable green nanotechnologies, Grant No. 7747845, CleanNanoCatalyze).

Improvement of the β-Ti alloy properties in bio-environment

Slađana Laketić[1,*], Bojan Međo[2], Miloš Momčilović[2], Jelena Bajat[2], Đorđe Veljović2, Vesna Kojić[3], Ivana Cvijović-Alagić[1]

[1] *Vinča Institute of Nuclear Sciences, University of Belgrade, P.O. Box 522, Belgrade, Serbia*

[2] *Faculty of Technology and Metallurgy, University of Belgrade, Karnegijeva 4, Belgrade, Serbia*

[3] *Oncology Institute of Vojvodina, Put doktora Goldmana 4, Sremska Kamenica, Serbia*

[*] *sladjana.laketic@vin.bg.ac.rs*

Abstract

The present study was focused on ensuring the β-type Ti-45Nb (mass%) alloy's long-term durability and appropriate behavior in harsh physiological conditions by improving the alloy surface, corrosive and biocompatible characteristics through the alloy microstructural alterations by high-pressure torsion (HPT) processing and the surface modifications by laser surface scanning technique. The alloy microstructural characterization showed that a change in the alloy phase composition did not occur during the HPT and laser irradiation processing. However, the alloy's HPT processing induced significant grain size reduction, while the laser treatment led to the surface chemical and morphological alterations that improved alloy's corrosion resistance and biocompatible properties in the bio-environment. This enhanced alloy's resistance to corrosion degradation and bioactive response is attributed to the formation of passive bioactivated bi-modal oxide layer and its significant thickening in a simulated body fluid environment. Obtained results indicated that metallic biomaterial's behavior in the bio-environment can be successfully improved through the combined HPT and laser surface treatment.

Keywords: *Ti-45Nb alloy; HPT process; laser surface scanning; corrosion resistance; biocompatibility.*

Introduction

Titanium alloys, due to their appropriate mechanical properties and corrosion resistance, as well as good biocompatibility and osseointegration with surrounding tissues in the human body, are particularly interesting for application as biomedical implants [1,2]. The disadvantages of this group of biomaterials are the possibility of their corrosion degradation in harsh bio-environmental conditions which can cause a problem during their interaction with the surrounding tissues [1,3]. Therefore, a new generation of β-Ti-based alloys has been developed to enhance hard-tissue implant biointegration properties and prevent the presence of cytotoxic elements in the human body that can cause allergic reactions and neurological disorders [1,2,4]. Above mentioned β-Ti alloys show outstanding corrosion resistance in the bio-environment as a result of the formation of a protective thin oxide layer on their surface. When this oxide layer is damaged or fractured, while the alloy is exposed to the bio-environment, the implant material deteriorates more rapidly [5]. Therefore, the formation of a compact and stable surface oxide layer is considered extremely desirable because it prevents the alloy's corrosion degradation and plays an important role in obtaining material excellent biocompatibility with the surrounding living tissues [6].

One way to attain favorable corrosive and biocompatible properties of implant materials is the application of a severe plastic deformation processing method, *i.e.* high-pressure torsion (HPT). Using this processing method the ultrafine-grained (UFG) microstructure with a high density of accumulated dislocations and grain size reduction can be obtained which leads to improved material characteristics [7,8]. Many authors showed in their research that the UFG metallic materials are characterized by improved physical properties, better corrosion resistance, and enhanced cell-implant interaction ability compared to their coarse-grained (CG) counterparts [8-11].

Given that the biomaterial's surface characteristics greatly determine its behavior in the human body, another way to obtain necessary implant material enhancements is to modify its surface [12-14]. Having this in mind, the laser surface scanning of biometallics has gained considerable attention in the last few years. Namely, laser beam irradiation can be used to modify the implant material surface properties and in that way enhance the corrosion resistance and biocompatibility of the hard-tissue implant [15,16]. Beneficial effects of the laser treatment include the formation of microstructural and morphological surface defects that exhibit a significant effect on the implant biointegration ability. Moreover, laser surface scanning leads to the appearance of more protective surface oxide layers which results in a more developed bioactive implant surface enabling in that way better osseointegration [15-18].
The aim of the present study was, therefore, to analyze the impact of the microstructural refinement and laser irradiation processing on the Ti-45Nb alloy surface morphology and damage-resistance characteristics, as well as on its electrochemical properties and biocompatibility in an aggressive bio-environment.

Experimental details

The β-type Ti-45Nb (mass%) alloy was selected for the present research and supplied in the form of hot-extruded rods. From the alloy rods, the samples were cut and metallographically prepared, *i.e.* ground by 180, 360, 600, and 1000 grit SiC papers, polished using a 2 μm polishing diamond suspension and cleaned in an ultrasonic bath with ethanol for 30 min.
The disk-shaped samples were then subjected to HPT and laser surface scanning processing. The alloy disk was for that purpose subjected to HPT deformation with 15 revolutions at room temperature under a pressure of 5.7 GPa. Additionally, the Ti-45Nb alloy samples in the HPT- unprocessed and processed form were irradiated using a Nd:YAG EKSPLA SL 212/SH/FH system operated at a 1064 nm wavelength by maintaining 5 mJ and 15 mJ output energy.
Obtained alloy alterations were analyzed using a filed-emission scanning electron microscope (FE-SEM) TESCAN Mira3 XMU, SEM JEOL JSM 5800, energy dispersive spectrometer (EDS) Oxford Inca 3.2, X-ray diffractometer (XRD) Rigaku Ultima IV and non-contact optical profilometer ZYGO NewView 7100. To estimate the effect of Ti-45Nb alloy microstructural refinement and laser surface modification on its corrosion resistance the potentiodynamic polarization and the electrochemical impedance spectroscopic (EIS) measurements were performed using a Gamry Reference 600 Potentiostat/Galvanostat/ZRA in the naturally aerated Ringer's solution at 37°C. Experimental EIS data were interpreted by a two-layer model and a good match between the EIS data and the applied model was obtained. The effect of the microstructural and surface modification on the cells' response and consequently the possibility of implanting investigated surface-modified alloy into the human body was investigated by its *in vitro* testing using the fibroblast MRC-5 cells. Examination of the cells' adhesion on the alloy surface was observed using the FE-SEM TESCAN Mira3 XMU microscope.

Results and discussion

FE-SEM micrographs presented in Figure 1 show that the laser irradiation of the CG and UFG Ti-45Nb alloy surface resulted in the formation of distinctive surface damage features in the form of unidirectional scan pattern lines parallel to the scanning direction with the appearance of periodic ripple-like structures and capillary waves.

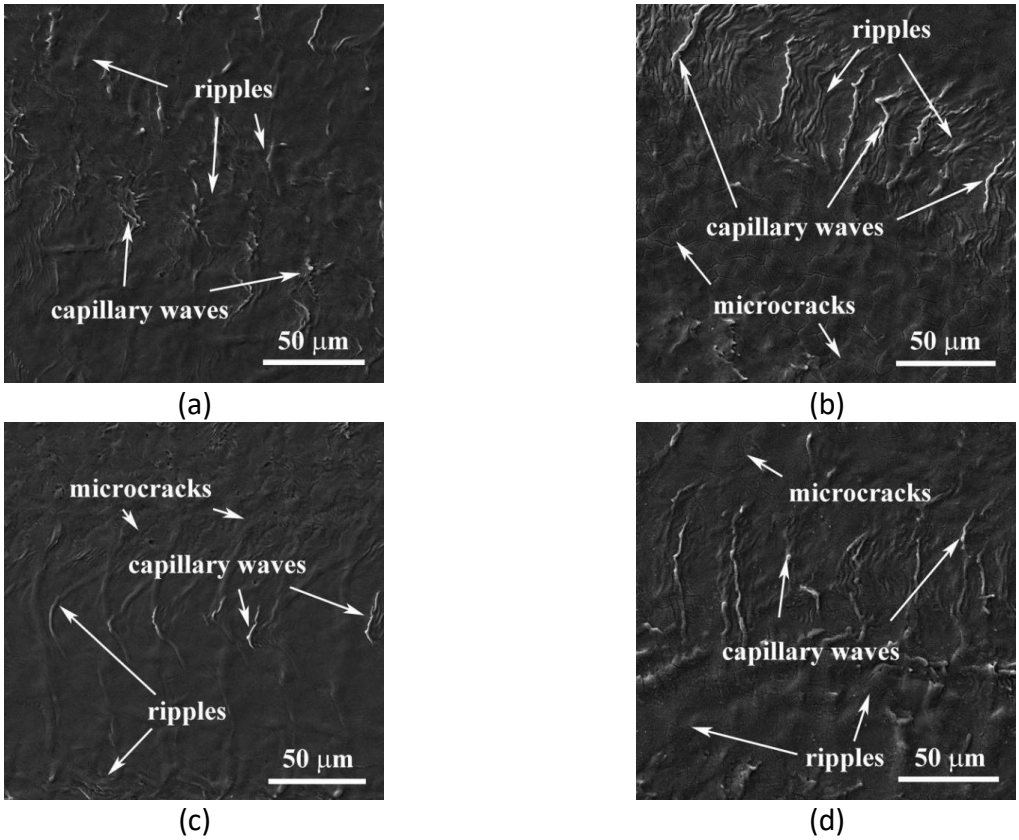

Figure 1. *FE-SEM micrographs of a),b) CG and c),d) UFG Ti-45Nb alloy surface after laser irradiation with a),c) 5 mJ and b),d) 15 mJ.*

Moreover, increasing the laser beam output energy from 5 mJ to 15 mJ resulted in the formation of more pronounced surface damage features and an enhanced alloy surface ablation took place (Figure 1b and 1d).

On the other hand, results obtained by the profilometric analysis given in Figure 2 indicated that the application of the higher laser pulse energy during the surface irradiation resulted in the appearance of a more pronounced alloy ablation process. The irradiated UFG Ti-45Nb alloy surface showed more pronounced damage features when compared to the CG alloy surface. Furthermore, the surface irradiation with 15 mJ caused the appearance of more distinctive damage characteristics than the surface irradiation with 5 mJ for both CG and UFG alloy samples.

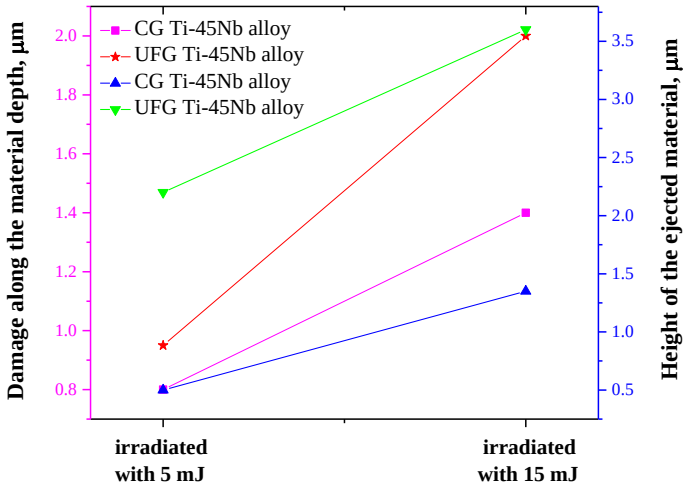

Figure 2. *Profilometric analysis of the CG and UFG Ti-45Nb alloy surface after the laser irradiation.*

Laser surface modification induced the creation of diverse surface topographies of both, CG and UFG, alloy samples. According to the results of surface roughness analysis presented in Figure 3, it can be concluded that the alloy microstructural and surface alterations led to the surface roughness increase which suggests the obtainment of improved alloy biointegration ability [17,18]. Moreover, the laser surface scanning with higher laser pulse energy caused a more pronounced increase in the surface roughness of CG and UFG alloy samples, although the highest roughness value was observed in the case of UFG Ti-45Nb alloy.

Furthermore, the analysis of the CG and UFG Ti-45Nb alloy surfaces after interaction with the laser beam in air showed that the absorbed energy caused not only morphological changes but also led to the change in alloy surface chemical composition. Results of the EDS analysis showed that Ti and Nb are present in similar proportions on the surface of all investigated samples after the laser treatment, while extremely high temperatures and the laser beam intensity redistribution achieved during the irradiation influenced the appearance of high oxygen concentrations in the analyzed irradiated areas (Figure 4). Moreover, an increase of the laser output energy from 5 mJ to 15 mJ stimulated the alloy surface oxidation process, which is extremely favorable when the improvement of the implant material bioactivity, corrosion resistance in the biological environment and biocompatibility are concerned [6,9,11,18]. In addition, it can be noted that the irradiated surface of the UFG Ti-45Nb alloy was characterized by a higher oxygen content compared to the irradiated CG Ti-45Nb alloy surface and that its highest value was detected when higher irradiation energy was applied. Moreover, the obtained results indicate the formation of a stable, thin surface layer, which consists of mixed Ti- and Nb-oxide, and its presence can in great merit affect the improvement of alloy corrosion behavior and biointegration properties due to the layer's high protective capacity [7,8,14,15].

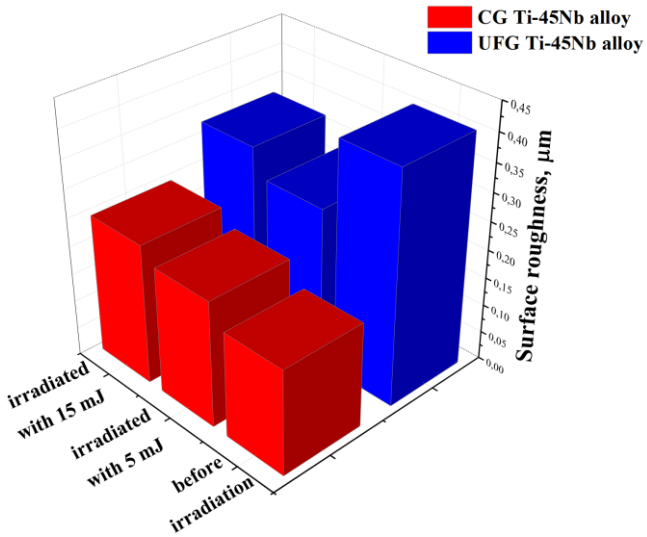

Figure 3. *Surface roughness of the CG and UFG Ti-45Nb alloy before and after laser surface irradiation.*

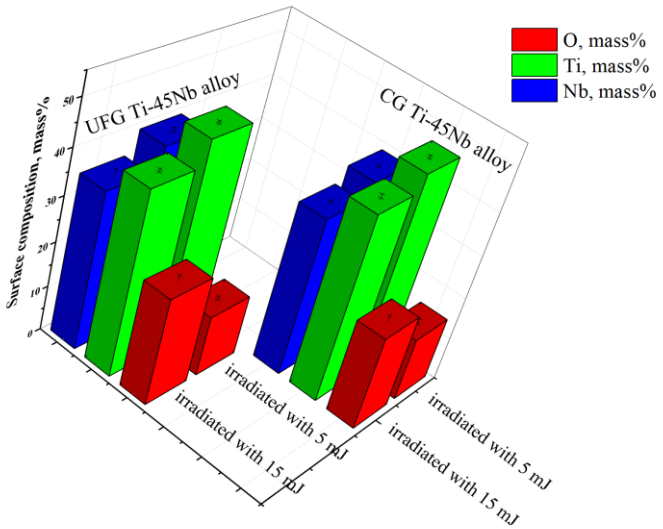

Figure 4. *Chemical composition of the laser-irradiated CG and UFG Ti-45Nb alloy surfaces as a dependence of the laser output energy.*

Figure 5 shows the XRD diffractograms obtained for the CG and UFG Ti-45Nb alloy before and after additional laser treatment. Due to the position and intensity of the peaks observed in the recorded diffractograms, it was confirmed that the HPT process and the laser surface scanning did not cause phase transformations in the investigated alloy microstructure. However, it can be noted that the laser treatment influenced the increase in the XRD peaks intensity, as well as the appearance of (Ti,Nb)O as a result of the Ti-45Nb alloy surface oxidation. A higher degree of oxidation was noticed after laser surface scanning of the UFG Ti-45Nb alloy with a lower output energy of 5 mJ.

Results obtained during electrochemical tests (Figure 6) showed that all investigated alloy samples exhibited similar electrochemical behavior. Namely, CG and UFG Ti-45Nb alloy before and after additional laser irradiation undergo spontaneous passivization in conditions that simulate the human body environment which results in developing a protective stable surface oxide layer comprised of mixed Ti- and Nb-oxides.

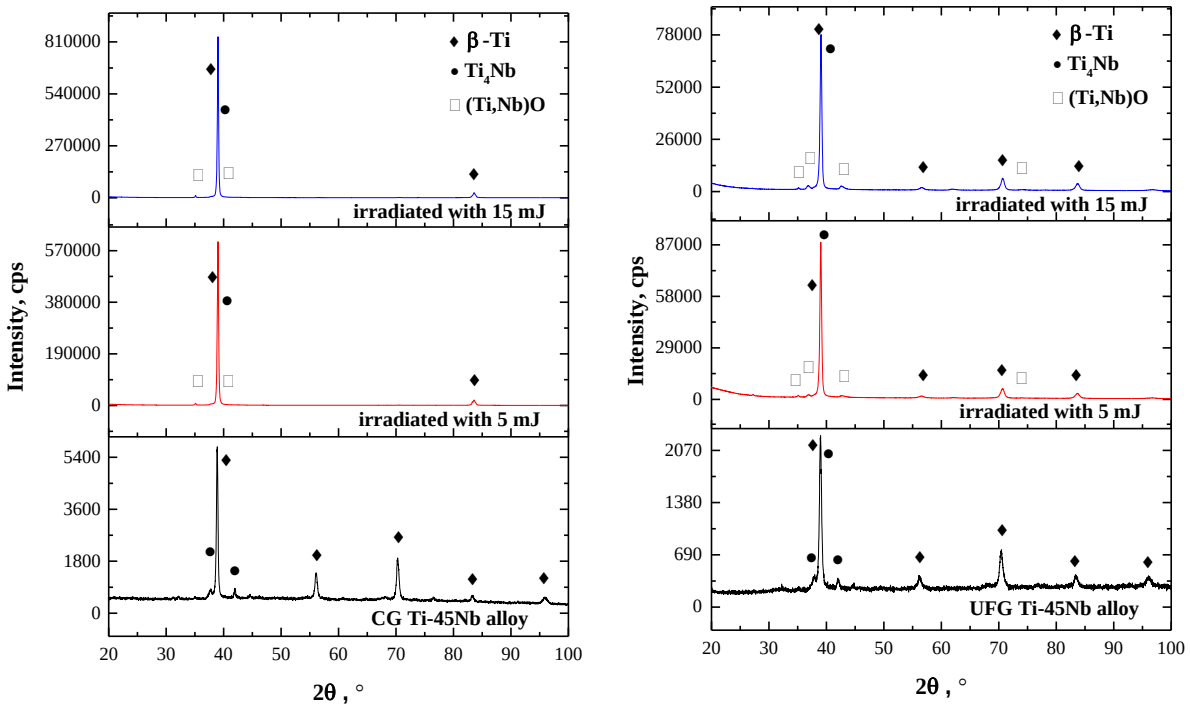

Figure 5. *XRD patterns of a) CG and b) UFG Ti-45Nb alloy before and after additional laser surface irradiation.*

The alloy corrosion behavior is best estimated through the corrosion current density j_{corr} value and the lower it is, the higher the corrosion resistance is. From the potentiodynamic curves, presented in Figure 6, it can be seen that the j_{corr} value was the lowest for the UFG Ti-45Nb alloy irradiated with 15 mJ and 5 mJ, respectively, followed by laser-treated CG alloy with 5 mJ and UFG alloy before laser surface modification with approximately the same values, then the CG Ti-45Nb alloy irradiated with 15 mJ and, finally, the CG Ti-45Nb alloy before laser irradiation characterized with the highest corrosion current density value. The obtained results showed that the UFG alloy exhibited a higher corrosion resistance than the alloy in its initial CG state, while the laser surface scanning induced the obtainment of the lowest j_{corr} which points out the formation of a more compact and protective surface layer. Furthermore, an increase in the corrosion potential is a characteristic of more stable oxide layer formation which, in turn, results in the j_{corr} value decrease and the oxide layer thickness increase. Therefore, the attained higher alloy corrosion stability was influenced by the formation of a bi-modal oxide surface layer consisting of an inner barrier and an outer porous layer.

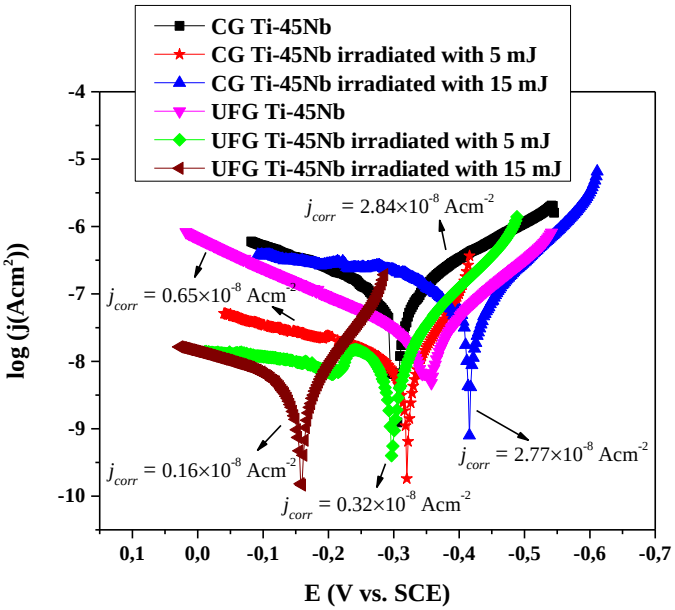

Figure 6. *Tafel curves of the CG and UFG Ti-45Nb alloy samples obtained in naturally aerated Ringer's solution at 37°C before and after the additional alloy irradiation.*

Table 1. Electrochemical parameters of the CG and UFG Ti-45Nb alloy samples obtained in naturally aerated Ringer's solution at 37°C before and after the additional alloy irradiation.

Ti-45Nb alloy		***CG***	***UFG***	***CG irradiated with 5 mJ***	***UFG irradiated with 5 mJ***	***CG irradiated with 15 mJ***	***UFG irradiated with 15 mJ***
Inner barrier layer	R_b , Ωcm^2	0.27×10^6	2.52×10^6	3.09×10^6	29.5×10^6	3.02×10^6	15.8×10^6
	C_b , $S^n\Omega^1cm^{-2}$	2.89×10^{-6}	0.77×10^{-6}	5.21×10^{-6}	1.43×10^{-6}	2.78×10^{-6}	6.44×10^{-6}
	d_b	$d_{b(UFG)} = 3.75d_{b(CG)}$		$d_{b(UFG+5mJ)} = 3.6d_{b(CG+5mJ)}$		$d_{b(CG+15mJ)} = 2.3d_{b(UFG+15mJ)}$	
Outer porous layer	R_p , Ωcm^2	39.2	109	130	150	144	32.5
	C_p , $S^n\Omega^{-1}cm^{-2}$	16.59×10^{-6}	20.29×10^{-6}	0.34×10^{-6}	4.15×10^{-6}	0.51×10^{-6}	2.87×10^{-6}
	d_p	$d_{p(CG)} = 1.22d_{p(UFG)}$		$d_{p(UFG+5mJ)} = 0.08d_{p(CG+5mJ)}$		$d_{p(UFG+15mJ)} = 0.2d_{p(CG+15mJ)}$	
Goodness of Fit		203.6×10^{-6}	54.8×10^{-6}	0.44×10^{-3}	447×10^{-6}	1.28×10^{-3}	199×10^{-6}

Additionally, the EIS measurements data was presented as the electrochemical parameters given in Table 1. As can be seen, the inner compact barrier layer resistance, R_b, and the outer porous layer resistance, R_p, that correspond to the CG and UFG Ti-45Nb alloy samples in the initial state are lower compared to the values attained for the laser-irradiated alloy samples. Moreover, R_b is significantly higher than R_p of the Ti-45Nb alloy samples before and after HPT and laser irradiation processing. These results demonstrated that the improved corrosion resistance of alloy samples was promoted with the laser surface irradiation due to an increase in the surface layer protective properties.

Also, the capacitance values of the barrier and porous layers, defined and presented in Table 1, were used to estimate the barrier and porous layer thickness [14]. The obtained results showed that in the case of the laser-untreated CG Ti-45Nb alloy, a thicker inner barrier layer was formed in bio-environmental conditions, while after laser surface irradiation treatment a thicker outer porous layer was formed. However, different results were obtained for the UFG Ti-45Nb alloy. Namely, the inner barrier layer thickness was higher for laser-modified samples, while higher outer porous layer thickness was observed on the alloy surface before additional laser treatment. Based on the attained results, it can be concluded that the CG alloy before surface treatment and the UFG alloy after surface treatment exhibited better corrosion resistance properties, while the CG alloy after laser surface treatment and the UFG alloy before laser surface treatment showed better osseointegration capacity.
Finally, according to the Tafel potentiodynamic curves and the EIS results it can be noticed that the corrosion behavior of the Ti-45Nb alloy is highly influenced by both the microstructural refinement and the surface texturing.
Surface analysis conducted to study cell integration showed that MRC-5 cells on the surfaces of CG and UFG Ti-45Nb alloy samples were elongated with pronounced cytoplasmic extensions, cells were connected to each other and attached to the alloy surface, especially after additional laser irradiation. Moreover, the cell morphology analysis demonstrated their good metabolic activity. Observed cell shape and the presence of filopodia on the unmodified and laser-modified CG and UFG Ti-45Nb alloy surfaces indicated their excellent biointegration abilities.
Results of the present study showed that the Ti-45Nb alloy is characterized by excellent biocompatibility characteristics.

Conclusion

Conducted research showed that the HPT processing and the laser irradiation resulted in significant alterations of the Ti-45Nb alloy properties. Attained microstructural refinement and surface texturing accompanied by the changed surface chemistry influenced the improvement of alloy corrosion resistance and, at the same time, enhanced live cell attachment, adhesion, and proliferation. These findings demonstrate that the combined HPT and laser surface processing can be effectively used to improve the metallic implant materials' behavior in the biological environment.

Acknowledgments

This work was financially supported by the Ministry of Science, Technological Development and Innovation of the Republic of Serbia through Contract No. 451-03-66/2024-03/200017 and the PhD fellowship of Slađana Laketić.

References

1. Q. Chen, G.A. Thouas, *Metallic implant biomaterials*, Mater. Sci. Eng. R Rep., 87, 1-57, 2015.
2. Y. Li, C. Yang, H. Zhao, S. Qu, X. Li, Y. Li, *New Developments of Ti-Based Alloys for Biomedical Applications*, Materials, 7, 1709-1800, 2014.
3. B.C. Costa, C.K. Tokuhara, L.A. Rocha, R.C. Oliveira, P.N. Lisboa-Filho, J. Costa Pessoa, *Vanadium ionic species from degradation of Ti-6Al-4V metallic implants: In vitro cytotoxicity and speciation evaluation*, Mater. Sci. Eng. C Mater. Biol. Appl., 96, 730-739, 2019.
4. L.-Y. Chen, Y.-W. Cui, L.-C. Zhang, Recent Development in Beta Titanium Alloys for Biomedical Applications, Metals, 10(9), 1139, 2020.
5. U. Nichul , V. Kumar, V. Hiwarkar, Electrochemical performance of heat-treated beta titanium alloy in artificial saliva: Key role of grain size, Mater. Today Commun. , 37, 106981, 2023.
6. I. Cvijović-Alagić, Z. Cvijović, J. Bajat, M. Rakin, Composition and processing effects on the electrochemical characteristics of biomedical titanium alloys, Corros. Sci., 83, 245-254, 2014.

7. D. Barjaktarević, B. Međo, P. Štefane, N. Gubeljak, I. Cvijović-Alagić, V. Đokić, M. Rakin, *Tensile and Corrosion Properties of Anodized Ultrafine-Grained Ti-13Nb-13Zr Biomedical Alloy Obtained by High-Pressure Torsion*, Met. Mater. Int., 27, 3325-3341, 2021.
8. I. Cvijović-Alagić, Z. Cvijović, J. Maletaškić, M. Rakin, Initial microstructure effect on the mechanical properties of Ti-6Al-4V ELI alloy processed by high-pressure torsion, Mat. Sci. Eng. A, 736, 175-192, 2018.
9. I. Cvijović-Alagić, S. Laketić, J. Bajat, A. Hohenwarter, M. Rakin, *Grain refinement effect on the Ti-45Nb alloy electrochemical behavior in simulated physiological solution*, Surf. Coat. Technol., 423, 127609, 2021.
10. C. Vasilescu, S.I. Drob, E.I. Neacsu, J.C. Mirza Rosca, Surface analysis and corrosion resistance of a new titanium base alloy in simulated body fluids, Corros. Sci., 65, 431-440, 2012.
11. K. Aniołek, B. Łosiewicz, J. Kubisztal, P. Osak, A. Stróz, A. Barylski, S. Kaptacz, Mechanical Properties, Corrosion Resistance and Bioactivity of Oxide Layers Formed by Isothermal Oxidation of Ti-6Al-7Nb Alloy, Coatings 11(5), 505, 2021.
12. L-C. Zhang, L-Y. Chen, L. Wang, Surface Modification of Titanium and Titanium Alloys: Technologies, Developments, and Future Interests, Adv. Eng. Mater., 22(5), 1901258, 2020.
13. S. Laketić, M. Rakin, M. Momčilović, J. Ciganović, Đ. Veljović, I. Cvijović-Alagić, *Surface modifications of biometallic commercially pure Ti and Ti-13Nb-13Zr alloy by picosecond Nd:YAG laser*, Int. J. Miner. Metall., 28, 285-295, 2021.
14. S. Laketić, M. Rakin, M. Momčilović, J. Ciganović, Đ. Veljović, I. Cvijović-Alagić, *Influence of laser irradiation parameters on the ultrafine-grained Ti-45Nb alloy surface characteristics*, Surf. Coat. Technol., 418, 127255, 2021.
15. H.K. Lin, G.Y. Li, S. Mortier, P. Bazarnik, Y. Huang, M. Lewandowska, T.G. Langdon, *Processing of CP-Ti by high-pressure torsion and the effect of surface modification using a post-HPT laser treatment*, J. Alloy. Compd., 784, 653-659, 2019.
16. M. von Allmen, *Laser Beam Interaction with Materials*, London, UK, Springer - Verlag, 1987.
17. Y. Wang, J. Zhang, K. Li, J. Hu, Surface characterization and biocompatibility of isotropic microstructure prepared by UV laser, J. Mater. Sci. Technol., 94, 136-146, 2021.
18. K. Anselme, P. Linez, M. Bigerelle, D. Le Maguer, A. Le Maguer, P. Hardouin, H.F. Hildebrand, A. Iost, J.M. Leroy, *The relative influence of the topography and chemistry of TiAl6V4 surfaces on osteoblastic cell behaviour*, Biomaterials 21(15), 1567-1577, 2000.

Enhanced photocatalytic removal of fluroxypyr using newly synthesized green ZnO nanocomposites under simulated solar irradiation

Vesna Despotović[1,*], Nataša Tot[2], Nina Finčur[1], Tamara Ivetić[3], Sabolč Bognar[1], Dušica Jovanović[1], Daniela Šojić Merkulov[1]

[1] *University of Novi Sad Faculty of Sciences, Department of Chemistry, Biochemistry and Environmental Protection, Trg Dositeja Obradovića 3, 21000 Novi Sad, Serbia*

[2] *Technical College of Applied Sciences in Zrenjanin, Đorđa Stratimirovića 23, 23000 Zrenjanin, Serbia*

[3] *University of Novi Sad Faculty of Sciences, Department of Physics, Trg Dositeja Obradovića 4, 21000 Novi Sad, Serbia*

[*] *vesna.despotovic@dh.uns.ac.rs*

Abstract

Fluroxypyr (FLU) is a herbicide from the class of pyridine carboxylic acids. The intensive application of FLU in agriculture leads to serious contamination of soil and water resources. The aim of this study was to investigate the photocatalytic activity of newly synthesized green ZnO nanocomposites based on banana peel extract (ZnO/banana peel) and tartaric acid (ZnO/tartaric acid) for the removal of FLU from aquatic environment in the presence of simulated solar irradiation. The photocatalytic reactor with xenon lamp was used for the removal of selected herbicide. The results showed that after 60 min of irradiation higher efficiency of FLU removal was achieved by using ZnO/tartaric acid as a photocatalyst compared to green nanopowders based on banana peel extract. In addition, to enhance the photocatalytic performance of ZnO/tartaric acid, the photocatalytic activity of a coupled semiconductor system SnO_2/ZnO/tartaric acid was also investigated.

Keywords: *fluroxypyr; photocatalysis; green ZnO nanocomposite*

Acknowledgements

This research was supported by the Science Fund of the Republic of Serbia (Grant No. 7747845, In situ pollutants removal from waters by sustainable green nanotechnologies – CleanNanoCatalyze) and the Ministry of Science, Technological Development and Innovation of the Republic of Serbia (Grant No. 451-03-66/2024-03/200125 and 451-03-65/2024-03/200125).

SPONSORS

SPONZORI


JADRAN

PROVEN ASSET PROTECTION ACROSS THE GLOBE

Sherwin-Williams Protective & Marine delivers world-class industry subject matter expertise, unparalleled technical and specification service, and unmatched regional commercial team support to our customers around the globe. Our broad portfolio of high-performance coatings and systems, including protective liquid and powder, fire protection, and flooring, excel at combating corrosion and help customers achieve smarter, time-tested asset protection. We serve a wide array of markets across our rapidly growing international distribution footprint, including Bridge & Highway, Energy, High-Value Infrastructure, Manufacturing and Processing, Marine, Rail, Power, and Water & Wastewater.

Visit our website or contact your Sherwin-Williams expert
Marko Nikolic: +381 60 4204 013 | marko.nikolic@sherwin.com

SHERWIN-WILLIAMS®

protectiveeu.sherwin-williams.com
protectiveemea.sherwin-williams.com


INTERNATIONAL SOCIETY OF ELECTROCHEMISTRY
ISE

Кнеза Милоша 7
11000 Београд

Савез инжењера и техничара Србије

Union of Engineers and Technicians of Serbia


KANSAI
HELIOS

ALFATERM d.o.o.

Firestop®
INTERNACIONAL

Inovativni protivpožarni premazi za sigurnu budućnost

Kompanija **Firestop Internacional** je sa svojim brendom **FIRESTOP** izbor broj 1 na tržištu Srbije i regiona u oblasti ekspandujućih protivpožarnih premaza za zaštitu čelika i drveta.

U svom portfoliju ima i **Tinto color** osnovne i završne premaze za zaštitu metala, koji se mogu koristiti samostalno ili u sklopu Firestop sistema zaštite.

Korišćenjem ovog inovativnog sistema premaza postiže se kompletna antikorozivna i protivpožarna zaštita.

Firestop Internacional d.o.o.
Gavrila Principa 20, 22330 Nova Pazova
Tel. 022 321 030, 326 342, 323 134 / Fax. 022 325 002
office@internacional.rs / www.firestopinternacional.rs

Protection upgraded



Custom Made Chemical Specialities for Surface Treatment

- Optimal solutions for all key applications of surface finishing
  - **Industrial Parts Cleaning**
  - **Metal Pre-treatment**
  - **Functional and Decorative Electroplating**
- Worldwide representatives in more than 50 countries
- A company of Freudenberg Group since 2011

SurTec doo Serbia

sales.serbia@surtec.com
www.SurTec.com

Preljinska baluga bb
32000 Cacak, Srbija

Tel. +381 32 538 1569
Fax. +381 32 538 1569

Institut za preventivu

zaštitu na radu, protivpožarnu zaštitu i razvoj d.o.o.

21000 Novi Sad • Kraljevića Marka 11 • tel/fax: 021 / 420-571, 420-572, 420-573
institut@izp.rs • www.izp.rs

ATC 04-010 АКРЕДИТОВАНО СЕРТИФИКАЦИОНО ТЕЛО SRPS EN 45011:2004

ATC 06-013 АКРЕДИТОВАНА КОНТРОЛНА ОРГАНИЗАЦИЈА SRPS ISO/IEC 17020:2002

ATC 01-069 АКРЕДИТОВАНА ЛАБОРАТОРИЈА ЗА ИСПИТИВАЊЕ SRPS ISO/IEC 17025:2006

- bezbednost i zdravlje na radu
- zaštita od požara i eksplozije
- zaštita životne sredine
- tehnički pregledi objekata
- izrada projektno tehničke dokumentacije
- katodna zaštita
- akreditovana tela
- sertifikacija i ispitivanje opreme u "Ex" izvedbi

ИНСТИТУТ ЗА ОПШТУ И ФИЗИЧКУ ХЕМИЈУ
INSTITUTE OF GENERAL AND PHYSICAL CHEMISTRY